frontiers | Research Topics

HIV/SIV basic research update

Edited by
Akio Adachi, Masako Nomaguchi and Takaaki Koma

Published in
Frontiers in Virology

ISSN 1664-8714
ISBN 978-2-8325-3264-5
DOI 10.3389/978-2-8325-3264-5

About Frontiers

Frontiers is more than just an open access publisher of scholarly articles: it is a pioneering approach to the world of academia, radically improving the way scholarly research is managed. The grand vision of Frontiers is a world where all people have an equal opportunity to seek, share and generate knowledge. Frontiers provides immediate and permanent online open access to all its publications, but this alone is not enough to realize our grand goals.

Frontiers journal series

The Frontiers journal series is a multi-tier and interdisciplinary set of open-access, online journals, promising a paradigm shift from the current review, selection and dissemination processes in academic publishing. All Frontiers journals are driven by researchers for researchers; therefore, they constitute a service to the scholarly community. At the same time, the *Frontiers journal series* operates on a revolutionary invention, the tiered publishing system, initially addressing specific communities of scholars, and gradually climbing up to broader public understanding, thus serving the interests of the lay society, too.

Dedication to quality

Each Frontiers article is a landmark of the highest quality, thanks to genuinely collaborative interactions between authors and review editors, who include some of the world's best academicians. Research must be certified by peers before entering a stream of knowledge that may eventually reach the public - and shape society; therefore, Frontiers only applies the most rigorous and unbiased reviews. Frontiers revolutionizes research publishing by freely delivering the most outstanding research, evaluated with no bias from both the academic and social point of view. By applying the most advanced information technologies, Frontiers is catapulting scholarly publishing into a new generation.

What are Frontiers Research Topics?

Frontiers Research Topics are very popular trademarks of the *Frontiers journals series*: they are collections of at least ten articles, all centered on a particular subject. With their unique mix of varied contributions from Original Research to Review Articles, Frontiers Research Topics unify the most influential researchers, the latest key findings and historical advances in a hot research area.

Find out more on how to host your own Frontiers Research Topic or contribute to one as an author by contacting the Frontiers editorial office: frontiersin.org/about/contact

HIV/SIV basic research update

Topic editors

Akio Adachi — Tokushima University, Japan

Masako Nomaguchi — Tokushima University, Japan

Takaaki Koma — Tokushima University, Japan

Citation

Adachi, A., Nomaguchi, M., Koma, T., eds. (2023). *HIV/SIV basic research update*. Lausanne: Frontiers Media SA. doi: 10.3389/978-2-8325-3264-5

Table of contents

frontiers | Frontiers in Virology

TYPE Editorial
PUBLISHED 02 August 2023
DOI 10.3389/fviro.2023.1253524

OPEN ACCESS

EDITED AND REVIEWED BY
Jeremy R. Thompson,
Plant Health & Environment Laboratories (MPI), New Zealand

*CORRESPONDENCE
Akio Adachi
adachi@tokushima-u.ac.jp
Masako Nomaguchi
nomaguchi@tokushima-u.ac.jp

RECEIVED 05 July 2023
ACCEPTED 24 July 2023
PUBLISHED 02 August 2023

CITATION
Adachi A, Koma T and Nomaguchi M (2023) Editorial: HIV/SIV basic research update.
Front. Virol. 3:1253524.
doi: 10.3389/fviro.2023.1253524

Editorial: HIV/SIV basic research update

Akio Adachi*, Takaaki Koma and Masako Nomaguchi*

Department of Microbiology, Graduate School of Medicine, Tokushima University, Tokushima, Tokushima, Japan

KEYWORDS

HIV/SIV, human retroviruses, molecular virology, accessory proteins, animal models, viral reservoirs, anti-HIV strategies

Editorial on the Research Topic
HIV/SIV basic research update

Since its identification as an etiological agent for acquired immunodeficiency syndrome (AIDS) and AIDS-related disease complex (ARC) in 1983, the extent of studies on human immunodeficiency virus type 1 (HIV-1) has been unprecedented (1). Because of the severity of the disease, its pandemic nature, and also the inherent intellectual curiosity of scientists for the novel virus, we virologists have made every effort to explore HIV-1 and related viruses in detail. From these far-reaching systemic studies performed by numerous virologists and their colleagues in different expert fields, we have gained a remarkably wide variety of basic and medical virological knowledge and insights on a range of HIV/AIDS issues (2–7). It should be noted here that the achievements in HIV-1 research in the four decades since its discovery (i.e., those of actual virological findings, virological concepts, strategic approaches, practical experimental tools/systems, scientific findings/concepts/research systems not confined to the virology research field, etc.) are applicable not only to HIV-1 and its related viruses but also to viruses of other families. In this regard, we would like to underscore the importance of the basic and applied HIV-1 research conducted so far for human virology as a whole.

In this Research Topic on HIV/SIV-related subjects (i.e., in our Research Topic designated "HIV/SIV basic research update"), there are nine full articles, six original research and three review articles, contributed by actively working researchers in the HIV/SIV-related fields in Canada, Japan, Rwanda, Uganda, and the USA. Each work presented addresses a currently crucial theme concordant with or closely relevant to the major aim of our Research Topic, as clearly expressed by its title and keywords. Meissner et al. comprehensively summarize the virology of representative primate retroviruses (HIV-1, HIV-2, and human T-cell leukemia virus type1 (HTLV-1)) in the first review article of this Research Topic. They provide a sophisticated overview of the viral replication cycle, genomic and biological diversity, and also of host cellular proteins that most notably affect viral replication. McAllister et al. investigate the Sp family proteins in cells of the monocyte-macrophage lineage and find that the binding of Sp1 to viral LTR increased relative to that of Sp3 following monocytic differentiation. It is also shown that the activity of Sp proteins is additionally regulated at the post-translational level. Miyakawa et al. identify a cellular transmembrane protein MAL that substantially inhibits HIV-1 virion production by the bioluminescence resonance energy transfer (NanoBRET) assay. Of note,

the antiviral activity of MAL was partially antagonized by that viral Nef protein. Umviligihozo et al. examine the sequence and function of viral Nef and Vpu proteins in a cohort of Rwandan long-term survivors with HIV-1 subtype A. It is suggested that the attenuated function of Nef, but not Vpu, is responsible for slowing disease progression. Kaku et al. produce five anti-idiotypic antibodies from mice immunized with 1C10, a ladle-type anti-HIV-1 subtype B V3 antibody, in order to analyze the epitope-paratope interactions between 1C10 and HIV-1 V3 loop. They demonstrate that the anti-idiotypic antibodies raised against the potent cross-neutralizing human antibody 1C10 recognize a key amino acid formation essential for steric interactions between the 1C10 and V3 loop. Curlin et al. evaluate virus replication kinetics, CD4+ T cell dynamics, and genetic adaptive changes in humanized BLT mice using three simian immunodeficiency viruses (SIVs) designated SIVmac239, SIV_{B670}, and SIV_{hu}. All three biologically distinct SIVs originating from SIVsm are shown to infect and replicate in these model animals and are found to be genetically adaptable in the hosts. The small model animals, susceptible to both SIV and HIV, may open a novel avenue for future comparative studies. Whitehurst et al. examine the effect of HIV co-infection on Epstein-Barr virus (EBV) replication and EBV-induced tumorigenesis using humanized NSG mice. They demonstrate that HIV co-infection enhances systemic EBV replication, host immune activation, and EBV-induced tumorigenesis. The results showing a direct effect of HIV co-infection on EBV pathogenesis and disease progression may facilitate detailed studies in the future. In their review article, Sukegawa and Takeuchi describe how cells of the monocyte/macrophage lineage influence HIV-1 infection. They focus on the monocyte/macrophage impact on HIV-1 replication and virus-reservoirs establishment. They also refer to recent approaches toward HIV-1 eradication by specific targeting of cells of a monocyte/macrophage lineage. Vargas and Sluis-Cremer outline the so-called "block and lock" therapeutic approach to a functional cure for HIV-1 infection in their review article. They focus on the small molecules, nucleic acids, and recombinant proteins reported to block and/or lock HIV-1 in the latent state, providing a clear overall picture of the "block and lock" approach against HIV-1.

Lastly, we briefly describe the HIV/AIDS issues that remain to be solved. From our perspective, major issues can be organized and summarized as follows: (i) detailed molecular biological understanding of viral replication and viral structural proteins (8–14); (ii) elucidation of viral adaptation and evolution in various circumstances and proactive prediction of viral adaptive mutations (15–17); (iii) clear determination of the biological significance of viral accessory proteins (18–21); (iv) establishment of animal models suitable for each research project (22, 23); (v) identification of viral reservoirs and a functional cure for HIV-1 infection (24–28). While we have accomplished many of the themes listed above in the past four decades, much still remains elusive. Anti-HIV-1 drugs have been successfully developed, and thus AIDS is no longer an incurable disease. However, a complete or functional cure is not yet achieved. Importantly, in addition, scientifically interesting and crucial but unsolved matters await clarification. In collaboration with experts in other research fields, we virologists have to seriously tackle the issues described above and move toward valid anti-HIV-1 strategies with a solid background in biological and molecular biological virology (29, 30).

Author contributions

AA: Conceptualization, Writing – original draft, Writing – review & editing. TK: Writing – review & editing. MN: Conceptualization, Writing – review & editing.

Conflict of interest

The authors declare that the research was conducted in the absence of any commercial or financial relationships that could be construed as a potential conflict of interest.

The authors MN, TK, and AA declared that they were an editorial board member of Frontiers, at the time of submission. This had no impact on the peer review process and the final decision.

Publisher's note

References

1. Barré-Sinoussi F, Chermann JC, Rey F, Nugeyre MT, Chamaret S, Gruest J, et al. Isolation of a T-lymphotropic retrovirus from a patient at risk for acquired immune deficiency syndrome (AIDS). *Science* (1983) 220:868–71. doi: 10.1126/science.6189183

2. Fauci AS. HIV and AIDS: 20 years of science. *Nat Med* (2003) 9:839–43. doi: 10.1038/nm0703-839

3. Ho DD, Bieniasz PD. HIV-1 at 25. *Cell* (2008) 133:561–65. doi: 10.1016/j.cell.2008.05.003

4. Barré-Sinoussi F, Ross AL, Delfraissy J-F. Past, present and future: 30 years of HIV research. *Nat Rev Microbiol* (2013) 11:877–83. doi: 10.1038/nrmicro3132

5. De Cock KM, Jaffe HW, Curran JW. Reflections on 30 years of AIDS. *Emerg Infect Dis* (2011) 17:1044–8. doi: 10.3201/eid/1706.100184

6. Li G, De Clercq E. HIV genome-wide protein associations: a review of 30 years of research. *Microbiol Mol Biol Rev* (2016) 80:679–731. doi: 10.1128/MMBR.00065-15

7. De Cock KM, Jaffe HW, Curran JW. Reflections on 40 years of AIDS. *Emerg Infect Dis* (2021) 27:1553–60. doi: 10.3201/eid2706.210284

8. Campbell EM, Hope TJ. HIV-1 capsid: the multifaceted key player in HIV-1 infection. *Nat Rev Microbiol* (2015) 13:471–83. doi: 10.1038/nrmicro3503

9. Freed EO. HIV-1 assembly, release and maturation. *Nat Rev Microbiol* (2015) 13:484–96. doi: 10.1038/nrmicro3490

10. Faust TB, Binning JM, Gross JD, Frankel AD. Making sense of multifunctional proteins: human Immunodeficiency virus type 1 accessory and regulatory proteins and connections to transcription. *Annu Rev Virol* (2017) 4:241–60. doi: 10.1146/annurev-virology-101416-041654

11. Colomer-Lluch M, Ruiz A, Moris A, Prado JG. Restriction factors: from intrinsic viral restriction to shaping cellular immunity against HIV-1. *Front Immunol* (2018) 9:2876. doi: 10.3389/fimmu.2018.02876

12. Ostermann PN, Ritchie A, Ptok J, Schaal H. Let it go: HIV-1 *cis*-acting repressive sequences. *J Virol* (2021) 95:e0034221. doi: 10.1128/JVI.00342-21

13. Müller TG, Zila V, Müller B, Kräusslich H-G. Nuclear capsid uncoating and reverse transcription of HIV-1. *Annu Rev Virol* (2022) 9:261–84. doi: 10.1146/annurev-virology-020922-110929

14. Zhao C, Li H, Swartz TH, Chen BK. The HIV Env glycoprotein conformational states on cells and viruses. *mBio* (2022) 13:e0182521. doi: 10.1128/mbio.01825-21

15. Nomaguchi M, Doi N, Koma T, Adachi A. HIV-1 mutates to adapt in fluxing environments. *Microbes Infect* (2018) 20:610–14. doi: 10.1016/j.micinf.2017.08.003

16. Hie B, Zhong ED, Berger B, Bryson B. Learning the language of viral evolution and escape. *Science* (2021) 371:284–8. doi: 10.1126/science.abd7331

17. Wertheim JO. When viruses become more virulent. *Science* (2022) 375:493–4. doi: 10.1126/science.abn4887

18. Sauter D, Kirchhoff F. Multilayered and versatile inhibition of cellular antiviral factors by HIV and SIV accessory proteins. *Cytokine Growth Factor Rev* (2018) 40:3–12. doi: 10.1016/j.cytogfr.2018.02.005

19. Chougui G, Margottin-Goguet F. HUSH, a link between intrinsic immunity and HIV latency. *Front Microbiol* (2019) 10:224. doi: 10.3389/fmicb.2019.00224

20. Buffalo CZ, Iwamoto Y, Hurley JH, Ren X. How HIV Nef proteins hijack membrane traffic to promote infection. *J Virol* (2019) 93:e01322–19. doi: 10.1128/JVI.01322-19

21. Evans JP, Liu S-L. Multifaceted roles of TIM-family proteins in virus-host interactions. *Trends Microbiol* (2020) 28:224–35. doi: 10.1016/j.tim.2019.10.004

22. Hatziioannou T, Evans DT. Animal models for HIV/AIDS research. *Nat Rev Microbiol* (2012) 10:852–67. doi: 10.1038/nrmicro2911

23. Nishimura Y, Martin MA. Of mice, macaques, and men: broadly neutralizing antibody immunotherapy for HIV-1. *Cell Host Microbe* (2017) 22:207–16. doi: 10.1016/j.chom.2017.07.010

24. Horsburgh BA, Palmer S. For viral reservoir studies, timing matters. *Trends Microbiol* (2019) 27:809–10. doi: 10.1016/j.tim.2019.08.003

25. Ndung'u T, McCune JM, Deeks SG. Why and where an HIV cure is needed and how it might be achieved. *Nature* (2019) 576:397–405. doi: 10.1038/s41586-019-1841-8

26. Henderson LJ, Reoma LB, Kovacs JA, Nath A. Advances toward curing HIV-1 infection in tissue reservoirs. *J Virol* (2020) 94:e00375–19. doi: 10.1128/JVI.00375-19

27. Rodari A, Darcis G, Van Lint CM. The current status of latency reversing agents for HIV-1 remission. *Annu Rev Virol* (2021) 8:491–514. doi: 10.1146/annurev-virology-091919-103029

28. Pasternak AO, Berkhout B. HIV persistence: silence or resistance? *Curr Opin Virol* (2023) 59:101301. doi: 10.1016/j.coviro.2023.101301

29. Adachi A. Frontiers in Virology: an innovative platform for integrative virus research. *Front Virol* (2021) 1:665473. doi: 10.3389/fviro.2021.665473

30. Nomaguchi M. Fundamental Virology: curiosity-oriented basic virus research. *Front Virol* (2021) 1:808768. doi: 10.3389/fviro.2021.808768

frontiers in Virology

ORIGINAL RESEARCH
published: 31 December 2021
doi: 10.3389/fviro.2021.813606

In vivo Infection Dynamics and Human Adaptive Changes of SIVsm-Derived Viral Siblings SIVmac239, SIV_{B670}, and SIVhu in Humanized Mice as a Paralog of HIV-2 Genesis

James Z. Curlin[1,2†], Kimberly Schmitt[1†], Leila Remling-Mulder[1], Ryan V. Moriarty[3], John J. Baczenas[3], Kelly Goff[4], Shelby O'Connor[3], Mark Stenglein[1], Preston A. Marx[4,5] and Ramesh Akkina[1]*

[1] Department of Microbiology, Immunology and Pathology, Colorado State University, Fort Collins, CO, United States, [2] Antiviral Discovery, Evaluation and Application Research (ADEAR) Training Program, Department of Medicine, University of Colorado, Aurora, CO, United States, [3] Department of Pathology and Laboratory Medicine, School of Medicine and Public Health, University of Wisconsin, Madison, WI, United States, [4] Department of Tropical Medicine, School of Public Health and Tropical Medicine, Tulane University, New Orleans, LA, United States, [5] Tulane National Primate Research Center, Covington, LA, United States

OPEN ACCESS

Edited by:
Akio Adachi,
Kansai Medical University, Japan

Reviewed by:
Scott Kitchen,
University of California, Los Angeles, United States
Fatah Kashanchi,
George Mason University, United States
Vicente Planelles,
The University of Utah, United States

***Correspondence:**
Ramesh Akkina
akkina@colostate.edu

† These authors have contributed equally to this work

Specialty section:
This article was submitted to Fundamental Virology, a section of the journal Frontiers in Virology

Received: *12 November 2021*
Accepted: *13 December 2021*
Published: *31 December 2021*

Citation:
Curlin JZ, Schmitt K, Remling-Mulder L, Moriarty RV, Baczenas JJ, Goff K, O'Connor S, Stenglein M, Marx PA and Akkina R (2021) In vivo Infection Dynamics and Human Adaptive Changes of SIVsm-Derived Viral Siblings SIVmac239, SIV_{B670}, and SIVhu in Humanized Mice as a Paralog of HIV-2 Genesis. Front. Virol. 1:813606. doi: 10.3389/fviro.2021.813606

Simian immunodeficiency virus native to sooty mangabeys (SIVsm) is believed to have given rise to HIV-2 through cross-species transmission and evolution in the human. SIVmac239 and SIV_{B670}, pathogenic to macaques, and SIVhu, isolated from an accidental human infection, also have origins in SIVsm. With their common ancestral lineage as that of HIV-2 from the progenitor SIVsm, but with different passage history in different hosts, they provide a unique opportunity to evaluate cross-species transmission to a new host and their adaptation/evolution both in terms of potential genetic and phenotypic changes. Using humanized mice with a transplanted human system, we evaluated *in vivo* replication kinetics, $CD4^+$ T cell dynamics and genetic adaptive changes during serial passage with a goal to understand their evolution under human selective immune pressure. All the three viruses readily infected hu-mice causing chronic viremia. While SIVmac and SIV_{B670} caused $CD4^+$ T cell depletion during sequential passaging, SIVhu with a deletion in *nef* gene was found to be less pathogenic. Deep sequencing of the genomes of these viruses isolated at different times revealed numerous adaptive mutations of significance that increased in frequency during sequential passages. The ability of these viruses to infect and replicate in humanized mice provides a new small animal model to study SIVs *in vivo* in addition to more expensive macaques. Since SIVmac and related viruses have been indispensable in many areas of HIV pathogenesis, therapeutics and cure research, availability of this small animal hu-mouse model that is susceptible to both SIV and HIV viruses is likely to open novel avenues of investigation for comparative studies using the same host.

Keywords: HIV origins and evolution from SIV, SIV cross-species transmission, a dual purpose humanized mouse model for HIV and SIV research, SIVmac and SIV_{B670} pathogenesis and evolution in humanized mice, viral adaptive changes and evolution, SIV evolution into HIV-2, origin of human pathogens in NHP, origin of human pandemic viruses

INTRODUCTION

The causative agents of AIDS, both HIV-1 and HIV-2, remain entrenched in the human population and continue their onslaught in the ongoing global health crisis. While HIV-1 receives the most attention due to its wider global distribution and prominence, studies on HIV-2 and its relatives have been relatively sparse and infrequent. Ten HIV-2 strains currently exist whose origins are traced back to a series of independent cross-species transmissions of simian immunodeficiency viruses (SIVsm) native to sooty mangabeys (1, 2). Several previous studies have sought to understand the genetic adaptations that were necessary for SIVsm to transition into HIV-2 (3, 4). Interestingly, besides human infections, SIVsm crossed the species barrier infecting additional non-human primate (NHP) species generating strains such as SIVmac and SIV_{B670} as well as other SIVsm derivatives such as SIVhu (5–10).

So far, over 40 other types of non-human primate derived SIVs have been identified, some with zoonotic potential. Thus, it is important to understand the nature of adaptations that these viruses undergo when transmitted to divergent host species (10). The SIVmac239 virus is a unique immunodeficiency causing virus resulting from an accidental transmission between two different NHP species, in this case from sooty mangabeys to rhesus macaques (5). While SIVsm is relatively harmless to its native host, SIVmac is highly pathogenic to rhesus macaques (9). The ability of SIVmac239 to cause the rapid onset of AIDS-like symptoms in rhesus macaques has led to SIVmac239 and its derivatives becoming important surrogate lentiviruses commonly used for understanding HIV pathogenesis (7, 8). Since the majority of endogenous SIVs do not cause AIDS-like symptoms in their native hosts (6, 11), SIVmac239 also serves as a useful tool for understanding the genetic adaptive changes contributing to the increased virological fitness and mobility between host species. Similar to SIVmac239, SIV_{B670} is widely used in non-human primate models to study lentivirus pathology (12, 13). SIV_{B670} is a derivative of SIVsm that was originally isolated from rhesus macaques that had been inoculated with cutaneous lepromatous leprosy lesion tissue homogenates from SIVsm infected sooty mangabeys. Infected macaque lymphoid tissues were then co-cultured with a human T cell line to isolate the virus SIV_{B670} (6, 14). This virus has been commonly used in HIV research due to its aggressive pathology and immunosuppression (15, 16).

In the context of rare accidental human laboratory exposures to SIVs, a laboratory worker in 1992 became exposed to SIV_{B670}. This subject became virus positive with a productive infection and was carefully monitored for several years (17, 18). While the subject never developed AIDS-like symptoms, viral reactive antibodies were detected and an SIV was isolated from the subject's PBMC. This viral isolate was termed SIVhu denoting its isolation from a human. Genetic analysis of the viral isolate revealed a small 4 bp deletion in the *nef* gene that is absent in the parental SIV_{B670} strain resulting in a premature stop codon leading to a truncated non-functional protein (18). Due to its replication in the human and isolation from this source as well as its parental origin from SIV_{B670}, SIVhu virus may represent an evolutionary intermediate variant between SIVsm and HIV-2. In essence, SIVmac239, SIVhu, SIV_{B670} and HIV-2, all have a common origin in the prototype SIVsm virus. Study of these viruses in a common *in vivo* setting is likely to provide interesting data in terms of their relative replicative ability and viral adaptation in a new host environment.

Host tropism of viruses and their adaptation to a new host are dictated by a complex interplay between various host and viral factors. Inherent differences exist between humans and non-human primates in terms of host factors and their respective immune environments thus restricting the cross-species transmission of lentiviruses in several ways. In addition to subtle differences in the CD4 and chemokine receptors necessary for viral entry, a number of host restriction factors play a role. Among some of these are tetherin, APOBEC3G (apolipoprotein B mRNA-editing enzyme catalytic polypeptide-like 3G) and TRIM5α (tripartite motif 5α protein), which are all involved in blocking viral production at various points in the viral replication cycle (19–23). While host restriction factors in human cells help impede SIV replication, they allow HIV replication and the reverse is true in simian cells (24–26). Many of the accessory proteins in HIV such as Vif, Vpx, Vpr, Vpu, and Nef are all well-known for their ability to counteract human host restriction factors (19, 27–32). Thus, counteracting restriction factors successfully is a key aspect for cross species viral transmissions.

A suitable and affordable model is necessary to effectively evaluate the initial transmission and gradual adaptation of these viruses. Non-human primate models (NHPs) have historically been important models to study HIV pathogenesis and curative strategies. However, to determine the genetic changes in SIVs that gave rise to HIV, an alternative model that can permit repeated SIV exposures to a human immune system is needed. Humanized mice, which are mice that have been xenografted with human hematopoietic stem cells (HSC), can provide a surrogative human immune environment to delineate the important questions on both SIV and HIV infection process and viral pathogenesis (3, 4, 33–39). Commonly used humanized mice models are hu-HSC and BLT mouse models. BLT mice are constructed by the transplantation of liver/thymus fragments surgically engrafted under the kidney capsule, while hu-HSC mice are derived through the direct injection of HSC (40–44). Both mouse models are capable of producing human T cells, B cells, macrophages, and dendritic cells *de novo*. Both the models permit HIV infection due to the presence of full immune cell repertoire and have been used widely to investigate areas such as HIV pathogenesis, transmission, and latency (33, 35, 44–47). We previously used the hu-mouse model as a human surrogate system to dissect various aspects of the initial cross-species transmission of SIV chimpanzee virus (SIVcpz) to the human giving rise to HIV-1 and the SIVsm progenitor virus in giving rise to HIV-2 (3, 4, 39, 48–50). These studies provided important insights into the important genetic changes these progenitor viruses had to undergo to quickly adapt to the human host and also shed light on the gradual genetic changes that arose as the viruses were serially passaged multiple times using this system.

The existence of three related viruses namely SIVmac239, SIVhu, SIV_{B670} that arose in different circumstances, but with a common origin in SIVsm which is a progenitor to HIV-2, provided a unique opportunity to evaluate their ability to cause a potential human infection in a human surrogate hu-mouse model and to ask important questions in an experimental setting. Here we determined if these viruses can infect humanized mice to simulate cross species transmission and serially passaged them *in vivo* to identify viral adaptive phenotypic and genetic changes with the goal to identify potential common adaptive changes between these three viruses. These studies also opened a new avenue to develop a cost-effective small animal model that can permit *in vivo* studies on SIVmac239 which is widely studied in more expensive NHP models. Our results show that all three viruses can productively infect humanized mice, cause chronic viremia and affect $CD4^+$ T cell dynamics. Furthermore, evaluation of these serially passaged viruses using this system mimics the necessary viral adaptation needed during the initial phases of viral encroachment into the human population to reveal important mutations among these three viruses.

RESULTS

SIVmac239, SIV_{B670}, and SIVhu Are All Capable of Productive and Chronic Infection in Humanized Mice

To determine if SIVmac239, SIV_{B670}, and SIVhu can establish productive infection, cohorts of five hu-HSC mice were inoculated with one of the three viruses and serially passaged for a total of three generations. Within 1 week of inoculation, SIVmac239 RNA was detected in the plasma using qRT-PCR in all five infected hu-HSC mice demonstrating that SIVmac239 can infect human cells *in vivo* (**Figure 1A**). During the first generation, the plasma viral loads continued to climb gradually until ∼64 days post-inoculation peaking at over 3.4×10^4 RNA copies/mL. This first generation proved successful chronic infection of human immune cells in hu-HSC mice by SIVmac239. After the virus was serially passaged into a second generation of hu-mice, the viral loads displayed a remarkably similar pattern to the first generation and were detected within 1 week. Interestingly, several individual mice in the third generation displayed drastically higher peak plasma viral loads than the others, reaching 1×10^6 RNA copies/mL within 21 days post-inoculation, suggesting that the virus had fundamentally adapted to human immune cells displaying increased viral fitness in these hu-mice (**Figure 1A**).

SIV_{B670} displayed a pattern of infection similar to that of SIVmac239. Following the initial inoculation, the virus was detected within the first week (1×10^4 RNA copies/mL) (**Figure 1B**). The viral loads gradually increased peaking (8×10^4 RNA copies/mL) around 35 days post-inoculation, at which point the viral loads showed a steady but persistent decline until the end of the first generation. In contrast, the second generation was not detected above the limit of detection until ∼21 days post-inoculation and the viral loads peaked (3×10^4 RNA copies/mL) lower than the first generation at around 49 days post-inoculation. Interestingly, the plasma viral loads of the third generation were initially over a log lower than those observed in the first generation. However, the third generation showed drastically less fluctuation than the second generation peaking (3.64×10^4 RNA copies/mL) by 63 days post-inoculation.

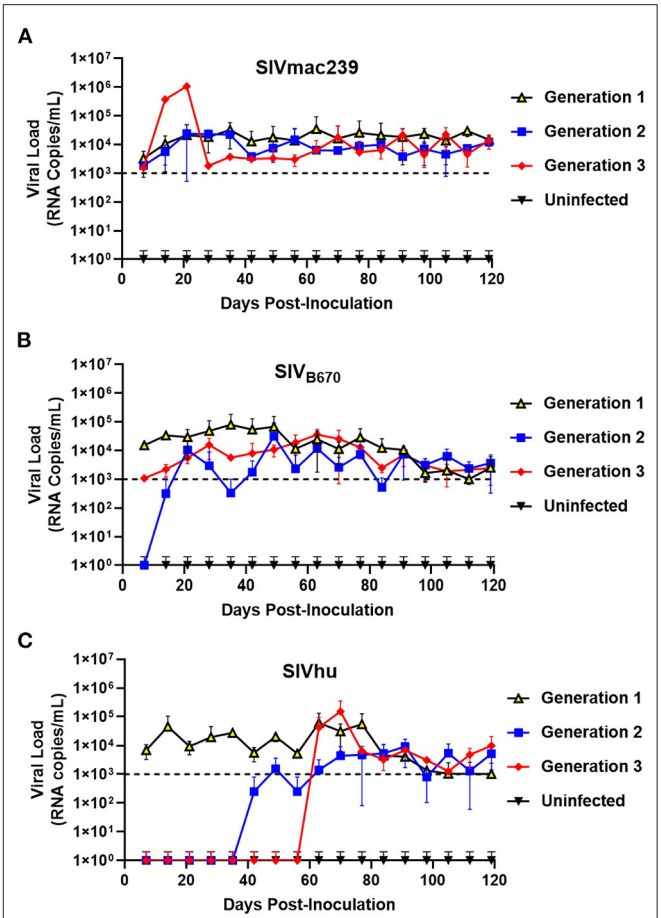

FIGURE 1 | SIVmac239, SIV_{B670}, and SIVhu can successfully initiate productive infection of hu-mice and are capable of serial transmission. **(A)** SIVmac239, **(B)** SIV_{B670}, and **(C)** SIVhu plasma viral loads during three generations of serial passage. Plasma viral loads were assessed using qRT-PCR on a weekly basis for the duration of each passage. The limit of detection was 1×10^3 RNA copies/mL.

Within the first generation of infection, SIVhu was initially detectable in the plasma by the first week and remained within a log of that before peaking (6×10^4 RNA copies/mL) around 63 days post-inoculation (**Figure 1C**). Following this viral peak, the viral loads rapidly dropped to around the limit of detection until the end of the generation. This demonstrated that SIVhu could readily infect human immune cells leading to productive viremia. After serial passaging, the virus struggled to replicate, and did not become detectable in the second generation until around 49 days post-inoculation. Similarly, the third generation was a continuation of the trend seen in the second generation, with the virus remaining undetected until around 63 days post-inoculation before shortly peaking (1.5×10^5 RNA copies/mL).

No positive viral loads were detected in any of the uninfected control mice from these studies (**Figure 1**).

SIVmac239 and SIV_{B670} Infection Results in $CD4^+$ T Cell Decline, but SIVhu Infection Does Not

One of the hallmarks of HIV infection in humans as well as hu-mice is the depletion of $CD4^+$ T cell lymphocytes during the course of infection (33, 41, 44, 51, 52). In the first generation, SIVmac239 displayed a slight decline in $CD4^+$ T cell levels within the first 100 days post-inoculation (**Figure 2A**). This resulted in no real net decrease of $CD4^+$ T cell levels. In contrast, the second generation showed an immediate decline in $CD4^+$ T cell levels through 70 days post-inoculation, while the third generation displayed a rapid decline in $CD4^+$ T cells beginning around 28 days post-inoculation as a result of the rapid increase in plasma viral loads. By the end of the third generation, there was a statistically significant difference in the $CD4^+$ T cell decline when compared to the uninfected control hu-mice similar to HIV-1 infection (two-tailed, Student's *t*-test, $p < 0.01$) demonstrating that serially passaging SIVmac239 results in a more rapid $CD4^+$ T cell depletion in the humanized mouse model (33, 41, 44, 51, 52).

The first generation of SIV_{B670} displayed a drastic decline in $CD4^+$ T cells compared to the controls within 14 days post-inoculation (**Figure 2B**). In contrast, the $CD4^+$ T cell levels in the second generation remained initially stable through 42 days post-inoculation, followed by a decrease in $CD4^+$ T cell levels. By the third generation, SIV_{B670} displayed a very consistent and gradual decline in $CD4^+$ T cell levels until 56 days post-inoculation, followed by significantly rapid $CD4^+$ T cell decline relative to the uninfected controls ($p < 0.05$). This data suggests that SIV_{B670} showed enhanced $CD4^+$ T cell depletion in the humanized mouse model indicative of increased viral fitness to human immune cells by the third generation.

Flow cytometric analysis showed that there was little to no significant $CD4^+$ T cell decline across any of the three generations of serial passaging among mice infected with SIVhu. In fact, the $CD4^+$ T cell levels remained relatively consistent across each generation (**Figure 2C**). Altogether, this data demonstrates that the truncated Nef protein in SIVhu may delay viral replication kinetics in human immune cells.

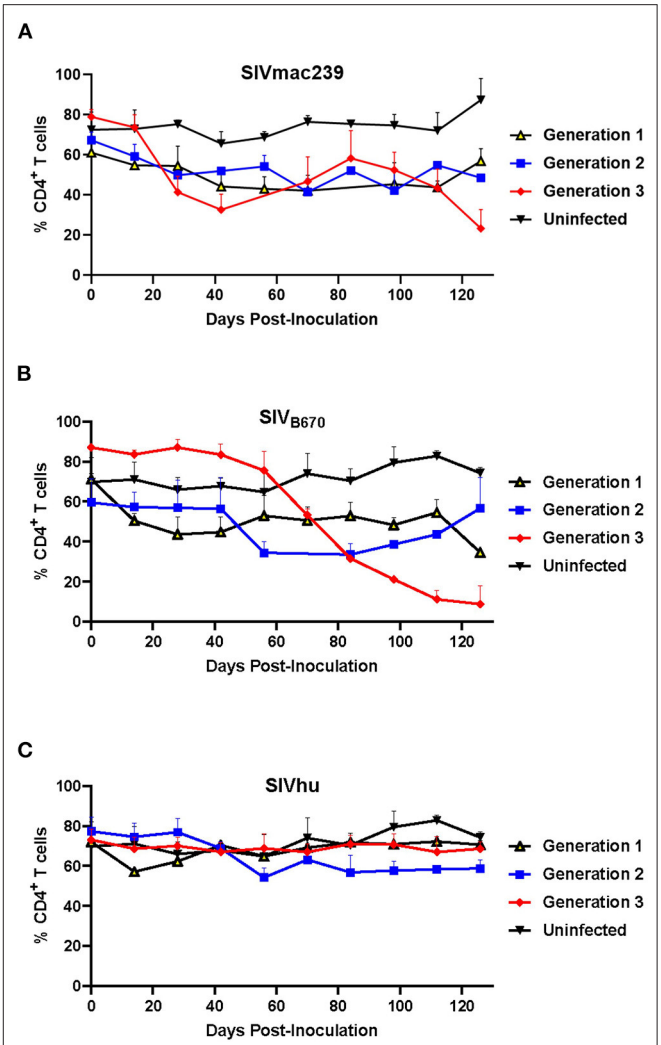

FIGURE 2 | $CD4^+$ T cells levels during three generations of serial passage of SIVmac239, SIV_{B670}, and SIVhu in humanized mice. **(A)** SIVmac239, **(B)** SIV_{B670}, and **(C)** SIVhu $CD4^+$ T cell levels over three generations. $CD4^+$ T cell levels were monitored bimonthly using flow cytometry. The percent of $CD4^+$ T cells is presented relative to that of $CD45^+/CD3^+$ cell populations. Statistically significant $CD4^+$ T cell depletion was seen in the third generation of SIVmac239 ($p < 0.01$) and SIV_{B670} ($p < 0.05$) infected hu-HSC mice relative to the uninfected control (two-tailed Student's *t*-test).

Evolutionary Genetic Adaptations Arise During Sequential Passaging of SIVmac239, SIV_{B670}, and SIVhu

In addition to the *in vivo* pathogenicity of these viruses, adaptation was assessed by identifying non-synonymous mutations that rose in frequency over time that could change the phenotype of the virus. Therefore, we used Illumina-based deep sequencing on plasma viral RNA from two mice (replicates) per generation collected at early, mid, and late timepoints across three serial passages. Paired end reads of the viruses were mapped to the consensus sequence of the starting viral stock. While there were numerous mutations that arose briefly and disappeared at later timepoints, the following criteria were used to identify truly significant variants: (1) Mutations must be non-synonymous and present in the coding sequence (CDS), (2) The mutations must be present in at least four of the data sets which means each variant is present beyond a single replicate in a single generation, (3) Mutations must increase in viral frequency over the subsequent generations, and (4) The frequency of the mutation in the viral population must average at least 50% at the last sequenced timepoint. Eight mutations were found in SIVmac239, 32 mutations were found in SIV_{B670}, and 11 mutations were found in SIVhu that matched

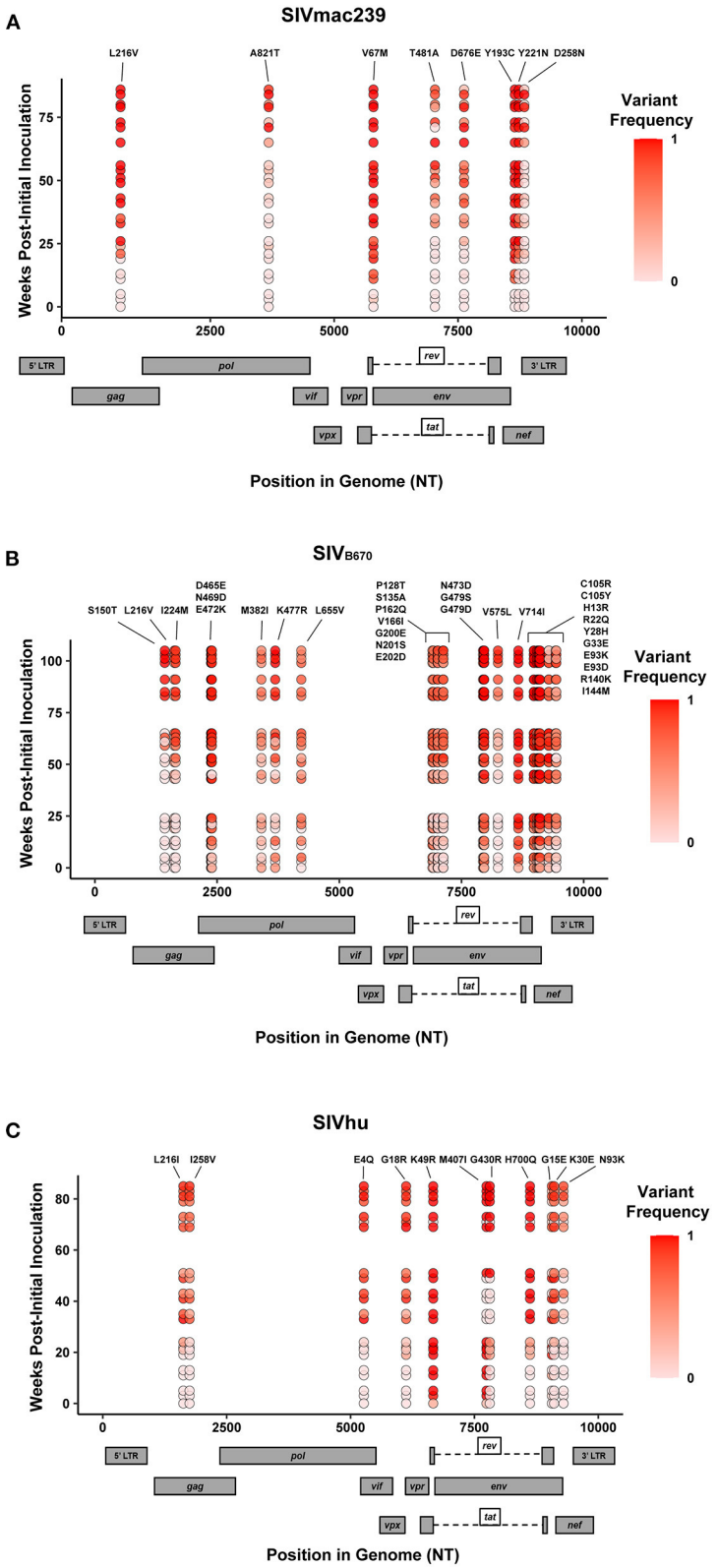

FIGURE 3 | Single nucleotide polymorphisms showing an increase in population frequency over three serial passages. Viral RNAs isolated from two infected hu-mice per viral strain per generation at early, middle, and late timepoints were sequenced. The non-synonymous mutations identified were present in the CDS, had an

(Continued)

FIGURE 3 | average endpoint frequency of at least 50%, and were found in at least four timepoints. **(A)** SIVmac239, **(B)** SIV_{B670}, and **(C)** SIVhu variants are plotted based on their position in the genome along the x-axis. The y-axis location denotes the time of collection weeks post-initial infection. Variant population frequency is denoted by the shading color scale for each point. Week 0 corresponds to the frequency in the viral stock pre-inoculation, with the second and third passages being plotted beginning at week 30 and 60, respectively. For each time point, replicates are offset vertically from each other. Both the residue changes and number for each position are listed above their respective locations.

TABLE 1 | Amino acid substitutions accumulated during three passages of SIVmac239 in hu-mice.

Protein	Position	Stock residue[a]	Variant residue[b]	Stock frequency[c]	P3 Endpoint frequency[d]	P3 Endpoint frequency[e]
Gag	216	L	V	0.00[f]	1.00	1.00
Pol	821	A	T	0.00[f]	1.00	0.94
Env	67	V	M	0.00[f]	1.00	1.00
Env	481	T	A	0.00[f]	0.85	0.84
Env	676	D	E	0.00[f]	0.95	0.23
Nef	193	Y	C	0.00[f]	1.00	1.00
Nef	221	Y	N	0.00[f]	1.00	1.00
Nef	258	D	N	0.00[f]	1.00	0.15

[a] *Consensus amino acid residue from sequenced stock virus.*
[b] *Variant amino acid residue from passaged virus.*
[c] *Frequency of variant residue in the stock virus population.*
[d] *Replicate 1 frequency of variant residue at the end of the third passage.*
[e] *Replicate 2 frequency of variant residue at the end of the third passage.*
[f] *The 0.00 indicates that the variant frequency was below the limit of detection of the variant identification pipeline.*

these criteria by the end of the third generation (**Figure 3**, **Tables 1**–**3**).

Non-synonymous mutations were identified in SIVmac239 after three generations of passage across a number of genes, with the largest concentration in *env* and *nef* (**Figure 3A**, **Table 1**). Of these mutations, Env D676E and Nef D258N had individual replicate samples in the third generation that had persistently low frequencies, while all the other identified mutations were near 100% population frequency in both replicates. SIV_{B670} had by far the largest number of qualifying mutations, with a large number of mutations found in *gag, pol, env,* and *nef* (**Figure 3B**, **Table 2**). Interestingly, though a number of these mutations did increase to a frequency of nearly 100%, quite a few mutations were still at lower frequencies, albeit they had still increased in frequency relative to the stock virus. SIVhu had fewer qualifying mutations than SIV_{B670}, with a relatively even distribution that was slightly weighted toward the 5′ end of the genome with *env* and *nef* having the most mutations (**Figure 3C**, **Table 3**). Interestingly, all of the mutations found in *env* were found to be at 100% frequency in the viral population of both replicates of the third generation. One mutation in particular at residue Gag 216, was present in all three viral strains, though the residue change was L → I in SIVhu and L → V in SIV_{B670} and SIVmac239, which may suggest some shared function in adaptation.

DISCUSSION

Here we described a unique human surrogate experimental setting that permitted the evaluation of *in vivo* infection features of three different SIVsm-derived viruses, namely SIVmac239, SIV_{B670}, and SIVhu in humanized mice. This system enables the simulation of cross-species viral transmission into the human and viral evolution under this selective pressure. Serial *in vivo* passaging of these viruses in hu-mice allowed for the identification of the genetic changes that potentially occur during the early stages of viral adaptation to humans. In this study, hu-mice mice were exposed to SIVmac239, SIVhu, and SIV_{B670} by i/p injection to first ascertain their potential for infection of human immune cells *in vivo*. Viruses isolated from the subsequent serial passages at different stages of infection were subjected to sequence analysis to identify and ascertain if any common changes could be found among these viruses given their shared ancestry. These studies also recapitulated some key aspects of cross-species transmission that we described previously in humanized mice that centered on SIVcpz and SIVsm to shed light on the origins of HIV-1 and HIV-2 from these respective progenitor viruses (3, 4, 48, 50). Of the key observations from this present study, one was that both SIVmac239 and SIV_{B670} were readily able to infect hu-mice (**Figures 1A,B**). Viremia was detected within a week following the initial inoculation and persisted for both the viruses beyond 120 days. Successful sequential serial passaging of these viruses in hu-mice imply that these viruses have the capacity for maintaining human-to-human transmission and can evolve further to increased viral fitness.

$CD4^+$ helper T cell loss was evaluated for these viruses across the three *in vivo* viral passages because this feature is a central hallmark of immunodeficiency and viral virulence (**Figure 2**). While the $CD4^+$ T cell levels remained steady during chronic infection in passages 1 and 2 of SIVmac239 and SIV_{B670}, a progressive and more rapid loss of these cells was observed during the 3rd passage indicating increased viral adaptation to these cells (**Figures 2A,B**). SIVhu also displayed productive infection upon the initial i/p inoculation followed by chronic

TABLE 2 | Amino acid substitutions accumulated during three passages of SIV_{B670} in hu-mice.

Protein	Position	Stock residue[a]	Variant residue[b]	Stock frequency[c]	P3 Endpoint frequency[d]	P3 Endpoint frequency[e]
Gag	150	S	T	0.00[f]	1.00	1.00
Gag	216	L	V	0.00[f]	0.70	0.96
Gag	224	I	M	0.00[f]	0.88	0.91
Gag	465	D	E	0.11	0.99	0.99
Gag	469	N	D	0.34	1.00	1.00
Gag	472	E	K	0.30	0.95	0.91
Pol	382	M	I	0.43	0.80	0.54
Pol	477	K	R	0.48	1.00	1.00
Pol	655	L	V	0.00[f]	0.55	0.59
Env	128	P	T	0.37	0.74	0.64
Env	135	S	A	0.09	0.72	0.65
Env	162	P	Q	0.44	1.00	1.00
Env	166	V	I	0.00[f]	0.71	0.82
Env	200	G	E	0.49	0.69	0.91
Env	201	N	S	0.49	0.78	0.94
Env	202	E	D	0.00[f]	0.66	0.91
Env	473	N	D	0.29	0.50	1.00
Env	479	G	S	0.37	0.50	1.00
Env	479	G	D	0.37	0.50	1.00
Env	481	R	Q	0.30	1.00	1.00
Env	575	V	L	0.00[f]	0.89	0.95
Env	714	V	I	0.34	1.00	1.00
Rev	105	C	R	0.50	1.00	0.99
Rev	105	C	Y	0.49	1.00	1.00
Nef	13	H	R	0.42	1.00	1.00
Nef	22	R	Q	0.46	1.00	1.00
Nef	28	Y	H	0.39	1.00	1.00
Nef	33	G	E	0.43	1.00	1.00
Nef	93	E	K	0.24	0.93	0.15
Nef	93	E	D	0.20	0.91	0.14
Nef	140	R	K	0.00	0.93	0.09
Nef	144	I	M	0.00[f]	0.87	0.43

[a] *Consensus amino acid residue from sequenced stock virus.*
[b] *Variant amino acid residue from passaged virus.*
[c] *Frequency of variant residue in the stock virus population.*
[d] *Replicate 1 frequency of variant residue at the end of the third passage.*
[e] *Replicate 2 frequency of variant residue at the end of the third passage.*
[f] *The 0.00 indicates that the variant frequency was below the limit of detection of the variant identification pipeline.*

viremia in during the first passage (**Figure 1C**). However, the SIVhu viral loads were lower compared to SIVmac239 and SIV_{B670} and it took longer to establish detectable viremia in the 2nd and 3rd passages. Also, in contrast to SIVmac239 and SIV_{B670}, no discernable $CD4^+$ T cell loss could be detected compared to uninfected control mice across all the 3 passages of SIVhu (**Figure 2C**). The lower replicative capacity of the SIVhu virus is likely due to the defective nature of this virus isolate harboring a deletion in the *nef* gene (see below).

Sequential serial passaging of each of these viruses for 3 generations in different cohorts of hu-mice allowed the original virus to adapt to the human immune cell environment *in vivo* and accumulate genetic mutations potentially conferring fitness (**Figure 3**, **Tables 1**–**3**). Overall, relative to SIVmac239 and SIVhu, SIV_{B670} accumulated the largest number of non-synonymous mutations with corresponding amino acid changes throughout the viral genome (**Figure 3B**, **Table 2**). The majority of these changes were found in the 3′ end of the viral genome similar to that found in previous studies on SIVsm and SIVcpz in hu-mouse studies (3, 37, 48–50). Interestingly, one of the most striking features amongst the three passaged viruses was the mutation at residue 216 in Gag that appeared within all three different strains of viruses in a highly conserved part of the genome (26, 53). This residue is part of the *gag* gene that encodes the capsid protein and is located within the cyclophilin binding loop. Furthermore, it is possible that this residue is involved in

TABLE 3 | Amino acid substitutions accumulated during three passages of SIVhu in hu-mice.

Protein	Position	Stock residue[a]	Variant residue[b]	Stock frequency[c]	P3 Endpoint frequency[d]	P3 Endpoint frequency[e]
Gag	216	L	I	0.00[f]	0.77	0.96
Gag	258	I	V	0.00[f]	0.79	0.95
Vif	4	E	Q	0.00[f]	0.85	0.99
Vpr	18	G	R	0.00[f]	0.82	0.97
Env	49	K	R	0.32	1.00	1.00
Env	407	M	I	0.25	1.00	1.00
Env	430	G	R	0.00[f]	1.00	1.00
Env	700	H	Q	0.00[f]	1.00	1.00
Nef	15	G	E	0.00[f]	0.31	0.90
Nef	30	K	E	0.00[f]	0.68	0.94
Nef	93	N	K	0.00[f]	0.51	0.85

[a] *Consensus amino acid residue from sequenced stock virus.*
[b] *Variant amino acid residue from passaged virus.*
[c] *Frequency of variant residue in the stock virus population.*
[d] *Replicate 1 frequency of variant residue at the end of the third passage.*
[e] *Replicate 2 frequency of variant residue at the end of the third passage.*
[f] *The 0.00 indicates that the variant frequency was below the limit of detection of the variant identification pipeline.*

TRIM5α antagonism and escape, which is an important barrier to overcome for successful cross-species transmission (54, 55). The dramatic increases in the frequency of viral populations bearing this mutation further supports its potential role in conferring improved fitness (56–58).

While functional studies are needed to fully understand the biological significance of these mutations, their occurrence in known motifs involved in binding interactions provide some potential clues. For example, the amino acid changes at Gag 465 and 469 in SIV_{B670} are located within a dileucine-motif shown to be responsible for particle association and uptake of Vpx and Vpr in SIVmac (59, 60). This interaction between the DXAXXLL motif and Vpr allows Vpr to be diverted away from the proteasome-degradative pathway, while deletion of this particular motif was shown to result in a total lack of incorporation of Vpx in SIVmac (60). The fact that this motif altered by the D465E mutation had no marked effect on pathogenicity for SIV_{B670} is notable. It could be due to the fact that the LXXLF motif at the C terminus of the $p6^{gag}$ region remained intact, and that they share some overlap in functionality (60). Just as compelling is that the Gag N469D mutation brings SIV_{B670} closer to amino acid sequences found in both SIVsmE041 and SIVmac239, which were already aspartic acid residues at this particular location (53). Very few notable mutations were identified in *vif, vpr,* and *vpx* in all three viruses studied. However, the SIVhu Vpr G18R residue change is immediately adjacent to a previously described DCAF-1 binding motif canonically found in both Vpr and Vpx which has been implicated in G2 arrest and SAMHD1 degradation, respectively (29).

Both *env* and *nef* genes displayed a large number of mutations in all three viruses that increased in frequency over time and may ultimately have functional implications regarding virus-host restriction factor interactions. The Env V67M mutation identified in SIVmac239 increased from 0% frequency in the starting stock virus to 100% by the end of the third passage. This mutation was previously shown to increase viral infectivity (61). The mechanism for this increased infectivity was not tied to neutralizing antibody escape, but was implicated in conferring macrophage tropism (62). Amino acid changes P128T and S135A of SIV_{B670} in the Env are located within the V1 hypervariable loop region implicated in neutralizing antibody susceptibility (63, 64). Since proline residues contributing to high degree of conformational rigidity are less frequent in protein binding sites, its substitution for a threonine could suggest a shift in functionality for this region of the protein (65). Other mutations such as Env G430R in SIVhu occurred in the V4 loop and could potentially affect neutralization. Additional mutations that were identified, but did not meet the previously described criteria, such as Env I421K, R425G, and Q428R all occurred in the V4 loop of SIV_{B670} and could be involved in neutralizing antibody escape due to undergoing variation early in infection (66–68). The R425G substitution, at approximately the equivalent P421 residue in SIVmac239, has been directly implicated in neutralizing antibody escape and increased infectivity when mutated into P421Q in SIVmac239 (61). Env N201S, and R481Q in SIV_{B670} and T481A in SIVmac239 occur within N-linked glycosylation motifs of the V2 and V5 loops. The effect of N-linked glycosylation motifs in the envelope proteins of HIV and SIV on antibody neutralization have been well-characterized. These motifs allow a glycan shield to form, which protects exposed epitopes from being bound by neutralizing antibodies (69, 70). The Rev-response element (RRE) is a critical binding motif necessary for the shuttling of transcripts from the nucleus to the cytoplasm. It is possible that Env V575L in SIV_{B670}, which falls within the RRE could be advantageously affecting this interaction, given that this mutation increased in frequency to make up nearly 90% of the viral population by the third generation.

While smaller in size than *env*, the *nef* gene accumulated a higher number of non-synonymous mutations. However, given that APOBEC3 deaminase activity begins on the 5′ end of the viral genome, it is possible that a restriction factor like APOBEC3 could play a role in the abundance of non-synonymous mutations occurring in *nef* though this requires further analysis (71). Similarly, to mutations seen in other genes, many of the substitutions in *nef* occur near previously characterized binding and interaction sites. For example, the Nef residue 93 changes that occur in both SIVhu and SIV_{B670} occur within a known PACS-1 binding site (72). The Nef Y193C substitution identified in SIVmac239 has a low evolutionary probability (**Supplementary Figure 1**) (73). This residue is found within a ExxxL (L/M) (di-leucine) motif in the α4 region of Nef, which is implicated as an AP interaction site involved in the downregulation of CD3 and CD4 (74). Additionally, this exact residue has also been implicated in tetherin antagonism (75). At a similar location in the stock viral sequences of SIVsmE041 and SIV_{B670} this residue is a cysteine. In HIV-2 and SIVmac, it has been shown that the di-leucine motif is flexible enough to form an alpha helix by binding to a hydrophobic crevice between α2 and α3 with Glu 190 and Leu 194 (74). Change in amino acid residue 193 to a cysteine could have a drastic impact on the ability of the di-leucine motif to bind to the hydrophobic crevice. Furthermore, Nef I144M from SIV_{B670} is located within the α3 region of Nef and is adjacent to a number of residues that have been shown to interact with the amino acid residues of the di-leucine sorting motif (76). However, this substitution is more biochemically favored than the others and may have less of an impact on binding for this region. The Nef Y221N substitution in SIVmac is located at the end of α5 helix and is a highly disfavored residue change based on the PAM1 matrix score (**Supplementary Figure 1A**). It is also adjacent to residue Y223 and Y226, which are involved in MHC-I downregulation and be functionally disrupted through substitutions (77). In SIV_{B670} residue Nef Y28H occurs at a conserved N-proximal tyrosine residue that has been found to be part of an adapter protein (AP) binding site that may be involved in mediating endocytosis (72, 78). Nef K30E in SIVhu also occurs at this same AP binding site.

Despite being the only strain of SIV isolated directly from a human subject, SIVhu displayed the lowest overall potential to gain increased fitness to the human among the three viruses tested during the serial passages. While the first generation showed viral loads comparable to the other two viruses, a clear decline in PVL and prolonged delay in establishing detectable viremia during subsequent passages suggests that SIVhu is slow to adapt to human immune cells (**Figure 1C**). Furthermore, the lack of significant $CD4^+$ T cell decline indicates that SIVhu is not yet capable of producing AIDS-like symptoms in humanized mice after three passages (**Figure 2C**). However, the increased peaks and general upward trend of the third generation of plasma viral loads suggest that SIVhu is still adapting, albeit slowly. The noted difficulty that SIVhu displays could be at least partially attributed to the documented frameshift deletion in *nef* that encodes a truncated protein (18). Nef has been shown to be involved in downregulating the CD4 and MHC class I molecules and helps to mitigate cell-mediated cytotoxicity (79–82). Additionally, Nef is involved in counteracting the action of host restriction factors such as tetherin and SERINC3/5 and is therefore critical for the virus to properly function (27, 30, 83). No restoring mutations meeting our selection criteria were present near the frameshift or premature truncation, which indicates that after three generations of serial passaging, the *nef* gene had not reverted, which is supported by the consistently low plasma viral loads.

In summary, the above data showed for the first time that SIVmac239 and SIV_{B670} both with origins in NHP macaques can infect hu-mice and that cross-species transmission studies simulating human infection are feasible in this system for future investigations of zoonosis centered on lentiviruses. We also established that SIVmac239 and SIVsm related viruses can cause chronic infection leading to $CD4^+$ T cell loss in hu-mice, thus mimicking key aspects of SIV pathogenesis. This has practical implications as this small animal model will permit novel studies *in vivo* using these primate lentiviruses that continue to play an important role in HIV pathogenesis and therapeutic studies. With regards to evolution, adaptive changes seen in all three viruses in the hu-mouse point to both unique and consensus changes in the viral genomes. Whether these evolving viruses resemble HIV-2 after prolonged and additional passages *in vivo* remains to be investigated and is something that we hope to explore in the future.

MATERIALS AND METHODS

Cell Culture

The 293T (ATCC CRL-3216) and the TZM-bl (ARP-8129) reporter cell lines were maintained with DMEM media that contained 1% L-glutamine, 10% heat inactivated fetal bovine serum (HI FBS), and 1% antibiotic-antimycotic mix (Thermo Fisher Scientific, Waltham, MA, United States). CEMx174 (ARP-272) cells were maintained with RPMI media that contained 10% HI FBS and 2× antibiotic-antimycotic mix (Thermo Fisher Scientific, Waltham, MA, United States). Whole blood filter packs were obtained from the Garth Englund Blood Center of Fort Collins, CO, United States. Mononuclear cells were isolated by Ficoll-Paque density centrifugation. PBMC were maintained in RPMI media with 1× antibiotic/antimycotic mix (Thermo Fisher Scientific, Waltham, MA, United States), 10% heat-inactivated fetal bovine serum, and 20 ng/mL IL-2 (R&D Systems, Inc., Minneapolis, MN, United States). For viral propagation, PBMC were CD8-depleted by positive selection and stimulated with 100 ng/mL of anti-CD3 and anti-CD28 soluble antibody (Miltenyi Biotec Inc., Auburn, CA, United States) for 48 h.

Generation of Hu-HSC and BLT Mice

All mice used in these studies were cared for in the Colorado State University Painter Animal Center. Fetal liver-derived human $CD34^+$ cells obtained from Advanced Bioscience Resources (ABR, Alameda CA), were isolated, column purified (Miltenyi Biotec, San Diego, CA), cultured and assessed for purity using flow cytometry (3, 4, 39, 48, 84, 85). To create humanized hematopoietic stem cell (hu-HSC) mice, neonatal (1–4 day old) Balb/c $Rag1^{-/-}\gamma c^{-/-}$ or Balb/c $Rag2^{-/-}\gamma c^{-/-}$ mouse

pups were sublethally irradiated (350 rads) prior to intrahepatic injection of 0.5–1 $\times$ 10^6 $CD34^+$ cells (3, 34, 86). For humanized bone marrow, liver, thymus (BLT) mice, adult Balb/c $Rag1^{-/-}\gamma c^{-/-}$ or Balb/c $Rag2^{-/-}\gamma c^{-/-}$ mice were surgically engrafted with a combination of human fetal liver and thymic tissue under the kidney capsule. This was followed by a tail-vein injection of autologous $CD34^+$ human hematopoietic stem cells from the same source as the liver and thymic tissue (40, 41, 44). Ten to twelve weeks after engraftment, peripheral blood was collected *via* tail vein puncture and used to assess human immune cell engraftment. Red blood cells were lysed with the Whole Blood Erythrocyte Lysing Kit (R & D Systems, Minneapolis, MN) according to the manufacturer's instructions. The fractioned white blood cells were stained for flow cytometry using fluorophore conjugated hCD45-FITC, hCD3-PE, and hCD4-PE/Cy5 (BD Pharmingen, San Jose, CA).

SIVmac239, SIVhu, and SIV_{B670} Viral Stock Preparation and *in vivo* Infection

The SIVmac239 molecular clone plasmid was transfected into 293T cells, and the viral supernatant was concentrated using ultracentrifugation as described previously (39, 50). A small aliquot from ultracentrifugation was set aside for a functional titer in TZM-bl reporter cells as previously described (50, 87, 88). SIVhu and SIV_{B670} viral supernatants were obtained from the NIH AIDS Reagent Program and were cultured according to their recommended guidelines (6, 18, 89). Cohorts of hu-HSC and/or BLT mice with high human hematopoietic engraftment levels were inoculated with ~200 μL of viral supernatant *via* intraperitoneal (i/p) injection with one of the respective progenitor viruses (SIVmac239: 1 $\times$ $10^{5.5}$ $TCID_{50}$/mL, SIVhu: 2 $\times$ 10^8 $TCID_{50}$/mL, SIV_{B670}: 5.78 $\times$ 10^7 $TCID_{50}$/mL).

Virus Propagation and Serial Passaging of SIVmac239, SIVhu, and SIV_{B670}

At 24 weeks post-infection, the viremic mice that showed the highest plasma viral loads were euthanized to propagate the virus from the first passage to the next. Whole blood was collected *via* cardiac puncture for PBMC and the spleen, lymph nodes and bone marrow were collected as previously described (50). Leukocyte fractions of the cells were collected by Ficoll-Paque density centrifugation and seeded at a density of 2–3 $\times$ 10^6 cells/mL. These cells were then activated for roughly 48 h using 100 ng/mL of anti-hCD3 and anti-hCD28 soluble antibody (Miltenyi Biotec Inc., Auburn, CA). To enhance viral infection of the next cohort of hu-mice, these cells were co-cultured for 48 h with freshly isolated splenocytes obtained from the new hu-mouse cohort used for serial passage. These cultured cells together with culture supernatants containing virus were then intraperitoneally inoculated into the next batch of hu-mice.

Plasma Viral Load Determination by qRT-PCR

During each passage, peripheral blood was collected on a weekly basis to assess plasma viral loads (PVL). Viral RNA from the plasma was extracted with the E.Z.N.A. Viral RNA kit as outlined by the manufacturer's recommendations (OMEGA bio-tek, Norcross, GA). This RNA was then used to determine PVL using qRT-PCR using the iScript One-Step RT-PCR kit with SYBR green (Bio Rad, Hercules, CA). Primers were designed for SIVmac239 based on the *ltr* sequence (GenBank accession: M33262.1), while SIVhu and SIV_{B670} used primers designed for a conserved region of the *ltr* sequence in SIVsmE041 (GenBank accession: HM059825.1). The primers used for PCR were as follows: 1. SIVmac239: forward 5′-GCAGGTAAGTGCAACACAAA-3′ and reverse 5′-CCTGACAAGACGGAGTTTCT-3′, Tm = 54°C and 2. SIV_{B670} and SIVhu: forward 5′-CCACAAAGGGGATGTTATGGGG-3′ and reverse 5′-AACCTCCCAGGGCTCAATCT-3′, Tm = 60°C. These primers were used with the following cycling reactions for qRT-PCR quantification: 50°C for 10 min, 95°C for 5 min, followed by 40 cycles of 95°C for 15 s and 54 or 60°C for 30 s using a Bio Rad C1000 Thermo Cycler and CFX96 Real-Time System (Bio Rad, Hercules, CA). The standard curve was determined using a series of 10-fold dilutions of viral SIVmac239, and SIVsmE041 *ltr* at a known concentration. The limit of detection was 1,000 copies/mL.

$CD4^+$ T Cell Level Determination

Peripheral blood was collected bi-monthly to assess human $CD4^+$ T cell engraftment levels using flow cytometry. Briefly, 5 μL of FcγR-block (Jackson ImmunoResearch Laboratories, Inc. West Grove, PA) was added to the blood for 5 min. Each blood sample was then stained with fluorophore conjugated hCD45-FITC, hCD3-PE and hCD4-PE/Cy5 (BD Pharmingen, San Jose, CA) for roughly 30 min. Erythrocytes were lysed with the Whole Blood Erythrocyte Lysing kit based on the manufacturer's guidelines (R&D Systems, Minneapolis, MN). Antibody-stained cells were then fixed in 1% paraformaldehyde/PBS and passed through a 0.45 μm filter. Samples were run on the BD Accuri C6 Flow Cytometer (BD Biosciences, San Jose, CA). $CD4^+$ T cell levels were assessed as a percentage of the $CD3^+/CD45^+$ cell population. Flow cytometry data was analyzed using the FlowJo v10.0.7 software package (FlowJo LLC, Ashland, OR). A two-tailed Student's *t*-test was used to determine $CD4^+$ T cell decline between the uninfected and infected mouse groups as indicated in the figure legend.

Amplicon and Illumina-Based Deep Sequencing Preparation

To identify potential adaptive mutations, viral RNA from two mice per passage at multiple timepoints from across the duration of the passage, i.e., 3, 11, 19, and 23 weeks post-inoculation, etc. as well as the starting stock viruses were used for sequencing. Briefly, cDNA was synthesized from the viral RNA with a SuperScript IV kit according to the manufacturer's guidelines (Invitrogen, Carlsbad, CA). Two multiplexed inter-overlapping primer pools that span the coding region of the viral genomes based on the SIVmac239 reference sequence (GenBank accession: M33262.1) and an independently sequenced SIVhu reference sequence for SIVhu and SIV_{B670} were designed using Primal Scheme

(https://primal.zibraproject.org) (90). These primer pools were then amplified using viral cDNA and Q5 Hot Start High Fidelity DNA Polymerase (New England Biolabs, Ipswich, MA) as described by Quick et al., to produce roughly 400 bp overlapping amplicons of the viral genomes (**Supplementary Tables 1**, **2**). Agencourt AMPure XP (Beckman Coulter Life Sciences, Indianapolis, IN) magnetic beads were used to purify the amplicons, which were further prepped for Illumina-based deep sequencing with the TruSeq Nano DNA HT Library Preparation Kit according to the manufacturer's guidelines (Illumina, San Diego, CA). Sequencing of the amplicon library was performed on a MiSeq Illumina desktop sequencer (Invitrogen, Carlsbad, CA) in the Pathogen Sequencing Services unit at the Wisconsin National Primate Research Center.

Calculation of Non-synonymous Single Nucleotide Polymorphism Frequencies

The deep sequencing reads were prepared for analysis by filtering out low quality reads, and by trimming the ∼30 bp primer sequences and adapter sequences off of the reads with cutadapt software v1.9.1 (91). Filtered reads were aligned to the stock virus sequence with bowtie2 software v2.2.5 (92). The resulting BAM format output was used as the input to call variants with lofreq software v2.1.2 (93). Variants identified here had >100 read depth and at least 1% frequency. Genome plots were generated using R and ggplot2 (ISBN: 0387981403). R scripts used to graph the plots can be found at https://github.com/stenglein-lab/viral_variant_explorer.

DATA AVAILABILITY STATEMENT

The raw data supporting the conclusions of this article are available on the sequence read archive (SRA) (Accession numbers: SRR17194541–SRR17194610).

ETHICS STATEMENT

The animal study was reviewed and approved by Colorado State University IACUC.

AUTHOR CONTRIBUTIONS

RA, JC, KS, MS, PM, and SO'C are responsible for the design and conduct of the project. LR-M, KG, JB, and RM provided technical assistance. All authors contributed to the article and approved the submitted version.

FUNDING

This work was supported by NIH, USA Grant R01 AI123234 to RA and in part by NIH, USA Grant R01 AI120021 to RA. In addition to the NIH grants listed above to RA, these experiments were further supported by the National Center for Research Resources, and the Office of Research Infrastructure Programs (ORIP) of the NIH through the grant OD011104 at the Tulane National Primate Research Center. Sequencing resources were provided through the NIH Grant P51OD011106 and the Wisconsin National Primate Research Center. Computational and sequencing analysis support was provided through the NIH/NCATS Colorado CTSA Grant Number UL1 TR002535. Partial support was also provided by the ADEAR Training Program NIH Grant T32AI150547.

ACKNOWLEDGMENTS

The following reagents were obtained through the NIH AIDS Reagent Program, Division of AIDS, NIAID, NIH: SIV B670 Virus from Dr. Michael Murphey-Corb, NIH: SIVhu Virus from Dr. Thomas Folks, NIH: 174xCEM Cells, ARP-272, contributed by Dr. Peter Cresswell, NIH: TZM-bl Cells, ARP-8129, contributed by Dr. John C. Kappes and Dr. Xiaoyun Wu. The 293T (ATCC CRL-3216) cells were obtained from the American Type Culture Collection (ATCC). Some of the data in this manuscript was part of a thesis by Curlin, J (94).

SUPPLEMENTARY MATERIAL

The Supplementary Material for this article can be found online at: https://www.frontiersin.org/articles/10.3389/fviro.2021.813606/full#supplementary-material

REFERENCES

1. Sharp PM, Hahn BH. Origins of HIV and the AIDS pandemic. *Cold Spring Harb Perspect Med.* (2011) 1:a006841. doi: 10.1101/cshperspect.a006841
2. Ayouba A, Akoua-Koffi C, Calvignac-Spencer S, Esteban A, Locatelli S, Li H, et al. Evidence for continuing cross-species transmission of SIVsmm to humans: characterization of a new HIV-2 lineage in rural Cote d'Ivoire. *AIDS.* (2013) 27:2488–91. doi: 10.1097/01.aids.0000432443.22684.50
3. Schmitt K, Mohan Kumar D, Curlin J, Remling-Mulder L, Stenglein M, O'Connor S, et al. Modeling the evolution of SIV sooty mangabey progenitor virus towards HIV-2 using humanized mice. *Virology.* (2017) 510:175–84. doi: 10.1016/j.virol.2017.07.005
4. Schmitt K, Curlin J, Kumar DM, Remling-Mulder L, Feely S, Stenglein M, et al. SIV progenitor evolution toward HIV: a humanized mouse surrogate model for SIVsm adaptation toward HIV-2. *J Med Primatol.* (2018) 47:298–301. doi: 10.1111/jmp.12380
5. Daniel MD, Letvin NL, King NW, Kannagi M, Sehgal PK, Hunt RD, et al. Isolation of T-cell tropic HTLV-III-like retrovirus from macaques. *Science.* (1985) 228:1201–4. doi: 10.1126/science.3159089
6. Murphey-Corb M, Martin LN, Rangan SR, Baskin GB, Gormus BJ, Wolf RH, et al. Isolation of an HTLV-III-related retrovirus from macaques with simian AIDS and its possible origin in asymptomatic mangabeys. *Nature.* (1986) 321:435–7. doi: 10.1038/321435a0
7. Naidu YM, Kestler HW, III, Li Y, Butler CV, Silva DP, Schmidt DK, et al. Characterization of infectious molecular clones of simian immunodeficiency virus (SIVmac) and human immunodeficiency virus type 2: persistent infection of rhesus monkeys with molecularly cloned SIVmac. *J Virol.* (1988) 62:4691–6. doi: 10.1128/jvi.62.12.4691-4696.1988
8. Kestler H, Kodama T, Ringler D, Marthas M, Pedersen N, Lackner A, et al. Induction of AIDS in rhesus monkeys by molecularly cloned simian immunodeficiency virus. *Science.* (1990) 248:1109–12. doi: 10.1126/science.2160735

9. Apetrei C, Kaur A, Lerche NW, Metzger M, Pandrea I, Hardcastle J, et al. Molecular epidemiology of simian immunodeficiency virus SIVsm in U.S. primate centers unravels the origin of SIVmac and SIVstm. *J Virol.* (2005) 79:8991–9005. doi: 10.1128/JVI.79.14.8991-9005.2005
10. Bell SM, Bedford T. Modern-day SIV viral diversity generated by extensive recombination and cross-species transmission. *PLoS Pathog.* (2017) 13:e1006466. doi: 10.1371/journal.ppat.1006466
11. Chahroudi A, Bosinger SE, Vanderford TH, Paiardini M, Silvestri G. Natural SIV hosts: showing AIDS the door. *Science.* (2012) 335:1188–93. doi: 10.1126/science.1217550
12. Andrieu JM, Lu W. A 30-year journey of trial and error towards a tolerogenic AIDS vaccine. *Arch Virol.* (2018) 163:2025–31. doi: 10.1007/s00705-018-3936-1
13. Moretti S, Virtuoso S, Sernicola L, Farcomeni S, Maggiorella MT, Borsetti A. Advances in SIV/SHIV non-human primate models of neuroAIDS. *Pathogens.* (2021) 10:1018. doi: 10.3390/pathogens10081018
14. Wolf RH, Gormus BJ, Martin LN, Baskin GB, Walsh GP, Meyers WM, et al. Experimental leprosy in three species of monkeys. *Science.* (1985) 227:529–31. doi: 10.1126/science.3917577
15. Zink WE, Zheng J, Persidsky Y, Poluektova L, Gendelman HE. The neuropathogenesis of HIV-1 infection. *FEMS Immunol Med Microbiol.* (1999) 26:233–41. doi: 10.1111/j.1574-695X.1999.tb01394.x
16. Dorsey JL, Mangus LM, Hauer P, Ebenezer GJ, Queen SE, Laast VA, et al. Persistent peripheral nervous system damage in simian immunodeficiency virus-infected macaques receiving antiretroviral therapy. *J Neuropathol Exp Neurol.* (2015) 74:1053–60. doi: 10.1097/NEN.0000000000000249
17. Khabbaz RF, Rowe T, Murphey-Corb M, Heneine WM, Schable CA, George JR, et al. Simian immunodeficiency virus needlestick accident in a laboratory worker. *Lancet.* (1992) 340:271–3. doi: 10.1016/0140-6736(92)92358-M
18. Khabbaz RF, Heneine W, George JR, Parekh B, Rowe T, Woods T, et al. Brief report: infection of a laboratory worker with simian immunodeficiency virus. *N Engl J Med.* (1994) 330:172–7. doi: 10.1056/NEJM199401203300304
19. Sheehy AM, Gaddis NC, Choi JD, Malim MH. Isolation of a human gene that inhibits HIV-1 infection and is suppressed by the viral Vif protein. *Nature.* (2002) 418:646–50. doi: 10.1038/nature00939
20. Sayah DM, Sokolskaja E, Berthoux L, Luban J. Cyclophilin A retrotransposition into TRIM5 explains owl monkey resistance to HIV-1. *Nature.* (2004) 430:569–73. doi: 10.1038/nature02777
21. Stremlau M, Owens CM, Perron MJ, Kiessling M, Autissier P, Sodroski J. The cytoplasmic body component TRIM5alpha restricts HIV-1 infection in Old World monkeys. *Nature.* (2004) 427:848–53. doi: 10.1038/nature02343
22. Neil SJ, Zang T, Bieniasz PD. Tetherin inhibits retrovirus release and is antagonized by HIV-1 Vpu. *Nature.* (2008) 451:425–30. doi: 10.1038/nature06553
23. Le Tortorec A, Neil SJ. Antagonism to and intracellular sequestration of human tetherin by the human immunodeficiency virus type 2 envelope glycoprotein. *J Virol.* (2009) 83:11966–78. doi: 10.1128/JVI.01515-09
24. Sauter D, Hue S, Petit SJ, Plantier JC, Towers GJ, Kirchhoff F, et al. HIV-1 Group P is unable to antagonize human tetherin by Vpu, Env or Nef. *Retrovirology.* (2011) 8:103. doi: 10.1186/1742-4690-8-103
25. Zhang X, Zhou T, Yang J, Lin Y, Shi J, Zhang X, et al. Identification of SERINC5-001 as the predominant spliced isoform for HIV-1 restriction. *J Virol.* (2017) 91:e00137–17. doi: 10.1128/JVI.00137-17
26. Sauter D, Kirchhoff F. Key viral adaptations preceding the AIDS pandemic. *Cell Host Microbe.* (2019) 25:27–38. doi: 10.1016/j.chom.2018.12.002
27. Jia B, Serra-Moreno R, Neidermyer W, Rahmberg A, Mackey J, Fofana IB, et al. Species-specific activity of SIV Nef and HIV-1 Vpu in overcoming restriction by tetherin/BST2. *PLoS Pathog.* (2009) 5:e1000429. doi: 10.1371/journal.ppat.1000429
28. Laguette N, Sobhian B, Casartelli N, Ringeard M, Chable-Bessia C, Segeral E, et al. SAMHD1 is the dendritic- and myeloid-cell-specific HIV-1 restriction factor counteracted by Vpx. *Nature.* (2011) 474:654–7. doi: 10.1038/nature10117
29. Wei W, Guo H, Han X, Liu X, Zhou X, Zhang W, et al. A novel DCAF1-binding motif required for Vpx-mediated degradation of nuclear SAMHD1 and Vpr-induced G2 arrest. *Cell Microbiol.* (2012) 14:1745–56. doi: 10.1111/j.1462-5822.2012.01835.x
30. Usami Y, Wu Y, Gottlinger HG. SERINC3 and SERINC5 restrict HIV-1 infectivity and are counteracted by Nef. *Nature.* (2015) 526:218–23. doi: 10.1038/nature15400
31. Lubow J, Collins KL. Vpr Is a VIP: HIV Vpr and infected macrophages promote viral pathogenesis. *Viruses.* (2020) 12:809. doi: 10.3390/v12080809
32. Lubow J, Virgilio MC, Merlino M, Collins DR, Mashiba M, Peterson BG, et al. Mannose receptor is an HIV restriction factor counteracted by Vpr in macrophages. *Elife.* (2020) 9:e51035. doi: 10.7554/eLife.51035.sa2
33. Berges BK, Wheat WH, Palmer BE, Connick E, Akkina R. HIV-1 infection and CD4 T cell depletion in the humanized Rag2-/-gamma c-/- (RAG-hu) mouse model. *Retrovirology.* (2006) 3:76. doi: 10.1186/1742-4690-3-76
34. Berges BK, Akkina SR, Folkvord JM, Connick E, Akkina R. Mucosal transmission of R5 and X4 tropic HIV-1 *via* vaginal and rectal routes in humanized Rag2-/- gammac -/- (RAG-hu) mice. *Virology.* (2008) 373:342–51. doi: 10.1016/j.virol.2007.11.020
35. Berges BK, Akkina SR, Remling L, Akkina R. Humanized Rag2(-/-)gammac(-/-) (RAG-hu) mice can sustain long-term chronic HIV-1 infection lasting more than a year. *Virology.* (2010) 397:100–3. doi: 10.1016/j.virol.2009.10.034
36. Yuan Z, Kang G, Ma F, Lu W, Fan W, Fennessey CM, et al. Recapitulating cross-species transmission of simian immunodeficiency virus SIVcpz to humans by using humanized BLT mice. *J Virol.* (2016) 90:7728–39. doi: 10.1128/JVI.00860-16
37. Sato K, Misawa N, Takeuchi JS, Kobayashi T, Izumi T, Aso H, et al. Experimental adaptive evolution of simian immunodeficiency virus SIVcpz to pandemic human immunodeficiency virus type 1 by using a humanized mouse model. *J Virol.* (2018) 92:e01905–17. doi: 10.1128/JVI.01905-17
38. Yuan Z, Kang G, Daharsh L, Fan W, Li Q. SIVcpz closely related to the ancestral HIV-1 is less or non-pathogenic to humans in a hu-BLT mouse model. *Emerg Microbes Infect.* (2018) 7:59. doi: 10.1038/s41426-018-0062-9
39. Curlin J, Schmitt K, Remling-Mulder L, Moriarty R, Stenglein M, O'Connor S, et al. SIVcpz cross-species transmission and viral evolution toward HIV-1 in a humanized mouse model. *J Med Primatol.* (2020) 49:40–3. doi: 10.1111/jmp.12440
40. Lan P, Tonomura N, Shimizu A, Wang S, Yang YG. Reconstitution of a functional human immune system in immunodeficient mice through combined human fetal thymus/liver and CD34+ cell transplantation. *Blood.* (2006) 108:487–92. doi: 10.1182/blood-2005-11-4388
41. Denton PW, Garcia JV. Humanized mouse models of HIV infection. *AIDS Rev.* (2011) 13:135–48.
42. Garcia S, Freitas AA. Humanized mice: current states and perspectives. *Immunol Lett.* (2012) 146:1–7. doi: 10.1016/j.imlet.2012.03.009
43. Shultz LD, Brehm MA, Garcia-Martinez JV, Greiner DL. Humanized mice for immune system investigation: progress, promise and challenges. *Nat Rev Immunol.* (2012) 12:786–98. doi: 10.1038/nri3311
44. Akkina R. New generation humanized mice for virus research: comparative aspects and future prospects. *Virology.* (2013) 435:14–28. doi: 10.1016/j.virol.2012.10.007
45. Neff CP, Ndolo T, Tandon A, Habu Y, Akkina R. Oral pre-exposure prophylaxis by anti-retrovirals raltegravir and maraviroc protects against HIV-1 vaginal transmission in a humanized mouse model. *PLoS ONE.* (2010) 5:e15257. doi: 10.1371/journal.pone.0015257
46. Choudhary SK, Archin NM, Cheema M, Dahl NP, Garcia JV, Margolis DM. Latent HIV-1 infection of resting CD4(+) T cells in the humanized Rag2(-)/(-) gammac(-)/(-) mouse. *J Virol.* (2012) 86:114–20. doi: 10.1128/JVI.05590-11
47. Charlins P, Schmitt K, Remling-Mulder L, Hogan LE, Hanhauser E, Hobbs KS, et al. A humanized mouse-based HIV-1 viral outgrowth assay with higher sensitivity than *in vitro* qVOA in detecting latently infected cells from individuals on ART with undetectable viral loads. *Virology.* (2017) 507:135–9. doi: 10.1016/j.virol.2017.04.011
48. Curlin J, Schmitt K, Remling-Mulder L, Moriarty R, Goff K, O'Connor S, et al. Evolution of SIVsm in humanized mice towards HIV-2. *J Med Primatol.* (2020) 49:280–3. doi: 10.1111/jmp.12486
49. Schmitt K, Curlin J, Remling-Mulder L, Moriarty R, Goff K, O'Connor S, et al. Mimicking SIV chimpanzee viral evolution toward HIV-1 during cross-species transmission. *J Med Primatol.* (2020) 49:284–7. doi: 10.1111/jmp.12485

50. Schmitt K, Curlin J, Remling-Mulder L, Moriarty R, Goff K, O'Connor S, et al. Cross-species transmission and evolution of SIV chimpanzee progenitor viruses toward HIV-1 in humanized mice. *Front Microbiol.* (2020) 11:1889. doi: 10.3389/fmicb.2020.01889
51. Aldrovandi GM, Feuer G, Gao L, Jamieson B, Kristeva M, Chen IS, et al. The SCID-hu mouse as a model for HIV-1 infection. *Nature.* (1993) 363:732–6. doi: 10.1038/363732a0
52. Baenziger S, Tussiwand R, Schlaepfer E, Mazzucchelli L, Heikenwalder M, Kurrer MO, et al. Disseminated and sustained HIV infection in CD34+ cord blood cell-transplanted Rag2-/-gamma c-/- mice. *Proc Natl Acad Sci USA.* (2006) 103:15951–6. doi: 10.1073/pnas.0604493103
53. Foley BL, Apetrei C, Hahn B, Mizrachi I, Mullins J, Rambaut A, ert al. *HIV Sequence Compendium 2018*. Los Alamos, New Mexico: Los Alamos National Laboratory, Theoretical Biology and Biophysics (2018).
54. Bukovsky AA, Weimann A, Accola MA, Gottlinger HG. Transfer of the HIV-1 cyclophilin-binding site to simian immunodeficiency virus from Macaca mulatta can confer both cyclosporin sensitivity and cyclosporin dependence. *Proc Natl Acad Sci USA.* (1997) 94:10943–8. doi: 10.1073/pnas.94.20.10943
55. Wu F, Kirmaier A, Goeken R, Ourmanov I, Hall L, Morgan JS, et al. TRIM5 alpha drives SIVsmm evolution in rhesus macaques. *PLoS Pathog.* (2013) 9:e1003577. doi: 10.1371/journal.ppat.1003577
56. Sanjuan R, Moya A, Elena SF. The distribution of fitness effects caused by single-nucleotide substitutions in an RNA virus. *Proc Natl Acad Sci USA.* (2004) 101:8396–401. doi: 10.1073/pnas.0400146101
57. Cuevas JM, Domingo-Calap P, Sanjuan R. The fitness effects of synonymous mutations in DNA and RNA viruses. *Mol Biol Evol.* (2012) 29:17–20. doi: 10.1093/molbev/msr179
58. Acevedo A, Brodsky L, Andino R. Mutational and fitness landscapes of an RNA virus revealed through population sequencing. *Nature.* (2014) 505:686–90. doi: 10.1038/nature12861
59. Pancio HA, Ratner L. Human immunodeficiency virus type 2 Vpx-Gag interaction. *J Virol.* (1998) 72:5271–5. doi: 10.1128/JVI.72.6.5271-5275.1998
60. Accola MA, Bukovsky AA, Jones MS, Gottlinger HG. A conserved dileucine-containing motif in p6(gag) governs the particle association of Vpx and Vpr of simian immunodeficiency viruses SIV(mac) and SIV(agm). *J Virol.* (1999) 73:9992–9. doi: 10.1128/JVI.73.12.9992-9999.1999
61. Sato S, Yuste E, Lauer WA, Chang EH, Morgan JS, Bixby JG, et al. Potent antibody-mediated neutralization and evolution of antigenic escape variants of simian immunodeficiency virus strain SIVmac239 *in vivo*. *J Virol.* (2008) 82:9739–52. doi: 10.1128/JVI.00871-08
62. Mori K, Ringler DJ, Kodama T, Desrosiers RC. Complex determinants of macrophage tropism in env of simian immunodeficiency virus. *J Virol.* (1992) 66:2067–75. doi: 10.1128/jvi.66.4.2067-2075.1992
63. Johnson WE, Morgan J, Reitter J, Puffer BA, Czajak S, Doms RW, et al. A replication-competent, neutralization-sensitive variant of simian immunodeficiency virus lacking 100 amino acids of envelope. *J Virol.* (2002) 76:2075–86. doi: 10.1128/jvi.76.5.2075-2086.2002
64. Saunders CJ, McCaffrey RA, Zharkikh I, Kraft Z, Malenbaum SE, Burke B, et al. The V1, V2, and V3 regions of the human immunodeficiency virus type 1 envelope differentially affect the viral phenotype in an isolate-dependent manner. *J Virol.* (2005) 79:9069–80. doi: 10.1128/JVI.79.14.9069-9080.2005
65. Betts M, Russell R. Amino acid properties and consequences of substitutions. In: Barnes M, editor. *Bioinformatics for Geneticists*. Hoboken: John Wiley & Sons (2003). p. 289—316.
66. Castro E, Belair M, Rizzardi GP, Bart PA, Pantaleo G, Graziosi C. Independent evolution of hypervariable regions of HIV-1 gp120: V4 as a swarm of N-Linked glycosylation variants. *AIDS Res Hum Retroviruses.* (2008) 24:106–13. doi: 10.1089/aid.2007.0139
67. Moore PL, Gray ES, Choge IA, Ranchobe N, Mlisana K, Abdool Karim SS, et al. The c3-v4 region is a major target of autologous neutralizing antibodies in human immunodeficiency virus type 1 subtype C infection. *J Virol.* (2008) 82:1860–9. doi: 10.1128/JVI.02187-07
68. Dieltjens T, Loots N, Vereecken K, Grupping K, Heyndrickx L, Bottieau E, et al. HIV type 1 subtype A envelope genetic evolution in a slow progressing individual with consistent broadly neutralizing antibodies. *AIDS Res Hum Retroviruses.* (2009) 25:1165–9. doi: 10.1089/aid.2008.0161
69. Chackerian B, Rudensey LM, Overbaugh J. Specific N-linked and O-linked glycosylation modifications in the envelope V1 domain of simian immunodeficiency virus variants that evolve in the host alter recognition by neutralizing antibodies. *J Virol.* (1997) 71:7719–27. doi: 10.1128/jvi.71.10.7719-7727.1997
70. Wei X, Decker JM, Wang S, Hui H, Kappes JC, Wu X, et al. Antibody neutralization and escape by HIV-1. *Nature.* (2003) 422:307–12. doi: 10.1038/nature01470
71. Chelico L, Pham P, Calabrese P, Goodman MF. APOBEC3G DNA deaminase acts processively 3' –> 5' on single-stranded DNA. *Nat Struct Mol Biol.* (2006) 13:392–9. doi: 10.1038/nsmb1086
72. Heusinger E, Deppe K, Sette P, Krapp C, Kmiec D, Kluge SF, et al. (2018). Preadaptation of simian immunodeficiency virus SIVsmm facilitated env-mediated counteraction of human tetherin by human immunodeficiency virus type 2. *J Virol* 92:e00276–18. doi: 10.1128/JVI.00276-18
73. Dayhoff MO. *Atlas of Protein Sequence and Structure*. Washington, DC: Georgetown University Medical Center (1972).
74. Manrique S, Sauter D, Horenkamp FA, Lulf S, Yu H, Hotter D, et al. Endocytic sorting motif interactions involved in Nef-mediated downmodulation of CD4 and CD3. *Nat Commun.* (2017) 8:442. doi: 10.1038/s41467-017-00481-z
75. Serra-Moreno R, Zimmermann K, Stern LJ, Evans DT. Tetherin/BST-2 antagonism by Nef depends on a direct physical interaction between Nef and tetherin, and on clathrin-mediated endocytosis. *PLoS Pathog.* (2013) 9:e1003487. doi: 10.1371/journal.ppat.1003487
76. Hirao K, Andrews S, Kuroki K, Kusaka H, Tadokoro T, Kita S, et al. Structure of HIV-2 nef reveals features distinct from HIV-1 involved in immune regulation. *iScience.* (2020) 23:100758. doi: 10.1016/j.isci.2019.100758
77. Swigut T, Iafrate AJ, Muench J, Kirchhoff F, Skowronski J. Simian and human immunodeficiency virus Nef proteins use different surfaces to downregulate class I major histocompatibility complex antigen expression. *J Virol.* (2000) 74:5691–701. doi: 10.1128/JVI.74.12.5691-5701.2000
78. Rowell JF, Stanhope PE, Siliciano RF. Endocytosis of endogenously synthesized HIV-1 envelope protein. Mechanism and role in processing for association with class II MHC. *J Immunol.* (1995) 155:473–88.
79. Aiken C, Konner J, Landau NR, Lenburg ME, Trono D. Nef induces CD4 endocytosis: requirement for a critical dileucine motif in the membrane-proximal CD4 cytoplasmic domain. *Cell.* (1994) 76:853–64. doi: 10.1016/0092-8674(94)90360-3
80. Rhee SS, Marsh JW. Human immunodeficiency virus type 1 Nef-induced down-modulation of CD4 is due to rapid internalization and degradation of surface CD4. *J Virol.* (1994) 68:5156–63. doi: 10.1128/jvi.68.8.5156-5163.1994
81. Chaudhuri R, Lindwasser OW, Smith WJ, Hurley JH, Bonifacino JS. Downregulation of CD4 by human immunodeficiency virus type 1 Nef is dependent on clathrin and involves direct interaction of Nef with the AP2 clathrin adaptor. *J Virol.* (2007) 81:3877–90. doi: 10.1128/JVI.02725-06
82. Veillette M, Desormeaux A, Medjahed H, Gharsallah NE, Coutu M, Baalwa J, et al. Interaction with cellular CD4 exposes HIV-1 envelope epitopes targeted by antibody-dependent cell-mediated cytotoxicity. *J Virol.* (2014) 88:2633–44. doi: 10.1128/JVI.03230-13
83. Zhang F, Wilson SJ, Landford WC, Virgen B, Gregory D, Johnson MC, et al. Nef proteins from simian immunodeficiency viruses are tetherin antagonists. *Cell Host Microbe.* (2009) 6:54–67. doi: 10.1016/j.chom.2009.05.008
84. Akkina RK, Rosenblatt JD, Campbell AG, Chen IS, Zack JA. Modeling human lymphoid precursor cell gene therapy in the SCID-hu mouse. *Blood.* (1994) 84:1393–8. doi: 10.1182/blood.V84.5.1393.1393
85. Bai J, Gorantla S, Banda N, Cagnon L, Rossi J, Akkina R. Characterization of anti-CCR5 ribozyme-transduced CD34+ hematopoietic progenitor cells *in vitro* and in a SCID-hu mouse model *in vivo*. *Mol Ther.* (2000) 1:244–54. doi: 10.1006/mthe.2000.0038
86. Veselinovic M, Charlins P, Akkina R. Modeling HIV-1 mucosal transmission and prevention in humanized mice. *Methods Mol Biol.* (2016) 1354:203–20. doi: 10.1007/978-1-4939-3046-3_14
87. Derdeyn CA, Decker JM, Sfakianos JN, Wu X, O'Brien WA, Ratner L, et al. Sensitivity of human immunodeficiency virus type 1 to the fusion inhibitor T-20 is modulated by coreceptor specificity defined by the V3 loop of gp120. *J Virol.* (2000) 74:8358–67. doi: 10.1128/JVI.74.18.8358-8367.2000

88. Wei X, Decker JM, Liu H, Zhang Z, Arani RB, Kilby JM, et al. Emergence of resistant human immunodeficiency virus type 1 in patients receiving fusion inhibitor (T-20) monotherapy. *Antimicrob Agents Chemother.* (2002) 46:1896–905. doi: 10.1128/AAC.46.6.1896-1905.2002
89. Baskin GB, Murphey-Corb M, Watson EA, Martin LN. Necropsy findings in rhesus monkeys experimentally infected with cultured simian immunodeficiency virus (SIV)/delta. *Vet Pathol.* (1988) 25:456–67. doi: 10.1177/030098588802500609
90. Quick J, Grubaugh ND, Pullan ST, Claro IM, Smith AD, Gangavarapu K, et al. Multiplex PCR method for MinION and illumina sequencing of Zika and other virus genomes directly from clinical samples. *Nat Protoc.* (2017) 12:1261–76. doi: 10.1038/nprot.2017.066
91. Martin M. Cutadapt removes adapter sequences from high-throughput sequencing reads. *EMBnet J.* (2011) 17:10–12. doi: 10.14806/ej.17.1.200
92. Langmead B, Salzberg SL. Fast gapped-read alignment with Bowtie 2. *Nat Methods.* (2012) 9:357–9. doi: 10.1038/nmeth.1923
93. Wilm A, Aw PP, Bertrand D, Yeo GH, Ong SH, Wong CH, et al. LoFreq: a sequence-quality aware, ultra-sensitive variant caller for uncovering cell-population heterogeneity from high-throughput sequencing datasets. *Nucleic Acids Res.* (2012) 40:11189–201. doi: 10.1093/nar/gks918
94. Curlin JZ. *Modeling the Evolution of SIV Progenitor Viruses Towards HIV-1 and HIV-2 in a Humanized Mouse Surrogate Model*. Ph.D. Fort Collins, CO: Colorado State University (2020).

Conflict of Interest: The authors declare that the research was conducted in the absence of any commercial or financial relationships that could be construed as a potential conflict of interest.

Publisher's Note: All claims expressed in this article are solely those of the authors and do not necessarily represent those of their affiliated organizations, or those of the publisher, the editors and the reviewers. Any product that may be evaluated in this article, or claim that may be made by its manufacturer, is not guaranteed or endorsed by the publisher.

frontiers in Virology

ORIGINAL RESEARCH
published: 11 March 2022
doi: 10.3389/fviro.2022.861628

HIV Co-infection Augments EBV-Induced Tumorigenesis *in vivo*

Christopher B. Whitehurst[1,2†‡], *Monica Rizk*[3,4,5†], *Adonay Teklezghi*[3,4,5], *Rae Ann Spagnuolo*[3,4,5], *Joseph S. Pagano*[1,2,6] *and Angela Wahl*[3,4,5*]

[1] Department of Microbiology and Immunology, University of North Carolina at Chapel Hill, Chapel Hill, NC, United States, [2] Lineberger Comprehensive Cancer Center, University of North Carolina at Chapel Hill, Chapel Hill, NC, United States, [3] International Center for the Advancement of Translational Science, University of North Carolina at Chapel Hill, Chapel Hill, NC, United States, [4] Division of Infectious Diseases, Department of Medicine, University of North Carolina at Chapel Hill, Chapel Hill, NC, United States, [5] Center for AIDS Research, University of North Carolina at Chapel Hill, Chapel Hill, NC, United States, [6] Department of Medicine, University of North Carolina at Chapel Hill, Chapel Hill, NC, United States

In most individuals, EBV maintains a life-long asymptomatic latent infection. However, EBV can induce the formation of B cell lymphomas in immune suppressed individuals including people living with HIV (PLWH). Most individuals who acquire HIV are already infected with EBV as EBV infection is primarily acquired during childhood and adolescence. Although antiretroviral therapy (ART) has substantially reduced the incidence of AIDS-associated malignancies, EBV positive PLWH are at an increased risk of developing lymphomas compared to the general population. The direct effect of HIV co-infection on EBV replication and EBV-induced tumorigenesis has not been experimentally examined. Using a humanized mouse model of EBV infection, we demonstrate that HIV co-infection enhances systemic EBV replication and immune activation. Importantly, EBV-induced tumorigenesis was augmented in EBV/HIV co-infected mice. Collectively, these results demonstrate a direct effect of HIV co-infection on EBV pathogenesis and disease progression and will facilitate future studies to address why the incidence of certain types of EBV-associated malignancies are stable or increasing in ART treated PLWH.

Keywords: Epstein-Barr Virus (EBV), human immunodeficiency virus (HIV), co-infection, replication, tumorigenesis, B cell lymphoma, humanized mice

OPEN ACCESS

Edited by:
Akio Adachi,
Kansai Medical University, Japan

Reviewed by:
Ramesh Akkina,
Colorado State University, United States
Kazutaka Terahara,
National Institute of Infectious Diseases (NIID), Japan
Larisa Y. Poluektova,
University of Nebraska Medical Center, United States

***Correspondence:**
Angela Wahl
angela_wahl@med.unc.edu

†Present address:
Christopher B. Whitehurst, Department of Pathology, Microbiology, and Immunology, New York Medical College, Valhalla, NY, United States

‡*These authors have contributed equally to this work and share first authorship*

Specialty section:
This article was submitted to Fundamental Virology, a section of the journal Frontiers in Virology

Received: *24 January 2022*
Accepted: *11 February 2022*
Published: *11 March 2022*

Citation:
Whitehurst CB, Rizk M, Teklezghi A, Spagnuolo RA, Pagano JS and Wahl A (2022) HIV Co-infection Augments EBV-Induced Tumorigenesis in vivo. Front. Virol. 2:861628. doi: 10.3389/fviro.2022.861628

INTRODUCTION

Epstein-Barr Virus (EBV) is a ubiquitous virus infecting over 90% of adults in developed and developing countries (1). EBV is an oncogenic herpesvirus that primarily infects B cells (2–4). Primary infection is characterized by the rapid proliferation of infected B cells until an effective immune response is elicited and/or EBV-infected B cells differentiate into latently-infected memory-like cells establishing a life-long infection of the B cell compartment (2–4).

In most individuals, EBV maintains a latent infection with intermittent periods of subclinical virus reactivation and shedding (5). However, EBV can induce the formation of B cell lymphomas in immune suppressed individuals including people living with HIV (PLWH) (4, 6, 7). Most individuals who acquire HIV are already infected with EBV as EBV infection is primarily acquired during childhood and adolescence (1). Without any interventions, EBV positive PLWH have over a 60-fold higher risk of developing lymphomas compared to the general population

(8). While antiretroviral therapy (ART) use has significantly decreased the incidence of AIDS-associated malignancies in PLWH, the incidence of certain types of EBV-associated cancers has remained elevated in PLWH (9–11). HIV mediated immune dysfunction may contribute to lymphomagenesis (12). A better understanding of how HIV co-infection affects EBV replication and tumorigenesis would facilitate the development and testing of novel interventions to ameliorate EBV-associated pathologies in PLWH.

Here, a humanized mouse model of EBV infection was used to evaluate the effect of HIV co-infection on EBV replication and tumorigenesis *in vivo*. Results demonstrate that HIV co-infection enhanced systemic EBV replication *in vivo* resulting in higher levels of virus in the peripheral blood and tissues. HIV co-infection also resulted in an enhancement of EBV-mediated $CD8^+$ T cell activation. Importantly, data directly demonstrated that HIV co-infection augmented EBV-associated tumorigenesis *in vivo*. These results will facilitate future studies to address how HIV-associated enhancement of EBV replication and EBV mediated immune activation and tumorigenesis is impacted by suppressive ART and why the incidence of certain types of EBV-associated malignancies are stable or increasing in ART treated PLWH.

RESULTS

Humanized mice reconstituted with human B cells and T cells were first exposed to EBV (**Supplementary Table 1**). To evaluate the effect of HIV co-infection on EBV replication and tumorigenesis *in vivo*, a subset of mice was subsequently exposed to HIV. EBV infection was assessed in mice by measuring EBV-DNA levels in peripheral blood (cells and plasma) longitudinally and in tissues at necropsy (16 weeks post exposure or earlier if mice experienced 20% weight loss and/or appeared lethargic). HIV infection was monitored over time by measuring peripheral blood plasma HIV-RNA levels. HIV-RNA was detected in the plasma of all mice exposed to HIV and virus replication sustained over time (**Supplementary Figure 1A**). By six weeks post-exposure, plasma HIV-RNA levels were higher in EBV/HIV co-infected mice ($P = 0.0317$) compared to mice infected with HIV-only (**Supplementary Figure 1A**).

Peak EBV Viremia Is Enhanced by HIV Co-infection

EBV-DNA was detected in the peripheral blood of all mice exposed to EBV only and 6/7 mice (86%) exposed to EBV and HIV (**Figure 1A**). No significant difference in EBV acquisition, as measured by the presence of detectable EBV-DNA in peripheral blood, was observed between groups of mice ($P = 0.5007$). While cell-free (plasma) and cell-associated EBV-DNA was detected in the peripheral blood of all EBV-positive mice, peak levels of cell-free and cell-associated EBV-DNA were 15-fold and 5-fold higher ($P = 0.0082$ and $P = 0.0350$, respectively) in EBV/HIV co-infected mice (**Figures 1B–D**). These results demonstrate that HIV co-infection enhanced EBV viremia.

Systemic EBV-Induced $CD8^+$ T Cell Activation Is Amplified by HIV Co-infection

EBV infection induces a $CD8^+$ T cell response in peripheral blood that is characterized by the expansion and activation of $CD8^+$ T cells and acquisition of a memory phenotype (13). At necropsy, regardless of HIV co-infection status, $CD8^+$ T cell levels were significantly higher in the peripheral blood of EBV positive mice (baseline: 4.5 ± 0.7% s.e.m.; necropsy: 29.6 ± 6.5% s.e.m.; $P = 0.0009$) compared to baseline pre-exposure levels (**Supplementary Table 2**). In addition, the frequencies of memory (baseline: 43.5 ± 6.9% s.e.m.; necropsy: 94.3 ± 2.2% s.e.m.; $P < 0.0001$) and activated (baseline: 12.9 ± 2.9% s.e.m.; necropsy: 47.1 ± 7.2% s.e.m.; $P = 0.0002$) $CD8^+$ T cells in peripheral blood were also significantly higher at necropsy compared to baseline pre-exposure levels (**Supplementary Table 2**). At necropsy, no significant differences in the levels of $CD8^+$ T cells in peripheral blood and tissues were observed between mice infected with EBV only or co-infected with EBV and HIV (**Figure 2A**; **Supplementary Table 2**). Notably, the vast majority of $CD8^+$ T cells in EBV positive mice expressed a memory phenotype in peripheral blood and tissues at necropsy (**Figure 2B**; **Supplementary Table 2**). However, the levels of activated $CD8^+$ T cells were significantly higher in the peripheral blood ($P = 0.0087$), spleen ($P = 0.0221$), liver ($P = 0.0140$), and lung ($P = 0.0047$) of EBV positive mice co-infected with HIV (**Figure 2C**; **Supplementary Table 2**). In the peripheral blood of mice infected with HIV only, the levels of activated $CD8^+$ T cells only transiently increased peaking at 2 weeks post-exposure indicating that EBV and HIV contribute to the higher levels of $CD8^+$ T cell activation observed in EBV/HIV co-infected mice (**Supplementary Figure 1B**). Collectively, these results suggest that HIV co-infection enhanced EBV-mediated immune activation.

HIV Co-infection Augments Systemic EBV Replication

To evaluate the effect of HIV on systemic EBV replication, EBV-DNA levels were measured in the peripheral blood, spleen, lymph nodes, bone marrow, liver, lung, and brain of EBV and EBV/HIV co-infected mice at necropsy. Significantly higher levels of cell-free and cell-associated EBV-DNA were observed in peripheral blood of EBV/HIV co-infected mice ($P = 0.0022$). EBV-DNA was detected in 39/41 tissues samples analyzed from mice infected with EBV only and in 42/42 tissue samples analyzed from EBV/HIV co-infected mice (**Supplementary Table 3**). EBV-DNA levels were significantly higher in the spleen ($P = 0.0047$), lymph nodes ($P = 0.0140$), bone marrow ($P = 0.0350$), liver ($P = 0.0082$), and lung ($P = 0.0221$) of EBV/HIV co-infected mice (**Figure 3**; **Supplementary Table 3**). Notably, EBV-DNA levels were also 60-fold higher in the brain of EBV/HIV co-infected mice (**Figure 3**, **Supplementary Table 3**).

HIV Co-infection Augments EBV-Induced Tumorigenesis *in vivo*

The presence of tumors in EBV and EBV/HIV infected mice was also analyzed at necropsy. HIV co-infection enhanced

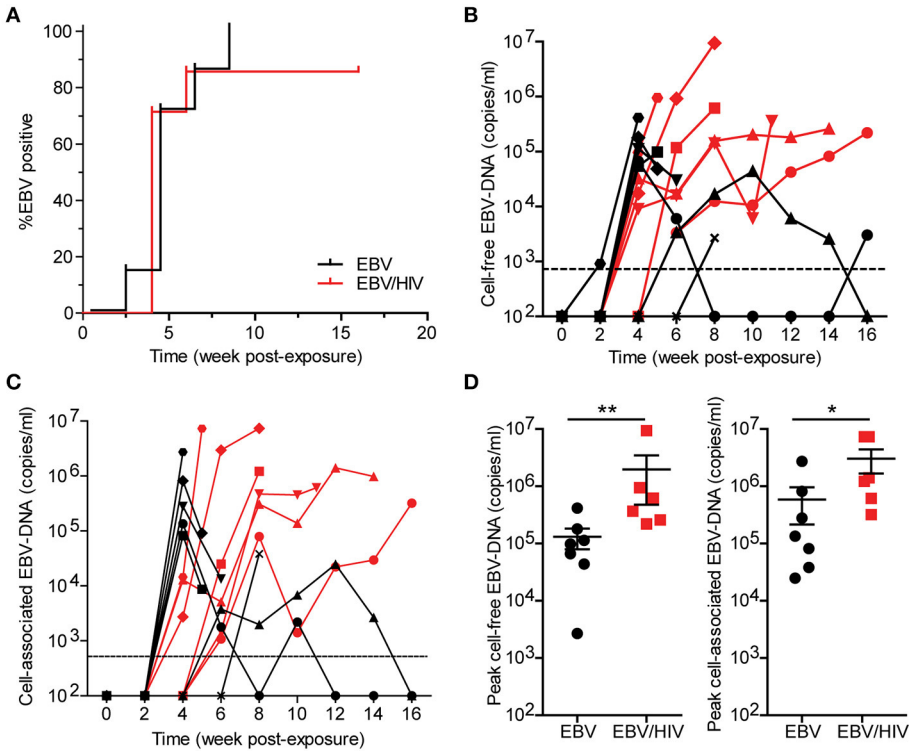

FIGURE 1 | HIV co-infection enhances EBV viremia. Humanized mice were inoculated intraperitoneally with EBV B95.8 ($n = 14$). Following EBV exposure, a group of mice ($n = 7$) were subsequently inoculated intravenously with HIV-1 LAI. EBV-DNA levels were monitored longitudinally in peripheral blood plasma (cell-free EBV-DNA) and cells (cell-associated EBV-DNA) of mice with real-time PCR. **(A)** A Kaplan Meier plot depicts the proportion of mice inoculated with EBV (black) or EBV/HIV (red) that became systemically infected with EBV as determined by the presence of EBV-DNA in peripheral blood. The **(B)** cell-free and **(C)** cell-associated EBV-DNA levels for individual mice systemically infected with EBV ($n = 7$ mice, black symbols) or EBV/HIV ($n = 6$ mice, red symbols) are shown. A dashed line indicates the assay limit of detection. **(D)** Peak cell-free and cell-associated EBV-DNA levels in the peripheral blood of EBV ($n = 7$ mice, black circles) and EBV/HIV ($n = 6$ mice, red squares) infected mice. The mean and standard error mean EBV-DNA levels are shown. Peak EBV-DNA levels between EBV and EBV/HIV infected animals were compared with a two-tailed Mann-Whitney test (*$p < 0.05$ and **$p < 0.01$).

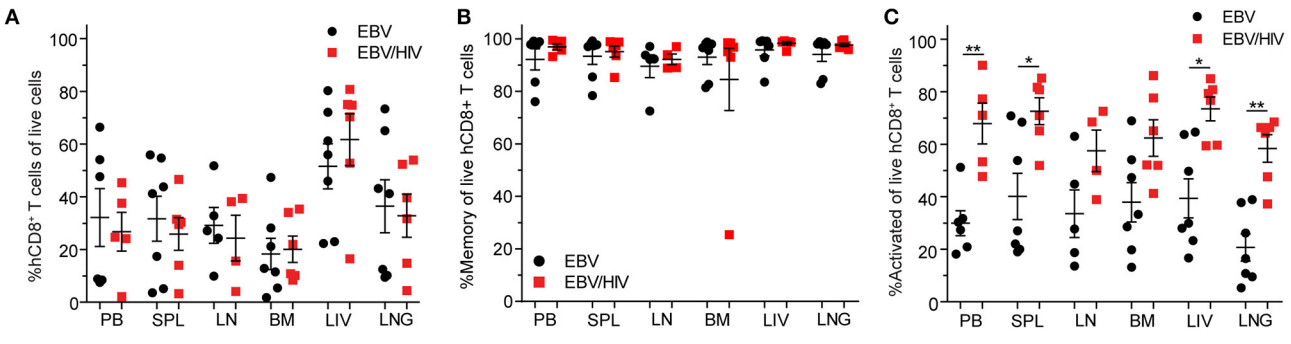

FIGURE 2 | Systemic EBV-induced $CD8^+$ T cell activation is amplified by HIV co-infection. **(A)** $CD8^+$ T cell, **(B)** memory ($CD45RA^{neg}$) $CD8^+$ T cell and **(C)** $CD8^+$ T cell activation ($HLA\text{-}DR^+CD38^+$) levels as determined by flow cytometric analysis in the peripheral blood (PB) and spleen (SPL), lymph node (LN), bone marrow (BM), liver (LIV) and lung (LNG) of EBV (SPL, BM, LIV, LNG: $n = 7$ mice, PB: $n = 6$ mice, LN: $n = 5$ mice, black circles) and EBV/HIV (SPL, BM, LIV, LNG: $n = 6$ mice, PB: $n = 5$ mice, LN: $n = 4$ mice, red squares) infected mice at necropsy. The mean and standard error mean are shown. $CD8^+$ T cell, memory $CD8^+$ T cell, and $CD8^+$ T cell activation levels in the PB and tissues of EBV and EBV/HIV infected animals were compared with a two-tailed Mann-Whitney test (*$p < 0.05$ and **$p < 0.01$).

EBV-induced tumorigenesis *in vivo*. Macroscopic tumors were readily observed in 7/7 EBV/HIV co-infected mice (**Figure 4A**; **Supplementary Table 3**). In contrast, only 4/7 mice infected with EBV only had macroscopic tumors (**Figure 4A**; **Supplementary Table 3**). Tumors were located in a greater number of distinct anatomical sites per mouse in EBV/HIV

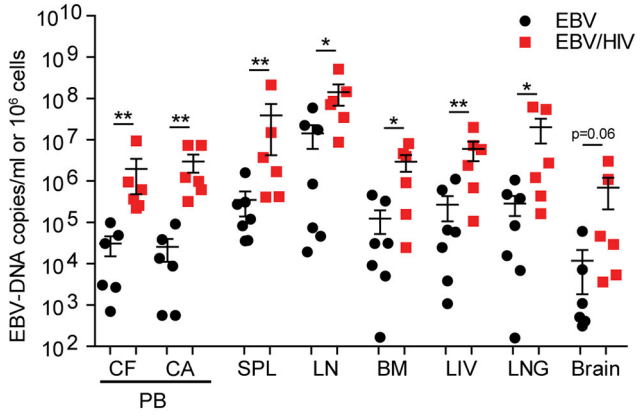

FIGURE 3 | HIV co-infection augments systemic EBV replication. EBV-DNA levels in the peripheral blood (PB, CF, cell-free; CA, cell-associated) and tissues (SPL, spleen; LN, lymph nodes; BM, bone marrow; LIV, liver; LNG, lung and brain) of EBV ($n = 7$ mice, black circles) and EBV/HIV ($n = 6$ mice, red squares) infected mice at necropsy. The mean and standard error mean EBV-DNA levels are shown. EBV-DNA levels between EBV and EBV/HIV infected animals were compared with a two-tailed Mann-Whitney test (*$p <$ 0.05 and **$p < 0.01$).

co-infected mice compared to mice infected with EBV only ($P = 0.0023$) (**Figure 4B**). Tumors were identified in one or two different tissues in mice infected with EBV only. In contrast, tumors were identified in up to five different tissues per mouse in mice co-infected with EBV and HIV (**Figure 4B**). In mice infected with EBV only tumors were only observed on the spleen and/or liver (**Figures 4C,D**; **Supplementary Table 3**). However, in EBV/HIV co-infected mice tumors could be observed on the spleen, liver, kidney, gastrointestinal tract, and/or salivary glands (**Figures 4C–E**; **Supplementary Table 3**). An analysis of viral gene expression in tumor samples collected from mice demonstrated that all tumors analyzed from EBV infected mice regardless of HIV co-infection status expressed LMP1 and EBNA2 (**Figure 4F**). This is characteristic of type III latency gene expression. Although HIV co-infection enhanced systemic EBV replication and EBV-induced tumorigenesis, no significant difference in survival ($P = 0.8372$) was observed between mice infected with EBV only or co-infected with EBV and HIV (**Supplementary Figure 2**).

DISCUSSION

Using a humanized mouse model of EBV infection (14–17), we directly demonstrated that HIV co-infection enhances systemic EBV replication, immune activation, and EBV-induced tumorigenesis *in vivo*. These data are consistent with studies reporting increased detection of EBV-DNA in the peripheral blood and saliva and the increased incidence of certain types of EBV-associated cancers in PLWH without any interventions (6–8, 18–21). In mice infected with EBV only, macroscopic tumors were only observed on the spleen and liver. In EBV/HIV co-infected animals, tumors were observed on the liver, spleen, kidneys, gastrointestinal tract, and salivary glands. These results suggest that HIV co-infection facilitates the spread of EBV-associated lymphomas and/or the simultaneous development of tumors at multiple different sites. Similar results were recently observed by another laboratory in humanized mice during a study focused on evaluating the effect of EBV infection on the cellular tropism of HIV (22). Several types of EBV positive lymphomas on extra nodal sites have been observed in PLWH including Hodgkin's lymphoma and diffuse large B cell lymphomas (6, 8). While we did not define the type of malignancies present, expression of EBV latency genes LMP1 and EBNA2 were detected in all tumors analyzed from humanized mice albeit at different levels. Co-expression of LMP1 and EBNA2 are indicative of type III latency (e.g. immunoblastic diffuse large B cell lymphomas) (4, 6).

Suppressive antiretroviral therapy (ART) reduces the incidence of AIDS-associated malignancies in PLWH (9, 10). The effect of ART on EBV reactivation and replication is less clear. For example, one study reported that incidence of EBV reactivation (as measured by the detection of EBV-DNA in saliva) was higher in PLWH compared to HIV negative controls regardless of ART use. However, the incidence of EBV reactivation was reduced in PLWH (ART +/–) with high $CD4^+$ T cell counts (23). Despite ART, the incidence of Hodgkin's lymphoma in PLWH has not decreased (9, 11). Most Hodgkin's lymphomas in PLWH are associated with EBV (7). While ART efficiently suppresses systemic HIV replication in PLWH, systemic immune activation and dysfunction persist presumably in part due to residual HIV replication and gut dysbiosis (24). Chronic immune activation and dysfunction in ART-suppressed PLWH may impair the formation of a robust immune response allowing for the formation of EBV-associated malignancies. Humanized mice could be used in the future to directly evaluate the effect of ART on systemic EBV replication and EBV-associated tumor formation and correlations between markers of chronic immune activation (e.g. LPS, sCD14, CRP, neopterin, TNFα, IL-6, IL-10, IFNγ, etc.) and EBV-associated disease.

Most PLWH acquire EBV infection prior HIV infection (1). Therefore, our study focused on the effect of HIV co-infection on EBV pathogenesis. However, EBV may influence the course of HIV infection. Here, we observed higher levels of HIV-RNA in the plasma of EBV/HIV co-infected mice compared to mice infected with HIV only by six weeks post-exposure. Even in healthy individuals, EBV periodically reactivates in the body which could stimulate local immune activation, potentially enhancing HIV replication (5). Studies in PLWH have attempted to evaluate associations between herpesvirus shedding (as determined by detectable virus in peripheral blood, throat washes, urine, stool, and/or semen) and HIV viral loads, however, given the high prevalence of other herpesviruses in PLWH, it is difficult to directly determine the effect of EBV on HIV replication and pathogenesis (25, 26). Humanized mice could serve as a model to directly evaluate the effect of EBV infection on HIV replication, pathogenesis and latency *in vivo*.

Limitations to our study include no uninfected control animals to serve as a comparison for the changes in the $CD8^+$ T cell compartment observed in EBV-infected mice. However,

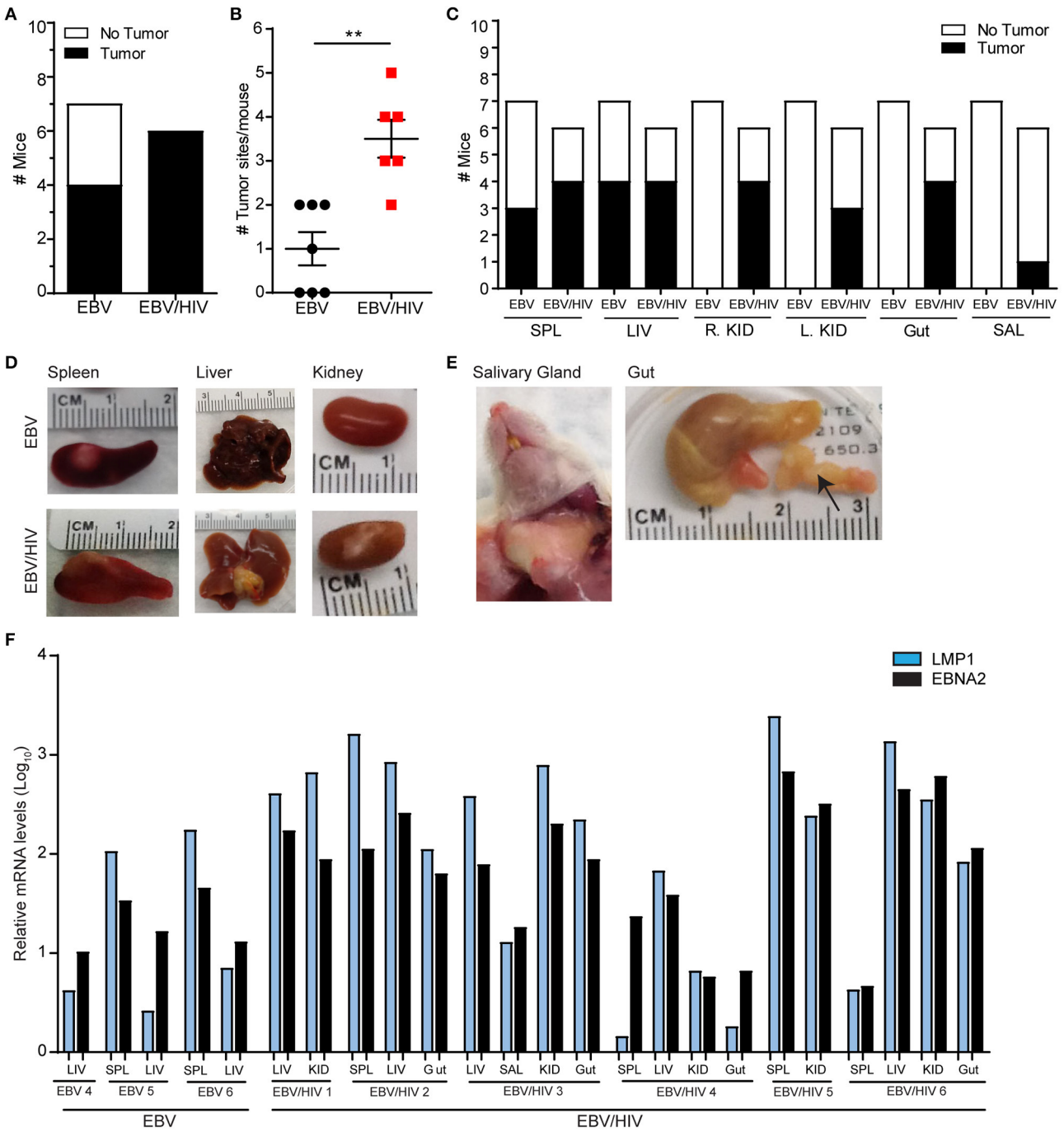

FIGURE 4 | HIV co-infection augments EBV-induced tumorigenesis *in vivo*. The presence of macroscopic tumors in the organs of EBV ($n = 7$ mice) and EBV/HIV ($n = 6$ mice) infected animals were noted at necropsy. **(A)** Tumor incidence in EBV and EBV/HIV infected mice (white: no tumors detected, black: tumors detected). **(B)** The number of different tissues with macroscopic tumors for each EBV (black circles) and EBV/HIV (red squares) infected mouse. The mean and standard error mean are shown. The number of tumor sites detected in EBV and EBV/HIV infected mice was compared with a two-tailed Mann-Whitney test (**$p < 0.01$). **(C)** Tumor incidence in the spleen (SPL), liver (LIV), right kidney (R.KID), left kidney (L.KID), gut and salivary glands (SAL) of EBV and EBV/HIV infected mice (white: no tumors detected, black: tumors detected). **(D)** Representative images of the spleen, liver, and kidney harvested from EBV and EBV/HIV infected mice. **(E)** Images of tumors detected in the salivary glands and gut (noted with an arrow) of EBV/HIV infected mice. **(F)** LMP1 and EBNA2 mRNA levels in tumors isolated from the spleen (SPL), liver (LIV), kidney (KID), gut and salivary glands (SAL) of EBV and EBV/HIV infected mice. Relative LMP1 (blue bars) and EBNA2 (black bars) mRNA levels were quantified using β-actin as an internal reference.

the effect of EBV infection on the $CD8^+$ T cell compartment including expansion, activation, and acquisition of a memory phenotype, has been well-documented in humans and in multiple humanized mouse models when compared to baseline levels and/or uninfected controls (13–15, 27–30). Furthermore, it has been shown that while the levels of human hematopoietic cells ($hCD45^+$) in the peripheral blood of mice is stable between 16 and 32 weeks post engraftment, the percentage of T cells that are $CD8^+$ decreases over time which is the opposite of what was observed in EBV-infected humanized mice (31). In addition, the short lifespan of humanized mice compared to humans requires experimental timelines to be condensed. Despite the shortened timeline between EBV and HIV exposures, our experimental data supports the clinical observation that the incidence of EBV-associated malignancies is higher in PLWH compared to the general population (6–8). In addition, while we anticipate that infection with a CCR5 or CXCR4 tropic strain of HIV would enhance EBV-associated tumorigenesis, a CXCR4 strain of HIV was chosen for this study to accelerate the development of HIV-associated pathogenesis.

In summary, we have implemented a model that permits the analysis of the effect of HIV infection on EBV. Our results demonstrate that HIV co-infection enhances EBV replication and the formation of EBV-associated malignancies. This work will facilitate future studies using humanized mouse models to address why the incidence of certain types of EBV-associated malignancies are stable or increasing in ART treated PLWH in contrast to the decline observed for many types of AIDS-associated malignancies.

MATERIALS AND METHODS

Preparation of Humanized Mice

Humanized mice were constructed by transplanting 12–15-week-old female and male irradiated (200 rads) NOD.Cg-*Prkdc*^{scid} *Il2rg*^{tm1Wjl}/SzJ mice (NSG; The Jackson Laboratory) with 2–3.5 x 10^5 human $CD34^+$ hematopoietic stem cells intravenously. Reconstitution of animals with human hematopoietic cells was monitored longitudinally with flow cytometry as previously described (14). Animals were maintained by the Division of Comparative Medicine at the University of North Carolina-Chapel Hill.

Production of Virus and Infection of Humanized Mice

Infectious EBV was reactivated by transfection of BZLF1 and gp110 into 293 cells harboring a B95.8 EBV bacmid (32). Cell supernatant fluid was passed through a 0.4 uM filter and concentrated with an Amicon ultra 100-kDa-molecular-mass-cutoff filter (Millipore). EBV stocks were titered on Raji cells as previously described (33). Stocks of HIV-1_{LAI} were generated by transient transfection of 293T cells and titered on TZM-BL indicator cells as previously described (34–40). Mice (16–24 weeks post-transplant) were exposed to 1–1.2 x 10^5 green Raji units (GRU) EBV via intraperitoneal injection. On the same day and following EBV exposure, a group of mice was also exposed intravenously to 3 x 10^4 TCIU HIV-1_{LAI} via tail vein injection.

Analysis of HIV Infection

HIV-RNA levels were measured longitudinally in the peripheral blood plasma of mice using real-time PCR as previously described (34–40).

Analysis of EBV Infection

EBV-DNA levels were measured longitudinally in peripheral blood and in tissues at necropsy using a real-time PCR assay as previously described (14). Flow cytometry was used to evaluate levels of $CD8^+$ T cells, memory ($CD45RA^{neg}$) $CD8^+$ T cells and $CD8^+$ T cell activation (HLA-DR+CD38+) in peripheral blood and tissues as previously described (14). Live cell gates were determined by forward and side scatter. Plasma was collected from peripheral blood following centrifugation (375 x g, 5 min). Cells were isolated from the peripheral blood, spleens, lymph nodes, bone marrow, livers, lungs and brains collected from mice for analysis by real-time PCR and flow cytometry as previously described (34–40). Liver, lung, and brain mononuclear cells were purified with a Percoll gradient. Mice were euthanized at 16 weeks post-exposure or earlier if they experienced 20% weight loss and/or appeared lethargic and a necropsy performed to assess the presence of tumors. Tumors were harvested, snap-frozen and stored at −80C for subsequent nucleic acid extraction and gene expression analysis. Tissue and tumor images were taken with an iSight color camera and the brightness adjusted in Adobe Photoshop CS6.

EBV Gene Expression Analysis

RNA was isolated from 100 mg of tissue from tumor samples using the TRIzol reagent (*Invitrogen*) according to manufacturer's instructions. Total RNA quantity and quality was determined using a Nanodrop 1000 (ThermoScientific). Total RNA (1 ug) was converted to cDNA using the iScript cDNA kit (BioRad) and random primers according to manufacturer's guidelines. qPCR was performed using iTaq Universal SYBR Green Supermix (BioRad) and the QuantStudio6 Real-Time PCR system (Applied Biosystems) under standard conditions. Samples were monitored for LMP1, EBNA2 and B-actin with the following primers: LMP1, 5′-AATTTGCACGGACAGGCATT-3′; (forward) and 5′-AAGGCCAAAAGCTGCCAGAT-3′ (reverse); EBNA2, 5′-GCTTAGCCAGTAACCCAGCACT-3′ (forward) and 5′-TGCTTAGAAGGTTGTTGGCATG-3′ (reverse), B-Actin, 5′-GTCTGCCTTGGTAGTGGATAATG-3′ (forward) and 5′-TCGAGGACGCCCTATCATGG-3′ (reverse). Relative levels of LMP1 and EBNA2 were quantified using β-actin as an internal reference.

Statistical Analyses

Statistical analyses were performed in Prism, version 6 (Graph Pad). A Log-rank Mantel-Cox test was used to compare the rates of EBV-DNA detection in the peripheral blood and survival between EBV and EBV/HIV exposed mice. A two-tailed Mann-Whitney U test was used to compare the peak peripheral blood cell-associated and cell-free HIV-DNA levels, tissue EBV-DNA levels, levels of $CD8^+$ T cells, memory $CD8^+$ T cells, and $CD8^+$ T cell activation in peripheral blood and tissues, and the number of tumor sites per mouse between EBV and EBV/HIV exposed mice.

A two-tailed Mann-Whitney U test was also used to compare $CD8^+$ T cells, memory $CD8^+$ T cells, and $CD8^+$ T cell activation levels in the peripheral blood of EBV infected mice (regardless of HIV co-infection status) at baseline and at necropsy.

DATA AVAILABILITY STATEMENT

The original contributions presented in the study are included in the article/**Supplementary Material**, further inquiries can be directed to the corresponding author.

ETHICS STATEMENT

The animal study was reviewed and approved by Institutional Animal Care and Use Committee at the University of North Carolina at Chapel Hill.

AUTHOR CONTRIBUTIONS

CW produced and titered stocks of EBV, performed the analysis of EBV latency gene expression, contributed to the experimental design, data interpretation, and manuscript writing. MR longitudinally monitored mouse health and survival, processed samples from EBV-exposed mice, performed flow cytometric analyses, performed the real-time PCR analysis of EBV-DNA levels in peripheral blood, tissue samples, and analyzed data. AT longitudinally monitored mouse health, survival and processed samples from EBV-exposed mice. RS performed and supervised the real-time PCR analysis of EBV-DNA. JP contributed to the experimental design and data interpretation. AW conceived, designed experiments, coordinated the study, contributed to data interpretation, data presentation, and manuscript writing.

FUNDING

This work was supported in part by funding from the National Institutes for Heath grants P01-CA019014-37, R01-AI123010, R01-AI140799, R01-DK131585, and R01-MH108179. This research was also supported by the University of North Carolina at Chapel Hill Center for AIDS Research (CFAR), an NIH funded program P30 AI050410.

ACKNOWLEDGMENTS

The authors thank current and past members of the UNC International Center for the Advancement of Translational Science for technical assistance. We also thank husbandry and veterinary staff in the UNC Division of Comparative Medicine.

SUPPLEMENTARY MATERIAL

The Supplementary Material for this article can be found online at: https://www.frontiersin.org/articles/10.3389/fviro.2022.861628/full#supplementary-material

REFERENCES

1. Hjalgrim H, Friborg J, Melbye M. The epidemiology of EBV and its association with malignant disease. In: Arvin A, Campadelli-Fiume G, Mocarski E, Moore PS, Roizman B, Whitley R, Yamanishi K, editors. *Human Herpesviruses: Biology, Therapy, and Immunoprophylaxis.* Cambridge: Cambridge University Press (2007). p. 929–959.
2. Rickinson AB, Callan MF, Annels NE. T-cell memory: lessons from Epstein-Barr virus infection in man. *Philos Trans R Soc Lond B Biol Sci.* (2000) 355:391–400. doi: 10.1098/rstb.2000.0579
3. Thorley-Lawson DA. EBV persistence–introducing the virus. *Curr Top Microbiol Immunol.* (2015) 390(Pt 1):151–209. doi: 10.1007/978-3-319-22822-8_8
4. Thorley-Lawson DA, Gross A. Persistence of the Epstein-Barr virus and the origins of associated lymphomas. *N Engl J Med.* (2004) 350:1328–37. doi: 10.1056/NEJMra032015
5. Maurmann S, Fricke L, Wagner HJ, Schlenke P, Hennig H, Steinhoff J, et al. Molecular parameters for precise diagnosis of asymptomatic Epstein-Barr virus reactivation in healthy carriers. *J Clin Microbiol.* (2003) 41:5419–28. doi: 10.1128/JCM.41.12.5419-5428.2003
6. Bibas M, Antinori A. EBV and HIV-related lymphoma. *Mediterr J Hematol Infect Dis.* (2009) 1:e2009032. doi: 10.4084/MJHID.2009.032
7. Carbone A, Volpi CC, Gualeni AV, Gloghini A. Epstein-Barr virus associated lymphomas in people with HIV. *Curr Opin HIV AIDS.* (2017) 12:39–46. doi: 10.1097/COH.0000000000000333
8. Grogg KL, Miller RF, Dogan A. HIV infection and lymphoma. *J Clin Pathol.* (2007) 60:1365–72. doi: 10.1136/jcp.2007.051953
9. Simard EP, Pfeiffer RM, Engels EA. Cumulative incidence of cancer among individuals with acquired immunodeficiency syndrome in the United States. *Cancer.* (2011) 117:1089–96. doi: 10.1002/cncr.25547
10. Rubinstein PG, Aboulafia DM, Zloza A. Malignancies in HIV/AIDS: from epidemiology to therapeutic challenges. *AIDS.* (2014) 28:453–65. doi: 10.1097/QAD.0000000000000071
11. Powles T, Robinson D, Stebbing J, Shamash J, Nelson M, Gazzard B, et al. Highly active antiretroviral therapy and the incidence of non-AIDS-defining cancers in people with HIV infection. *J Clin Oncol.* (2009) 27:884–90. doi: 10.1200/JCO.2008.19.6626
12. Epeldegui M, Vendrame E, Martinez-Maza O. HIV-associated immune dysfunction and viral infection: role in the pathogenesis of AIDS-related lymphoma. *Immunol Res.* (2010) 48:72–83. doi: 10.1007/s12026-010-8168-8
13. Roos MT, van Lier RA, Hamann D, Knol GJ, Verhoofstad I, van Baarle D, et al. Changes in the composition of circulating CD8+ T cell subsets during acute epstein-barr and human immunodeficiency virus infections in humans. *J Infect Dis.* (2000) 182:451–8. doi: 10.1086/315737
14. Wahl A, Linnstaedt SD, Esoda C, Krisko JF, Martinez-Torres F, Delecluse HJ, et al. A cluster of virus-encoded microRNAs accelerates acute systemic Epstein-Barr virus infection but does not significantly enhance virus-induced oncogenesis *in vivo*. *J Virol.* (2013) 87:5437–46. doi: 10.1128/JVI.00281-13
15. Strowig T, Gurer C, Ploss A, Liu YF, Arrey F, Sashihara J, et al. Priming of protective T cell responses against virus-induced tumors in mice with human immune system components. *J Exp Med.* (2009) 206:1423–34. doi: 10.1084/jem.20081720
16. Yajima M, Imadome K, Nakagawa A, Watanabe S, Terashima K, Nakamura H, et al. A new humanized mouse model of Epstein-Barr virus infection that reproduces persistent infection, lymphoproliferative disorder, and cell-mediated and humoral immune responses. *J Infect Dis.* (2008) 198:673–82. doi: 10.1086/590502
17. Whitehurst CB Li G, Montgomery SA, Montgomery ND, Su L, Pagano JS. Knockout of Epstein-Barr virus BPLF1 retards B-cell transformation and lymphoma formation in humanized mice. *MBio.* (2015) 6:e01574–15. doi: 10.1128/mBio.01574-15

18. Lucht E, Biberfeld P, Linde A. Epstein-Barr virus (EBV) DNA in saliva and EBV serology of HIV-1-infected persons with and without hairy leukoplakia. *J Infect.* (1995) 31:189–94. doi: 10.1016/S0163-4453(95)80025-5
19. Ling PD, Vilchez RA, Keitel WA, Poston DG, Peng RS, White ZS, et al. Epstein-Barr virus DNA loads in adult human immunodeficiency virus type 1-infected patients receiving highly active antiretroviral therapy. *Clin Infect Dis.* (2003) 37:1244–9. doi: 10.1086/378808
20. Pan R, Liu X, Zhou S, Ning Z, Zheng H, Gao M, et al. Differential prevalence and correlates of whole blood Epstein-Barr virus DNA between HIV-positive and HIV-negative men who have sex with men in Shanghai, China. *Epidemiol Infect.* (2017) 145:2330–40. doi: 10.1017/S0950268817001054
21. Byrne CM, Johnston C, Orem J, Okuku F, Huang ML, Rahman H, et al. Examining the dynamics of Epstein-Barr virus shedding in the tonsils and the impact of HIV-1 coinfection on daily saliva viral loads. *PLoS Comput Biol.* (2021) 17:e1009072. doi: 10.1371/journal.pcbi.1009072
22. McHugh D, Myburgh R, Caduff N, Spohn M, Kok YL, Keller CW, et al. EBV renders B cells susceptible to HIV-1 in humanized mice. *Life Sci Alliance.* (2020) 3:e202000640. doi: 10.26508/lsa.202000640
23. Yan Y, Ren Y, Chen R, Hu J, Ji Y, Yang J, et al. Evaluation of Epstein-Barr virus salivary shedding in HIV/AIDS patients and HAART use: a retrospective cohort study. *Virol Sin.* (2018) 33:227–33. doi: 10.1007/s12250-018-0028-z
24. Williams LD, Amatya N, Bansal A, Sabbaj S, Heath SL, Sereti I, et al. Immune activation is associated with CD8 T cell interleukin-21 production in HIV-1-infected individuals. *J Virol.* (2014) 88:10259–63. doi: 10.1128/JVI.00764-14
25. Agudelo-Hernandez A, Chen Y, Bullotta A, Buchanan WG, Klamar-Blain CR, Borowski L, et al. Subclinical herpesvirus shedding among HIV-1-infected men on antiretroviral therapy. *AIDS.* (2017) 31:2085–94. doi: 10.1097/QAD.0000000000001602
26. Gianella S, Moser C, Vitomirov A, McKhann A, Layman L, Scott B, et al. Presence of asymptomatic cytomegalovirus and Epstein–Barr virus DNA in blood of persons with HIV starting antiretroviral therapy is associated with non-AIDS clinical events. *AIDS.* (2020) 34:849–57. doi: 10.1097/QAD.0000000000002484
27. Zdimerova H, Murer A, Engelmann C, Raykova A, Deng Y, Gujer C, et al. Attenuated immune control of Epstein-Barr virus in humanized mice is associated with the multiple sclerosis risk factor HLA-DR15. *Eur J Immunol.* (2021) 51:64–75. doi: 10.1002/eji.202048655
28. Heuts F, Rottenberg ME, Salamon D, Rasul E, Adori M, Klein G, et al. T cells modulate Epstein-Barr virus latency phenotypes during infection of humanized mice. *J Virol.* (2014) 88:3235–45. doi: 10.1128/JVI.02885-13
29. Traggiai E, Chicha L, Mazzucchelli L, Bronz L, Piffaretti JC, Lanzavecchia A, et al. Development of a human adaptive immune system in cord blood cell-transplanted mice. *Science.* (2004) 304:104–7. doi: 10.1126/science.1093933
30. Melkus MW, Estes JD, Padgett-Thomas A, Gatlin J, Denton PW, Othieno FA, et al. Humanized mice mount specific adaptive and innate immune responses to EBV and TSST-1. *Nat Med.* (2006) 12:1316–22. doi: 10.1038/nm1431
31. Audige A, Rochat MA Li D, Ivic S, Fahrny A, Muller CKS, et al. Long-term leukocyte reconstitution in NSG mice transplanted with human cord blood hematopoietic stem and progenitor cells. *BMC Immunol.* (2017) 18:28. doi: 10.1186/s12865-017-0209-9
32. Delecluse HJ, Hilsendegen T, Pich D, Zeidler R, Hammerschmidt W. Propagation and recovery of intact, infectious Epstein-Barr virus from prokaryotic to human cells. *Proc Natl Acad Sci U S A.* (1998) 95:8245–50. doi: 10.1073/pnas.95.14.8245
33. Kumar R, Whitehurst CB, Pagano JS. The Rad6/18 ubiquitin complex interacts with the Epstein-Barr virus deubiquitinating enzyme, BPLF1, and contributes to virus infectivity. *J Virol.* (2014) 88:6411–22. doi: 10.1128/JVI.00536-14
34. Nixon CC, Mavigner M, Sampey GC, Brooks AD, Spagnuolo RA, Irlbeck DM, et al. Systemic HIV and SIV latency reversal via non-canonical NF-kappaB signalling in vivo. *Nature.* (2020) 578:160–5. doi: 10.1038/s41586-020-1951-3
35. Honeycutt JB, Liao B, Nixon CC, Cleary RA, Thayer WO, Birath SL, et al. T cells establish and maintain CNS viral infection in HIV-infected humanized mice. *J Clin Invest.* (2018) 128:2862–76. doi: 10.1172/JCI98968
36. Wahl A, Ho PT, Denton PW, Garrett KL, Hudgens MG, Swartz G, et al. Predicting HIV pre-exposure prophylaxis efficacy for women using a preclinical pharmacokinetic-pharmacodynamic *in vivo* model. *Sci Rep.* (2017) 7:41098. doi: 10.1038/srep41098
37. Kovarova M, Shanmugasundaram U, Baker CE, Spagnuolo RA De C, Nixon CC, et al. HIV pre-exposure prophylaxis for women and infants prevents vaginal and oral HIV transmission in a preclinical model of HIV infection. *J Antimicrob Chemother.* (2016) 71:3185–94. doi: 10.1093/jac/dkw283
38. Olesen R, Swanson MD, Kovarova M, Nochi T, Chateau M, Honeycutt JB, et al. ART influences HIV persistence in the female reproductive tract and cervicovaginal secretions. *J Clin Invest.* (2016) 126:892–904. doi: 10.1172/JCI64212
39. Wahl A, Baker C, Spagnuolo RA, Stamper LW, Fouda GG, Permar SR, et al. Breast Milk of HIV-positive mothers has potent and species-specific *in vivo* HIV-inhibitory activity. *J Virol.* (2015) 89:10868–78. doi: 10.1128/JVI.01702-15
40. Wahl A, Swanson MD, Nochi T, Olesen R, Denton PW, Chateau M, et al. Human breast milk and antiretrovirals dramatically reduce oral HIV-1 transmission in BLT humanized mice. *PLoS Pathog.* (2012) 8:e1002732. doi: 10.1371/journal.ppat.1002732

Conflict of Interest: The authors declare that the research was conducted in the absence of any commercial or financial relationships that could be construed as a potential conflict of interest.

frontiers in Virology

ORIGINAL RESEARCH
published: 23 March 2022
doi: 10.3389/fviro.2022.836125

MAL Inhibits the Production of HIV-1 Particles by Sequestering Gag to Intracellular Endosomal Compartments

Kei Miyakawa[1]*, *Mayuko Nishi*[1], *Sundararaj Stanleyraj Jeremiah*[1], *Yuko Morikawa*[2] *and Akihide Ryo*[1]*

[1] Department of Microbiology, School of Medicine, Yokohama City University, Kanagawa, Japan, [2] Graduate School of Infection Control Sciences, Kitasato University, Tokyo, Japan

The host innate immune response is the first line of defense against human immunodeficiency virus (HIV) infection. The type I interferon (IFN) response is a robust anti-viral response that induces the transcription of several IFN-stimulated genes (ISGs). However, the effects of ISGs, particularly on the HIV-1 Gag protein, remain largely unknown. Hence, we screened ISG-encoded proteins by bioluminescence resonance energy transfer to identify the crucial host effectors that suppressed Gag function. Consequently, we identified the transmembrane protein MAL as a Gag-interacting ISG product. In fact, ectopic expression of MAL substantially inhibited the production of HIV-1 particles, leading to the translocation, accumulation, and eventual lysosomal degradation of Gag in the host endosomal compartments. Owing to the conserved N-terminal region of MAL, which specifically interacts with HIV-1 Gag, this particular antiviral function of MAL targeting Gag is also conserved among orthologs of various animal species. Notably, the antiviral activity of MAL was partially antagonized by the viral accessory protein Nef, as it interfered with the interaction between MAL and Gag. Therefore, this study reveals a previously unidentified antiviral function of MAL and its viral counteraction. It also sheds new light on therapeutic strategies against HIV-1 infection based on the intrinsic antiviral immunity of host cells.

Keywords: HIV-1, interferon-stimulated genes, Gag, antiviral immunity, innate immunity

OPEN ACCESS

Edited by:
Akio Adachi,
Kansai Medical University, Japan

Reviewed by:
Mikako Fujita,
Kumamoto University, Japan
Kazuaki Monde,
Kumamoto University, Japan

***Correspondence:**
Kei Miyakawa
keim@yokohama-cu.ac.jp
Akihide Ryo
aryo@yokohama-cu.ac.jp

Specialty section:
This article was submitted to Fundamental Virology, a section of the journal Frontiers in Virology

Received: *15 December 2021*
Accepted: *07 March 2022*
Published: *23 March 2022*

Citation:
Miyakawa K, Nishi M, Jeremiah SS, Morikawa Y and Ryo A (2022) MAL Inhibits the Production of HIV-1 Particles by Sequestering Gag to Intracellular Endosomal Compartments. Front. Virol. 2:836125. doi: 10.3389/fviro.2022.836125

INTRODUCTION

Human immunodeficiency virus type 1 (HIV-1) is the causative agent of acquired immunodeficiency syndrome (AIDS). Its genome comprises nine genes: three structural genes (*gag*, *pol*, and *env*), two regulatory genes (*rev* and *tat*), and four accessory genes (*nef*, *vpu*, *vif*, and *vpr*) (1). The Gag structural protein is synthesized as a precursor polyprotein ($Pr55^{Gag}$) consisting of four major domains: matrix

Abbreviations: HIV-1, Human immunodeficiency virus 1; IFN, Interferon; ISG, Interferon-stimulated gene; AIDS, Acquired immunodeficiency syndrome; MA, Matrix; MVBs, Multivesicular bodies; PM, Plasma membrane; NanoLuc, NanoLuciferase; NanoBRET, NanoLuciferase-based bioluminescence resonance energy transfer.

(MA), capsid (CA), nucleocapsid (NC), and p6, and two spacer sequences: SP1 and SP2. During late HIV-1 replication, the Gag protein is transported to the plasma membrane (PM) where it is assembled and multimerized for viral budding (2, 3). The MA domain of the Gag polyprotein helps transport it to the PM by interacting with anionic membrane lipids, such as phosphatidylinositol 4,5-bisphosphate (PIP2) (4, 5).

In the infected cells, HIV-1 targets various host factors to promote the production of progeny virions. On the other hand, host cells express antiviral factors that inhibit key steps of viral replication (6). Interferons (IFNs) are antiviral signaling proteins that are secreted by an infected cell during viral infection. They induce the expression of an array of antiviral proteins in both the infected and the surrounding non-infected cells. Furthermore, IFNs are classified into three categories: types I, II, and III. Notably, type I and type III IFNs are involved in establishing an antiviral tissue environment (7). These IFNs inhibit HIV replication at various stages of the viral life cycle by promoting the expression of IFN-stimulated gene (ISG) products. For example, the ISG-encoded proteins APOBEC3G and BST2/tetherin abrogate HIV replication by targeting reverse transcription of the HIV genome and the release of the virus, respectively (8). However, HIV has evolved and acquired accessory proteins, such as Vif and Vpu, to counter the function of the antiviral ISG products (9, 10). Indeed, these ISG products are specifically targeted for degradation by the host ubiquitin-proteasomal pathway or lysosome pathway, sustaining viral replication.

Previously studies have shown that several host proteins induced by type I and type III IFNs suppress the production of viral particles (11, 12). However, which ISG product targets the translocation of $Pr55^{Gag}$ to the PM and its multimerization for the production and assembly of viral particles during HIV-1 biogenesis is not fully clarified. We therefore screened for intracellular protein-protein interactions by generating a library of ISGs using NanoLuciferase (NanoLuc)-based bioluminescence resonance energy transfer (NanoBRET). In this study, we utilized the NanoBRET technology to identify putative host proteins that bind to Gag and potently restrict HIV replication. Consequently, we identified the tetraspanin membrane protein MAL as a novel ISG product that targets Gag and exhibits anti-HIV activities. Additionally, we found that the HIV accessory protein Nef antagonizes the antiviral function of MAL, sustaining viral replication.

MATERIALS AND METHODS

Cells and Plasmids

We cultured HEK293 cells (ATCC, #CRL-1573) in Dulbecco's Modified Eagle Medium supplemented with 10% fetal bovine serum (FBS). Additionally, we cultured PC3 (ATCC, #CRL-1435) and CEM cells in RPMI supplemented with 10% FBS. The human codon-optimized $HIV\text{-}1_{NL4\text{-}3}$ Gag and Nef, and non-human MAL cDNAs were synthesized and subcloned into pEGFP- or pcDNA-based vectors. Mutants were generated by PCR-based mutagenesis procedures. The HIV-1 molecular clone pNL4-3, pNL4-3/Gag-EGFP, pNL4-3/Fyn10WT and pNL4-3/Fyn10ΔMA have been described previously (13, 14). We obtained the pNL4-3 plasmid defective in *nef* from the NIH HIV reagent program (catalogue number ARP-12755). Expression vectors encoding HaloTag-conjugated ISG-encoded proteins were collected by Kazusa Genome Technologies (Chiba, Japan) and purchased from Promega. Plasmids encoding GFP-tagged LC3 and RhoB were obtained from Addgene (catalogue number #11546) and Takara-Bio (catalogue number #632490), respectively. NCBI accession numbers of MAL genes are: *Homo sapiens* (AB529205), *Macaca mulatta* (XM_015112833), *Mus musculus* (NM_010762), *Gallus gallus* (NM_001199391), and *Danio rerio* (NM_001017686).

NanoBRET

We transfected HEK293 cells in 96-well white plates with vectors encoding the HaloTag-fused ISG-encoded protein (100 ng) and NanoLuc-fused Gag or Nef (1 ng). The NanoBRET activity was measured at 48 h post-transfection using the NanoBRET Nano-Glo Detection System (Promega). First, cells were co-transfected with C-terminal NanoLuciferase (NL)-conjugated Gag and N-terminal HaloTag (HT)-fused ISG expression vectors. Subsequently, the HT-618 ligand and furimazine substrate were added. If two proteins were within 200 nm of each other, NanoBRET signals were detected. The NanoBRET signals of the interaction between Gag-NL and Gag-HT was used as a positive control.

HIV-1 Production Assay

HEK293 or PC3 cells seeded in 12-well plates were co-transfected with pNL4-3 and either an ISG-encoded protein expression vector or an empty vector using Effectene (Qiagen) for HEK293 cells or Lipofectamine 3000 (Thermo) for PC3 cells. In experiments with siRNA, cells were transfected with 20 pmol of siRNA using Lipofectamine RNAiMAX (Thermo) one day prior to transfection with pNL4-3. Two days post-transfection, cell lysates and supernatants were harvested and subjected to immunoblotting. In some experiments, 10 μM MG132 (Merck #474790) or 100 μM chloroquine (Cayman Chemical #14194) were added 16 h before cells were harvested. The p24 antigen levels in the supernatants were measured using an ELISA kit (Zepto Metrix). siRNAs were purchased from Qiagen (catalogue number #SI03650318 for the negative control and #SI00627214 and #SI00627228 for MAL).

HIV-1 Multicycle Assay

Replication-competent HIV-1 stocks were produced by transient transfection of HEK293 cells with the pNL4-3 or pNL4-3ΔNef plasmids. Culture supernatants containing HIV-1were collected 48 h after transfection and filtered through a 0.45 μm Millex-HV filter (Merck).

CEM cells (10^6 cells) were transfected with 50 pmol of siRNAs using a 4D-Nucleofector (Lonza) with electroporation program CL-120, following the manufacturer's instructions. At 24 h post-transfection, the CEM cells were infected with 25 ng of the HIV-1 p24 antigen. The cells were then centrifuged for 90 min at 800 x *g*

with 5 μg/ml polybrene, and subsequently washed three times with PBS to remove the added viruses. Thereafter, we periodically collected the nascent virions that were produced by the infected cells and measured the p24 levels as described in section 2.3.

Immunoprecipitation

HEK293 cells seeded in six-well plates were transfected with Gag-FLAG-encoding vector and the HT-tagged protein expression plasmid with or without the Nef expression plasmid (500 ng each). At 48 h post-transfection, the cells were lysed with an HBST buffer (10 mM HEPES pH 7.4, 150 mM NaCl, and 0.5% Triton-X-100) containing a protease inhibitor cocktail (Merck #11697498001). The cell lysates were immunoprecipitated using an anti-FLAG EZview Red Affinity Gel (Merck #F2426) for 16 h, and the bound proteins were analyzed by immunoblotting as follows. Samples dissolved in SDS loading buffer were loaded and electrophoresed using 10% polyacrylamide gels, and the separated proteins were blotted onto PVDF membranes (Merck). Subsequently, the membranes were probed with primary antibodies and horseradish peroxidase-conjugated secondary antibodies (Cytiva). The detected proteins were visualized using a FluorChem imaging system (Alpha Innotech) or LuminoGraph imaging system (Atto). Protein bands were analyzed using ImageJ software (NIH). Primary antibodies used in this study included the following: HaloTag (Promega #G9211), FLAG (Merck #F3165), GFP (MBL #598), vinculin (Merck #V9131), p24 (NIH HIV reagent program #ARP-3537), and Nef (Thermo #MA1-71501).

Immunofluorescence

For the immunofluorescence assay, HepG2 cells were seeded onto glass cover slips one day before transfection. At 24 or 48 h post-transfection, the cells were fixed with 4% paraformaldehyde and permeabilized with 0.5% Triton X-100. Thereafter, the cells were stained with anti-HaloTag (Promega #G9281) and Alexa Fluor594-conjugated secondary antibody (Thermo #A48284).

RESULTS

Identification of Gag-Binding Proteins That Inhibit HIV-1 Production

We prepared a human cDNA library comprising 723 ISG products based on the Interferome database (http://www.interferome.org/). While preparing this library, we only selected the ISG products whose expression was induced more than 1.5-fold following treatment with type I or III IFNs (15). Subsequently, to identify the ISG products that interacted with Gag, we performed a high-throughput screening of the library by co-expressing the C-terminus of the NanoLuc-conjugated HIV-1 Gag protein with each of the 723 ISG products in HEK293 cells. Moreover, we analyzed the protein–protein interactions by NanoBRET. In the first screening, we selected 62 ISGs as potential candidates whose products bind to the Gag protein (**Figure 1A**). Since Gag is the major structural protein required for viral particle formation, we investigated whether these candidates hindered viral particle production. To this end, we performed a second screening wherein we co-transfected HEK293 cells with the candidate ISG products and pNL4-3 and estimated the Gag p24 antigen levels in the culture supernatant by ELISA. We found that five ISG-encoded proteins (MAL, ZNF36L2, ZNF36, TCIRG1, and BCMP1) significantly inhibited the production of HIV-1 particles without causing apparent cytotoxicity (**Figure 1B**). Indeed, they inhibited viral particle production more prominently than the known antiviral factor IFITM2, which also targets Gag (16).

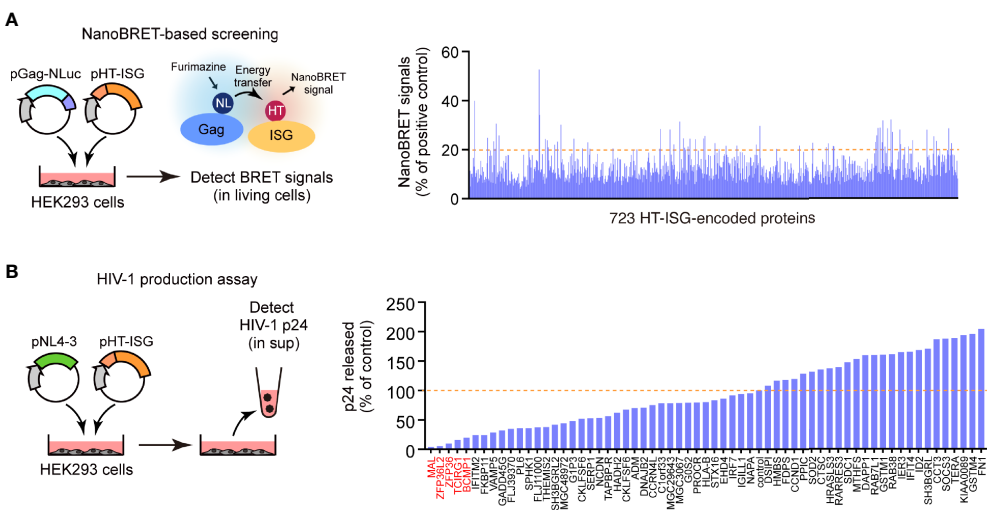

FIGURE 1 | Identification of Gag-binding proteins that inhibit HIV-1 production. **(A)** NanoBRET-based screening identified 723 Gag-interacting proteins encoded by interferon-stimulated genes (ISGs) in HEK293 cells. **(B)** HIV particle production assay. HEK293 cells were co-transfected with the HIV molecular clone pNL4-3 and ISG-encoded protein expression vectors. Two days post-transfection, viral p24 antigen levels in the culture supernatants were measured by ELISA.

Moreover, a single round of infection using VSVg-pseudotyped reporter viruses revealed that these proteins did not interfere with the early stages of the HIV life cycle (from cell entry to reporter gene expression; **Supplementary Figure S1**). Therefore, we selected these five candidate proteins for further in-depth functional analyses.

MAL Inhibits Gag Protein Assembly at the Plasma Membrane

Our immunoprecipitation analysis validated the interactions between the candidate proteins and Gag, as all the candidate proteins co-immunoprecipitated with Gag (**Figure 2A** and **Supplementary Figure S2A**). We also found that these proteins decreased viral particle production in a dose-dependent manner; this decrease was accompanied by a massive reduction in intracellular Gag levels (**Figure 2B**). Since, the Gag protein accumulates, assembles, and multimerizes on the PM prior to HIV-1 particle formation, we examined its localization upon overexpressing the five candidate proteins with Gag-GFP. Notably, Gag was localized on the PM in cells that overexpressed ZNF36, TCIRG1, BCMP1, and ZNF36L2 (**Supplementary Figure S2B**). However, Gag was mostly located in the cytoplasmic puncta and hardly localized to the PM in cells overexpressing MAL (**Figure 3A** and **Supplementary Figure S3**). Since MAL primarily localizes to the PM and endosomes (17), we hypothesized that Gag accumulated in the endosomal puncta in the MAL-overexpressing cells. Consistent with this hypothesis, we discovered that Gag was co-localized with the endosomal marker RhoB, but not with the autophagosomal marker LC3 (**Figure 3B**). Furthermore, we found that chloroquine (a lysosome inhibitor) and not MG132 (a proteasome inhibitor) inhibited MAL-mediated Gag degradation (**Figure 3C**). Thus, we deduced that MAL hindered the translocation of Gag to the PM by sequestering it to endosomal compartments, eventually leading to its lysosomal degradation.

Antiviral Effect of Endogenous MAL Against HIV-1

We next examined the effect of endogenous expression of MAL on HIV-1 production in PC3 cells, which are known to functionally express MAL (18). We treated the cells with two different MAL-targeting siRNAs, which had 90% knockdown efficiencies, and then transfected them with pNL4-3 (**Figure 4A** and **Supplementary Figure S4**). Compared with the control cell supernatants, the MAL-knockdown cell supernatants had a 3- to 4-fold increase in p24 levels, reflecting increased HIV-1 production (**Figure 4B**). To further investigate the function of MAL in multi-round HIV-1 infection, we transduced CEM cells with MAL-targeting siRNA and infected them with replication-competent HIV-1. Subsequent calculation of p24 levels revealed that viral infection was significantly enhanced in MAL-silenced CEM cells compared to those in control cells (**Figures 4C, D**). We confirmed an incremental increase in cellular $Pr55^{Gag}$ in cells with MAL knockdown (**Figures 4B, D**). Together, these results indicate that endogenous MAL negatively regulates HIV-1 replication by degrading $Pr55^{Gag}$.

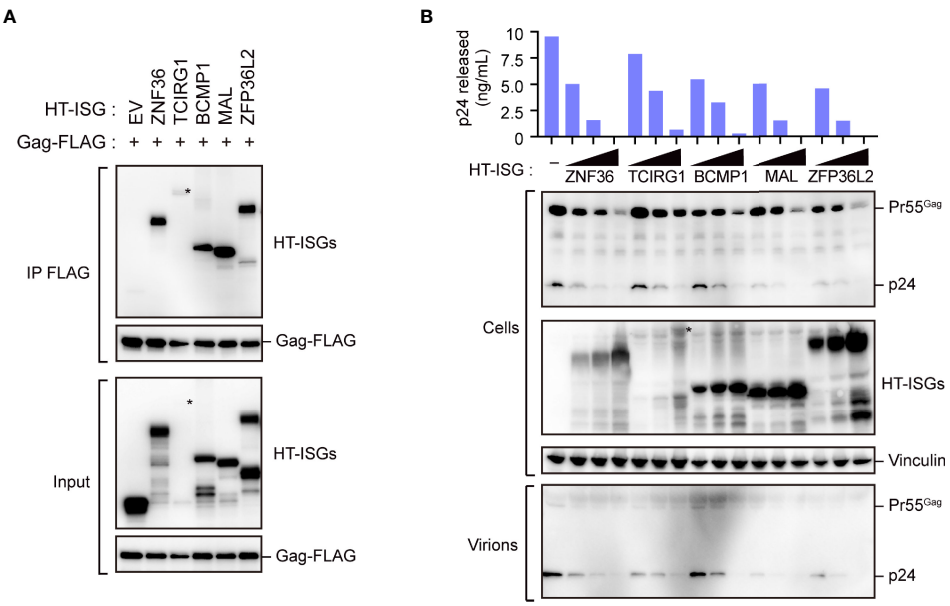

FIGURE 2 | Characterization of Gag-binding proteins. **(A)** Immunoprecipitation of HEK293 cells with Gag-FLAG and indicated HaloTag (HT)- interferon-stimulated gene (ISG)-encoded protein expression vectors. Cell lysates were precipitated with anti-FLAG, followed by immunoblotting. Asterisks on the blot indicate TCIRG1 expression. Longer exposure blot of input sample is shown in **Supplementary Figure S2A**. **(B)** HIV particle production assay. HEK293 cells were co-transfected with the HIV molecular clone pNL4-3 and the indicated ISG-encoded protein expression vectors. Two days post-transfection, cell lysates (Cells) and the culture supernatants (Virions) were subjected to immunoblotting. Viral p24 antigen in the culture supernatants was measured by ELISA.

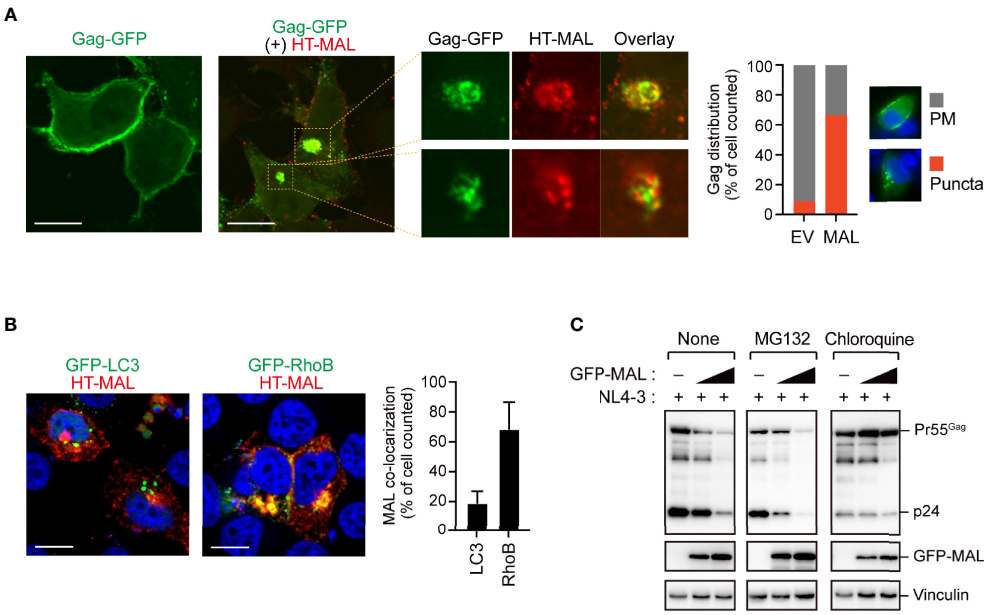

FIGURE 3 | MAL inhibits translocation of Gag to the plasma membrane. **(A)** Confocal microscopy images of HepG2 cells expressing pNL4-3/Gag-EGFP and HaloTag (HT)-conjugated MAL proteins. The third image in this panel is the expanded view. Note that other viral proteins except Pol were expressed in this experiment. Scale bar, 10μm. Low magnification images, including other cells, are shown in **Supplementary Figure S3**. The graph on the right shows the percentage of cells in which Gag-GFP localized at the PM or in cytoplasmic puncta (n > 20 cells). **(B)** Confocal micrographs showing HepG2 cells expressing HT-MAL and either GFP-LC3 (autophagosomal marker) or GFP-Rho3 (endosomal marker). Nuclei were stained with DAPI. Scale bar, 10μm. The graph on the right shows the percentage of cells in which MAL localized to LC3- or RhoB-positive structures (n > 20 cells). **(C)** Lysosomal inhibitor blocks MAL-mediated Gag degradation. HEK293 cells were co-transfected with pNL4-3 and the MAL expression vectors. Two days post-transfection, cell lysates were subjected to immunoblotting. The compounds indicated in the figure were added 16 h before the cells were harvested.

The Gag MA Domain Is a Key Target of MAL-Mediated Inhibition

Since the MA and NC domains of the Gag protein are specifically involved in localizing Gag to the PM (3), we next mapped the MAL-binding sites on $Pr55^{Gag}$ using several domain mutants. Our immunoprecipitation analysis revealed that the polyprotein mutant lacking the MA domain, but not the NC domain, exhibited reduced binding to MAL (**Figure 5A**). This suggested that the MA domain is responsible for the interaction of Gag with MAL. Since MAL has four transmembrane domains, we generated MAL mutants lacking either the N-terminus or the C-terminus for further immunoprecipitation analysis. Consequently, we observed that Gag could interact with the MAL mutant that lacked the C-terminal region (**Figure 5B**). Consistently, the MA domain of Gag interacted with the N-terminal half of MAL, indicating that Gag binds to the N-terminal domain of MAL. To investigate whether this interaction is a prerequisite for the anti-HIV activity of MAL, we examined its inhibitory effect on Gag mutants lacking the MA domain. To this end, we co-transfected cells with GFP-MAL and pNL4-3 encoding either wild-type Gag or MA-deleted Gag with the Fyn peptide (Fyn10WT or Fyn10ΔMA), which can associate with the PM (5). Subsequent immunoblotting analysis revealed that the amount of MA-deleted Gag was not reduced in the cells, whereas that of the wild-type Gag was prominently reduced under identical conditions (**Figure 5C**). These results suggested that MAL inhibits Gag *via* the MA domain. We further found that both Gag mutants, which lack PM-targeting activity due to the absence of a myristoyl group (G2A) or highly basic domain (6A2T), had low binding activity to MAL (**Supplementary Figures S5A, B**). Together, these results suggest that the PM targeting of Gag is necessary for MAL interaction.

Since the N-terminus of MAL is conserved among animal species (**Figure 5D**), we analyzed whether the inhibitory function of MAL is also conserved across the orthologs of other animal species, including *Macaca mulatta* (rhesus monkey), *Mus musculus* (mouse), *Gallus gallus* (chicken), and *Danio rerio* (zebrafish). Our results revealed that all orthologs could reduce intracellular Gag levels (**Figure 5D**), suggesting that the antiviral function of MAL has been conserved during evolution.

Nef Partially Overcomes the Antiviral Activity of MAL

As our above results suggested that HIV-1 can replicate to an extent even in MAL-expressing T cells (**Figure 4D**), we hypothesized that HIV-1 can possibly counteract the antiviral activity of endogenous MAL. A previous study reported that the HIV-1 accessory protein Nef induces MAL-dependent massive secretion of exosomal markers, inducing the efficient fusion of the endosomes with the PM (19). Thus, we examined whether Nef could regulate the antiviral effect of MAL using wild-type HIV-1 and HIV-1 lacking the Nef, Vpu, and Env proteins, which

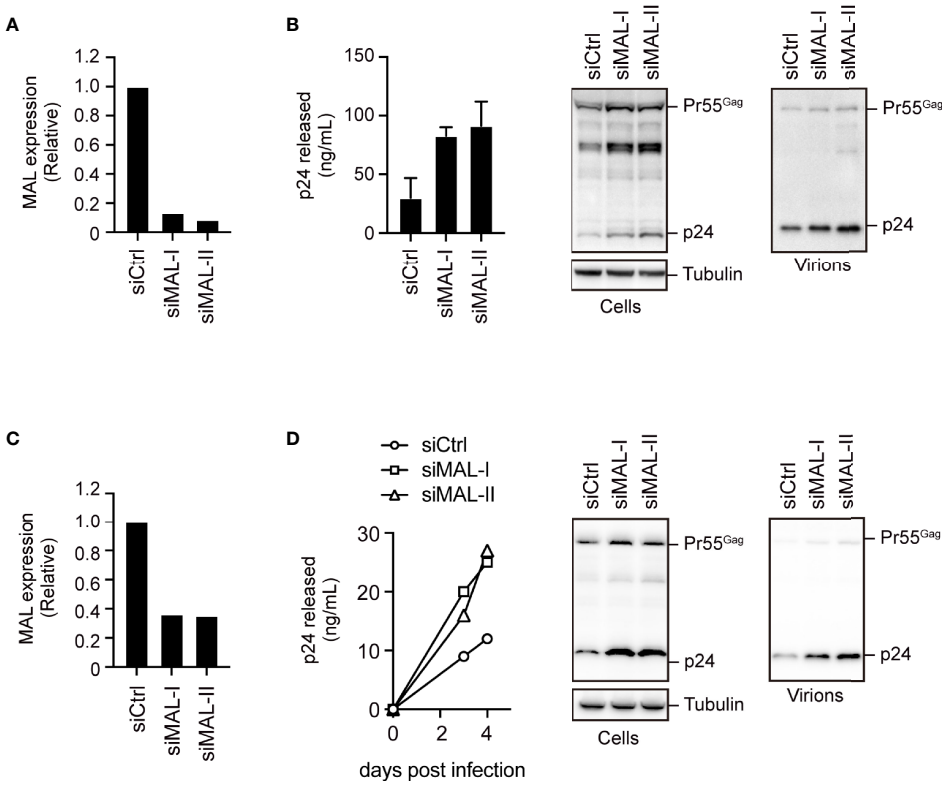

FIGURE 4 | Endogenous MAL expression inhibits HIV-1 production. **(A, B)** PC3 cells transduced with control-(Ctrl) or MAL-targeting siRNAs (siMAL-I and siMAL-II) were transfected with pNL4-3. MAL knockdown was confirmed by RT-PCR **(A)**. Following transfection, cell lysates (Cells) and the culture supernatants (Virions) were subjected to immunoblotting and p24 levels were measured by ELISA **(B)**. **(C, D)** CEM T cells transduced with indicated siRNAs were infected with HIV-1. MAL knockdown was confirmed by RT-PCR **(C)**. The supernatants were harvested at 3 and 4 days post-infection and p24 levels were measured by ELISA. At 4 days post-infection, cell lysates and the culture supernatants (virions) were subjected to immunoblotting **(D)**.

might bind to the host membrane proteins. Our results demonstrated that the antiviral activity of MAL was enhanced in HIV-1 lacking Nef, but not in HIV-1 lacking Vpu and Env (**Figure 6A**). In MAL-expressing cells, the levels of $Pr55^{Gag}$ in the ΔNef virus were reduced compared to that of the WT virus (**Figure 6B**). In PC3 cells, the production of ΔNef virus was lower than that of the WT virus, but this reduction was not observed in MAL-depleted PC3 cells (**Figure 6C**). Consistent with this, intracellular $Pr55^{Gag}$ levels of ΔNef virus were recovered by MAL knockdown (**Figure 6D**). Moreover, multi-round HIV-1 infection analysis revealed that reduced ΔNef virus replication was also recovered by MAL knockdown (**Figure 6E**). Together, these results suggest that Nef may rescue MAL-mediated Gag degradation, promoting HIV production.

In fact, we detected a proximal interaction between Nef and MAL using NanoBRET (**Figure 6F**), suggesting that they are in close proximation in living cells. Interestingly, Nef mutants devoid of their membrane-targeting ability (G2A mutants) exhibited reduced NanoBRET signals. In contrast, Nef mutants lacking the PxxP motifs, which are important for binding of Nef to Src kinases (20), could still bind to MAL (**Figure 6F**). These results suggested that Nef was adjacent to MAL at the host PM. Notably, our immunoprecipitation analysis revealed that Nef interfered with the binding between MAL and Gag (**Figure 6G**), implying that Nef impedes the antiviral function of MAL against Gag. The immunofluorescence analysis also showed that in the absence of Nef, MAL was present in both the PM and intracellular endosomes. However, in the presence of Nef, MAL was primarily localized to the PM without localizing to the endosomes (**Figure 6H** and **Supplementary Figure S6**). These results suggest that Nef attenuates the antiviral activity of MAL by interfering with its localization to the PM and the endosomes, inhibiting accumulation of Gag in the endosomal compartments.

DISCUSSION

In this study, we identified several novel Gag-binding ISG-products that negatively regulate HIV-1 particle production. We revealed that MAL has an anti-HIV function, as it sequesters Gag into the endosomal components. We also found that the viral accessory protein Nef antagonizes the antiviral function of MAL by interfering with the binding between MAL and Gag (**Figure 7**).

MAL is a 17 kDa membrane protein consisting of four transmembrane domains. It was first identified in human T

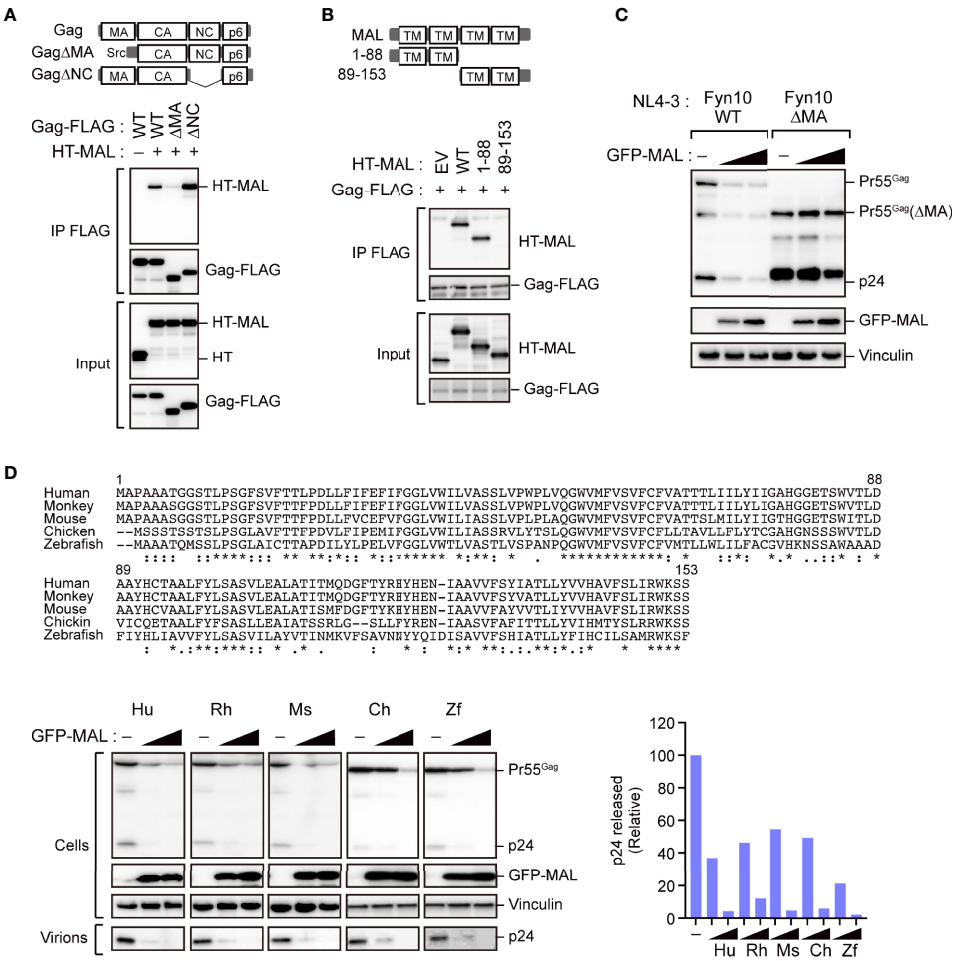

FIGURE 5 | The matrix domain of Gag is a major target for MAL-mediated inhibition. **(A)** MAL binds to the MA domain of Gag. Immunoprecipitation assays of HEK293 cells expressing the specified Gag-FLAG mutants and HaloTag (HT)-MAL. Cell lysates were precipitated with anti-FLAG antibodies, followed by immunoblotting. WT, wild-type; Δ, gene deletion. **(B)** N-terminus of MAL binds to Gag. Immunoprecipitation assays of HEK293 cells expressing the indicated HT-MAL mutants and Gag-FLAG. Cell lysates were precipitated with anti-FLAG antibodies, followed by immunoblotting. **(C)** MA-deleted Gag is resistant to MAL. HEK293 cells were co-transfected with pNL4-3/Fyn(10)full MA or pNL4-3/Fyn(10)ΔMA and GFP-MAL. Two days post-transfection, cell lysates were subjected to immunoblotting. **(D)** Antiviral activity of MAL is conserved across animal species. Sequence alignment of MAL across the specified animal species (top). The symbols below the alignment show the conserved residues (*), conservative substitutions (:) and semi-conservative substitutions (.). HEK293 cells were co-transfected with the HIV molecular clone pNL4-3 and the specified MAL expression vectors. Two days post-transfection, cell lysates (Cells) and the culture supernatants (Virions) were subjected to immunoblotting (bottom left). p24 antigen levels in the culture supernatants were also measured by ELISA (bottom right).

lymphocytes (21). Moreover, it localizes to lipid raft microdomains of the PM, endosomes, and trans-Golgi networks (17), and is expressed in human T cells, epithelial cells, and myelin-forming cells (22). In T cells, MAL is involved in transporting proteins to the cell membrane, the secretion of exosomes or multivesicular bodies (MVBs), and in organizing immune synapses (23–25). Although the role of MAL in HIV-1 replication has not been reported to date, a previous study did report its involvement in the viral propagation of HSV-1 (26). Here, we demonstrate that MAL also targets the HIV-1 protein Gag and interferes with its transport to the PM, where HIV-1 particles are formed.

Although previous studies have shown that translocation of Gag to the PM and sorting of endosomes is crucial for efficient viral production, the precise molecular mechanisms underlying the intracellular dynamics of Gag remain unclear. The Gag protein is transported to the PM *via* N-terminal myristoylation and the basic patch on the MA domain (27, 28). However, the role of endosomes or MVBs in active transportation has not been well characterized. Indeed, the MA domain contains a myristoyl group that enables the stable binding of Gag to PIP2 on the PM and is involved in its stable localization to the PM (4, 5, 29). This localization is necessary and sufficient to trigger viral assembly. Our results revealed that MAL promotes the localization of Gag to intracellular endosomal vesicles rather than the PM *via* interacting with the MA domain; however, the detailed molecular mechanism underlying this phenomenon remains elusive.

We also found that Nef antagonizes the antiviral function and interaction of MAL with Gag. Previous studies have

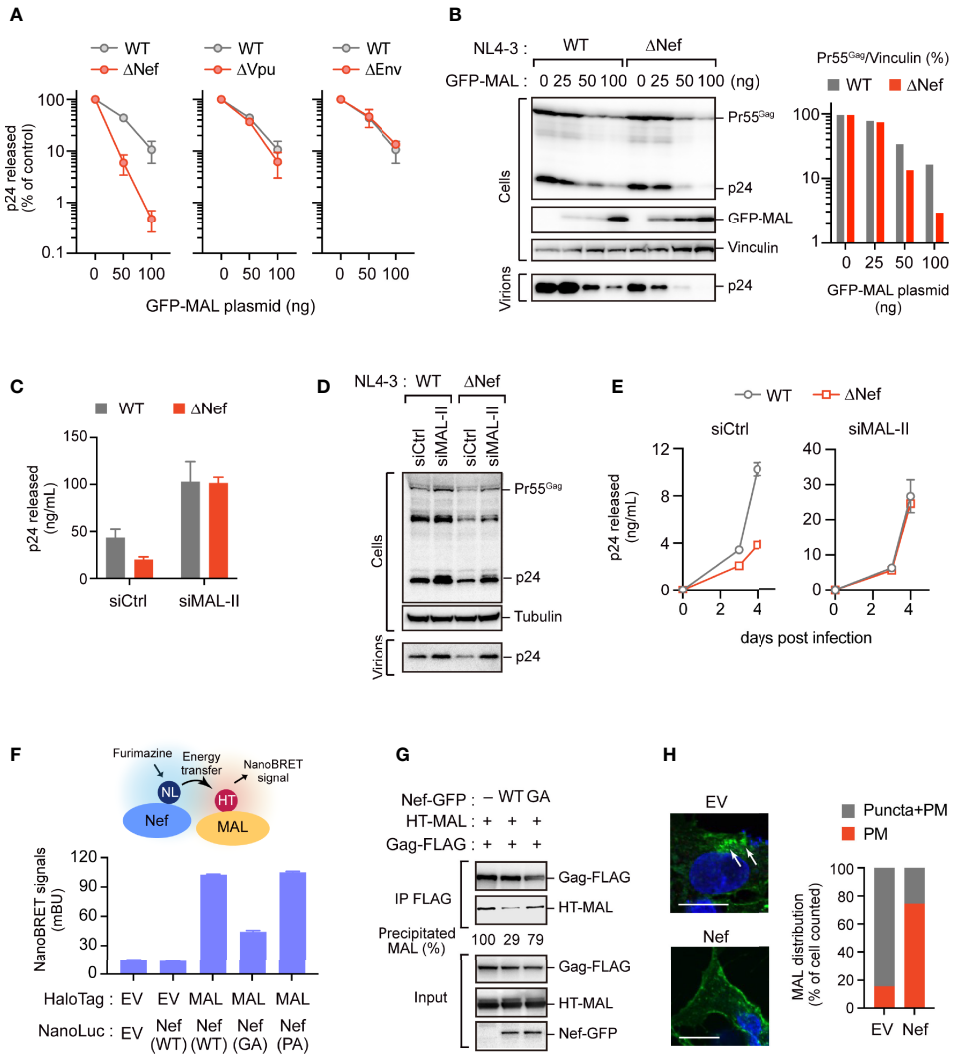

FIGURE 6 | Nef partially overcomes the antiviral activity of MAL. **(A, B)** HEK293 cells were transfected with the HIV-1 molecular clone pNL4-3 lacking *nef*, *vpu*, or *env*, and the GFP-MAL expression vector. Two days post-transfection, p24 levels in the supernatants were assessed by ELISA **(A)**. Cell lysates were subjected to immunoblotting **(B)**. Bar graph shows the relative $Pr55^{Gag}$ levels normalized to vinculin levels as determined by densitometry. WT, wild-type; Δ, gene deletion. **(C, D)** PC3 cells transduced with control-(Ctrl) or MAL-targeting siRNA (siMAL-II) were transfected with pNL4-3 or pNL4-3ΔNef. Cell lysates (Cells) and supernatants (Virions) were subjected to immunoblotting and p24 levels were measured by ELISA. **(E)** CEM T cells transduced with Ctrl or siMAL-II were infected with HIV-1 or Nef-deficient HIV-1. The supernatants were harvested at 3 and 4 days post-infection and p24 levels were measured by ELISA. **(F)** Nef associates with MAL. HEK293 cells were co-transfected with C-terminal NanoLuciferase (NL)-conjugated Nef and HaloTag (HT)-MAL expression vectors. Two days post-transfection, NanoBRET signals from cells were measured. WT, wild-type; GA, G2A mutation; PA, P72,75A mutation. **(G)** Nef inhibits the Gag-MAL interaction. Immunoprecipitation assays of HEK293 cells expressing Gag-FLAG and HT-MAL in the presence or absence of Nef. Cell lysates were precipitated with anti-FLAG antibodies, followed by immunoblotting analysis. Precipitated MAL levels (relative) were also shown, determined by densitometry. **(H)** Nef inhibits the internalization of MAL. Confocal microscopy images of HepG2 cells expressing GFP-MAL and Nef-FLAG. Note that no other viral proteins were expressed in this experiment. Nuclei were stained with DAPI. Arrows indicate internalized MAL. Scale bar, 10μm. Low magnification images, including other cells, are shown in **Supplementary Figure S6**. The graph on the right shows the percentage of cells in which GFP-MAL localized at the PM or in cytoplasmic puncta ($n > 20$ cells).

demonstrated that Nef stabilizes the localization of Gag to the PM; nevertheless, the underlying mechanism is as yet unknown (30, 31). In this study, we found that Nef possibly stabilizes the localization of Gag to the PM by antagonizing the antiviral function of endogenous MAL. Consistently, we also observed that despite endogenous MAL exhibiting antiviral activity, a low level of virus particles was still produced. These results suggest that the stoichiometric relationship between Nef and MAL can determine the efficiency of viral replication.

Multiple studies have reported the functional interactions between HIV-1 Nef and MAL. Indeed, Nef promotes the secretion of exosomes and microvesicles, which is mediated by MAL (32–34). Consistently, the activity of Nef is inhibited upon knockdown of MAL (19). In our current study, we revealed an

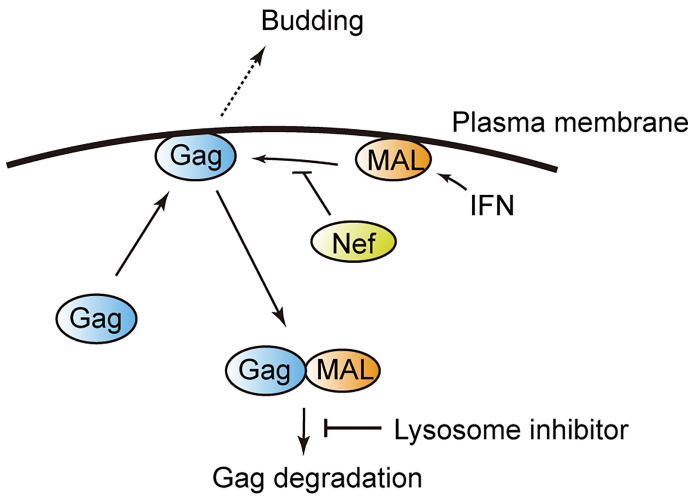

FIGURE 7 | Model illustrating MAL-induced Gag degradation. MAL targets the matrix domain of the HIV-1 Gag protein and induces its degradation *via* the endolysosomal pathway. The viral protein Nef inhibits this interaction, overcoming the antiviral activity of MAL.

additional function of MAL in inhibiting HIV-1 particle production *via* sequestrating Gag to endosomal compartments. It is possible that Nef directs the function of MAL for exosome secretion rather than HIV-1 inhibition, sustaining HIV-1 particle production. This interesting hypothesis needs to be addressed in the future.

Our immunoprecipitation data reveal that Nef physically associates with MAL, blocking its binding to Gag. However, other mechanism(s) of its action on Gag need to be further explored. For example, Nef is known to alter the lipid content and protein properties of the PM (35, 36). Likewise, it is possible that Nef also alters the content, properties, and structure of MAL in the PM.

Owing to our analysis of the MAL orthologs in different species, we verified the antiviral effects of MAL derived from zebrafish; the MAL amino acid sequence of zebrafish has approximately 50% homology to that of human MAL. Thus, we deduced that a conserved region of these sequences is possibly crucial for HIV-1 inhibition. In this regard, we discovered that the N-terminus of the MAL protein is conserved among different animal species and is important for its binding to Gag. Nevertheless, the functional significance of the N-terminus of MAL binding to the Gag MA domain and sequestering Gag to the endosomal compartments is still undetermined. Although we found that the membrane binding activity of the MA domain is required for the interaction between Gag and MAL, it is interesting that the anti-retroviral function of MAL is conserved across multiple animal species.

In summary, our results demonstrate that MAL is an anti-HIV factor that targets Gag. It also facilitates the internalization and degradation of Gag-expressing viral particles. However, its antiviral effect is antagonized by the viral protein Nef. Thus, our findings shed new light on the molecular mechanisms underlying the HIV-1 degradation pathway in the innate immune system. Importantly, MAL and other molecules of this pathway are potential novel therapeutic targets for AIDS and related disorders.

DATA AVAILABILITY STATEMENT

The original contributions presented in the study are included in the article/**Supplementary Material**. Further inquiries can be directed to the corresponding authors.

AUTHOR CONTRIBUTIONS

KM designed and performed the research, analyzed the data, and wrote the manuscript. MN and SJ performed the research and analyzed the data. YM contributed reagents and analyzed the data. AR directed the research, analyzed the data, and wrote the manuscript. All authors contributed to the article and approved the submitted version.

FUNDING

This work was supported in part by JSPS KAKENHI Grants (JP19K07594 and JP20H03498) and AMED Grants (JP20fk0410020 and JP21fk0410039).

ACKNOWLEDGMENTS

The authors thank Dr. Akira Ono for providing NL4-3/Fyn10WT and pNL4-3/Fyn10ΔMA, and Kazufusa Takahashi and Kenji Yoshihara for their technical assistance. The following reagents were obtained through the NIH HIV

Reagent Program, Division of AIDS, NIAID, NIH: Anti- HIV-1 p24 Monoclonal (183-H12-5C), ARP-3537, contributed by Dr. Bruce Chesebro and Kathy Wehrly; and HIV-1 NL4-3 ΔNef Infectious Molecular Clone, ARP-12755, contributed by Dr. Olivier Schwartz.

SUPPLEMENTARY MATERIAL

The Supplementary Material for this article can be found online at: https://www.frontiersin.org/articles/10.3389/fviro.2022.836125/full#supplementary-material

REFERENCES

1. Freed EO. HIV-1 Replication. *Somat Cell Mol Genet* (2001) 26:13–33. doi: 10.1023/A:1021070512287
2. Adamson CS, Freed EO. Human Immunodeficiency Virus Type 1 Assembly, Release, and Maturation. *Adv Pharmacol* (2007) 55:347–87. doi: 10.1016/S1054-3589(07)55010-6
3. Freed EO. HIV-1 Assembly, Release and Maturation. *Nat Rev Microbiol* (2015) 13:484–96. doi: 10.1038/nrmicro3490
4. Ono A, Ablan SD, Lockett SJ, Nagashima K, Freed EO. Phosphatidylinositol (4,5) Bisphosphate Regulates HIV-1 Gag Targeting to the Plasma Membrane. *Proc Natl Acad Sci USA* (2004) 101:14889–94. doi: 10.1073/pnas.0405596101
5. Chukkapalli V, Ono A. Molecular Determinants That Regulate Plasma Membrane Association of HIV-1 Gag. *J Mol Biol* (2011) 410:512–24. doi: 10.1016/j.jmb.2011.04.015
6. Yan N, Chen ZJ. Intrinsic Antiviral Immunity. *Nat Immunol* (2012) 13:214–22. doi: 10.1038/ni.2229
7. Lazear HM, Schoggins JW, Diamond MS. Shared and Distinct Functions of Type I and Type III Interferons. *Immunity* (2019) 50:907–23. doi: 10.1016/j.immuni.2019.03.025
8. Colomer-Lluch M, Ruiz A, Moris A, Prado JG. Restriction Factors: From Intrinsic Viral Restriction to Shaping Cellular Immunity Against HIV-1. *Front Immunol* (2018) 9:2876. doi: 10.3389/fimmu.2018.02876
9. Strebel K. HIV Accessory Proteins *Versus* Host Restriction Factors. *Curr Opin Virol* (2013) 3:692–9. doi: 10.1016/j.coviro.2013.08.004
10. Malim MH, Bieniasz PD. HIV Restriction Factors and Mechanisms of Evasion. *Cold Spring Harb Perspect Med* (2012) 2:a006940. doi: 10.1101/cshperspect.a006940
11. Barr SD, Smiley JR, Bushman FD. The Interferon Response Inhibits HIV Particle Production by Induction of TRIM22. *PLoS Pathog* (2008) 4:e1000007. doi: 10.1371/journal.ppat.1000007
12. Wilson SJ, Schoggins JW, Zang T, Kutluay SB, Jouvenet N, Alim MA, et al. Inhibition of HIV-1 Particle Assembly by 2',3'-Cyclic-Nucleotide 3'-Phosphodiesterase. *Cell Host Microbe* (2012) 12:585–97. doi: 10.1016/j.chom.2012.08.012
13. Miyakawa K, Nishi M, Matsunaga S, Okayama A, Anraku M, Kudoh A, et al. The Tumour Suppressor APC Promotes HIV-1 Assembly *via* Interaction With Gag Precursor Protein. *Nat Commun* (2017) 8:14259. doi: 10.1038/ncomms14259
14. Chukkapalli V, Hogue IB, Boyko V, Hu WS, Ono A. Interaction Between the Human Immunodeficiency Virus Type 1 Gag Matrix Domain and Phosphatidylinositol-(4,5)-Bisphosphate Is Essential for Efficient Gag Membrane Binding. *J Virol* (2008) 82:2405–17. doi: 10.1128/JVI.01614-07
15. Rusinova I, Forster S, Yu S, Kannan A, Masse M, Cumming H, et al. Interferome V2.0: An Updated Database of Annotated Interferon-Regulated Genes. *Nucleic Acids Res* (2013) 41:D1040–6. doi: 10.1093/nar/gks1215
16. Tartour K, Appourchaux R, Gaillard J, Nguyen XN, Durand S, Turpin J, et al. IFITM Proteins Are Incorporated Onto HIV-1 Virion Particles and Negatively Imprint Their Infectivity. *Retrovirology* (2014) 11:103. doi: 10.1186/s12977-014-0103-y
17. Puertollano R, Alonso MA. MAL, an Integral Element of the Apical Sorting Machinery, Is an Itinerant Protein That Cycles Between the Trans-Golgi Network and the Plasma Membrane. *Mol Biol Cell* (1999) 10:3435–47. doi: 10.1091/mbc.10.10.3435
18. Llorente A, de Marco MC, Alonso MA. Caveolin-1 and MAL Are Located on Prostasomes Secreted by the Prostate Cancer PC-3 Cell Line. *J Cell Sci* (2004) 117:5343–51. doi: 10.1242/jcs.01420
19. Ventimiglia LN, Fernandez-Martin L, Martinez-Alonso E, Anton OM, Guerra M, Martinez-Menarguez JA, et al. Cutting Edge: Regulation of Exosome Secretion by the Integral MAL Protein in T Cells. *J Immunol* (2015) 195:810–4. doi: 10.4049/jimmunol.1500891
20. Saksela K, Cheng G, Baltimore D. Proline-Rich (PxxP) Motifs in HIV-1 Nef Bind to SH3 Domains of a Subset of Src Kinases and Are Required for the Enhanced Growth of Nef+ Viruses But Not for Down-Regulation of CD4. *EMBO J* (1995) 14:484–91. doi: 10.1002/j.1460-2075.1995.tb07024.x
21. Millan J, Alonso MA. MAL, a Novel Integral Membrane Protein of Human T Lymphocytes, Associates With Glycosylphosphatidylinositol-Anchored Proteins and Src-Like Tyrosine Kinases. *Eur J Immunol* (1998) 28:3675–84. doi: 10.1002/(SICI)1521-4141(199811)28:11<3675::AID-IMMU3675>3.0.CO;2-5
22. Copie-Bergman C, Plonquet A, Alonso MA, Boulland ML, Marquet J, Divine M, et al. MAL Expression in Lymphoid Cells: Further Evidence for MAL as a Distinct Molecular Marker of Primary Mediastinal Large B-Cell Lymphomas. *Mod Pathol* (2002) 15:1172–80. doi: 10.1097/01.MP.0000032534.81894.B3
23. Anton O, Batista A, Millan J, Andres-Delgado L, Puertollano R, Correas I, et al. An Essential Role for the MAL Protein in Targeting Lck to the Plasma Membrane of Human T Lymphocytes. *J Exp Med* (2008) 205:3201–13. doi: 10.1084/jem.20080552
24. Anton OM, Andres-Delgado L, Reglero-Real N, Batista A, Alonso MA. MAL Protein Controls Protein Sorting at the Supramolecular Activation Cluster of Human T Lymphocytes. *J Immunol* (2011) 186:6345–56. doi: 10.4049/jimmunol.1003771
25. Ventimiglia LN, Alonso MA. Biogenesis and Function of T Cell-Derived Exosomes. *Front Cell Dev Biol* (2016) 4:84. doi: 10.3389/fcell.2016.00084
26. Lopez-Guerrero JA, de la Nuez C, Praena B, Sanchez-Leon E, Krummenacher C, Bello-Morales R. Herpes Simplex Virus 1 Spread in Oligodendrocytic Cells Is Highly Dependent on MAL Proteolipid. *J Virol* (2020) 94:e01739–19. doi: 10.1128/JVI.01739-19
27. Vlach J, Saad JS. Trio Engagement *via* Plasma Membrane Phospholipids and the Myristoyl Moiety Governs HIV-1 Matrix Binding to Bilayers. *Proc Natl Acad Sci USA* (2013) 110:3525–30. doi: 10.1073/pnas.1216655110
28. Olety B, Ono A. Roles Played by Acidic Lipids in HIV-1 Gag Membrane Binding. *Virus Res* (2014) 193:108–15. doi: 10.1016/j.virusres.2014.06.015
29. Monde K, Chukkapalli V, Ono A. Assembly and Replication of HIV-1 in T Cells With Low Levels of Phosphatidylinositol-(4,5)-Bisphosphate. *J Virol* (2011) 85:3584–95. doi: 10.1128/JVI.02266-10
30. Malbec M, Sourisseau M, Guivel-Benhassine F, Porrot F, Blanchet F, Schwartz O, et al. HIV-1 Nef Promotes the Localization of Gag to the Cell Membrane and Facilitates Viral Cell-to-Cell Transfer. *Retrovirology* (2013) 10:80. doi: 10.1186/1742-4690-10-80
31. Collette Y, Olive D. The Primate Lentivirus-Encoded Nef Protein can Regulate Several Steps of the Viral Replication Cycle. *Virology* (1999) 265:173–7. doi: 10.1006/viro.1999.0053
32. Campbell TD, Khan M, Huang MB, Bond VC, Powell MD. HIV-1 Nef Protein Is Secreted Into Vesicles That Can Fuse With Target Cells and Virions. *Ethn Dis* (2008) 18:S2–14-9.
33. Muratori C, Cavallin LE, Kratzel K, Tinari A, De Milito A, Fais S, et al. Massive Secretion by T Cells Is Caused by HIV Nef in Infected Cells and by Nef Transfer to Bystander Cells. *Cell Host Microbe* (2009) 6:218–30. doi: 10.1016/j.chom.2009.06.009
34. Lenassi M, Cagney G, Liao M, Vaupotic T, Bartholomeeusen K, Cheng Y, et al. HIV Nef is Secreted in Exosomes and Triggers Apoptosis in Bystander CD4+ T Cells. *Traffic* (2010) 11:110–22. doi: 10.1111/j.1600-0854.2009.01006.x
35. Bregnard C, Zamborlini A, Leduc M, Chafey P, Camoin L, Saib A, et al. Comparative Proteomic Analysis of HIV-1 Particles Reveals a Role for Ezrin and EHD4 in the Nef-Dependent Increase of Virus Infectivity. *J Virol* (2013) 87:3729–40. doi: 10.1128/JVI.02477-12

36. Brugger B, Krautkramer E, Tibroni N, Munte CE, Rauch S, Leibrecht I, et al. Human Immunodeficiency Virus Type 1 Nef Protein Modulates the Lipid Composition of Virions and Host Cell Membrane Microdomains. *Retrovirology* (2007) 4:70. doi: 10.1186/1742-4690-4-70

Conflict of Interest: The authors declare that the research was conducted in the absence of any commercial or financial relationships that could be construed as a potential conflict of interest.

Publisher's Note: All claims expressed in this article are solely those of the authors and do not necessarily represent those of their affiliated organizations, or those of the publisher, the editors and the reviewers. Any product that may be evaluated in this article, or claim that may be made by its manufacturer, is not guaranteed or endorsed by the publisher.

frontiers | Frontiers in Virology

REVIEW
published: 02 June 2022
doi: 10.3389/fviro.2022.872599

Molecular Biology and Diversification of Human Retroviruses

Morgan E. Meissner[1,2], *Nathaniel Talledge*[1,3,4] *and Louis M. Mansky*[1,2,3,4]*

[1] Institute for Molecular Virology, University of Minnesota – Twin Cities, Minneapolis, MN, United States, [2] Molecular, Cellular, Developmental Biology and Genetics Graduate Program, University of Minnesota – Twin Cities, Minneapolis, MN, United States, [3] Division of Basic Sciences, School of Dentistry, University of Minnesota – Twin Cities, Minneapolis, MN, United States, [4] Masonic Cancer Center, University of Minnesota – Twin Cities, Minneapolis, MN, United States

Studies of retroviruses have led to many extraordinary discoveries that have advanced our understanding of not only human diseases, but also molecular biology as a whole. The most recognizable human retrovirus, human immunodeficiency virus type 1 (HIV-1), is the causative agent of the global AIDS epidemic and has been extensively studied. Other human retroviruses, such as human immunodeficiency virus type 2 (HIV-2) and human T-cell leukemia virus type 1 (HTLV-1), have received less attention, and many of the assumptions about the replication and biology of these viruses are based on knowledge of HIV-1. Existing comparative studies on human retroviruses, however, have revealed that key differences between these viruses exist that affect evolution, diversification, and potentially pathogenicity. In this review, we examine current insights on disparities in the replication of pathogenic human retroviruses, with a particular focus on the determinants of structural and genetic diversity amongst HIVs and HTLV.

Keywords: retrovirus, molecular biology, diversification, human T-cell leukemia virus, human immunodeficiency virus

OPEN ACCESS

Edited by:
Akio Adachi,
Kansai Medical University, Japan

Reviewed by:
Fatah Kashanchi,
George Mason University, United States
Mikako Fujita,
Kumamoto University, Japan
Eric O. Freed,
National Cancer Institute at Frederick (NIH), United States

***Correspondence:**
Louis M. Mansky
mansky@umn.edu

Specialty section:
This article was submitted to Fundamental Virology, a section of the journal Frontiers in Virology

Received: *09 February 2022*
Accepted: *07 March 2022*
Published: *02 June 2022*

Citation:
Meissner ME, Talledge N and Mansky LM (2022) Molecular Biology and Diversification of Human Retroviruses. Front. Virol. 2:872599. doi: 10.3389/fviro.2022.872599

PATHOGENIC HUMAN RETROVIRUSES

Human Immunodeficiency Viruses

Human immunodeficiency virus (HIV) is the etiologic agent of acquired immunodeficiency syndrome (AIDS) (1, 2). Nearly 40 years after its discovery, HIV remains a chronic global public health concern. Since its emergence in the human population, HIV has infected approximately 75 million people and is responsible for the deaths of almost 32 million individuals (3). As of 2018, an estimated 38 million people are infected with HIV around the world (4). Despite advancements in the understanding of viral transmission and antiviral drug development, approximately 1.7 million new infections and 770,000 HIV-related deaths still occur annually (4).

Most HIV infections are caused by HIV type 1 (HIV-1), which is the primary driver of the pandemic. A much smaller subset of HIV infections are caused by HIV type 2 (HIV-2), which accounts for only about 1 to 2 million infections and is almost exclusively geographically constrained to West Africa (5). Both HIV-1 and HIV-2 belong to the *Retroviridae* family of viruses. Retroviruses are a unique class of viruses that challenge the central dogma of biology, such that their RNA genomes are first reverse transcribed into DNA. The DNA copy of the viral genome is then integrated into the host DNA, which contributes to lifelong, persistent infections. Messenger

RNA (mRNA) and viral genomic RNA (vRNA) are both transcribed from the integrated genome, which allows for sustained propagation of viral progeny so long as the host cell survives.

Both HIV-1 and HIV-2 infect immune cells that express the CD4 molecule on their surface, namely CD4+ T cells and macrophages. During the acute stage, which represents the first weeks of infection, CD4+ T cells are robustly depleted from the lymphoid system. This is driven by both direct targeting of virally-infected cells as well as the activation-induced death of bystander T cells (6). Infected individuals may experience mononucleosis-like symptoms, such as fever, headache, and muscle pains. These symptoms may be so mild that many individuals do not realize they are infected. The acute stage of infection is followed by a long period of clinical latency, known as the asymptomatic phase, which typically lasts about 6 to 8 years (7). During this time, the concentration of CD4+ T cell continues to decline and viremia increases. When CD4+ T cell counts drop below 500 cells/μL, patients enter the symptomatic phase of infection, at which point viremia rapidly increases and progression to AIDS (defined as CD4+ T cell concentration <200 cells/μL) typically occurs within a couple of years (7). Left untreated, 52% of patients will die within 2 years of progression to AIDS and 82% will die within 6 years (8).

Compared with HIV-1, HIV-2 exhibits a significantly attenuated disease phenotype, characterized by lower viral loads within individuals, lower rates of both vertical and sexual transmissibility, and a slower progression to AIDS (9–14). In areas where HIV-2 has historically been endemic, rates of HIV-2 infection are decreasing while the prevalence of HIV-1 is on the rise (15–17). For example, in Guinea-Bissau, the prevalence of HIV-1 rose from 0.5% in 1990 to 3.6% in 2007, whereas HIV-2 prevalence dropped from 8.3% to 4.7% in the same timeframe (17). Even in the absence of antiretrovirals, the prognosis for HIV-2-infected individuals is better than for HIV-1-infected individuals. A study of women with HIV-1 and HIV-2 infections from 1985 to 1993 found that the 5-year AIDS-free survival rate for HIV-1-infected women was 67% compared with 100% for HIV-2-infected women (14).

The reason for the attenuated disease progression of HIV-2 compared with HIV-1 remains unclear. Humanized mice studies in HIV-2 are lacking, and no head-to-head comparisons have been done, but preliminary studies suggest that viral loads in HIV-2-infected humanized mice are an order of magnitude lower than those of HIV-1-infected humanized mice during the first several months of infection (18, 19). Studies of HIV-1 elite controllers and long-term non-progressors (i.e., those individuals who maintain high CD4+ T-cell counts in the absence of treatment) have found that these patients have lower levels of proviral DNA and smaller pools of latently infected cells compared with viremic individuals (20–22). However, results comparing HIV-1 and HIV-2 long-term non-progressors have been conflicting. One study found that differences in proviral loads between HIV-1- and HIV-2-infected individuals may explain disparities in viremia and disease progression (23). However, another group demonstrated that low plasma viral load was independent of proviral load in HIV-2-infected individuals, which were comparable with proviral loads for HIV-1-infected individuals at similar disease states (24).

Human T-Cell Leukemia Virus Type 1

Human T cell leukemia virus type 1 (HTLV-1) represents the other major pathogenic human retrovirus. HTLV-1 was the first human retrovirus discovered, laying the groundwork for much of the work that has been done to understand HIV-1 infection (25, 26). HTLV-1 is in the *deltaretrovirus* genus, whereas HIV-1 and HIV-2 are in the *lentivirus* genus. Like HIV-1 and HIV-2, HTLV-1 predominantly infects CD4+ T cells, but also infects a wide variety of other immune cells, endothelial cells, myeloid cells, and fibroblasts (27–31). Although HTLV-1 is also characterized by relatively low rates of transmission between individuals, an estimated 5 to 10 million people are infected worldwide, and the seroprevalence may reach as high as 40% in endemic regions such as Japan, the Caribbean, central Africa, Brazil, parts of the Middle East, and the Pacific Islands, including Australia (32, 33).

While most HTLV-1 infections remain asymptomatic, there is a 0.25% to 3% lifetime risk for pathogenicity for infected individuals (32). In these individuals, the disease may manifest as a lymphoproliferative adult T cell leukemia/lymphoma (ATL) or as a collection of neurological disorders, namely HTLV-1-associated myelopathy/tropical spastic paraparesis (HAM/TSP) (25, 34–36). HTLV-1 is also associated with a number of other inflammatory disorders, including bronchiectasis. A recent study found that in Indigenous adults in central Australia, HTLV-1 proviral loads are 8-fold higher in patients with bronchiectasis compared with healthy controls, and patients with an HTLV-1 proviral load greater than 1000 copies per 100,000 peripheral blood leukocytes were over 12-times more likely to develop bronchiectasis (37).

Compared with HIV-1, both HIV-2 and HTLV-1 have been significantly understudied. A search of the online PubMed database performed December 2021 yields over 100,000 results using the search terms "HIV-1" or "human immunodeficiency virus type-1", compared with approximately 6,300 results for "HIV-2" or "human immunodeficiency virus type-2" and 6,600 to 8,500 results for "HTLV-1" or "human T cell leukemia virus type-1". Although the viruses share many similarities, it is important to consider both HIV-2 and HTLV-1 independently, as there are key differences that distinguish these viruses from HIV-1 that have important implications for replication, disease pathogenesis, and treatment.

THE RETROVIRAL LIFECYCLE

HIV-1, HIV-2, and HTLV-1 Genomes

At the most basic level, retroviral genomes consist of at least 3 core genes which are encoded in a 5'-*gag-pol-env*-3' structure. The proteins encoded by these genes facilitate the fundamental steps in viral replication: attachment/entry, genome replication, particle assembly, and egress. All 3 major human retroviruses also encode a set of auxiliary genes, known as accessory genes,

which are dispensable for replication in certain *in vitro* cell culture systems (**Figure 1**). The proteins encoded by these genes play a variety of important roles within the host system and help facilitate transmission and replication. Two identical copies of the single-stranded RNA genome are packaged into viral particles and serve as the templates for the generation of a single proviral genome, which is integrated into the host DNA.

The HIV-1 genome is approximately 9,200 to 9,600 nucleotides and is flanked at both ends by long terminal repeat (LTR) sequences. There are 9 protein-coding viral genes encoded by overlapping reading frames: *gag*, *pol*, *vif*, *vpr*, *tat*, *rev*, *vpu*, *env*, and *nef*. The RNA genome also contains a number of highly structured elements that regulate replication, including the 5' trans-activation response (TAR) element, primer binding site (PBS), dimerization initiation sequence (DIS), and the Rev response element (RRE) (38).

The HIV-2 genome is structurally very similar to the HIV-1 genome and is approximately 9,800 nucleotides in length. The most prominent difference between them is the absence of *vpu*, which is replaced instead with *vpx*. At the sequence level, however, HIV-1 and HIV-2 are highly divergent. The viruses emerged in the human population *via* distinct zoonotic transmissions of simian immunodeficiency viruses (SIVs) from either chimpanzees or gorillas (HIV-1) or sooty mangabeys (HIV-2) (39). As result, HIV-1 and HIV-2 share approximately 60% identity at the amino acid level and just 48% identity at the nucleotide level (40).

The HTLV-1 genome is approximately 9,000 nucleotides in length and, similarly to HIV-1 and HIV-2, is flanked by LTR sequences. In addition to the 3 core genes, HTLV-1 also contains a regulatory *pX* region, which encodes the viral accessory proteins Tax-1, Rex, p8/p12, p13, p30, and HBZ (encoded in the antisense direction) (41). Several of these unique accessory factors, namely Tax and HBZ, have been implicated in oncogenesis and serve to partly explain the distinct disease pathogeneses of HTLV-1 from HIVs (42). HTLV-1 is genetically distinct from both HIV-1 and HIV-2 and is the result of multiple zoonotic transmissions of simian T-lymphotropic virus type 1 (STLV-1) from apes to humans. Whereas this transmission is thought to have occurred relatively recently for HIV-1 and HIV-2, likely sometime between 1920 and 1940 (43, 44), HTLV-1 is thought to be a much older human pathogen, with some transmission events estimated to have occurred as early as the Paleolithic period (45, 46). Indeed, preserved HTLV-1 proviral DNA has been identified in 1500-year-old Andean mummies (47). Even in the most conserved structural regions of the genome, such as the capsid (CA) domain of the Gag protein, HTLV-1 shares only about 50% amino acid identity with HIV-1 (48).

Attachment, Fusion, and Entry

Viral entry into target cells is facilitated by the envelope glycoprotein (Env) on the surface of the viral particle (**Figure 2A**) . Env is initially translated as a polyprotein precursor which is subsequently cleaved into the surface protein (SU) and a transmembrane protein (TM), the latter of which is anchored within the lipid membrane of the viral envelope. The mature Env protein consists of a trimer of the SU-TM heterodimers that is heavily glycosylated during protein trafficking to the plasma membrane of the host cell (49–51). The SU protein binds to a series of receptors on the host cell which facilitate viral uptake. For both HIV-1 and HIV-2, the primary cellular receptor is CD4. CD4 is abundantly expressed on the surface of CD4+ T cells but is also expressed on a number of other immune cell types, including hematopoietic progenitor cells (52). Subsequent interaction with a coreceptor on the cell

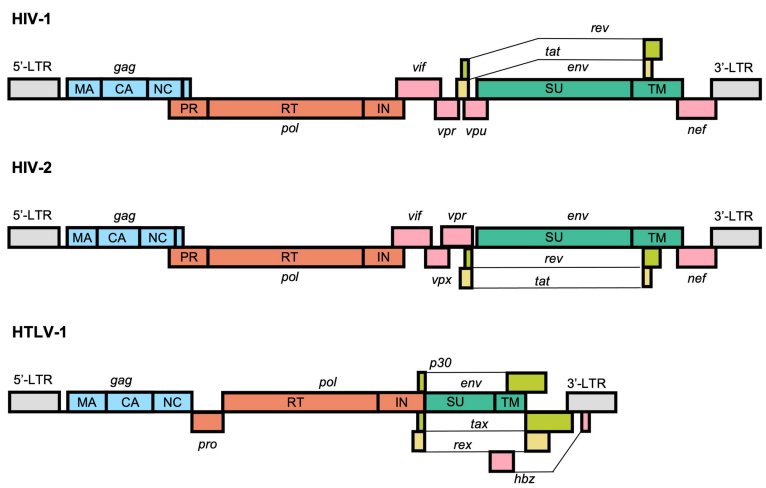

FIGURE 1 | Schematic representation of the typical structure of the HIV-1, HIV-2, and HTLV-1 proviral genomes. All retroviruses encode a core set of genes in a 5'-*gag-pol-env*-3' structure flanked by long-terminal repeats (LTRs) that facilitate replication and integration within the genome. HIV-1, HIV-2, and HTLV-1 also encode a unique set of accessory genes, shown in pink, lime green, and yellow, that help facilitate genomic replication and immune evasion and counteract cellular defense mechanisms against the virus.

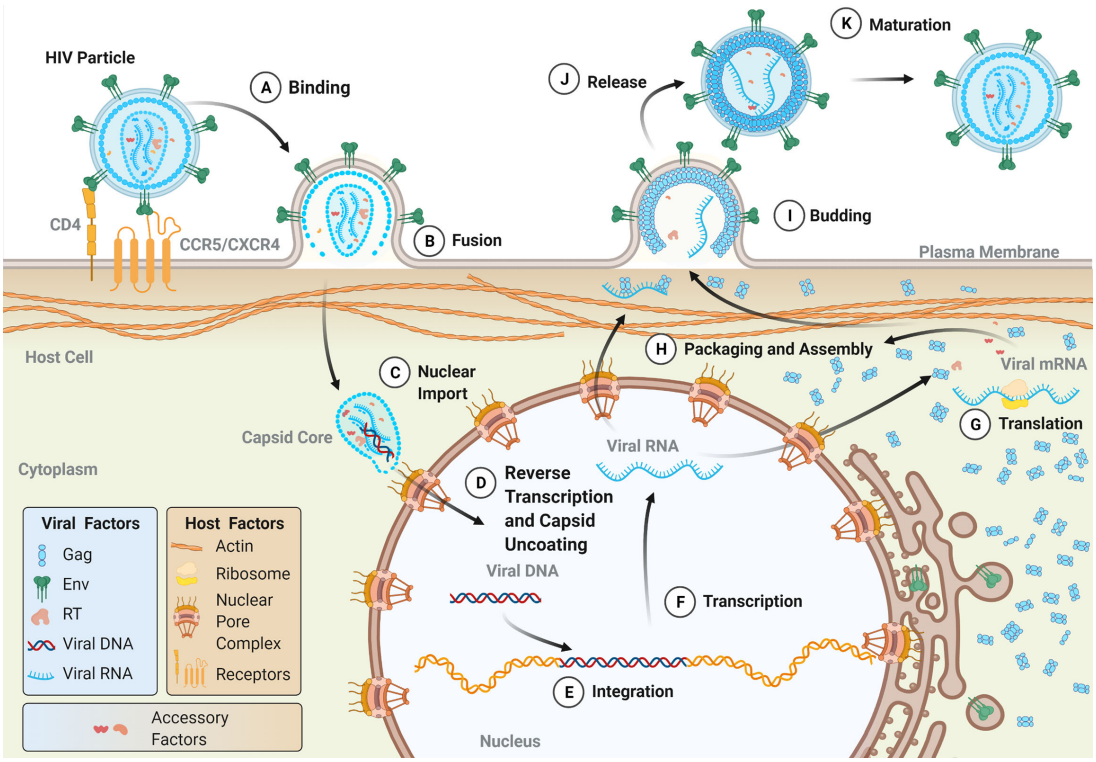

FIGURE 2 | The lifecycle of human retroviruses. The major steps of the retroviral lifecycle are shown. Viral proteins are colored according to those used in the genomic structure diagram in **Figure 1**. **(A)** The retroviral lifecycle begins when the envelope proteins of a mature, infectious virion attach to the appropriate receptor (for HIV-1, CD4) and co-receptor (CCR5 or CXRC4) on the surface of the cell, which facilitates viral membrane fusion with the plasma membrane. Following release into the cytoplasm **(B)**, the intact (or near intact) capsid core is trafficked to nuclear pore complexes (NPCs) on the nuclear envelope. During or shortly after nuclear import **(C)**, capsid uncoating and reverse transcription occur **(D)** (see **Figure 3** for more details on reverse transcription). The double-stranded DNA product is subsequently integrated into the host genome by integrase **(E)**. Host machinery transcribes the proviral genome **(F)** into both the viral genomic RNA (vRNA) and mRNA, which templates the translation of viral proteins both in the cytosol and on the surface of the ER, with co-translational insertion of the transmembrane Env protein occurring in the ER **(G)**. A milieu of viral and host proteins traffics along with vRNA to the plasma membrane where they are packaged into nascent budding particles **(H)**. Following the budding **(I)** and release of the particle from the plasma membrane **(J)**, the viral protease cleaves Gag resulting in the formation of a mature, infectious particle **(K)**.

surface, namely one of the chemokine receptors CCR5 or CXCR4, triggers a conformational change within Env which results in the fusion of the viral and cellular membranes mediated by the TM protein. The process is similar for HTLV-1, except that HTLV-1 SU first interacts with heparin sulfate proteoglycans (HSPGs), followed by neuropilin-1 (NRP-1), and finally glucose transporter 1 (GLUT1). Binding to NRP-1 induces a conformational change within SU which allows for interaction with GLUT1 which subsequently facilitates fusion of the viral and cellular membranes (53).

Reverse Transcription and Integration

Following membrane fusion, the viral capsid core is released into the cytoplasm of the cell along with a host of viral and cellular proteins, including reverse transcriptase (RT), integrase (IN), and cellular proviral and restriction factors (**Figure 2B**). The early stages of genomic replication within the cell have remained a topic of debate. Reverse transcription is intimately linked to the dissociation of the capsid core structure, known as uncoating, and perturbation of uncoating kinetics can disrupt reverse transcription events (54–58). While it was historically believed that capsid core uncoating and reverse transcription occurred in the cytoplasm, recent evidence suggests that capsid cores remain largely intact until they reach nuclear pore complexes (NPCs) on the nuclear envelope (59–63). Recent reports suggest that these cores are subsequently trafficked through the NPC in an intact state, and that both uncoating and reverse transcription occur in the nucleus (59–61). Others, however, suggest that capsid remodeling or partial uncoating occur at the NPC, and that the early formation of viral DNA products occurs at or near the nuclear envelope (**Figures 2C, D**) (62, 63). Such studies, which have reshaped our understanding of the timing of capsid uncoating and reverse transcription, have been aided by advancements in molecular imaging techniques. Further improvements in live cell imaging microscopy will allow for deeper insights into the relationship between uncoating and reverse transcription, as well as the timing of these processes.

The details of reverse transcription are shown in **Figure 3**. Cellular tRNAs serve as the primer for initiation of reverse transcription ($tRNA^{Lys3}$ for HIV-1 and HIV-2, $tRNA^{Pro}$ for HTLV-1), which bind to the PBS at the 5' end of the RNA genome (64). From this primer, the RT enzyme begins synthesis of the negative-sense strand of single-stranded DNA (-ssDNA) in a 5'-to-3' direction. As RT proceeds with DNA synthesis, the RNase H domain of the enzyme degrades the RNA genome behind it. RT proceeds through the unique 5' (U5) and repeated (R) regions of the 5' leader sequence of the RNA genome, at which point the first strand transfer occurs. The R region is thusly named as it is repeated at both ends of the genome, allowing for binding of the newly synthesized ssDNA to the 3' end of the genome. DNA elongation continues through the unique 3' (U3) region, generating the first of the LTRs. As synthesis of the -ssDNA continues, RNase H continues to degrade the viral RNA genome, until it reaches the centrally located polypurine tract (PPT). This portion of the RNA is resistant to RNase H cleavage and serves as the template for generation of the positive-sense single-stranded DNA (+ssDNA).

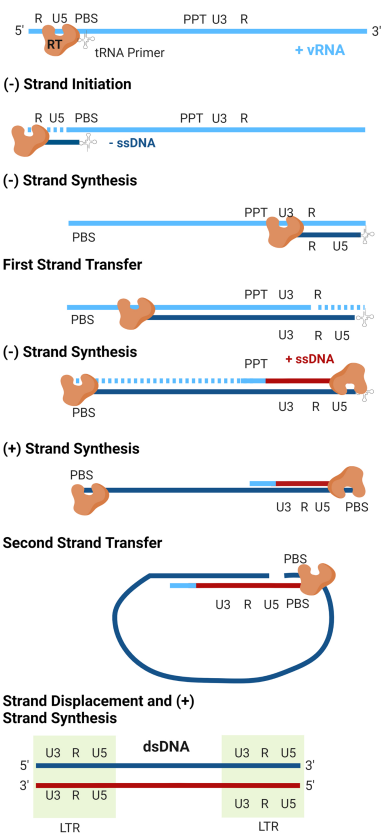

FIGURE 3 | Reverse transcription. The virally encoded reverse transcriptase (RT) converts the viral genomic RNA (vRNA) into double-stranded DNA. As replication occurs, the RNaseH activity of RT degrades the vRNA template (dashed lines). Following completion of plus-strand synthesis, the double-stranded DNA product is integrated into the host genome by integrase to form a transcriptionally active provirus (not shown).

As synthesis of the -ssDNA continues, +ssDNA elongation proceeds to the 3' end of the genome through U3, R, and U5. The second strand transfer occurs, in which the PBS from both ssDNA molecules hybridize. Both strands are allowed to complete synthesis using one another as templates and the dsDNA genome is completed.

Within the nucleus, the dsDNA product exists as a ribonucleotide complex made up of viral and cellular proteins, known as the pre-integration complex (PIC). Included within the PIC is IN, which acts to catalyze the integration of the viral dsDNA into the host genome, forming a completed provirus (**Figure 2E**). Integration of retroviral genomes occurs in a semi-random fashion. Research suggests that both HIV-1 and HIV-2 preferentially integrate within or adjacent to protein-coding regions and in CpG-rich regions (65–70). One study found that during *in vitro* infection of peripheral blood mononuclear cells, 82% of HIV-2 integrations occurred within annotated genes (68). On the other hand, HTLV-1 does not exhibit a preference for integration within open reading frames (71, 72). According to one analysis of integration sites in cells from HTLV-1-infected individuals, HTLV-1 proviruses integrate within gene transcriptional units at a frequency similar to what is expected based on random chance (71). Although specific genomic hotspots have not been identified, research suggests that HTLV-1 may preferentially integrate at palindromic targets near transcription start sites (72).

Retroviral transcription from integrated proviruses is driven by promoter and enhancer elements within the LTR (73, 74). A number of structures and sequences are included within the LTRs that promote viral gene transcription, including the TATA box, the 5' trans-activating response (TAR) element, and a collection of host transcription factor binding sites. Together, these factors recruit the cellular RNA polymerase II, which catalyzes the transcription of viral mRNAs as well as genomic RNA starting at the U3 region of the LTR (73). Because HIV-1 and HIV-2 integrate near or within transcriptionally active regions of the genome, enhancement of transcription from the proviral LTRs can also affect the gene expression profile of infected cells (75). Additionally, some of the cellular factors recruited to the proviral LTR, including NF-κB and CBF-1, also recruit histone deacetylases (HDACs) that suppress viral gene transcription and help establish viral latency (76–78).

Assembly, Budding, and Maturation

Viral particle assembly occurs as the vRNA and transcribed proteins (**Figure 2G**), including Gag, Gag-Pol, Env, and a collection of accessory proteins (**Figure 2F**), traffic to the plasma membrane (**Figure 2H**). A key step in this process is the oligomerization of Gag proteins, which promotes the formation of the immature Gag lattice of the viral particle. For HIV-1, Gag oligomerization is driven by interactions between the C-terminal domains within the CA region of different Gag proteins (79). In contrast, HTLV-1 Gag oligomerization is driven by a variety of Gag-Gag interactions across the full length of the protein, including in the N-terminal domain of CA as well as in the matrix (MA) and nucleocapsid (NC) domains (80, 81). In the

case of HIV-1 infection, Gag oligomers form primarily in the cytoplasm before trafficking to the plasma membrane (82). HTLV-1 Gag is instead thought to traffic to the plasma membrane as a monomer before oligomerizing on the inner leaflet of the plasma membrane (82). The MA domain of Gag is responsible for the membrane-binding activity of the protein, which anchors the protein within lipid rafts at the plasma membrane (83–87). For both HIV-1 and HTLV-1, electrostatic interactions between the highly basic region of MA and phosphatidylinositol 4,5-bisphosphate [$PI(4,5)P_2$] are key regulators of membrane binding, though recent research suggests that co-translational myristoylation of the G2 position in MA is the primary driver of HTLV-1 Gag membrane binding (88, 89).

Although NC is thought to be the main driver of Gag vRNA-binding activity, MA can bind to vRNA as well (90–93). It is currently unknown whether HIV-1 and HTLV-1 Gag proteins bind to vRNA within the cytoplasm of the cell and traffic to the membrane together, or whether vRNA reaches sites of particle assembly *via* transient diffusion (94–96). Preliminary evidence from *in vitro* biophysical studies suggests that ribonucleoprotein complexes, including Gag-RNA complexes, may be partially excluded from the plasma membrane-adjacent space *via* the actin cortex, which may act as a steric hinderance to particle assembly (97). Although the biological implications of these observations remain to be elucidated, these results suggest that the actin cortex may serve as a physical determinant of particle assembly sites on the plasma membrane.

The curvature of the Gag lattice at the plasma membrane causes the formation of a roughly spherical particle, the budding and release of which is catalyzed by host proteins including the ESCRT machinery (98–102). During or shortly after virus particle release, the viral PR cleaves Gag, triggering the maturation of the immature virus particle (**Figures 2I–K**). The mature particle contains MA embedded along the inner surface of the viral envelope; a CA core surrounding the viral genomic RNA, which is studded with NC, RT, and IN proteins; and a myriad of host and viral accessory proteins within the tegument of the particle. The maturation process is the final step in the development of an infectious viral particle that contains all the necessary factors to infect a naïve target cell (95, 103).

MORPHOLOGICAL DIVERSITY IN HUMAN RETROVIRUS PARTICLES

Mature HIV-1 and HIV-2 particles exhibit an iconic conical capsid core structure (104, 105). Lentiviral core structure is unique among retroviruses, though, and the *Retroviridae* family exhibits a great deal of structural diversity, both among mature and immature particles (106, 107). Similar to other retroviruses, including murine leukemia virus (MLV), Rous sarcoma virus (RSV), and foamy viruses, HTLV-1 mature particles have been found to be roughly polygonal in nature (108–111). However, in analyses of HTLV-1 mature core morphology using chronically infected T cell lines, populations of particles with distinct morphologies have been identified (111, 112). In these analyses, particles with a distinct core-like structure accounted for just 10% to 15% of particles observed, and an additional 5% to 20% contained what were termed "partially mature" capsid cores, in which the capsid structure appeared incomplete. Still another 60% to 70% exhibited uniform electron density within the viral particle, with no discernable core-like structure observed (111, 112). The large proportion of HTLV-1 particles lacking CA organization and containing partially mature CA cores provides a plausible hypothesis to explain the decreased transmissibility and infectivity of HTLV-1 particles in a cell-free environment, though further research is needed to define this relationship.

Significant structural diversity has also been observed in immature particle structure across different human and animal retroviral species. In a comprehensive analysis of the structure of immature retroviral particles, it was determined that immature HTLV-1 particles are distinct among all retroviruses, characterized by discontinuous Gag lattices and flat regions of multimerized CA that appear disconnected from the plasma membrane (106, 113). The retroviral Gag lattice is the most prominent feature in both mature and immature particles, and the complex arrangement of these lattices is dictated by intermolecular protein interactions located primarily within the CA domain (79–81). While the structural determinants of HIV-1 Gag oligomerization have been extensively studied in authentic particles (114–116), virus-like particles (117–119), and *in vitro* assemblies of purified CA proteins (120), high resolution of the structure of the HTLV-1 has been limited to nuclear magnetic resonance (NMR) studies of the HTLV-1 CA domain (121). Comparative studies probing residues within CA have identified many of the key interaction interfaces required for maintaining replication and morphology of HIV-1 (122, 123), HIV-2 (124), and HTLV-1 (81), including those that dictate the formation of structural features such as the six-helix bundle of CA-SP1 and the two- and three-fold CA interfaces. Recent determination of the structure of the HIV-2 immature lattice demonstrates a similar hexameric organization to that of HIV-1 (125), further emphasizing the unique nature of HTLV-1 among human retroviruses.

Understanding structural diversity, and its impact on infectivity, in retroviruses is important, as form dictates function. As Moshe Safdie wrote in his 1970 novel *Beyond Habitat*, "nature makes form, and form is a by-product of evolution." Using point mutations introduced into the HIV-1 CA protein that either increase or decrease the stability of the CA core structure, research has demonstrated that core stability and disassembly are finely tuned processes, and that structural abnormalities that disrupt their kinetics in either direction inhibit viral replication (56, 58). This is likely due to the observation that CA core uncoating is connected to reverse transcription kinetics; consequently, disruption of core disassembly may perturb replication of the viral genome (126, 127). There is therefore a need to better understand the structural diversity within retroviruses, and particularly within HTLV-1,

and how this relates to viral replication and infectivity. In addition, more quantitative analyses identifying the differences in viral and host protein incorporation into particles, properties of Gag oligomerization, and maturation dynamics are critical to support the next generation of comparative studies of human retroviral particles.

GENETIC DIVERSITY IN HUMAN RETROVIRUSES

A high rate of viral evolution is a hallmark feature of HIV-1 that drives the rapid diversification of viral genomes, both within and between hosts. The genetic diversity of HIV-1 within a single infected individual is comparable with the genetic diversity observed in influenza sequences circulating around the globe within a given year (128). The genetic diversity of the virus has led to the classification of HIV-1 into groups, subtypes, and sub-subtypes (**Figure 4A**). HIV-1 can be classified as group M, N, O, or P; group M consists of subtypes A, B, C, D, F, G, H, J, and K, and subtypes A and F can be further classified into sub-subtypes A1, A2, A3, A4, F1, and F2 (129). The genetic variability between subtypes generally ranges from about 25% to 35%, and within subtype variability can be as high as 20% (130). The various HIV-1 groups are thought to have originated *via* distinct zoonotic transmission events, with the further diversification of HIV-1 group M driven by a high rate of viral mutation.

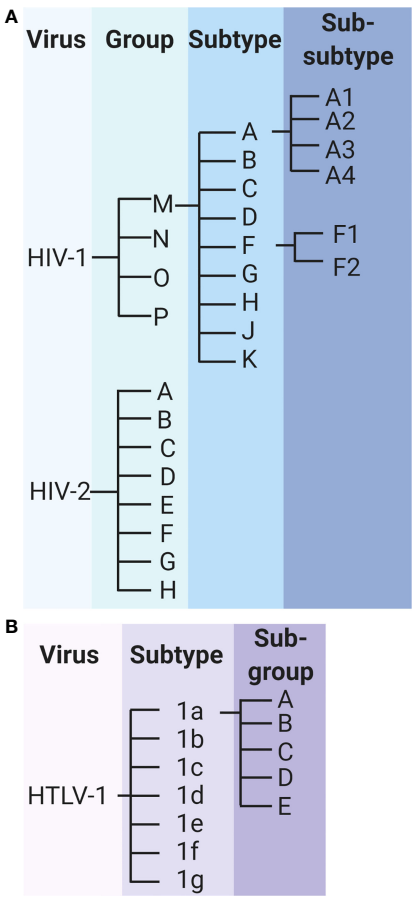

FIGURE 4 | Classification of HIV-1, HIV-2 and HTLV-1. **(A)** Classification of HIV-1 and HIV-2 groups, subtypes, and sub-subtypes. **(B)** Classification of HTLV-1 subtypes and subgroups.

The genetic diversity of HIV-1 has important consequences for the clinical progression of disease. A diverse pool of viral genomes promotes immune evasion, cell tropism changes, and the emergence of antiretroviral drug resistance (131). The rapid evolution of HIV-1 has necessitated a shift in the HIV-1 treatment paradigm towards combination active antiretroviral therapy (cART, or simply ART), which uses a customized combination of different classes of antiretrovirals to suppress HIV replication. The use of ART has significantly increased the proportion of people living with HIV who remain progression-free and can delay the progression to AIDS by 85% and the risk for AIDS-related death by 98% (132, 133). However, resistance to ART has already started emerging globally. In 2019, the World Health Organization reported that more than 10% of adults infected with HIV in 12 countries in Africa, Asia, and Central and South America have developed drug resistance to efavirenz and nevirapine, two non-nucleoside analog reverse transcriptase inhibitors that form the backbone of many ART regimens. In sub-Saharan Africa, the prevalence of ART resistance is especially high, with approximately 50% of newly diagnosed infants within the region being infected with a strain of HIV that is resistant to one or both of these drugs (134).

Like HIV-1, HIV-2 is further characterized into groups A through H (**Figure 4A**). Preliminary research suggested that the genetic diversity between these groups may reach as high as 25% (135), but these data are nearly 3 decades old and do not reflect the potential genetic diversity in newly identified HIV-2 groups. In addition to the sparsity of research, a clear understanding of HIV-2 diversification has been confounded by conflicting results from *in vivo* studies of HIV-2 evolution. In a 2007 study of *env* gene evolution among 8 HIV-2-infected individuals from Senegal over approximately 10 years, HIV-2 evolution was found to be significantly slower than that of HIV-1 sequences over a similar time period (136). In contrast, a similar study published in 2010, which compared HIV-1 and HIV-2 *env* sequence evolution among 22 Swedish and Portuguese patients, reported significantly faster rates of genetic evolution for HIV-2 compared with HIV-1 over up to 13 years of follow up (137). In a more recent study exploring the selective pressure of the immune system on HIV-1 and HIV-2, HIV-2 was found to be under greater purifying selection than HIV-1, suggestive of stronger constraints on viral evolution (138). The discrepancies in results may be related to the regions of the *env* gene sequenced, as HIV-2 evolution has been found to vary significantly across various regions of *env* (139). Similarly incongruent results have been observed in *in vitro* studies of HIV-1 and HIV-2 RT fidelity and kinetics (140, 141). However, single-cycle replication studies suggest that HIV-2 accumulates significantly fewer mutations during a single round of replication than does HIV-1 (142, 143).

HTLV-1 is divided into 7 subtypes (1a through 1g), of which subtype 1a is further characterized into subgroups A through E (**Figure 4B**). The diversity between these subtypes is considerably lower than is observed for HIV-1 or HIV-2, with one study estimating less than 1% genetic divergence between isolates of HTLV-1 subtypes (144). This diversity represents the result of thousands of years of evolution within the human population, underscoring the extremely low rate of HTLV-1 evolution (45–47). Studies estimate that substitutions accumulate within the HTLV-1 genome at a frequency of approximately 1% per thousand years (145, 146).

Research on the determinants of viral mutagenesis and evolution suggest that the diversification of retroviruses is driven by a complex interplay of internal and external factors. For example, while the error rate of HTLV-1 RT has been found to be several orders of magnitude lower than that of HIV-1 RT (147, 148), studies analyzing virus replication suggest that the substitution rate of HTLV-1 is comparable with those observed in HIV-1 and HIV-2 (137, 139, 149, 150). These results suggest that human retroviral evolution is driven by multiple factors beyond intrinsic replication errors alone. Indeed, retroviral evolution is thought to be driven by a combination of viral mutation, the pace of viral replication, the longevity of infection, and the size of the replicating viral population (131). The relative contribution of these factors has been found to vary considerable between retroviruses. For example, while HTLV-1 diversification is thought to be driven primarily by clonal expansion of infected cells (33), a high viral mutation rate and rapid replication of the virus are thought to be key contributors to viral evolution of HIV-1. Historical studies have estimated that the HIV-1 mutation rate is between 1.4 and 3.4 x 10^{-5} mutations per base pair (mut/bp), although more recent studies have estimated that the mutation rate may be closer to 4.1 x 10^{-3} mut/bp per cell *in vivo* (151–155).

The occurrence of multiple zoonotic transmission events of SIVs are also thought to contribute to the genetic diversity of HIV-1 and HIV-2. While most strains of HIV-1 exhibit the highest level of similarity to SIVs from chimpanzees, group O viruses are more closely related to SIVs isolated from gorillas, indicating distinct transmission events that have contributed to the pool of circulating HIV-1. Additionally, phylogenetic analyses demonstrate that HIV-2 isolates are genetically interspersed with SIV strains from sooty mangabey monkeys, suggesting multiple cross-species transmissions (156). Zoonotic transmission events are undoubtedly an important earlier driver of the genetic diversity of human retroviruses, as adaptive mutations have been found to coincide with cross-species transmission events (157).

MOLECULAR DETERMINANTS OF RETROVIRAL MUTAGENESIS

Reverse Transcriptase

The error-prone RT encoded by the virus is thought to be the primary driver of HIV-1 mutagenesis (158). *In vitro* studies suggest that the error rate of the HIV-1 group M RT (subtype B) is approximately 0.6 to 2.0 x 10^{-4} mut/bp, nearly 100- to 1000-times greater than cellular DNA polymerases (148). The extremely high error rates associated with HIV-1 and other retroviral polymerases are due in part to a lack of intrinsic proofreading ability, which corrects up to 99% of mistakes encoded by cellular DNA polymerases (159). Instead, polymerase errors become fixed within the retroviral genome and contribute to viral diversification.

A variety of intrinsic and extrinsic factors can modulate the fidelity of retroviral polymerases. Mutations within the *pol* gene that encode for drug resistance-associated mutations, for example, can significantly increase or decrease the fidelity of RT. The M184V mutation in HIV-1, which confers resistance to the nucleoside analogue reverse transcriptase inhibitors (NRTIs) lamivudine (3TC) and emtricitabine (FTC), is associated with a 20% reduction in the relative HIV-1 mutant frequency (160). In contrast, the K65R mutation, which confers resistance to the NRTIs 3TC, abacavir (ABC), and tenofovir disoproxil fumarate (TDF) in both HIV-1 and HIV-2, increases the mutant frequency of HIV-2 by approximately 10% compared with WT (141, 161). Small molecules and NRTIs themselves can also affect viral mutagenesis and can be used to increase the viral mutation rate above a theoretical error threshold to promote viral population collapse (a novel therapeutic strategy known as *lethal mutagenesis*) (160, 162–165). Retroviral polymerases are also prone to "slipping" and "jumping", which often occur at runs of repeated nucleotides and can result in deletions and frameshift mutations (166).

The fidelity of retroviral polymerases can also be affected by cellular concentrations of deoxynucleoside triphosphates (dNTPs), which are needed for generation of viral genomic DNA products (167). The mutation rate of HIV-1 has been found to differ by up to 30% between macrophages and T cells, which have drastically different dNTP concentrations based on their dividing status (168). In the absence of dNTPs, ribonucleotides are frequently incorporated during HIV-1 replication in macrophages, which can result in viral mutation if unrepaired (169). Indeed, recent research suggests that perturbations of dNTP pools within macrophages results in a 20% to 30% increase in the viral mutant frequency (170). However, the misincorporation of ribonucleotides during retroviral replication in macrophages is reduced following expression of the HIV-2/SIV accessory protein viral protein X (Vpx) (171). Vpx counteracts the cellular HIV-restriction factor SAMHD1 (sterile alpha motif and HD domain-containing protein 1), which acts as a deoxynucleoside triphosphohydrolase in non-dividing myeloid-lineage cells and depletes cellular dNTP pools (172). Collectively, these results suggest that depletion of dNTPs within macrophages by SAMHD1 contributes to HIV mutagenesis, but direct evidence of this effect remains to be observed. However, in further support of this activity, SAMHD1 expression is associated with perturbations in dNTP levels similar to those observed with the ribonucleoside reductase inhibitors, which have been shown to increase the HIV-1 mutagenic properties of nucleoside analogs (173–175).

The retroviral polymerase, RT, is also highly prone to recombination, which further promotes diversification.

Retroviruses, including HIV-1, HIV-2, and HTLV-1, are considered pseudodiploid, meaning that viral particles each contain two complete copies of the viral genomic RNA. During replication of the viral genome and synthesis of the DNA provirus, template switching may occur, in which the viral RT enzyme "jumps" between RNA copies to complete reverse transcription (176). When identical copies of the RNA genome are packaged, no effect is observed. However, mutations can arise when genetically distinct copies of the RNA genome are packaged, either as a result of superinfection (infection of the host cell with more than one virus) or, much less frequently, errors resulting from host DNA polymerases (176). Recombination itself can also lead to mutations. One study demonstrated that 15% to 20% of all mutations that occur during reverse transcription in cell culture are associated with recombination events (177).

In endemic regions where individuals may be repeatedly exposed to HIV, recombination can occur between HIV subtypes within the context of host superinfection, resulting in the formation of recombinant forms of the virus (178). As of June 2021, 102 circulating recombinant forms (CRFs) of HIV-1 have been identified in the Los Alamos National Laboratory HIV sequence database (179). Recombination between subtypes of HIV-2, however, is much less common, and only one HIV-2 CRF has been identified to date (179, 180). Recombination between HTLV-1 strains has been observed similarly infrequently (33, 181).

Recombination is an essential process in retroviral replication and occurs frequently during the course of infection. Early *in vitro* studies estimated that over 20% of proviruses within a population are the result of recombination events after as little as 15 days (182). Blocking recombination results in a reduction in HIV-1 viral titers and significant deletions within genomes that are able to propagate, indicating that recombination is essential for maintaining genomic integrity (183). Studies of HIV-1 suggest that retroviral recombination is dependent on regions of high sequence similarity between templates as well as RNA secondary structures (40, 184–186). Low levels of cellular dNTP pools may also promote recombination, as macrophages have been found to have recombination rates up to 4-fold higher than observed in T cells, and HIV-1 template switching in macrophages is reduced to T cell levels following degradation of SAMHD1 *via* Vpx (168, 187).

APOBEC3 Proteins

Host cellular factors, including the APOBEC3 (apolipoprotein B mRNA editing-enzyme catalytic polypeptide-like 3; A3) family of restriction factors, also contribute to viral mutagenesis (**Figure 5**). These proteins are a family of cytosine deaminases that catalyze the deamination of cytosine (C) to uracil (U) within ssDNA substrates (188, 189). During reverse transcription, these C-to-U mutations template the improper insertion of adenine (A) in place of guanine (G) in the complimentary DNA strand, effectively catalyzing G-to-A mutations within the positive-sense DNA strand (188, 190). Of the 7 APOBEC3 proteins encoded within the human genome (A3A-D, A3F-H), A3D, A3F, A3G, and A3H (haplotypes II, V, and VII) have been shown to restrict HIV-1 infection *via* the introduction of G-to-A mutations during reverse transcription (191–195). Editing by APOBEC3 proteins is dependent on both DNA structure and sequence, with A3G preferentially targeting cytosines within a 5'-CC-3' (5'-GG-3') context and all other A3 proteins more potently mutagenizing cytosines within a 5'-TC-3' (5'-GA-3') context (189, 196–200). APOBEC3 proteins, particularly A3G, can introduce several G-to-A mutations within an HIV-1 genome during a single round of replication, a phenomenon termed *hypermutation*. One study found that up to 10% of plus-strand guanines in the HIV-1 viral genome were converted to adenines by A3G during a single round of replication; some individual base pairs were especially prone to mutagenesis, being changed to adenines at frequencies ranging from 33% to 100% (196). APOBEC3-induced G-to-A mutations are often lethal, as a G-to-A transition within a 5'-TGG-3' context results in the generation of any one of the 3 translational stop codons (TAG, TAA, or TGA). In an analysis of the HIV-1 *gag* gene, it was found that over 80% of proviruses contained stop codons introduced by A3G editing within a cell culture system (196).

HIV-1 escapes restriction by APOBEC3 proteins *via* expression of the Vif (viral infectivity factor) protein. In viral producer cells, Vif interacts with the cellular cofactor CBF-β to catalyze the formation of an active E3 ubiquitin ligase complex, comprised of CUL5, ELOB, ELOC, and RBX1, to promote the ubiquitination and subsequent proteasomal degradation of APOBEC3 proteins (188, 201–205). In the absence of Vif, APOBEC3 proteins are packaged into budding particles along with viral proteins and genomic RNA. Following infection of a target cell, they exert their antiviral activity by deaminating cytosines within the nascent ssDNA. Targeting of the APOBEC3 proteins for degradation within the producer cell by Vif prevents their incorporation into viral particles and allows the virus to circumvent APOBEC3-mediated restriction.

However, even in the presence of Vif expression, sublethal levels of G-to-A mutations are observed within the HIV-1 genome, indicating that suppression of APOBEC3-mediated restriction is incomplete (142, 143, 158, 206, 207). These mutations have important implications within the context of viral infection, and have been linked to changes in coreceptor usage, immune evasion, and the failure of ART (208–214). One study found that incomplete neutralization of A3G and A3F was associated with a significant increase in the presence of CXCR4-tropic viruses in the population, a shift that has previously been found to correlate with cell tropism changes, disease progression, and a more rapid decline in CD4+ T cell counts in HIV-1 infected individuals (209, 215). In a study of 88 Indian HIV-1-positive patients (87 infected with subtype C, 1 infected with a recombinant A1C strain), 11.4% exhibited evidence of A3G-mediated hypermutation within proviral sequences, and patients failing ART were nearly 5-times more likely to exhibit evidence of lethal G-to-A hypermutation than treatment naïve patients (214). Collectively with other *in vitro* and *in vivo* studies, these results suggest that, despite their relatively minor contribution to the HIV-1 mutation rate (158), G-to-A mutations resulting from sublethal APOBEC3-mediated mutagenesis are important drivers of HIV-1 diversification and evolution.

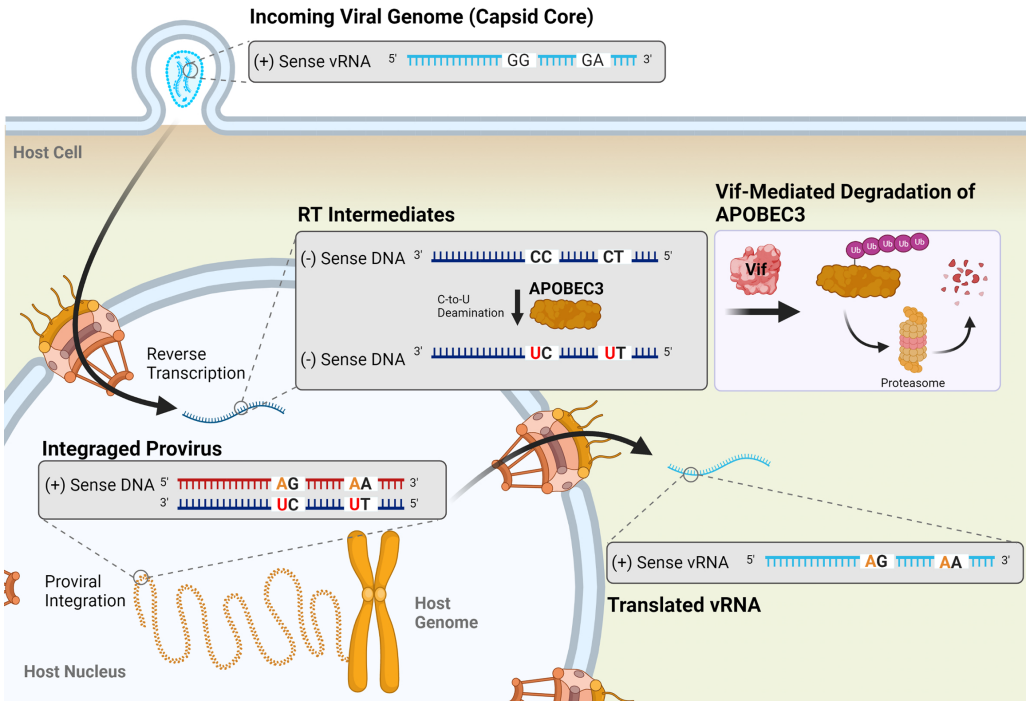

FIGURE 5 | Mutagenesis by APOBEC3 proteins results in G-to-A transition mutations in HIV-1 proviruses. Four APOBEC3 proteins (A3D, A3F, A3G, and A3H) are known to restrict HIV-1 infection by catalyzing the deamination of cytosine in single-stranded DNA (ssDNA) into a uracil (red) during reverse transcription. This templates the improver insertion of an adenine (orange) in place of a guanine, resulting in a G-to-A mutation in the positive-sense DNA strand of the resulting provirus. These mutations preferentially occur in a 5'-GG-3' or 5'-GA-3' dinucleotide context. APOBEC3 activity is inhibited by the viral accessory protein Vif (shown in pink box), which targets APOBEC3 proteins for degradation by the proteasome. Vif suppression of APOBEC3 activity is incomplete, though, and sublethal levels of G-to-A mutations can be observed in HIV-1 proviruses.

The restrictive activity of APOBEC3 proteins against other human retroviruses has remained largely uncharacterized relative to HIV-1. Studies on the anti-HIV-2 activity of APOBEC3 proteins have largely been conducted in a piecewise fashion, primarily as an evolutionary comparator with HIV-1 and SIV (216–218). However, one study demonstrated that HIV-1 and HIV-2 Vif proteins interact with A3G and A3F *via* disparate moieties in both the Vif and APOBEC3 proteins (218). Additionally, our group has demonstrated that HIV-2 is characterized by a relative lack of G-to-A mutations, and specifically hypermutations, relative to HIV-1 (142, 143). Consistent with these observations, restriction of HIV-2 was found to be mediated by a smaller subset of APOBEC3 proteins than HIV-1 (A3F, A3G, and A3H), with only A3F and A3G serving as potent mutagens of HIV-2 (219). Collectively, these results indicate that APOBEC3-mediated restriction of HIV-2 is distinct from that of HIV-1.

The effects of APOBEC3 proteins on HTLV-1 have been studied, but with somewhat inconclusive results. In a single cell culture study, A3A and A3B were found to restrict HTLV-1 infection in a deaminase-dependent manner (220). A3G and A3H (haplotype II) have also been found to restrict HTLV-1 infection *in vitro*, though these proteins are thought to act in a deaminase-independent manner and the exact mechanisms remain to be established (220, 221). However, two studies independently examined proviral sequences obtained from the blood of HTLV-1-infected individuals to determine the effects of APOBEC3 editing *in vivo*. While one study found no evidence of G-to-A hypermutation within HTLV-1 proviruses (222), the other reported extensive editing of proviral sequences within dinucleotide contexts suggestive of APOBEC3-mediated mutagenesis (220). A more recent study examining the evolutionary footprint of APOBEC3 proteins within the genome of human viruses found that the HBZ-encoding region of the HTLV-1 genome is relatively depleted of 5'-NTC-3' codons, indicative of historic APOBEC3-mediated editing throughout the evolution of the virus (223). More research is needed to fully understand the effects of the HTLV-1-restrictive activity of APOBEC3, but studies have been confounded by difficulties propagating the virus in cell culture (224–226).

ADAR Proteins

Host ADAR (adenosine deaminases acting on RNA) proteins have also been implicated as potential sources of mutation during HIV-1 replication (**Figure 6A**). ADAR proteins are RNA-editing enzymes that catalyze the deamination of adenosine into the purine nucleoside inosine (I) in double-stranded RNA structures (227, 228). During splicing and

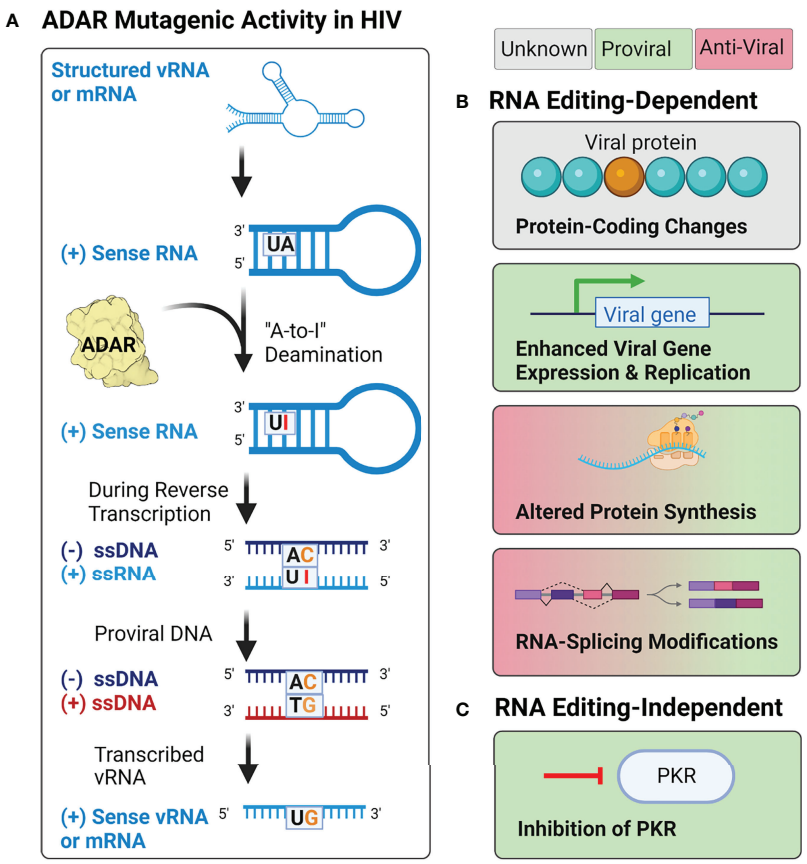

FIGURE 6 | Potential effects of ADAR activity during HIV-1, HIV-2, and HTLV-1 infection. **(A)** Adenosine deamination reactions by ADAR proteins during retroviral replication are thought to induce A-to-I mutations within structured RNA elements from both the incoming vRNA genome and transcribed mRNA products. When these mutations occur during reverse transcription, it may lead to the introduction of A-to-G mutations in the integrated provirus. **(B)** Proposed RNA editing-dependent enzymatic activities of ADAR during retroviral infection have reported pro- and antiviral effects on protein synthesis, viral gene expression and replication, rates of protein synthesis, and RNA-splicing. **(C)** Proposed RNA editing-independent effects include inhibition of PKR.

translation events, cellular machinery treat inosine as guanosine, resulting in changes to both splicing patterns and protein amino acid sequences (228–230). This also results in the introduction of A-to-G mutations in proviral DNA when these editing events occur during reverse transcription (154, 231). A-to-G, and U-to-C, hypermutation have been observed in many negative-sense RNA viruses but are observed relatively infrequently in retroviruses such as HIV-1 and HIV-2 (142, 154, 207, 232, 233).

Research on the effects of ADAR editing on HIV-1 infectivity has yielded conflicting results (**Figure 6B**). Several studies have demonstrated that ADAR1 and ADAR2, the two ADAR proteins expressed throughout the body, serve as proviral factors for HIV-1 (and HTLV-1) infection (234–238). Studies of ADAR1 overexpression in HIV-1 producer cells have demonstrated that editing by ADAR1 in the 5'UTR, as well as the *env*, *rev*, and *tat* genes, results in enhanced expression of the viral genome and increased protein production (234, 236). Experimental evidence using both HIV-1 and HTLV-1 suggest that the proviral activity of ADAR1 is also mediated by ADAR1-induced inhibition of PKR (protein kinase RNA activated), an antiviral protein that inhibits translational initiation of viral RNAs (**Figure 6C**) (235, 238). However, although ADAR1 has been shown to facilitate HIV-1 replication in CD4+ T cells (238), it has been found to inhibit HIV-1 replication in human alveolar macrophages (233). In these cells, overexpression of ADAR1 inhibited viral replication, but did not affect transcription of viral genes, suggesting the antiviral activity may be regulated post-transcriptionally (233). This hypothesis is supported by evidence from a variety of cell lines (293T, HeLa, Jurkat T, and primary CD4+ T cells), which found that ADAR1-induced A-to-G mutations in highly structured regions of the genome (i.e., *rev*, *env*, and the RRE) inhibited viral protein synthesis, but not viral RNA synthesis (239). The conflicting results observed in existing studies, as well as the lack of research on the effects of ADAR1 and ADAR2 on HIV-2 replication, highlight the need for further research on the cellular sources of genetic diversity within human retroviruses, and their effects on viral replication.

CONCLUSION

Much of our current knowledge on the biology of human retroviruses is based on studies of HIV-1, the most prominent and deadly of the human pathogenic *Retroviridae*. However, comparative studies demonstrate key genetic, morphological, and physiologic differences between HIV-1 and other retroviruses including HIV-2 and HTLV-1. Historically, assumptions about these viruses, particularly HIV-2, have been made based on what is known about HIV-1. Indeed, even clinical guidelines for the treatment of HIV-2-infected individuals are based on extrapolation of data from the treatment of HIV-1, as clinical trials and formal studies in HIV-2 patients are lacking (240). As indicated in this review, the available research demonstrates that significant diversity exists among human retroviruses, and each should be studied independently for a complete understanding of their biology, including the cellular and molecular determinants of replication and mutagenesis. Comparative analysis among the human retroviruses can be powerful in understanding their replication, evolution, persistence, and pathogenicity.

AUTHOR CONTRIBUTIONS

Writing—original draft preparation, MM. Writing—reviewing and editing, MM, NT, and LM. Visualization, MM and NT. All authors contributed to the article and approved the submitted version.

FUNDING

This work was supported by National Institutes of Health grant R01 AI150468 (to LM). MM was supported by NIH grants T32 AI083196 and F31 AI 50487. NT was supported by NIH grants T32 DA007097, F32 AI150351, and American Cancer Society Postdoctoral Fellowship PF-21-189-01-MPC.

ACKNOWLEDGMENTS

We thank Dr. Nikunj Somia for his thoughtful comments and advice on this manuscript. Figures were created with BioRender.com.

REFERENCES

1. Barre-Sinoussi F, Chermann JC, Rey F, Nugeyre MT, Chamaret S, Gruest J, et al. Isolation of a T-Lymphotropic Retrovirus From a Patient at Risk for Acquired Immune Deficiency Syndrome (AIDS). *Science* (1983) 220 (4599):868–71. doi: 10.1126/science.6189183
2. Gallo RC, Sarin PS, Gelmann EP, Robert-Guroff M, Richardson E, Kalyanaraman VS, et al. Isolation of Human T-Cell Leukemia Virus in Acquired Immune Deficiency Syndrome (AIDS). *Science* (1983) 220 (4599):865–7. doi: 10.1126/science.6601823
3. UNAIDS. *Global HIV & AIDS Statistics — 2019 Fact Sheet* (2020). Available at: https://www.unaids.org/en/resources/fact-sheet.
4. World Health Organization. *HIV Data and Statistics* (2020). Available at: https://www.who.int/hiv/data/en/.
5. Visseaux B, Damond F, Matheron S, Descamps D, Charpentier C. Hiv-2 Molecular Epidemiology. *Infect Genet Evol* (2016) 46:233–40. doi: 10.1016/j.meegid.2016.08.010
6. Walker B, McMichael A. The T-Cell Response to HIV. *Cold Spring Harb Perspect Med* (2012) 2(11). doi: 10.1101/cshperspect.a007054
7. Pantaleo G, Fauci AS. Immunopathogenesis of HIV Infection. *Annu Rev Microbiol* (1996) 50:825–54. doi: 10.1146/annurev.micro.50.1.825
8. Poorolajal J, Sarr AD, Travers KU, Guèye-Ndiaye A, Mboup S, Essex ME, et al. Survival Rate of AIDS Disease and Mortality in HIV-Infected Patients: A Meta-Analysis. *Public Health* (2016) 139:3–12. doi: 10.1016/j.puhe.2016.05.004
9. Popper SJ, Hooshmand E, Mahjub H, Esmailnasab N, Jenabi E. Lower Human Immunodeficiency Virus (HIV) Type 2 Viral Load Reflects the Difference in Pathogenicity of HIV-1 and HIV-2. *J Infect Dis* (1999) 180 (4):1116–21. doi: 10.1086/315010
10. Andersson S, Norrgren H, da Silva Z, Biague A, Bamba S, Kwok S, et al. Plasma Viral Load in HIV-1 and HIV-2 Singly and Dually Infected Individuals in Guinea-Bissau, West Africa: Significantly Lower Plasma Virus Set Point in HIV-2 Infection Than in HIV-1 Infection. *Arch Intern Med* (2000) 160(21):3286–93. doi: 10.1001/archinte.160.21.3286
11. Kanki PJ, Travers KU, S MB, Hsieh CC, Marlink RG, Gueye NA, et al. Slower Heterosexual Spread of HIV-2 Than HIV-1. *Lancet* (1994) 343(8903):943–6. doi: 10.1016/S0140-6736(94)90065-5
12. Adjorlolo-Johnson G, Norrgren H, da Silva Z, Biague A, Bamba S, Kwok S, et al. Prospective Comparison of Mother-to-Child Transmission of HIV-1 and HIV-2 in Abidjan, Ivory Coast. *JAMA* (1994) 272(6):462–6. doi: 10.1001/jama.1994.03520060062033
13. O'Donovan D, Ariyoshi K, Milligan P, Ota M, Yamuah L, Sarge-Njie R, et al. Maternal Plasma Viral RNA Levels Determine Marked Differences in Mother-to-Child Transmission Rates of HIV-1 and HIV-2 in The Gambia. MRC/Gambia Government/University College London Medical School Working Group on Mother-Child Transmission of HIV. *AIDS* (2000) 14(4):441–8.
14. Marlink R, Kanki P, Thior I, Travers K, Marlink R, et al. Reduced Rate of Disease Development After HIV-2 Infection as Compared to HIV-1. *Science* (1994) 265(5178):1587–90. doi: 10.1126/science.7915856
15. van der Loeff MF, Awasana AA, Sarge-Njie R, van der Sande M, Jaye A, Sabally S, et al. Sixteen Years of HIV Surveillance in a West African Research Clinic Reveals Divergent Epidemic Trends of HIV-1 and HIV-2. *Int J Epidemiol* (2006) 35(5):1322–8. doi: 10.1093/ije/dyl037
16. da Silva ZJ, Oliveira I, Andersen A, Dias F, Rodrigues A, Holmgren B, et al. Changes in Prevalence and Incidence of HIV-1, HIV-2 and Dual Infections in Urban Areas of Bissau, Guinea-Bissau: Is HIV-2 Disappearing? *AIDS* (2008) 22(10):1195–202. doi: 10.1097/QAD.0b013e328300a33d
17. Tienen C, van der Loeff MS, Zaman SM, Vincent T, Sarge-Njie R, Peterson I, et al. Two Distinct Epidemics: The Rise of HIV-1 and Decline of HIV-2 Infection Between 1990 and 2007 in Rural Guinea-Bissau. *J Acquir Immune Defic Syndr* (2010) 53(5):640–7. doi: 10.1097/QAI.0b013e3181bf1a25
18. Berges BK, Akkina SR, Remling L, Akkina R. Humanized Rag2(-/-)Gammac (-/-) (RAG-Hu) Mice can Sustain Long-Term Chronic HIV-1 Infection Lasting More Than a Year. *Virology* (2010) 397(1):100–3. doi: 10.1016/j.virol.2009.10.034
19. Hu S, Neff CP, Kumar DM, Habu Y, Akkina SR, Seki T, et al. A Humanized Mouse Model for HIV-2 Infection and Efficacy Testing of a Single-Pill Triple-Drug Combination Anti-Retroviral Therapy. *Virology* (2017) 501:115–8. doi: 10.1016/j.virol.2016.11.013
20. Julg B, Pereyra F, Buzon MJ, Piechocka-Trocha A, Clark MJ, Baker BM, et al. Infrequent Recovery of HIV From But Robust Exogenous Infection of Activated CD4(+) T Cells in HIV Elite Controllers. *Clin Infect Dis* (2010) 51(2):233–8. doi: 10.1086/653677
21. Garcia M, Gorgolas M, Cabello A, Estrada V, Ligos JM, Fernandez-Guerrero M, et al. Peripheral T Follicular Helper Cells Make a Difference in HIV Reservoir Size Between Elite Controllers and Patients on Successful cART. *Sci Rep* (2017) 7(1):16799. doi: 10.1038/s41598-017-17057-y
22. Sharaf R, Lee GQ, Sun X, Etemad B, Aboukhater LM, Hu Z, et al. HIV-1 Proviral Landscapes Distinguish Posttreatment Controllers From Noncontrollers. *J Clin Invest* (2018) 128(9):4074–85. doi: 10.1172/JCI120549
23. Gueudin M, Damond F, Braun J, Taieb A, Lemee V, Plantier JC, et al. Differences in Proviral DNA Load Between HIV-1- and HIV-2-Infected Patients. *AIDS* (2008) 22(2):211–5. doi: 10.1097/QAD.0b013e3282f42429
24. Popper SJ, Sarr AD, Gueye-Ndiaye A, Mboup S, Essex ME, Kanki PJ. Low Plasma Human Immunodeficiency Virus Type 2 Viral Load is Independent

of Proviral Load: Low Virus Production *In Vivo*. *J Virol* (2000) 74(3):1554–7. doi: 10.1128/JVI.74.3.1554-1557.2000
25. Yoshida M, Miyoshi I, Hinuma Y. Isolation and Characterization of Retrovirus From Cell Lines of Human Adult T-Cell Leukemia and its Implication in the Disease. *Proc Natl Acad Sci USA* (1982) 79(6):2031–5. doi: 10.1073/pnas.79.6.2031
26. Popovic M, Sarin PS, Robert-Gurroff M, Kalyanaraman VS, Mann D, Minowada J, et al. Isolation and Transmission of Human Retrovirus (Human T-Cell Leukemia Virus). *Science* (1983) 219(4586):856–9. doi: 10.1126/science.6600519
27. Yamamoto N, Matsumoto T, Koyanagi Y, Tanaka Y, Hinuma Y. Unique Cell Lines Harbouring Both Epstein-Barr Virus and Adult T-Cell Leukaemia Virus, Established From Leukaemia Patients. *Nature* (1982) 299(5881):367–9. doi: 10.1038/299367a0
28. Longo DL, Gelmann EP, Cossman J, Young RA, Gallo RC, O'Brien SJ, et al. Isolation of HTLV-Transformed B-Lymphocyte Clone From a Patient With HTLV-Associated Adult T-Cell Leukaemia. *Nature* (1984) 310(5977):505–6. doi: 10.1038/310505a0
29. Ho DD, Rota TR, Hirsch MS. Infection of Human Endothelial Cells by Human T-Lymphotropic Virus Type I. *Proc Natl Acad Sci USA* (1984) 81 (23):7588–90. doi: 10.1073/pnas.81.23.7588
30. Yoshikura H, Nishida J, Yoshida M, Kitamura Y, Takaku F, Ikeda S, et al. Isolation of HTLV Derived From Japanese Adult T-Cell Leukemia Patients in Human Diploid Fibroblast Strain IMR90 and the Biological Characters of the Infected Cells. *Int J Cancer* (1984) 33(6):745–9. doi: 10.1002/ijc.2910330606
31. Koyanagi Y, Itoyama Y, Nakamura N, Takamatsu K, Kira J, Iwamasa T, et al. *In Vivo* Infection of Human T-Cell Leukemia Virus Type I in non-T Cells. *Virology* (1993) 196(1):25–33. doi: 10.1006/viro.1993.1451
32. Gessain A, Mahieux R. Tropical Spastic Paraparesis and HTLV-1 Associated Myelopathy: Clinical, Epidemiological, Virological and Therapeutic Aspects. *Rev Neurol (Paris)* (2012) 168(3):257–69. doi: 10.1016/j.neurol.2011.12.006
33. Afonso PV, Cassar O, Gessain A. Molecular Epidemiology, Genetic Variability and Evolution of HTLV-1 With Special Emphasis on African Genotypes. *Retrovirology* (2019) 16(1):39. doi: 10.1186/s12977-019-0504-z
34. Yoshida M, Seiki M, Yamaguchi K, Takatsuki K. Monoclonal Integration of Human T-Cell Leukemia Provirus in All Primary Tumors of Adult T-Cell Leukemia Suggests Causative Role of Human T-Cell Leukemia Virus in the Disease. *Proc Natl Acad Sci USA* (1984) 81(8):2534–7. doi: 10.1073/pnas.81.8.2534
35. Gessain A, Barin F, Vernant JC, Gout O, Maurs L, Calender A, et al. Antibodies to Human T-Lymphotropic Virus Type-I in Patients With Tropical Spastic Paraparesis. *Lancet* (1985) 2(8452):407–10. doi: 10.1016/S0140-6736(85)92734-5
36. Osame M, Usuku K, Izumo S, Ijichi N, Amitani H, Igata A, et al. HTLV-I Associated Myelopathy, a New Clinical Entity. *Lancet* (1986) 1(8488):1031–2. doi: 10.1016/S0140-6736(86)91298-5
37. Einsiedel L, Pham H, Au V, Hatami S, Wilson K, Spelman T, et al. Predictors of non-Cystic Fibrosis Bronchiectasis in Indigenous Adult Residents of Central Australia: Results of a Case-Control Study. *ERJ Open Res* (2019) 5 (4). doi: 10.1183/23120541.00001-2019
38. Watts JM, Dang KK, Gorelick RJ, Leonard CW, Bess JWJr, Swanstrom R, et al. Architecture and Secondary Structure of an Entire HIV-1 RNA Genome. *Nature* (2009) 460(7256):711–6. doi: 10.1038/nature08237
39. Tebit DM, Arts EJ. Tracking a Century of Global Expansion and Evolution of HIV to Drive Understanding and to Combat Disease. *Lancet Infect Dis* (2011) 11(1):45–56. doi: 10.1016/S1473-3099(10)70186-9
40. Dilley KA, Ni N, Nikolaitchik OA, Chen J, Galli A, Hu WS. Determining the Frequency and Mechanisms of HIV-1 and HIV-2 RNA Copackaging by Single-Virion Analysis. *J Virol* (2011) 85(20):10499–508. doi: 10.1128/JVI.05147-11
41. Harrod R. Silencers of HTLV-1 and HTLV-2: The pX-Encoded Latency-Maintenance Factors. *Retrovirology* (2019) 16(1):25. doi: 10.1186/s12977-019-0487-9
42. Bangham CR, Ratner L. How Does HTLV-1 Cause Adult T-Cell Leukaemia/Lymphoma (ATL)? *Curr Opin Virol* (2015) 14:93–100. doi: 10.1016/j.coviro.2015.09.004
43. Sharp PM, Hahn BH. Origins of HIV and the AIDS Pandemic. *Cold Spring Harb Perspect Med* (2011) 1(1):a006841. doi: 10.1101/cshperspect.a006841
44. German Advisory Committee Blood, S. A. o. P. T. b. B. Human Immunodeficiency Virus (HIV). *Transfus Med Hemother* (2016) 43 (3):203–22.
45. Sonoda S, Li HC, Tajima K. Ethnoepidemiology of HTLV-1 Related Diseases: Ethnic Determinants of HTLV-1 Susceptibility and its Worldwide Dispersal. *Cancer Sci* (2011) 102(2):295–301. doi: 10.1111/j.1349-7006.2010.01820.x
46. Paiva A, Casseb J. Origin and Prevalence of Human T-Lymphotropic Virus Type 1 (HTLV-1) and Type 2 (HTLV-2) Among Indigenous Populations in the Americas. *Rev Inst Med Trop Sao Paulo* (2015) 57(1):1–13. doi: 10.1590/S0036-46652015000100001
47. Sonoda S, Li HC, Cartier L, Nunez L, Tajima K. Ancient HTLV Type 1 Provirus DNA of Andean Mummy. *AIDS Res Hum Retroviruses* (2000) 16 (16):1753–6. doi: 10.1089/08892220050193263
48. Rayne F, Bouamr F, Lalanne J, Mamoun RZ. The NH2-Terminal Domain of the Human T-Cell Leukemia Virus Type 1 Capsid Protein is Involved in Particle Formation. *J Virol* (2001) 75(11):5277–87. doi: 10.1128/JVI.75.11.5277-5287.2001
49. Bernstein HB, Tucker SP, Hunter E, Schutzbach JS, Compans RW. Human Immunodeficiency Virus Type 1 Envelope Glycoprotein is Modified by O-Linked Oligosaccharides. *J Virol* (1994) 68(1):463–8. doi: 10.1128/jvi.68.1.463-468.1994
50. Allan JS, Coligan JE, Barin F, McLane MF, Sodroski JG, Rosen CA, et al. Major Glycoprotein Antigens That Induce Antibodies in AIDS Patients are Encoded by HTLV-III. *Science* (1985) 228(4703):1091–4. doi: 10.1126/science.2986290
51. Leonard CK, Spellman MW, Riddle L, Harris RJ, Thomas JN, Gregory TJ. Assignment of Intrachain Disulfide Bonds and Characterization of Potential Glycosylation Sites of the Type 1 Recombinant Human Immunodeficiency Virus Envelope Glycoprotein (Gp120) Expressed in Chinese Hamster Ovary Cells. *J Biol Chem* (1990) 265(18):10373–82. doi: 10.1016/S0021-9258(18)86956-3
52. Sebastian NT, Zaikos TD, Terry V, Taschuk F, McNamara LA, Onafuwa-Nuga A, et al. CD4 is Expressed on a Heterogeneous Subset of Hematopoietic Progenitors, Which Persistently Harbor CXCR4 and CCR5-Tropic HIV Proviral Genomes *In Vivo*. *PloS Pathog* (2017) 13(7): e1006509. doi: 10.1371/journal.ppat.1006509
53. Ghez D, Lepelletier Y, Jones KS, Pique C, Hermine O. Current Concepts Regarding the HTLV-1 Receptor Complex. *Retrovirology* (2010) 7:99. doi: 10.1186/1742-4690-7-99
54. Temin HM, Mizutani S. RNA-Dependent DNA Polymerase in Virions of Rous Sarcoma Virus. *Nature* (1970) 226(5252):1211–3. doi: 10.1038/2261211a0
55. Baltimore D. RNA-Dependent DNA Polymerase in Virions of RNA Tumour Viruses. *Nature* (1970) 226(5252):1209–11. doi: 10.1038/2261209a0
56. Forshey BM, von Schwedler U, Sundquist WI, Aiken C. Formation of a Human Immunodeficiency Virus Type 1 Core of Optimal Stability is Crucial for Viral Replication. *J Virol* (2002) 76(11):5667–77. doi: 10.1128/JVI.76.11.5667-5677.2002
57. Hulme AE, Perez O, Hope TJ. Complementary Assays Reveal a Relationship Between HIV-1 Uncoating and Reverse Transcription. *Proc Natl Acad Sci USA* (2011) 108(24):9975–80. doi: 10.1073/pnas.1014522108
58. Hulme AE, Kelley Z, Okocha EA, Hope TJ. Identification of Capsid Mutations That Alter the Rate of HIV-1 Uncoating in Infected Cells. *J Virol* (2015) 89(1):643–51. doi: 10.1128/JVI.03043-14
59. Dharan A, Bachmann N, Talley S, Zwikelmaier V, Campbell EM. Nuclear Pore Blockade Reveals That HIV-1 Completes Reverse Transcription and Uncoating in the Nucleus. *Nat Microbiol* (2020) 5(9):1088–95. doi: 10.1038/s41564-020-0735-8
60. Li C, Burdick RC, Nagashima K, Hu WS, Pathak VK. HIV-1 Cores Retain Their Integrity Until Minutes Before Uncoating in the Nucleus. *Proc Natl Acad Sci USA* (2021) 118(10). doi: 10.1073/pnas.2019467118
61. Zila V, Margiotta E, Turonova B, Muller TG, Zimmerli CE, Mattei S, et al. Cone-Shaped HIV-1 Capsids are Transported Through Intact Nuclear Pores. *Cell* (2021) 184(4):1032–1046.e1018. doi: 10.1016/j.cell.2021.01.025

62. Blanco-Rodriguez G, Gazi A, Monel B, Frabetti S, Scoca V, Mueller F, et al. Remodeling of the Core Leads HIV-1 Preintegration Complex Into the Nucleus of Human Lymphocytes. *J Virol* (2020) 94(11). doi: 10.1128/JVI.00135-20
63. Guedan A, Donaldson CD, Caroe ER, Cosnefroy O, Taylor IA, Bishop KN. HIV-1 Requires Capsid Remodelling at the Nuclear Pore for Nuclear Entry and Integration. *PloS Pathog* (2021) 17(9):e1009484. doi: 10.1371/journal.ppat.1009484
64. Jin D, Musier-Forsyth K. Role of Host tRNAs and aminoacyl-tRNA Synthetases in Retroviral Replication. *J Biol Chem* (2019) 294(14):5352–64. doi: 10.1074/jbc.REV118.002957
65. Kitamura Y, Lee YM, Coffin JM. Nonrandom Integration of Retroviral DNA *In Vitro*: Effect of CpG Methylation. *Proc Natl Acad Sci USA* (1992) 89 (12):5532–6. doi: 10.1073/pnas.89.12.5532
66. Schroder AR, Shinn P, Chen H, Berry C, Ecker JR, Bushman F. HIV-1 Integration in the Human Genome Favors Active Genes and Local Hotspots. *Cell* (2002) 110(4):521–9. doi: 10.1016/S0092-8674(02)00864-4
67. Holman AG, Coffin JM. Symmetrical Base Preferences Surrounding HIV-1, Avian Sarcoma/Leukosis Virus, and Murine Leukemia Virus Integration Sites. *Proc Natl Acad Sci USA* (2005) 102(17):6103–7. doi: 10.1073/pnas.0501646102
68. MacNeil A, Sankale JL, Meloni ST, Sarr AD, Mboup S, Kanki P. Genomic Sites of Human Immunodeficiency Virus Type 2 (HIV-2) Integration: Similarities to HIV-1 *In Vitro* and Possible Differences *In Vivo*. *J Virol* (2006) 80(15):7316–21. doi: 10.1128/JVI.00604-06
69. Soto MJ, Pena A, Vallejo FG. A Genomic and Bioinformatics Analysis of the Integration of HIV in Peripheral Blood Mononuclear Cells. *AIDS Res Hum Retroviruses* (2011) 27(5):547–55. doi: 10.1089/aid.2010.0182
70. Kok YL, Vongrad V, Chaudron SE, Shilaih M, Leemann C, Neumann K, et al. HIV-1 Integration Sites in CD4+ T-Cells During Primary, Chronic, and Late Presentation of HIV-1 Infection. *JCI Insight* (2021). doi: 10.1172/jci.insight.143940
71. Doi K, Wu X, Taniguchi Y, Yasunaga J, Satou Y, Okayama A, et al. Preferential Selection of Human T-Cell Leukemia Virus Type I Provirus Integration Sites in Leukemic Versus Carrier States. *Blood* (2005) 106 (3):1048–53. doi: 10.1182/blood-2004-11-4350
72. Derse D, Crise B, Li Y, Princler G, Lum N, Stewart C, et al. Human T-Cell Leukemia Virus Type 1 Integration Target Sites in the Human Genome: Comparison With Those of Other Retroviruses. *J Virol* (2007) 81(12):6731–41. doi: 10.1128/JVI.02752-06
73. Pluta A, Jaworski JP, Cortes-Rubio CN. Balance Between Retroviral Latency and Transcription: Based on HIV Model. *Pathogens* (2020) 10(1). doi: 10.3390/pathogens10010016
74. Pluta A, Jaworski JP, Douville RN. Regulation of Expression and Latency in BLV and HTLV. *Viruses* (2020) 12(10). doi: 10.3390/v12101079
75. Ciuffi A, Bushman FD. Retroviral DNA Integration: HIV and the Role of LEDGF/P75. *Trends Genet* (2006) 22(7):388–95. doi: 10.1016/j.tig.2006.05.006
76. He G, Margolis DM. Counterregulation of Chromatin Deacetylation and Histone Deacetylase Occupancy at the Integrated Promoter of Human Immunodeficiency Virus Type 1 (HIV-1) by the HIV-1 Repressor YY1 and HIV-1 Activator Tat. *Mol Cell Biol* (2002) 22(9):2965–73. doi: 10.1128/MCB.22.9.2965-2973.2002
77. Williams SA, Chen LF, Kwon H, Ruiz-Jarabo CM, Verdin E, Greene WC. NF-kappaB P50 Promotes HIV Latency Through HDAC Recruitment and Repression of Transcriptional Initiation. *EMBO J* (2006) 25(1):139–49. doi: 10.1038/sj.emboj.7600900
78. Keedy KS, Archin NM, Gates AT, Espeseth A, Hazuda DJ, Margolis DM. A Limited Group of Class I Histone Deacetylases Acts to Repress Human Immunodeficiency Virus Type 1 Expression. *J Virol* (2009) 83(10):4749–56. doi: 10.1128/JVI.02585-08
79. Lanman J, Lam TT, Barnes S, Sakalian M, Emmett MR, Marshall AG, et al. Identification of Novel Interactions in HIV-1 Capsid Protein Assembly by High-Resolution Mass Spectrometry. *J Mol Biol* (2003) 325(4):759–72. doi: 10.1016/S0022-2836(02)01245-7
80. Martin JL, Mendonca LM, Angert I, Mueller JD, Zhang W, Mansky LM. Disparate Contributions of Human Retrovirus Capsid Subdomains to Gag-Gag Oligomerization, Virus Morphology, and Particle Biogenesis. *J Virol* (2017) 91(14). doi: 10.1128/JVI.00298-17
81. Martin JL, Mendonca LM, Marusinec R, Zuczek J, Angert I, Blower RJ, et al. Critical Role of the Human T-Cell Leukemia Virus Type 1 Capsid N-Terminal Domain for Gag-Gag Interactions and Virus Particle Assembly. *J Virol* (2018) 92(14). doi: 10.1128/JVI.00333-18
82. Eichorst JP, Chen Y, Mueller JD, Mansky LM. Distinct Pathway of Human T-Cell Leukemia Virus Type 1 Gag Punctum Biogenesis Provides New Insights Into Enveloped Virus Assembly. *mBio* (2018) 9(5). doi: 10.1128/mBio.00758-18
83. Chukkapalli V, Hogue IB, Boyko V, Hu WS, Ono A. Interaction Between the Human Immunodeficiency Virus Type 1 Gag Matrix Domain and Phosphatidylinositol-(4,5)-Bisphosphate is Essential for Efficient Gag Membrane Binding. *J Virol* (2008) 82(5):2405–17. doi: 10.1128/JVI.01614-07
84. Ono A. HIV-1 Assembly at the Plasma Membrane: Gag Trafficking and Localization. *Future Virol* (2009) 4(3):241–57. doi: 10.2217/fvl.09.4
85. Inlora J, Collins DR, Trubin ME, Chung JY, Ono A. Membrane Binding and Subcellular Localization of Retroviral Gag Proteins are Differentially Regulated by MA Interactions With Phosphatidylinositol-(4,5)-Bisphosphate and RNA. *mBio* (2014) 5(6):e02202. doi: 10.1128/mBio.02202-14
86. Maldonado JO, Martin JL, Mueller JD, Zhang W, Mansky LM. New Insights Into Retroviral Gag-Gag and Gag-Membrane Interactions. *Front Microbiol* (2014) 5:302. doi: 10.3389/fmicb.2014.00302
87. Thornhill D, Murakami T, Ono A. Rendezvous at Plasma Membrane: Cellular Lipids and tRNA Set Up Sites of HIV-1 Particle Assembly and Incorporation of Host Transmembrane Proteins. *Viruses* (2020) 12(8). doi: 10.3390/v12080842
88. Herrmann D, Zhou LW, Hanson HM, Willkomm NA, Mansky LM, Saad JS. Structural Insights Into the Mechanism of Human T-Cell Leukemia Virus Type 1 Gag Targeting to the Plasma Membrane for Assembly. *J Mol Biol* (2021) 433(19):167161. doi: 10.1016/j.jmb.2021.167161
89. Ono A, Ablan SD, Lockett SJ, Nagashima K, Freed EO. Phosphatidylinositol (4,5) Bisphosphate Regulates HIV-1 Gag Targeting to the Plasma Membrane. *Proc Natl Acad Sci USA* (2004) 101(41):14889–94. doi: 10.1073/pnas.0405596101
90. Sun M, Grigsby IF, Gorelick RJ, Mansky LM, Musier-Forsyth K. Retrovirus-Specific Differences in Matrix and Nucleocapsid Protein-Nucleic Acid Interactions: Implications for Genomic RNA Packaging. *J Virol* (2014) 88 (2):1271–80. doi: 10.1128/JVI.02151-13
91. Kroupa T, Datta SAK, Rein A. Distinct Contributions of Different Domains Within the HIV-1 Gag Polyprotein to Specific and Nonspecific Interactions With RNA. *Viruses* (2020) 12(4). doi: 10.3390/v12040394
92. Mouhand A, Pasi M, Catala M, Zargarian L, Belfetmi A, Barraud P, et al. Overview of the Nucleic-Acid Binding Properties of the HIV-1 Nucleocapsid Protein in Its Different Maturation States. *Viruses* (2020) 12(10). doi: 10.3390/v12101109
93. Wu W, Hatterschide J, Syu YC, Cantara WA, Blower RJ, Hanson HM, et al. Human T-Cell Leukemia Virus Type 1 Gag Domains Have Distinct RNA-Binding Specificities With Implications for RNA Packaging and Dimerization. *J Biol Chem* (2018) 293(42):16261–76. doi: 10.1074/jbc.RA118.005531
94. Chen J, Grunwald D, Sardo L, Galli A, Plisov S, Nikolaitchik OA, et al. Cytoplasmic HIV-1 RNA is Mainly Transported by Diffusion in the Presence or Absence of Gag Protein. *Proc Natl Acad Sci USA* (2014) 111 (48):E5205-5213. doi: 10.1073/pnas.1413169111
95. Martin JL, Maldonado JO, Mueller JD, Zhang W, Mansky LM. Molecular Studies of HTLV-1 Replication: An Update. *Viruses* (2016) 8(2). doi: 10.3390/v8020031
96. Comas-Garcia M, Davis SR, Rein A. On the Selective Packaging of Genomic RNA by HIV-1. *Viruses* (2016) 8(9). doi: 10.3390/v8090246
97. Angert CI, Kakura SR, Mansky LM, Mueller JD. Partitioning of Ribonucleoprotein Complexes From the Cellular Actin Cortex. *bioRxiv* (2021). doi: 10.1101/2021.10.01.462753
98. Demirov DG, Freed EO. Retrovirus Budding. *Virus Res* (2004) 106(2):87–102. doi: 10.1016/j.virusres.2004.08.007

99. Morita E, Sundquist WI. Retrovirus Budding. *Annu Rev Cell Dev Biol* (2004) 20:395–425. doi: 10.1146/annurev.cellbio.20.010403.102350
100. Weiss ER, Gottlinger H. The Role of Cellular Factors in Promoting HIV Budding. *J Mol Biol* (2011) 410(4):525–33. doi: 10.1016/j.jmb.2011.04.055
101. Sundquist WI, Krausslich HG. HIV-1 Assembly, Budding, and Maturation. *Cold Spring Harb Perspect Med* (2012) 2(7):a006924.
102. Ehrlich LS, Carter CA. HIV Assembly and Budding: Ca(2+) Signaling and Non-ESCRT Proteins Set the Stage. *Mol Biol Int* (2012) 2012:851670. doi: 10.1155/2012/851670
103. Konvalinka J, Krausslich HG, Muller B. Retroviral Proteases and Their Roles in Virion Maturation. *Virology* (2015) 479-480:403–17. doi: 10.1016/j.virol.2015.03.021
104. Goto T, Ashina T, Fujiyoshi Y, Kume N, Yamagishi H, Nakai M. Projection Structures of Human Immunodeficiency Virus Type 1 (HIV-1) Observed With High Resolution Electron Cryo-Microscopy. *J Electron Microsc (Tokyo)* (1994) 43(1):16–9.
105. Kewalramani VN, Emerman M. Vpx Association With Mature Core Structures of HIV-2. *Virology* (1996) 218(1):159–68. doi: 10.1006/viro.1996.0176
106. Martin JL, Cao S, Maldonado JO, Zhang W, Mansky LM. Distinct Particle Morphologies Revealed Through Comparative Parallel Analyses of Retrovirus-Like Particles. *J Virol* (2016) 90(18):8074–84. doi: 10.1128/JVI.00666-16
107. Zhang W, Cao S, Martin JL, Mueller JD, Mansky LM. Morphology and Ultrastructure of Retrovirus Particles. *AIMS Biophys* (2015) 2(3):343–69. doi: 10.3934/biophy.2015.3.343
108. Yeager M, Wilson-Kubalek EM, Weiner SG, Brown PO, Rein A. Supramolecular Organization of Immature and Mature Murine Leukemia Virus Revealed by Electron Cryo-Microscopy: Implications for Retroviral Assembly Mechanisms. *Proc Natl Acad Sci USA* (1998) 95(13):7299–304. doi: 10.1073/pnas.95.13.7299
109. Butan C, Winkler DC, Heymann JB, Craven RC, Steven AC. RSV Capsid Polymorphism Correlates With Polymerization Efficiency and Envelope Glycoprotein Content: Implications That Nucleation Controls Morphogenesis. *J Mol Biol* (2008) 376(4):1168–81. doi: 10.1016/j.jmb.2007.12.003
110. Effantin G, Estrozi LF, Aschman N, Renesto P, Stanke N, Lindemann D, et al. Cryo-Electron Microscopy Structure of the Native Prototype Foamy Virus Glycoprotein and Virus Architecture. *PloS Pathog* (2016) 12(7):e1005721. doi: 10.1371/journal.ppat.1005721
111. Cao S, Maldonado JO, Grigsby IF, Mansky LM, Zhang W. Analysis of Human T-Cell Leukemia Virus Type 1 Particles by Using Cryo-Electron Tomography. *J Virol* (2015) 89(4):2430–5. doi: 10.1128/JVI.02358-14
112. Meissner ME, Mendonca LM, Zhang W, Mansky LM. Polymorphic Nature of Human T-Cell Leukemia Virus Type 1 Particle Cores as Revealed Through Characterization of a Chronically Infected Cell Line. *J Virol* (2017) 91(16). doi: 10.1128/JVI.00369-17
113. Maldonado JO, Cao S, Zhang W, Mansky LM. Distinct Morphology of Human T-Cell Leukemia Virus Type 1-Like Particles. *Viruses* (2016) 8(5). doi: 10.3390/v8050132
114. Mattei S, Glass B, Hagen WJ, Krausslich HG, Briggs JA. The Structure and Flexibility of Conical HIV-1 Capsids Determined Within Intact Virions. *Science* (2016) 354(6318):1434–7. doi: 10.1126/science.aah4972
115. Schur FK, Hagen WJ, Rumlova M, Ruml T, Muller B, Krausslich HG, et al. Structure of the Immature HIV-1 Capsid in Intact Virus Particles at 8.8 A Resolution. *Nature* (2015) 517(7535):505–8. doi: 10.1038/nature13838
116. Ni T, Zhu Y, Yang Z, Xu C, Chaban Y, Nesterova T, et al. Structure of Native HIV-1 Cores and Their Interactions With IP6 and CypA. *Sci Adv* (2021) 7 (47):eabj5715. doi: 10.1126/sciadv.abj5715
117. Mattei S, Tan A, Glass B, Muller B, Krausslich HG, Briggs JAG. High-Resolution Structures of HIV-1 Gag Cleavage Mutants Determine Structural Switch for Virus Maturation. *Proc Natl Acad Sci USA* (2018) 115(40):E9401–10. doi: 10.1073/pnas.1811237115
118. Schur FK, Obr M, Hagen WJ, Wan W, Jakobi AJ, Kirkpatrick JM, et al. An Atomic Model of HIV-1 Capsid-SP1 Reveals Structures Regulating Assembly and Maturation. *Science* (2016) 353(6298):506–8. doi: 10.1126/science.aaf9620
119. Mendonca L, Sun D, Ning J, Liu J, Kotecha A, Olek M, et al. CryoET Structures of Immature HIV Gag Reveal Six-Helix Bundle. *Commun Biol* (2021) 4(1):481. doi: 10.1038/s42003-021-01999-1
120. Li S, Hill CP, Sundquist WI, Finch JT. Image Reconstructions of Helical Assemblies of the HIV-1 CA Protein. *Nature* (2000) 407(6802):409–13. doi: 10.1038/35030177
121. Khorasanizadeh S, Campos-Olivas R, Clark CA, Summers MF. Sequence-Specific 1H, 13C and 15N Chemical Shift Assignment and Secondary Structure of the HTLV-I Capsid Protein. *J Biomol NMR* (1999) 14(2):199–200. doi: 10.1023/A:1008307507462
122. Ganser-Pornillos BK, von Schwedler UK, Stray KM, Aiken C, Sundquist WI. Assembly Properties of the Human Immunodeficiency Virus Type 1 CA Protein. *J Virol* (2004) 78(5):2545–52. doi: 10.1128/JVI.78.5.2545-2552.2004
123. von Schwedler UK, Stray KM, Garrus JE, Sundquist WI. Functional Surfaces of the Human Immunodeficiency Virus Type 1 Capsid Protein. *J Virol* (2003) 77(9):5439–50. doi: 10.1128/JVI.77.9.5439-5450.2003
124. Yang H, Talledge N, Arndt WG, Zhang W, Mansky LM. Human Immunodeficiency Virus Type 2 Capsid Protein Mutagenesis Defines the Determinants for Gag-Gag Interactions. *BioRxiv* (2022). doi: 10.1101/2022.01.31.478542
125. Talledge N, Yang H, Shi K, Yu G, Arndt WG, Mendonca LM, et al. HIV-2 Immature Particle Morphology Provides Insights Into Gag Lattice Stability and Virus Maturation. *BioRxiv* (2022). doi: 10.1101/2022.02.01.478508
126. Rankovic S, Deshpande A, Harel S, Aiken C, Rousso I. HIV-1 Uncoating Occurs *via* a Series of Rapid Biomechanical Changes in the Core Related to Individual Stages of Reverse Transcription. *J Virol* (2021). doi: 10.1101/2021.01.16.426924
127. Christensen DE, Ganser-Pornillos BK, Johnson JS, Pornillos O, Sundquist WI. Reconstitution and Visualization of HIV-1 Capsid-Dependent Replication and Integration *In Vitro*. *Science* (2020) 370(6513). doi: 10.1126/science.abc8420
128. Korber B, Gaschen B, Yusim K, Thakallapally R, Kesmir C, Detours V. Evolutionary and Immunological Implications of Contemporary HIV-1 Variation. *Br Med Bull* (2001) 58:19–42. doi: 10.1093/bmb/58.1.19
129. Taylor BS, Sobieszczyk ME, McCutchan FE, Hammer SM. The Challenge of HIV-1 Subtype Diversity. *N Engl J Med* (2008) 358(15):1590–602. doi: 10.1056/NEJMra0706737
130. Hemelaar J, Gouws E, Ghys PD, Osmanov S. Global and Regional Distribution of HIV-1 Genetic Subtypes and Recombinants in 2004. *AIDS* (2006) 20(16):W13–23. doi: 10.1097/01.aids.0000247564.73009.bc
131. Coffin J, Swanstrom R. HIV Pathogenesis: Dynamics and Genetics of Viral Populations and Infected Cells. *Cold Spring Harb Perspect Med* (2013) 3(1):a012526. doi: 10.1101/cshperspect.a012526
132. Tancredi MV, Waldman EA. Predictors of Progression to AIDS After HIV Infection Diagnosis in the Pre- and Post-HAART Eras in a Brazilian AIDS-Free Cohort. *Trans R Soc Trop Med Hyg* (2014) 108(7):408–14. doi: 10.1093/trstmh/tru078
133. Jiang H, Xie N, Cao B, Tan L, Fan Y, Zhang F, et al. Determinants of Progression to AIDS and Death Following HIV Diagnosis: A Retrospective Cohort Study in Wuhan, China. *PloS One* (2013) 8(12):e83078. doi: 10.1371/journal.pone.0083078
134. Mega ER. Alarming Surge in Drug-Resistant HIV Uncovered. *Nature* (2019). doi: 10.1038/d41586-019-02316-x
135. Gao F, Yue L, Robertson DL, Hill SC, Hui H, Biggar RJ, et al. Genetic Diversity of Human Immunodeficiency Virus Type 2: Evidence for Distinct Sequence Subtypes With Differences in Virus Biology. *J Virol* (1994) 68 (11):7433–47. doi: 10.1128/jvi.68.11.7433-7447.1994
136. MacNeil A, Sankale JL, Meloni ST, Sarr AD, Mboup S, Kanki P. Long-Term Intrapatient Viral Evolution During HIV-2 Infection. *J Infect Dis* (2007) 195 (5):726–33. doi: 10.1086/511308
137. Skar H, Borrego P, Wallstrom TC, Mild M, Marcelino JM, Barroso H, et al. HIV-2 Genetic Evolution in Patients With Advanced Disease is Faster Than That in Matched HIV-1 Patients. *J Virol* (2010) 84(14):7412–5. doi: 10.1128/JVI.02548-09
138. de Silva TI, Leligdowicz A, Carlson J, Garcia-Knight M, Onyango C, Miller N, et al. HLA-Associated Polymorphisms in the HIV-2 Capsid Highlight Key Differences Between HIV-1 and HIV-2 Immune Adaptation. *AIDS* (2018) 32 (6):709–14. doi: 10.1097/QAD.0000000000001753

139. Rocha C, Calado R, Borrego P, Marcelino JM, Bartolo I, Rosado L, et al. Evolution of the Human Immunodeficiency Virus Type 2 Envelope in the First Years of Infection is Associated With the Dynamics of the Neutralizing Antibody Response. *Retrovirology* (2013) 10:110. doi: 10.1186/1742-4690-10-110
140. Lenzi GM, Domaoal RA, Kim DH, Schinazi RF, Kim B. Mechanistic and Kinetic Differences Between Reverse Transcriptases of Vpx Coding and Non-Coding Lentiviruses. *J Biol Chem* (2015) 290(50):30078–86. doi: 10.1074/jbc.M115.691576
141. Alvarez M, Sebastian-Martin A, Garcia-Marquina G, Menendez-Arias L. Fidelity of Classwide-Resistant HIV-2 Reverse Transcriptase and Differential Contribution of K65R to the Accuracy of HIV-1 and HIV-2 Reverse Transcriptases. *Sci Rep* (2017) 7:44834. doi: 10.1038/srep44834
142. Rawson JM, Gohl DM, Reilly CS, Mansky LM. HIV-1 and HIV-2 Exhibit Similar Mutation Frequencies and Spectra in the Absence of G-To-A Hypermutation. *Retrovirology* (2015) 12:60. doi: 10.1186/s12977-015-0180-6
143. Rawson JMO, Gohl DM, Landman SR, Roth ME, Meissner ME, Peterson TS, et al. Single-Strand Consensus Sequencing Reveals That HIV Type But Not Subtype Significantly Impacts Viral Mutation Frequencies and Spectra. *J Mol Biol* (2017). doi: 10.1016/j.jmb.2017.05.010
144. Nozuma S, Matsuura E, Kodama D, Tashiro Y, Matsuzaki T, Kubota R, et al. Effects of Host Restriction Factors and the HTLV-1 Subtype on Susceptibility to HTLV-1-Associated Myelopathy/Tropical Spastic Paraparesis. *Retrovirology* (2017) 14(1):26. doi: 10.1186/s12977-017-0350-9
145. Sherman MP, Saksena NK, Dube DK, Yanagihara R, Poiesz BJ. Evolutionary Insights on the Origin of Human T-Cell Lymphoma/Leukemia Virus Type I (HTLV-I) Derived From Sequence Analysis of a New HTLV-I Variant From Papua New Guinea. *J Virol* (1992) 66(4):2556–63. doi: 10.1128/jvi.66.4.2556-2563.1992
146. Gessain A, Mahieux R, de The G. Genetic Variability and Molecular Epidemiology of Human and Simian T Cell Leukemia/Lymphoma Virus Type I. *J Acquir Immune Defic Syndr Hum Retrovirol* (1996) 13 Suppl 1: S132–145. doi: 10.1097/00042560-199600001-00022
147 . Mansky LM. *In Vivo* Analysis of Human T-Cell Leukemia Virus Type 1 Reverse Transcription Accuracy. *J Virol* (2000) 74(20):9525–31. doi: 10.1128/JVI.74.20.9525-9531.2000
148. Menendez-Arias L. Mutation Rates and Intrinsic Fidelity of Retroviral Reverse Transcriptases. *Viruses* (2009) 1(3):1137–65. doi: 10.3390/v1031137
149. Nobre AFS, Almeida DS, Ferreira LC, Ferreira DL, Junior ECS, Viana M, et al. Low Genetic Diversity of the Human T-Cell Lymphotropic Virus (HTLV-1) in an Endemic Area of the Brazilian Amazon Basin. *PloS One* (2018) 13(3):e0194184. doi: 10.1371/journal.pone.0194184
150. Patino-Galindo JA, Gonzalez-Candelas F. The Substitution Rate of HIV-1 Subtypes: A Genomic Approach. *Virus Evol* (2017) 3(2):vex029. doi: 10.1093/ve/vex029
151. Mansky LM, Temin HM. Lower *In Vivo* Mutation Rate of Human Immunodeficiency Virus Type 1 Than That Predicted From the Fidelity of Purified Reverse Transcriptase. *J Virol* (1995) 69(8):5087–94. doi: 10.1128/jvi.69.8.5087-5094.1995
152. Mansky LM. Forward Mutation Rate of Human Immunodeficiency Virus Type 1 in a T Lymphoid Cell Line. *AIDS Res Hum Retroviruses* (1996) 12 (4):307–14. doi: 10.1089/aid.1996.12.307
153. Kim T, Mudry RA Jr, Rexrode CA 2nd, Pathak VK. Retroviral Mutation Rates and A-To-G Hypermutations During Different Stages of Retroviral Replication. *J Virol* (1996) 70(11):7594–602. doi: 10.1128/jvi.70.11.7594-7602.1996
154. Abram ME, Ferris AL, Shao W, Alvord WG, Hughes SH. Nature, Position, and Frequency of Mutations Made in a Single Cycle of HIV-1 Replication. *J Virol* (2010) 84(19):9864–78. doi: 10.1128/JVI.00915-10
155. Cuevas JM, Geller R, Garijo R, Lopez-Aldeguer J, Sanjuan R. Extremely High Mutation Rate of HIV-1 *In Vivo*. *PloS Biol* (2015) 13(9):e1002251. doi: 10.1371/journal.pbio.1002251
156. Sharp PM, Hahn BH. The Evolution of HIV-1 and the Origin of AIDS. *Philos Trans R Soc Lond B Biol Sci* (2010) 365(1552):2487–94. doi: 10.1098/rstb.2010.0031
157. Mansky LM, Cunningham KS. Virus Mutators and Antimutators: Roles in Evolution, Pathogenesis and Emergence. *Trends Genet* (2000) 16(11):512–7. doi: 10.1016/S0168-9525(00)02125-9
158. Delviks-Frankenberry KA, Nikolaitchik OA, Burdick RC, Gorelick RJ, Keele BF, Hu WS. Minimal Contribution of APOBEC3-Induced G-To-A Hypermutation to HIV-1 Recombination and Genetic Variation. *PloS Pathog* (2016) 12(5):e1005646. doi: 10.1371/journal.ppat.1005646
159. Pray L. DNA Replication and Causes of Mutation. *Nat Educ* (2008) 1(1):214.
160. Mansky LM, Bernard LC. 3'-Azido-3'-Deoxythymidine (AZT) and AZT-Resistant Reverse Transcriptase can Increase the *In Vivo* Mutation Rate of Human Immunodeficiency Virus Type 1. *J Virol* (2000) 74(20):9532–9. doi: 10.1128/JVI.74.20.9532-9539.2000
161. Brenner BG, Coutsinos D. The K65R Mutation in HIV-1 Reverse Transcriptase: Genetic Barriers, Resistance Profile and Clinical Implications. *HIV Ther* (2009) 3(6):583–94. doi: 10.2217/hiv.09.40
162. Domingo E, Sheldon J, Perales C. Viral Quasispecies Evolution. *Microbiol Mol Biol Rev* (2012) 76(2):159–216. doi: 10.1128/MMBR.05023-11
163. Dapp MJ, Patterson SE, Mansky LM. Back to the Future: Revisiting HIV-1 Lethal Mutagenesis. *Trends Microbiol* (2013) 21(2):56–62. doi: 10.1016/j.tim.2012.10.006
164. Domingo E, Perales C. Viral Quasispecies. *PloS Genet* (2019) 15(10): e1008271. doi: 10.1371/journal.pgen.1008271
165. Rawson JM, Daly MB, Xie J, Clouser CL, Landman SR, Reilly CS, et al. 5-Azacytidine Enhances the Mutagenesis of HIV-1 by Reduction to 5-Aza-2'-Deoxycytidine. *Antimicrob Agents Chemother* (2016) 60(4):2318–25. doi: 10.1128/AAC.03084-15
166. Pathak VK, Temin HM. Broad Spectrum of *In Vivo* Forward Mutations, Hypermutations, and Mutational Hotspots in a Retroviral Shuttle Vector After a Single Replication Cycle: Substitutions, Frameshifts, and Hypermutations. *Proc Natl Acad Sci USA* (1990) 87(16):6019–23. doi: 10.1073/pnas.87.16.6019
167. Julias JG, Pathak VK. Deoxyribonucleoside Triphosphate Pool Imbalances *In Vivo* are Associated With an Increased Retroviral Mutation Rate. *J Virol* (1998) 72(10):7941–9. doi: 10.1128/JVI.72.10.7941-7949.1998
168. Cromer D, Schlub TE, Smyth RP, Grimm AJ, Chopra A, Mallal S, et al. HIV-1 Mutation and Recombination Rates Are Different in Macrophages and T-Cells. *Viruses* (2016) 8(4):118. doi: 10.3390/v8040118
169. Kennedy EM, Amie SM, Bambara RA, Kim B. Frequent Incorporation of Ribonucleotides During HIV-1 Reverse Transcription and Their Attenuated Repair in Macrophages. *J Biol Chem* (2012) 287(17):14280–8. doi: 10.1074/jbc.M112.348482
170. Shepard C, Xu J, Holler J, Kim DH, Mansky LM, Schinazi RF, et al. Effect of Induced dNTP Pool Imbalance on HIV-1 Reverse Transcription in Macrophages. *Retrovirology* (2019) 16(1):29. doi: 10.1186/s12977-019-0491-0
171. Oo A, Kim DH, Schinazi RF, Kim B. Viral Protein X Reduces the Incorporation of Mutagenic Noncanonical rNTPs During Lentivirus Reverse Transcription in Macrophages. *J Biol Chem* (2020) 295(2):657–66. doi: 10.1074/jbc.RA119.011466
172. St Gelais C, Wu L. SAMHD1: A New Insight Into HIV-1 Restriction in Myeloid Cells. *Retrovirology* (2011) 8:55. doi: 10.1186/1742-4690-8-55
173. Hollenbaugh JA, Tao S, Lenzi GM, Ryu S, Kim DH, Diaz-Griffero F, et al. dNTP Pool Modulation Dynamics by SAMHD1 Protein in Monocyte-Derived Macrophages. *Retrovirology* (2014) 11:63. doi: 10.1186/s12977-014-0063-2
174. Rawson JM, Roth ME, Xie J, Daly MB, Clouser CL, Landman SR, et al. Synergistic Reduction of HIV-1 Infectivity by 5-Azacytidine and Inhibitors of Ribonucleotide Reductase. *Bioorg Med Chem* (2016) 24(11):2410–22. doi: 10.1016/j.bmc.2016.03.052
175. Rawson JM, Roth ME, Xie J, Daly MB, Clouser CL, Landman SR, et al. 5,6-Dihydro-5-Aza-2'-Deoxycytidine Potentiates the Anti-HIV-1 Activity of Ribonucleotide Reductase Inhibitors. *Bioorg Med Chem* (2013) 21 (22):7222–8. doi: 10.1016/j.bmc.2013.08.023
176. Onafuwa-Nuga A, Telesnitsky A. The Remarkable Frequency of Human Immunodeficiency Virus Type 1 Genetic Recombination. *Microbiol Mol Biol Rev* (2009) 73(3):451–80. doi: 10.1128/MMBR.00012-09
177. Schlub TE, Grimm AJ, Smyth RP, Cromer D, Chopra A, Mallal S, et al. Fifteen to Twenty Percent of HIV Substitution Mutations are Associated With Recombination. *J Virol* (2014) 88(7):3837–49. doi: 10.1128/JVI.03136-13
178. Bbosa N, Kaleebu P, Ssemwanga D. HIV Subtype Diversity Worldwide. *Curr Opin HIV AIDS* (2019) 14(3):153–60. doi: 10.1097/COH.0000000000000534

179. LANL HIV Sequence Database. *HIV Circulating Recombinant Forms (CRFs)* . Available at: https://www.hiv.lanl.gov/content/sequence/HIV/CRFs/CRFs.html.
180. Ibe S, Yokomaku Y, Shiino T, Tanaka R, Hattori J, Fujisaki S, et al. HIV-2 CRF01_AB: First Circulating Recombinant Form of HIV-2. *J Acquir Immune Defic Syndr* (2010) 54(3):241–7. doi: 10.1097/QAI.0b013e3181dc98c1
181. Desrames A, Cassar O, Gout O, Hermine O, Taylor GP, Afonso PV, et al. Northern African Strains of Human T-Lymphotropic Virus Type 1 Arose From a Recombination Event. *J Virol* (2014) 88(17):9782–8. doi: 10.1128/JVI.01591-14
182. Kuwata T, Miyazaki Y, Igarashi T, Takehisa J, Hayami M. The Rapid Spread of Recombinants During a Natural *In Vitro* Infection With Two Human Immunodeficiency Virus Type 1 Strains. *J Virol* (1997) 71(9):7088–91. doi: 10.1128/jvi.71.9.7088-7091.1997
183. Rawson JMO, Nikolaitchik OA, Keele BF, Pathak VK, Hu WS. Recombination is Required for Efficient HIV-1 Replication and the Maintenance of Viral Genome Integrity. *Nucleic Acids Res* (2018) 46 (20):10535–45. doi: 10.1093/nar/gky910
184. An W, Telesnitsky A. Effects of Varying Sequence Similarity on the Frequency of Repeat Deletion During Reverse Transcription of a Human Immunodeficiency Virus Type 1 Vector. *J Virol* (2002) 76(15):7897–902. doi: 10.1128/JVI.76.15.7897-7902.2002
185. Motomura K, Chen J, Hu W. Genetic Recombination Between Human Immunodeficiency Virus Type 1 (HIV-1) and HIV-2, Two Distinct Human Lentiviruses. *J Virol* (2008) 82(4):1923–33. doi: 10.1128/JVI.01937-07
186. Simon-Loriere E, Martin DP, Weeks KM, Negroni M. RNA Structures Facilitate Recombination-Mediated Gene Swapping in HIV-1. *J Virol* (2010) 84(24):12675–82. doi: 10.1128/JVI.01302-10
187. Nguyen LA, Kim DH, Daly MB, Allan KC, Kim B . Host SAMHD1 Protein Promotes HIV-1 Recombination in Macrophages. *J Biol Chem* (2014) 289 (5):2489–96. doi: 10.1074/jbc.C113.522326
188. Harris RS, Dudley JP. APOBECs and Virus Restriction. *Virology* (2015) 479-480:131–45. doi: 10.1016/j.virol.2015.03.012
189. McDaniel YZ, Wang D, Love RP, Adolph MB, Mohammadzadeh N, Chelico L, et al. Deamination Hotspots Among APOBEC3 Family Members are Defined by Both Target Site Sequence Context and ssDNA Secondary Structure. *Nucleic Acids Res* (2020) 48(3):1353–71. doi: 10.1093/nar/gkz1164
190. Okada A, Iwatani Y. APOBEC3G-Mediated G-To-A Hypermutation of the HIV-1 Genome: The Missing Link in Antiviral Molecular Mechanisms. *Front Microbiol* (2016) 7:2027. doi: 10.3389/fmicb.2016.02027
191. Hultquist JF, Lengyel JA, Refsland EW, LaRue RS, Lackey L, Brown WL, et al. Human and Rhesus APOBEC3D, APOBEC3F, APOBEC3G, and APOBEC3H Demonstrate a Conserved Capacity to Restrict Vif-Deficient HIV-1. *J Virol* (2011) 85(21):11220–34. doi: 10.1128/JVI.05238-11
192. Chaipan C, Smith JL, Hu WS, Pathak VK. APOBEC3G Restricts HIV-1 to a Greater Extent Than APOBEC3F and APOBEC3DE in Human Primary CD4+ T Cells and Macrophages. *J Virol* (2013) 87(1):444–53. doi: 10.1128/JVI.00676-12
193. Ooms M, Brayton B, Letko M, Maio SM, Pilcher CD, Hecht FM, et al. HIV-1 Vif Adaptation to Human APOBEC3H Haplotypes. *Cell Host Microbe* (2013) 14(4):411–21. doi: 10.1016/j.chom.2013.09.006
194. Refsland EW, Hultquist JF, Luengas EM, Ikeda T, Shaban NM, Law EK, et al. Natural Polymorphisms in Human APOBEC3H and HIV-1 Vif Combine in Primary T Lymphocytes to Affect Viral G-To-A Mutation Levels and Infectivity. *PloS Genet* (2014) 10(11):e1004761. doi: 10.1371/journal.pgen.1004761
195. Krisko JF, Begum N, Baker CE, Foster JL, Garcia JV. APOBEC3G and APOBEC3F Act in Concert To Extinguish HIV-1 Replication. *J Virol* (2016) 90(9):4681–95. doi: 10.1128/JVI.03275-15
196. Yu Q, Konig R, Pillai S, Chiles K, Kearney M, Palmer S, et al. Single-Strand Specificity of APOBEC3G Accounts for Minus-Strand Deamination of the HIV Genome. *Nat Struct Mol Biol* (2004) 11(5):435–42. doi: 10.1038/nsmb758
197. Chelico L, Pham P, Calabrese P, Goodman MF. APOBEC3G DNA Deaminase Acts Processively 3' –> 5' on Single-Stranded DNA. *Nat Struct Mol Biol* (2006) 13(5):392–9. doi: 10.1038/nsmb1086
198. Hache G, Liddament MT, Harris RS. The Retroviral Hypermutation Specificity of APOBEC3F and APOBEC3G is Governed by the C-Terminal DNA Cytosine Deaminase Domain. *J Biol Chem* (2005) 280 (12):10920–4. doi: 10.1074/jbc.M500382200
199. Rathore A, Carpenter MA, Demir O, Ikeda T, Li M, Shaban NM, et al. The Local Dinucleotide Preference of APOBEC3G can be Altered From 5'-CC to 5'-TC by a Single Amino Acid Substitution. *J Mol Biol* (2013) 425(22):4442–54. doi: 10.1016/j.jmb.2013.07.040
200. Holtz CM, Sadler HA, Mansky LM. APOBEC3G Cytosine Deamination Hotspots are Defined by Both Sequence Context and Single-Stranded DNA Secondary Structure. *Nucleic Acids Res* (2013) 41(12):6139–48. doi: 10.1093/nar/gkt246
201. Yu X, Yu Y, Liu B, Luo K, Kong W, Mao P, et al. Induction of APOBEC3G Ubiquitination and Degradation by an HIV-1 Vif-Cul5-SCF Complex. *Science* (2003) 302(5647):1056–60. doi: 10.1126/science.1089591
202. Shirakawa K, Takaori-Kondo A, Kobayashi M, Tomonaga M, Izumi T, Fukunaga K, et al. Ubiquitination of APOBEC3 Proteins by the Vif-Cullin5-ElonginB-ElonginC Complex. *Virology* (2006) 344(2):263–6. doi: 10.1016/j.virol.2005.10.028
203. Jager S, Kim DY, Hultquist JF, Shindo K, LaRue RS, Kwon E, et al. Vif Hijacks CBF-Beta to Degrade APOBEC3G and Promote HIV-1 Infection. *Nature* (2011) 481(7381):371–5.
204. Zhang W, Du J, Evans SL, Yu Y, Yu XF. T-Cell Differentiation Factor CBF-Beta Regulates HIV-1 Vif-Mediated Evasion of Host Restriction. *Nature* (2011) 481(7381):376–9.
205. Guo Y, Dong L, Qiu X, Wang Y, Zhang B, Liu H, et al. Structural Basis for Hijacking CBF-Beta and CUL5 E3 Ligase Complex by HIV-1 Vif. *Nature* (2014) 505(7482):229–33. doi: 10.1038/nature12884
206. Sadler HA, Stenglein MD, Harris RS, Mansky LM. APOBEC3G Contributes to HIV-1 Variation Through Sublethal Mutagenesis. *J Virol* (2010) 84(14):7396–404. doi: 10.1128/JVI.00056-10
207. Meissner ME, Julik EJ, Badalamenti JP, Arndt WG, Mills LJ, Mansky LM. Development of a User-Friendly Pipeline for Mutational Analyses of HIV Using Ultra-Accurate Maximum-Depth Sequencing. *Viruses* (2021) 13(7). doi: 10.3390/v13071338
208. Sato K, Takeuchi JS, Misawa N, Izumi T, Kobayashi T, Kimura Y, et al. APOBEC3D and APOBEC3F Potently Promote HIV-1 Diversification and Evolution in Humanized Mouse Model. *PloS Pathog* (2014) 10(10):e1004453. doi: 10.1371/journal.ppat.1004453
209. Alteri C, Surdo M, Bellocchi MC, Saccomandi P, Continenza F, Armenia D, et al. Incomplete APOBEC3G/F Neutralization by HIV-1 Vif Mutants Facilitates the Genetic Evolution From CCR5 to CXCR4 Usage. *Antimicrob Agents Chemother* (2015) 59(8):4870–81. doi: 10.1128/AAC.00137-15
210. Monajemi M, Woodworth CF, Zipperlen K, Gallant M, Grant MD, Larijani M. Positioning of APOBEC3G/F Mutational Hotspots in the Human Immunodeficiency Virus Genome Favors Reduced Recognition by CD8+ T Cells. *PloS One* (2014) 9(4):e93428. doi: 10.1371/journal.pone.0093428
211. Squires KD, Monajemi M, Woodworth CF, Grant MD, Larijani M. Impact of APOBEC Mutations on CD8+ T Cell Recognition of HIV Epitopes Varies Depending on the Restricting HLA. *J Acquir Immune Defic Syndr* (2015) 70 (2):172–8. doi: 10.1097/QAI.0000000000000689
212. Mulder LC, Harari A, Simon V. Cytidine Deamination Induced HIV-1 Drug Resistance. *Proc Natl Acad Sci USA* (2008) 105(14):5501–6. doi: 10.1073/pnas.0710190105
213. Kim EY, Bhattacharya T, Kunstman K, Swantek P, Koning FA, Malim MH, et al. Human APOBEC3G-Mediated Editing can Promote HIV-1 Sequence Diversification and Accelerate Adaptation to Selective Pressure. *J Virol* (2010) 84(19):10402–5. doi: 10.1128/JVI.01223-10
214. Neogi U, Shet A, Sahoo PN, Bontell I, Ekstrand ML, Banerjea AC, et al. Human APOBEC3G-Mediated Hypermutation is Associated With Antiretroviral Therapy Failure in HIV-1 Subtype C-Infected Individuals. *J Int AIDS Soc* (2013) 16:18472. doi: 10.7448/IAS.16.1.18472
215. Connor RI, Sheridan KE, Ceradini D, Choe S, Landau NR. Change in Coreceptor Use Correlates With Disease Progression in HIV-1–Infected Individuals. *J Exp Med* (1997) 185(4):621–8. doi: 10.1084/jem.185.4.621
216. Wiegand HL, Doehle BP, Bogerd HP, Cullen BR. A Second Human Antiretroviral Factor, APOBEC3F, is Suppressed by the HIV-1 and HIV-2 Vif Proteins. *EMBO J* (2004) 23(12):2451–8. doi: 10.1038/sj.emboj.7600246
217. Ribeiro AC, Maia e Silva A, Santa-Marta M, Pombo A, Moniz-Pereira J, Goncalves J, et al. Functional Analysis of Vif Protein Shows Less Restriction of Human Immunodeficiency Virus Type 2 by APOBEC3G. *J Virol* (2005) 79 (2):823–33. doi: 10.1128/JVI.79.2.823-833.2005

218. Smith JL, Izumi T, Borbet TC, Hagedorn AN, Pathak VK. HIV-1 and HIV-2 Vif Interact With Human APOBEC3 Proteins Using Completely Different Determinants. *J Virol* (2014) 88(17):9893–908. doi: 10.1128/JVI.01318-14
219. Meissner ME, Willkomm NA, Lucas J, Arndt WG, Aitken SF, Julik EJ, et al. Differential Activity of APOBEC3F, APOBEC3G, and APOBEC3H in the Restriction of HIV-2. *J Mol Biol* (2021), 167355.
220. Ooms M, Krikoni A, Kress AK, Simon V, Munk C. APOBEC3A, APOBEC3B, and APOBEC3H Haplotype 2 Restrict Human T-Lymphotropic Virus Type 1. *J Virol* (2012) 86(11):6097–108. doi: 10.1128/JVI.06570-11
221. Sasada A, Takaori-Kondo A, Shirakawa K, Kobayashi M, Abudu A, Hishizawa M, et al. APOBEC3G Targets Human T-Cell Leukemia Virus Type 1. *Retrovirology* (2005) 2:32. doi: 10.1186/1742-4690-2-32
222. Mahieux R, Suspene R, Delebecque F, Henry M, Schwartz O, Wain-Hobson S, et al. Extensive Editing of a Small Fraction of Human T-Cell Leukemia Virus Type 1 Genomes by Four APOBEC3 Cytidine Deaminases. *J Gen Virol* (2005) 86(Pt 9):2489–94. doi: 10.1099/vir.0.80973-0
223. Poulain F, Lejeune N, Willemart K, Gillet NA. Footprint of the Host Restriction Factors APOBEC3 on the Genome of Human Viruses. *PloS Pathog* (2020) 16(8):e1008718. doi: 10.1371/journal.ppat.1008718
224. Kimata JT, Wong FH, Wang JJ, Ratner L. Construction and Characterization of Infectious Human T-Cell Leukemia Virus Type 1 Molecular Clones. *Virology* (1994) 204(2):656–64. doi: 10.1006/viro.1994.1581
225. Derse D, Hill SA, Lloyd PA, Chung H, Morse BA. Examining Human T-Lymphotropic Virus Type 1 Infection and Replication by Cell-Free Infection With Recombinant Virus Vectors. *J Virol* (2001) 75(18):8461–8. doi: 10.1128/JVI.75.18.8461-8468.2001
226. Ohsugi T, Kumasaka T, Ohsugi T. Construction of a Full-Length Human T Cell Leukemia Virus Type I Genome From MT-2 Cells Containing Multiple Defective Proviruses Using Overlapping Polymerase Chain Reaction. *Anal Biochem* (2004) 329(2):281–8. doi: 10.1016/j.ab.2004.02.036
227. Bass BL. RNA Editing by Adenosine Deaminases That Act on RNA. *Annu Rev Biochem* (2002) 71:817–46. doi: 10.1146/annurev.biochem.71.110601.135501
228. Nishikura K. Editor Meets Silencer: Crosstalk Between RNA Editing and RNA Interference. *Nat Rev Mol Cell Biol* (2006) 7(12):919–31. doi: 10.1038/nrm2061
229. Basilio C, Wahba AJ, Lengyel P, Speyer JF, Ochoa S. Synthetic Polynucleotides and the Amino Acid Code. V. *Proc Natl Acad Sci USA* (1962) 48:613–6.
230. Rueter SM, Dawson TR, Emeson RB. Regulation of Alternative Splicing by RNA Editing. *Nature* (1999) 399(6731):75–80. doi: 10.1038/19992
231. Steele EJ, Lindley RA, Wen J, Weiller GF. Computational Analyses Show A-To-G Mutations Correlate With Nascent mRNA Hairpins at Somatic Hypermutation Hotspots. *DNA Repair (Amst)* (2006) 5(11):1346–63. doi: 10.1016/j.dnarep.2006.06.002
232. Cattaneo R. Biased (A–>I) Hypermutation of Animal RNA Virus Genomes. *Curr Opin Genet Dev* (1994) 4(6):895–900. doi: 10.1016/0959-437X(94)90076-0
233. Weiden MD, Hoshino S, Levy DN, Li Y, Kumar R, Burke SA , et al. Adenosine Deaminase Acting on RNA-1 (ADAR1) Inhibits HIV-1 Replication in Human Alveolar Macrophages. *PloS One* (2014) 9(10):e108476. doi: 10.1371/journal.pone.0108476
234. Phuphuakrat A, Kraiwong R, Boonarkart C, Lauhakirti D, Lee TH, Auewarakul P. Double-Stranded RNA Adenosine Deaminases Enhance Expression of Human Immunodeficiency Virus Type 1 Proteins. *J Virol* (2008) 82(21):10864–72. doi: 10.1128/JVI.00238-08
235. Clerzius G, Gelinas JF, Daher A, Bonnet M, Meurs EF, Gatignol A. ADAR1 Interacts With PKR During Human Immunodeficiency Virus Infection of Lymphocytes and Contributes to Viral Replication. *J Virol* (2009) 83(19):10119–28. doi: 10.1128/JVI.02457-08
236. Doria M, Neri F, Gallo M, Farace MG, Michienzi A. Editing of HIV-1 RNA by the Double-Stranded RNA Deaminase ADAR1 Stimulates Viral Infection. *Nucleic Acids Res* (2009) 37(17):5848–58. doi: 10.1093/nar/gkp604
237. Cuadrado E, Booiman T, van Hamme JL, Jansen MH, van Dort KA, Vanderver A, et al. ADAR1 Facilitates HIV-1 Replication in Primary CD4 + T Cells. *PloS One* (2015) 10(12):e0143613. doi: 10.1371/journal.pone.0143613
238. Cachat A, Alais S, Chevalier SA, Journo C, Fusil F, Dutartre H, et al. ADAR1 Enhances HTLV-1 and HTLV-2 Replication Through Inhibition of PKR Activity. *Retrovirology* (2014) 11:93. doi: 10.1186/s12977-014-0093-9
239. Biswas N, Wang T, Ding M, Tumne A, Chen Y, Wang Q, et al. ADAR1 is a Novel Multi Targeted Anti-HIV-1 Cellular Protein. *Virology* (2012) 422(2):265–77. doi: 10.1016/j.virol.2011.10.024
240. DHHS Panel on Antiretroviral Guidelines for Adults and Adolescents. *Guidelines for the Use of Antiretroviral Agents in Adults and Adolescents With HIV: HIV-2 Infection* . Available at: https://clinicalinfo.hiv.gov/sites/default/files/guidelines/documents/AdultARV_GL_HIV-2.pdf.

Conflict of Interest: The authors declare that the research was conducted in the absence of any commercial or financial relationships that could be construed as a potential conflict of interest.

Publisher's Note: All claims expressed in this article are solely those of the authors and do not necessarily represent those of their affiliated organizations, or those of the publisher, the editors and the reviewers. Any product that may be evaluated in this article, or claim that may be made by its manufacturer, is not guaranteed or endorsed by the publisher.

frontiers | Frontiers in Virology

ORIGINAL RESEARCH
published: 16 June 2022
doi: 10.3389/fviro.2022.917902

Attenuated HIV-1 Nef But Not Vpu Function in a Cohort of Rwandan Long-Term Survivors

*Gisele Umviligihozo[1], Jaclyn K. Mann[2], Steven W. Jin[1], Francis M. Mwimanzi[1], Hua-Shiuan A. Hsieh[3], Hanwei Sudderuddin[4], Guinevere Q. Lee[5], Helen Byakwaga[6,7], Conrad Muzoora[5], Peter W. Hunt[6], Jeff N. Martin[6], Jessica E. Haberer[8,9], Etienne Karita[10], Susan Allen[11], Eric Hunter[11,12], Zabrina L. Brumme[1,4] and Mark A. Brockman[1,3,4]**

[1] Faculty of Health Sciences, Simon Fraser University, Burnaby, BC, Canada, [2] HIV Pathogenesis Programme, University of KwaZulu-Natal, Durban, South Africa, [3] Department of Molecular Biology and Biochemistry, Simon Fraser University, Burnaby, BC, Canada, [4] British Columbia Centre for Excellence in HIV/AIDS, Vancover, BC, Canada, [5] Department of Medicine, Weill Cornell Medical College, New York, NY, United States, [6] Department of Community Health, Mbarara University of Science and Technology, Mbarara, Uganda, [7] Department of Medicine, University of California, San Francisco, CA, United States, [8] Center for Global Health, Massachusetts General Hospital, Boston, MA, United States, [9] Department of Medicine, Harvard Medical School, Boston, MA, United States, [10] Centre for Family Health Research, Kigali, Rwanda, [11] Department of Pathology and Laboratory Medicine, Emory University, Atlanta, GA, United States, [12] Emory Vaccine Center at Yerkes National Primate Research Center, Atlanta, GA, United States

OPEN ACCESS

Edited by:
Akio Adachi,
Kansai Medical University, Japan

Reviewed by:
Kenzo Tokunaga,
National Institute of Infectious Diseases (NIID), Japan
Ai Kawana-Tachikawa,
National Institute of Infectious Diseases, Japan
Sarah Rowland-Jones,
University of Oxford, United Kingdom

***Correspondence:**
Mark A. Brockman
mark_brockman@sfu.ca

Specialty section:
This article was submitted to Fundamental Virology, a section of the journal Frontiers in Virology

Received: *11 April 2022*
Accepted: *13 May 2022*
Published: *16 June 2022*

Citation:
Umviligihozo G, Mann JK, Jin SW, Mwimanzi FM, Hsieh H-SA, Sudderuddin H, Lee GQ, Byakwaga H, Muzoora C, Hunt PW, Martin JN, Haberer JE, Karita E, Allen S, Hunter E, Brumme ZL and Brockman MA (2022) Attenuated HIV-1 Nef But Not Vpu Function in a Cohort of Rwandan Long-Term Survivors. Front. Virol. 2:917902. doi: 10.3389/fviro.2022.917902

HIV-1 accessory proteins Nef and Vpu enhance viral pathogenesis through partially overlapping immune evasion activities. Attenuated Nef or Vpu functions have been reported in individuals who display slower disease progression, but few studies have assessed the relative impact of these proteins in non-B HIV-1 subtypes or examined paired proteins from the same individuals. Here, we examined the sequence and function of matched Nef and Vpu clones isolated from 29 long-term survivors (LTS) from Rwanda living with HIV-1 subtype A and compared our results to those of 104 Nef and 62 Vpu clones isolated from individuals living with chronic untreated HIV-1 subtype A from the same geographic area. *Nef* and *vpu* coding regions were amplified from plasma HIV RNA and cloned. The function of one intact, phylogenetically-validated Nef and Vpu clone per individual was then quantified by flow cytometry following transient expression in an immortalized CD4+ T-cell line. We measured the ability of each Nef clone to downregulate CD4 and HLA class I, and of each Vpu clone to downregulate CD4 and Tetherin, from the cell surface. Results were normalized to reference clones (Nef-SF2 and Vpu-NL4.3). We observed that Nef-mediated CD4 and HLA downregulation functions were lower in LTS compared to the control cohort (Mann-Whitney $p=0.03$ and $p<0.0001$, respectively). Moreover, we found a positive correlation between Nef-mediated CD4 downregulation function and plasma viral load in LTS and controls (Spearman $\rho= 0.59$, $p=0.03$ and $\rho=0.30$, $p=0.005$, respectively). In contrast, Vpu-mediated functions were similar between groups and did not correlate with clinical markers. Further analyses identified polymorphisms at Nef codon 184 and Vpu codons 60-62 that were associated with

function, which were confirmed through mutagenesis. Overall, our results support attenuated function of Nef, but not Vpu, as a contributor to slower disease progression in this cohort of long-term survivors with HIV-1 subtype A.

Keywords: HIV non-progressors, viral accessory proteins, immune evasion, pathogenesis, downregulation, CD4, tetherin, HLA

INTRODUCTION

The rate of disease progression following human immunodeficiency virus type 1 (HIV-1) infection can vary widely (1). In the absence of combination antiretroviral therapy (cART), symptoms of acquired immunodeficiency syndrome (AIDS) may appear within as little as one year or as long as ten years (or more) after infection (2, 3). Such heterogeneity has prompted studies of people living with HIV (PLWH) who display extreme protective phenotypes, as defined by prolonged maintenance of favorable clinical measures such as high CD4+ T cell counts and low plasma HIV-1 viral loads (pVL) in the absence of therapy (4, 5). The small subset of PLWH who remain healthy for many years in the absence of cART are variously known as long-term non-progressors, elite controllers, elite suppressors or long-term survivors (LTS), with somewhat overlapping definitions based on the specific classification criteria used (5).

Both host and viral genetic factors are associated with HIV non-progressor phenotypes (6). Host factors include polymorphisms in cellular genes required for HIV-1 replication such as the viral co-receptor CCR5 (7) as well as natural variation in immune genes including the Human Leukocyte Antigens (HLA) (8). Stochastic differences in the host immune response to infection such as the development of higher avidity and more cross-reactive antiviral T cells have also been described (9). Viral genetic variation influences HIV-1 set point viral load (10) and mutations that attenuate viral replication and pathogenesis contribute specifically: deletions or polymorphisms that impair the function of viral structural proteins such as Gag or Env, as well as those affecting accessory proteins such as Nef, Vpu or Vpr can influence disease outcome (11).

HIV-1 Nef and Vpu enhance viral pathogenicity through partially overlapping immune evasion functions (12–14). Both proteins downregulate the viral entry receptor CD4 from the cell surface, thereby shielding the infected cell from elimination by antibody-dependent cellular cytotoxicity (ADCC), which requires Env on the cell surface to be in its CD4-bound confirmation (15–17). Nef also prevents antigen presentation by internalizing HLA class I, while Vpu enhances virion release and protects infected cells from ADCC by internalizing Tetherin (12, 18, 19). Studies of humans and non-human primates have demonstrated that impairment of Nef or Vpu is associated with slower disease progression (20–22). Additionally, attenuated Nef or Vpu function has been reported in some non-progressors (23–26). Most studies however have focused only on HIV-1 subtype B and few reports have assessed both Nef and Vpu function in the same individuals. The relative roles of Nef and Vpu in the context of non-progression thus remain incompletely understood, particularly in the context of non-B subtypes.

In the present study, we analysed the sequence and *in vitro* function of autologous Nef and Vpu clones isolated from 29 LTS from Rwanda with chronic HIV-1 subtype A infection. Data were compared to an existing panel of 104 Nef and 62 Vpu clones isolated from individuals from the same geographic area with chronic HIV-1 subtype A infection. Our results indicate that impaired function of Nef, but not Vpu, is associated with slower disease progression in this cohort of African LTS.

MATERIALS AND METHODS

Study Participants and Ethics Approvals

LTS plasma samples were obtained from a longitudinal cohort of PLWH from Rwanda, which was established in 1986 by Projet San Francisco and the Centre for Family Health Research. Control plasma samples were obtained from participants of the Heterosexual Transmission [HT] study in Kigali, Rwanda. Previously-generated Vpu (27) and Nef (28) clones from participants of the Uganda AIDS Rural Treatment Outcomes [UARTO] study in Mbarara, Uganda were also included as controls. All participants provided written informed consent prior to enrolment. The present study was approved by the Rwanda National Ethics committee, the Emory University Institutional Review Board, and the Simon Fraser University Research Ethics Board.

Amplification and Sequencing of *Nef and Vpu*

HIV-1 RNA was extracted from plasma using the NucliSENS EasyMag system (bioMérieux). The *nef* and *vpu* coding regions were amplified by reverse transcription-polymerase chain reaction (RT-PCR) using the Superscript III one-step RT-PCR system with Platinum *Taq* HiFi (Invitrogen) as described previously for Nef (28, 29) and Vpu (27). First-round amplicons were subjected to a nested second-round PCR reaction using the Expand High-Fidelity Plus PCR system (Roche) and primers containing AscI and SacII restriction enzyme sites to facilitate cloning. First-round *nef* primers, designed to accommodate HIV-1 subtype diversity, were: forward 5'- TAGCAGTAGCTGRGKGRACAGATAG-3' (HXB2 nt 8683-8707); reverse 5'-TACAGGCAAAAAGCAGCTG CTTATATGYAG- 3' (HXB2 nt 9536-9507). Second-round *nef* primers were: forward 5'-AGAGCACCGGCGC GCC**TCCACATACCTASAAGAATMAGACARG**- 3', (HXB2 nt 8746-8772 in bold text; AscI restriction site is underlined); reverse 5'- GCCTCCGCGGATCGAT**CAGGCCACRCC TCCCTGGAAASKCCC**- 3', (HXB2 nt 9474-9449, in bold text;

SacII restriction site is underlined). First-round *vpu* primers were: forward, 5′-TTGGGTGYCRRCAYAGCAGRATAGG-3′ (HXB2 nt 5780-5804); reverse, 5′-ATRTGCTTTVGCATCTGAT GCACARAATA-3′ (HXB2 nt 6407-6379). Second-round *vpu* primers were: forward, 5′-AGAGGGCGCGCC**ATCAARHTY CTVTAYCAAAGCAGTAAGTA**-3′; (HXB2 nt 6024-6052 in bold; AscI restriction site is underlined); reverse 5′-GCCTCCGCG GATCGAT**GGTACCCCATARTAGACHGTRACCCA**-3′ (HXB2 nt 6352-6327 in bold; SacII restriction site is underlined). Amplicons were Sanger sequenced on a 3730xl automated Genetic Analyzer (Applied Biosystems Inc.). Chromatograms were assembled using Sequencher v5.0.1 software (GeneCodes).

Nef and Vpu Cloning

Nef and *vpu* amplicons were cloned into eukaryotic expression vectors as described (28, 30). Briefly, second-round products were purified using the E.Z.N.A Cycle Pure kit (Omega Bio-tek). Each *nef* or *vpu* amplicon was then cloned into a modified version of pSELECT-GFPzeo (*In vivo*Gen) that contained 5' AscI and 3' SacII sites, where expression is driven by a composite hEF1-HTLV promoter. pSELECT-GFPzeo also features an independent CMV/HTLV promoter driving the expression of GFP. The pSELECT-GFPzeo vector used for *vpu* cloning was further modified to include the HIV-1 Rev Responsive Element (RRE) sequence downstream of the multiple cloning site to enhance Vpu expression (pSELECT-RRE-GFP). Following ligation, DNA products were transformed into *E. cloni* 10G chemically competent cells (Lucigen) and plated on Luria-Bertani (LB) agar containing Zeocin. Colonies were isolated, grown in LB medium containing Zeocin, and plasmid DNA was purified using the E.Z.N.A Plasmid DNA Mini kit (Omega Bio-tek). Plasmid clones were validated by Sanger sequencing. Following phylogenetic authentication (see below), one intact *nef* and one intact *vpu* clone per participant was selected for *in vitro* functional analysis (**Supplementary Figure 1**).

Phylogenetic Analysis and Subtype Determination

Alignments of intact clonal sequences and their original bulk plasma sequences were generated using HIV Align (www.hiv.lanl.gov/content/sequence/VIRALIGN/viralign.html) (31) and manually edited using Aliview (32). Maximum likelihood phylogenetic trees were inferred using using PhyML (33) and visualized using FigTree v1.4.4 (http://tree.bio.ed.ac.uk/software/figtree/) (34). HIV subtype classification was performed using the Recombinant Identification Program (RIP) (www.hiv.lanl.gov/content/sequence/RIP/RIP.html) (35), using a window size of 100 and confidence threshold of 95%.

Flow Cytometry

To examine Nef function, 2.0 µg of pSELECT-Nef-GFP was transfected into 1 x 10^6 CEM T cells resuspended in 50 µl Opti-MEM-I medium (Life Technologies) by electroporation using a Bio-Rad GenePulser MxCell instrument (single 25-ms square-wave pulse at 250 V, 2,000 µF, infinite Ω). All electroporations were performed in a 96-well plate (Bio-Rad cat #1652681). To examine Vpu function, 1.5 µg of pSELECT-Vpu-RRE-GFP plus 2.0 µg of pSELECT-Rev was transfected into 0.5 x 10^6 CEM cells using the same protocol. Transfected cells were resuspended in 400 µl RPMI 1640 medium, supplemented with 2 mM L-glutamine, 1,000 U/ml penicillin and 1 mg/ml streptomycin (all from Sigma-Aldrich) plus 10% fetal bovine serum (Life Technologies) and incubated for 24 h at 37°C with 5% CO_2. For Nef, 0.25 x 10^6 cells were stained with allophycocyanin (APC) labeled anti-human CD4 (clone RPA-T4; BD Biosciences) and phycoerythrin (PE) labeled anti-human HLA-A*02 (clone BB7.2; BioLegend) antibodies. For Vpu, 0.25 x 10^6 cells were stained with allophycocyanin (APC) labeled anti-human CD4 (clone RPA-T4; BD Biosciences) and phycoerythrin (PE) labeled anti-human CD317/BST2/tetherin (clone RS38E; BioLegend) antibodies. Stained cells were incubated at 4°C for 30 min, washed twice using phosphate-buffered saline (PBS) solution (Sigma-Aldrich), then resuspended in 250 µl PBS and analyzed on a CytoFlex S flow cytometer (Beckman Coulter). Data were analyzed using FlowJo 10.8.1 software (BD Biosciences). Sample gating was standardized using CEM cells transfected with positive (SF2 strain Nef; NL4.3 strain Vpu) and negative controls (empty plasmids).

To quantify the relative function of each LTS-derived Nef or Vpu clone, the difference in median fluorescence intensity (MFI) of each antibody label was calculated between the GFP-positive (i.e., Nef/Vpu-transfected) and GFP-negative (*i.e.*, untransfected) cell gates. These values were then normalized to those of the positive control, which was examined in parallel, using the following formula: $[(MFI_{Neg}-MFI_{clone})]/[(MFI_{Neg}-MFI_{control})]$. A value of <1.0 indicates a relative function that is less than that of the positive control (SF2 for Nef or NL4.3 for Vpu), whereas a value of >1.0 indicates a relative function greater than that of the relevant control. Each Nef and Vpu clone was tested in at least three independent experiments, and results are reported as the mean.

Mutagenesis

Participant-derived Nef or Vpu clones were subjected to site-directed mutagenesis to evaluate the impact of specific polymorphisms on protein function. Individual mutations were introduced into the parental gene sequence, which was then codon optimized (Codon Optimization tool; Integrated DNA Technologies) and synthesized commercially (eBlocks; Integrated DNA Technologies). Products were cloned into pSELECT-GFPzeo, sequence-validated and assessed for function as described. Codon optimized parental clones were used as controls. Each mutant clone was tested at least three times in independent experiments, and representative results are shown.

Statistical Analysis

Statistical analyses were performed using Prism v9.0 (GraphPad). The Mann-Whitney *U*-test was used to compare Nef and Vpu functions in LTS and controls. It was also used to assess the relationship between population-level Nef and Vpu amino acid variation and protein function on a codon-by-codon basis, where multiple comparisons were addressed using a q-value approach (36). Fisher's exact test was used to compare Nef and Vpu amino acid frequencies at specific residues between groups. Spearman's correlation was used to analyze the relationship between *Nef* and *Vpu* functions within the same

participant, as well as between protein functions and the participant's clinical parameters (CD4+ T-cell count and pVL). An unpaired *t*-test was used to compare the function of the mutant to that of the parental clone.

Data Availability

Nef and *vpu* sequences from LTS and a subset of *Nef* controls have been submitted to GenBank accession numbers ON044919-ON044988. Control *nef* sequences with accession numbers KC906733-KC907077 (28) and control *vpu* sequences with accession numbers MT116441-MT116772 (27) were deposited in GenBank previously. All clone sequences are provided in the **Supplementary Data File**; **Tables S1** and **S2**. Full results of sequence-function analyses are provided in the **Supplementary Data File**; **Tables S3–S6**.

RESULTS

LTS and Control Study Participants

Our research group has promoted couples-based HIV counseling and testing in Rwanda since the mid-1980s (37). In 1994 however, the genocide against the Tutsi in Rwanda interrupted this work for nearly 6 years. Upon re-initiating the project, we identified 103 former clients who had been diagnosed with HIV-1 in 1986 and who had lived for more than a decade without access to cART. While their extended longevity fulfills a core criterion used to define the non-progressor phenotype, no other clinical information is available prior to the year 2000. To reflect this limitation, we refer to these individuals as long-term survivors (LTS). Since relatively few studies of HIV-1 non-progressors have been conducted in Africa, we were interested to explore the potential role of viral accessory protein function in this unique group. Plasma samples of varying quantity and quality, collected between 2000-2003, were available from 103 LTS, from which we were able to amplify paired *nef* and *vpu* sequences from 34 participants (**Figure 1**). As the majority of these clones (n=30 for *nef* and N=29 for *vpu*) were subtype A, we focused our subsequent functional analyses on the 29 LTS with subtype A *nef* and *vpu* sequences. These 29 LTS had remained healthy for a median [IQR] of 19.3 [15.9-24.6] years without cART (**Table 1**). As a comparator group, we used data from 166 clones (104 Nef and 62 Vpu) isolated from the plasma of 143 participants with chronic untreated HIV-1 subtype A infection (27, 28). Of these, 20 participants were enrolled in the Rwandan Heterosexual Transmission [HT] prospective study in Kigali, Rwanda from 2005-2009, and 123 participants were enrolled in the Uganda AIDS Rural Treatment Outcomes [UARTO] cohort in Mbarara, Uganda from 2002-2009 (**Table 1**).

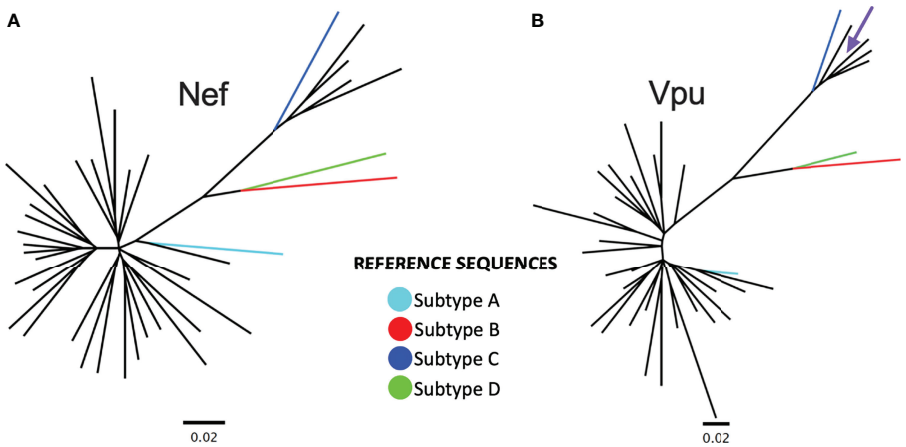

FIGURE 1 | *Nef* and *Vpu* phylogenies from the survivor cohort. **(A)** Unrooted phylogeny inferred from an alignment comprising 34 *nef* sequences from Rwandan long-term survivors (LTS) along with HIV-1 subtype A, B, C and D reference sequences. The scale, shown below the phylogeny, is measured in estimated nucleotide substitutions per site. **(B)** A corresponding phylogeny for 34 *vpu* sequences. The arrow points to a *vpu* sequence with a branch length too short to see.

TABLE 1 | Characteristics of Rwandan long-term survivors and controls.

Characteristic	LTS cohort Vpu and Nef (subtype A) (N = 29)	Comparison cohort Vpu (subtype A) (N = 62)	Comparison cohort Nef (subtype A) (N = 104)
Female Sex, N (%)	29 (100)	34 (54.8)	56 (53.8)
Follow up in years before ART, median [IQR]	19.3 [15.9-24.6]	–	–
Age at cohort entry in years, median [IQR]	24 [23-27]	37 [32-40]	35 [30-40.5]
Country of origin (%)	Rwanda (100)	Rwanda (24.2); Uganda (75.8)	Rwanda (11.5); Uganda (88.5)
Most recent pVL pre-ART, median [IQR]	4.12 [3.55-4.72]	4.93 [4.41-5.45]	4.84 [4.42-5.53]
CD4 count at time of sampling, median [IQR]	320 [147-563]	154 [88-199]	170 [101-243]

Phylogenetic Analysis of Nef and Vpu From LTS and Chronic Controls

Given the temporal and geographic variation between the LTS and control *nef* and *vpu* sequences, we first investigated these sequences for evidence of genetic clustering that could influence results interpretation. Maximum-likelihood phylogenies inferred from LTS and chronic *nef* and *vpu* sequence alignments however showed that LTS sequences interspersed relatively evenly among the chronic comparison sequences, with no overt segregation, supporting the latter as reasonable controls (**Figures 2A, B**). Some differences nevertheless existed between LTS and control consensus amino acid sequences, which differed at four of Nef's 206 codons (56, 85, 133 and 184) and three of Vpu's 81 codons (2, 32, and 44) (**Figures 2C, D**).

Nef Function Is Reduced in LTS Clones

To assess whether Nef function is impaired in LTS, we examined Nef-mediated downregulation of CD4 and HLA

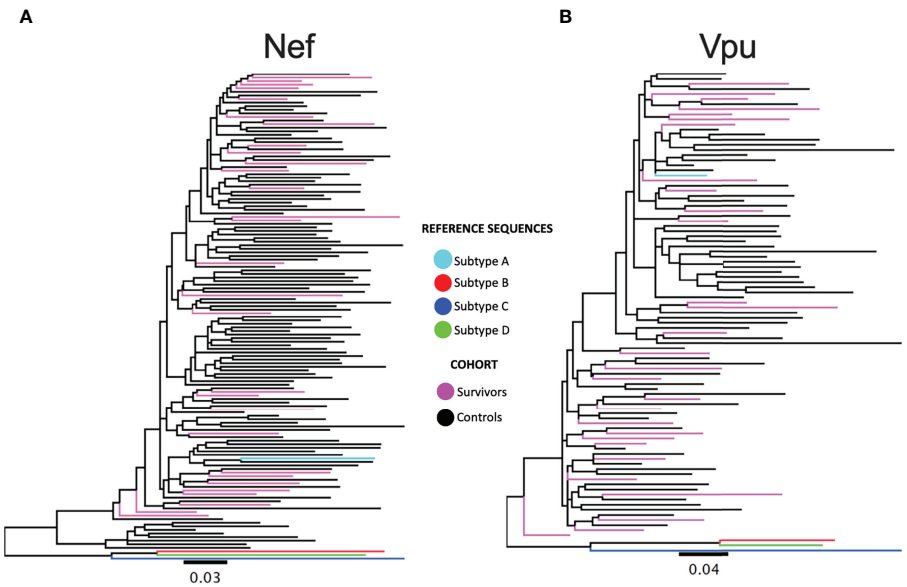

C

```
HXB2_NEF   MGGKWSKSSV IGWPTVRERM RRAEPAADRV GAASRDLEKH GAITSSNTAA
Survivors  MGGKWSKSSI VGWPEVRERM RRTPPAATGV GAVSQDLDKH GAVTSSNI..  50
 Controls  ---------- ---------- ---------- ---------- --------..

HXB2_NEF   TNAACAWLEA QEEEEVGFPV TPQVPLRPMT YKAAVDLSHF LKEKGGLEGL
Survivors  NHPSCVWLEA QEEEEVGFPV RPQVPLRPMT YKGALDLSHF LKEKGGLDGL  100
 Controls  -----A---- ---------- ---------- ----F----- ----------

HXB2_NEF   IHSQRRQDIL DLWIYHTQGY FPDXQNYTPG PGVRYPLTFG WCYKLVPVEP
Survivors  IYSRKRQEIL DLWVYHTQGY FPDWQNYTPG PGTRYPLTFG WCFKLVPVDP  150
 Controls  ---------- ---------- ---------- --V------- ----------

HXB2_NEF   DKIEEANKGE NTSLLHPVSL HGMDDPEREV LEWRFDSRLA FHHVARELHP
Survivors  DEVEKATEGE NNSLLHPICQ HGMDDEERET LMWRFDSRLA LKHRARELHP  200
 Controls  ---------- ---------- ---------- ---K------ ----------

HXB2_NEF   EYFKNC
Survivors  EFYKDC  206
 Controls  ------
```

D

```
HXB2_VPU   TQPIPIVAIV ALVVAIIIAI VVWSIVIIEY RKILRQRKID RLIDRLIERA
Survivors  MTPLEICAIV GLIVALILAI VVWTIVGIEY KKLLKQRKID RLIERIRERA  50
 Controls  -L-------- ---------- ---------- -R-------- ---K------

HXB2_VPU   EDSGNESEG. ..EISALVEM GVEMGHHAPW DVDDL
Survivors  EDSGNESDGD TEELSKL... .VEMGNYDLG DDNNL  81
 Controls  ---------- --------... .--------- -----
```

FIGURE 2 | Phylogenetic trees of subtype A sequences from survivors and controls. **(A)** Phylogeny inferred from alignments of HIV-1 subtype A *nef* sequences from LTS and control participants, along with HIV-1 subtype **(A–D)** reference sequences. Sequences are colored by cohort (LTS in pink, controls in black). The tree is midpoint-rooted. Scale in estimated nucleotide substitutions per site. (B) Corresponding phylogeny for HIV-1 subtype A *vpu* sequences. **(C)** *nef* consensus sequences from LTS and control cohorts aligned to HXB2 subtype B reference. Residue numbering is based on HXB2. **(D)** *vpu* consensus sequences from LTS and control cohorts aligned to HXB2 subtype B reference. Residues 60-62 (DTE) shown in orange were present in the native subtype A sequences, but missing in HXB2. Likewise, HXB2 contains an insertion at residues 65-68, which were excluded from numbering. As such, the residue numbering for Vpu is based on the participant consensus.

class I using an established reporter cell assay where Nef clones are transfected into an immortalized $CD4^+$ T-cell line that also expresses HLA-A*02 (representative raw data and normalized protein functions shown in **Figure 3A**). Each LTS Nef clone was examined in at least three independent experiments, with results reported as the mean of these measurements, while results for each Nef control clone is reported as the mean of two independent experiments (**Supplementary Figure 2**). Note that downregulation data for the 104 chronic Nef clones was obtained as part of our previously published study (28). To confirm the reproducibility of these historical data in the present context, we retested 25 chronic Nef clones from the previous dataset along with LTS clones and confirmed a high degree of correlation with no bias in the difference between historic and re-tested measures (**Supplementary Figure 3**).

Overall, Nef-mediated CD4 downregulation function was modestly lower among the 29 LTS clones compared to the 104 chronic clones: the normalized median activity of LTS clones was 0.96 (interquartile range [IQR] 0.89-0.99], while the median activity of chronic clones was 0.98 [IQR 0.94-1.0] (Mann-Whitney p=0.03; **Figure 3B**). Nef-mediated HLA class I downregulation was substantially lower among LTS clones: the normalized median activity of LTS clones was 0.63 [IQR 0.39-0.70], while the median activity of chronic clones was 0.83 [0.74-0.89] (Mann Whitney p<0.0001; **Figure 3C**). Moreover, and consistent with some prior studies, we found a weak positive correlation between these two Nef functions in the combined LTS and control data (ρ=0.38, p<0.0001), as well as within the control group (ρ=0.33, p=0.0007) (**Figure 3D**).

Vpu Function Is Similar in LTS and Chronic Controls

To examine possible impairments in Vpu function in LTS, we used an established reporter cell assay where each Vpu clone was co-transfected with Rev into an immortalized $CD4^+$T-cell line, and its ability to downregulate CD4 and Tetherin was measured by flow cytometry (representative raw data and normalized protein functions shown in **Figure 4A**). Both functions are reported as the mean of three independent replicate measurements (**Supplementary Figure 4**). Normalized Vpu function among the 29 LTS clones was compared to that of 62 Vpu clones previously isolated from individuals with chronic HIV-1 Subtype A infection (27).

Overall, the median Vpu-mediated CD4 downregulation function of the LTS clones was 0.89 [IQR 0.74-1.04], compared to 0.97 [IQR 0.83-1.17] in the chronic clones; however, this activity was variable within groups and the difference was not statistically significant (p=0.13) (**Figure 4B**). Similarly, median Tetherin downregulation function was 0.93 [IQR 0.78-1.0] in LTS clones, compared to 0.91 [IQR 0.84-0.97] in the control clones (p=0.72) (**Figure 4C**). We observed a positive correlation between these Vpu functions in our combined data from LTS and chronic clones (ρ=0.5, p<0.0001), as well as within the control group (ρ=0.6, p<0.0001) (**Figure 4D**).

No Relationship Between Nef and Vpu Function in Paired LTS Clones

Given their complementary immune evasion activities, within-host Nef and Vpu proteins could in theory compensate for impaired function in the other protein (12, 38, 39), in which case the function of within-host *nef* and *vpu* sequences would correlate inversely. Our analysis of paired Nef and Vpu clones from 29 LTS provided an opportunity to assess this. We observed no significant association between within-host Nef and Vpu functions however (**Figure 5**), suggesting that the activities of these viral proteins were largely independent.

Associations Between Nef and Vpu Functions, and HIV Clinical Parameters

The downregulation functions of Nef and Vpu enhance viral pathogenicity (14, 18, 22), and attenuated Nef and Vpu functions have previously been associated with slower disease progression (24, 26). We therefore analyzed the relationship between each Nef or Vpu function and clinical HIV-1 markers (CD4 cell count and plasma viral load (pVL)) (**Figure 6**). In combined data from LTS and control clones, Nef-mediated CD4 downregulation function correlated inversely with CD4 T cell count (ρ= –0.24, p=0.01) (**Figure 6A**) and positively with pVL (ρ=0.4, p=0.0001) (**Figure 6C**). The positive correlation between Nef-mediated CD4 downregulation function and pVL was also statistically significant when LTS and controls were analyzed separately (ρ= 0.59, p=0.03 and ρ= 0.3, p=0.005, respectively) (**Figure 6C**). In combined data from LTS and control clones, Nef-mediated HLA downregulation function also correlated positively with pVL (ρ=0.25, p=0.01) (**Figure 6D**); however, no association was observed between Nef-mediated HLA downregulation and CD4 cell count (**Figure 6B**). Similar associations between Nef function and clinical markers were typically not observed when LTS clones were analyzed alone, which may be due to limited statistical power, relatively lower function and/or less variable clinical phenotypes within this group. In contrast, no significant associations were found between Vpu function and HIV-1 clinical markers (**Figures 6E-H**). Overall, these observations support the notion that impaired Nef function is associated with slower disease progression.

Nef and *Vpu* Sequence Polymorphisms Associated With Function

As previous studies have identified naturally occurring *nef* and *vpu* polymorphisms associated with downregulation function (27, 40, 41), we examined this question using linked sequence-function data from LTS and control participants. When aligning subtype A study sequences, we noted that Vpu residues 60-62 (typically DAE, DTE, or DTD), which were present in all of our sequences as well as most sequences from other subtypes published in the Los Alamos National Laboratory (LANL) HIV Sequence Database, were absent in the subtype B HXB2 reference sequence that is used to define the standard HIV-1 numbering convention. These residues were also absent in the NL4.3 Vpu clone that was used as a reference for functional assays. Furthermore, we noted that Vpu residues VEMG were

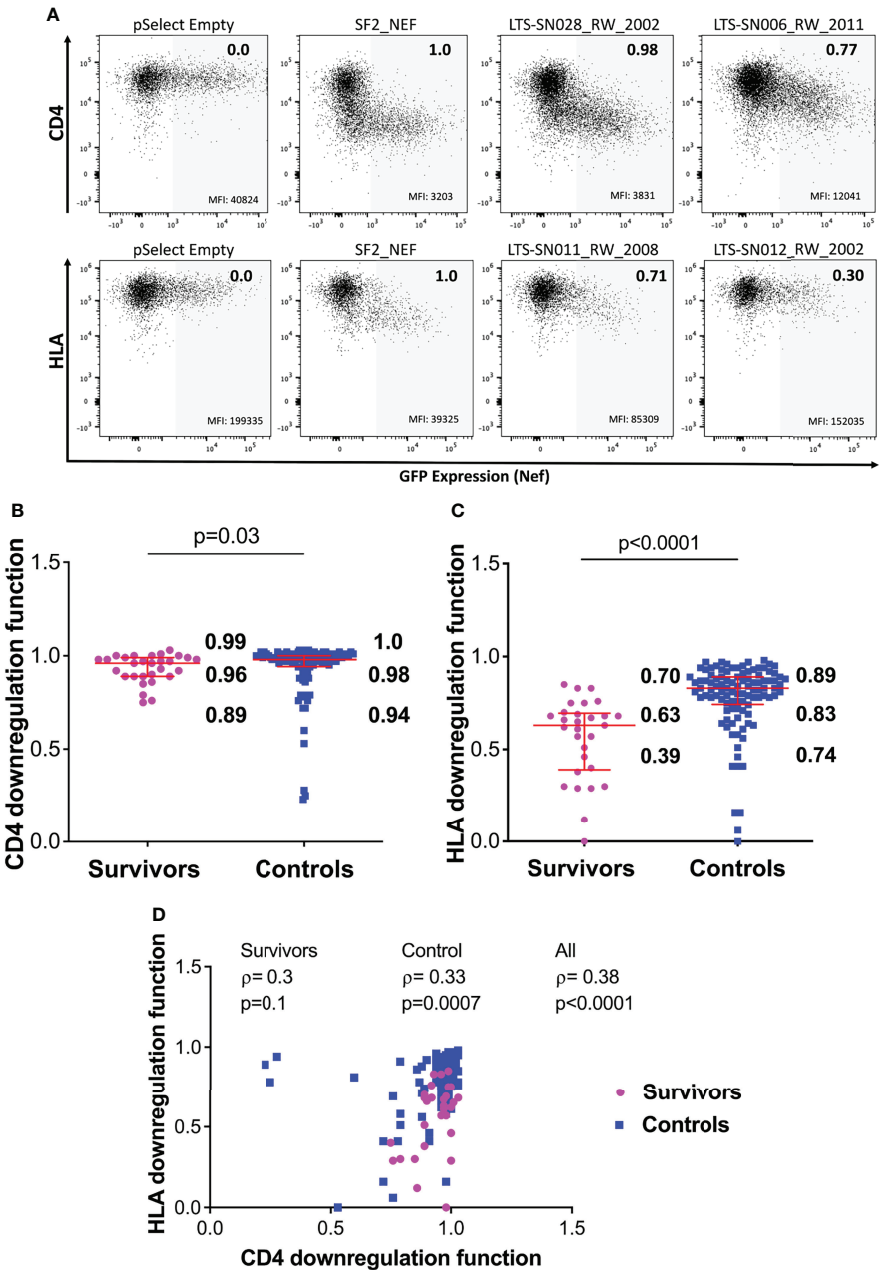

FIGURE 3 | Nef-mediated CD4 and HLA downregulation function in survivors and controls. **(A)** Representative flow cytometry plots showing downregulation of CD4 (top) or HLA (bottom) following transfection of negative control (pSelect empty vector), positive control (SF2 Nef), a representative functional clone and a representative poorly-functional clone. Gray shading denotes the GFP-positive (Nef-expressing) gate that was used for quantification. Median fluorescence intensity (MFI) of receptor expression is indicated at the bottom of each gate, and the SF2-normalized downregulation function value (calculated as described in the Methods) is indicated in the top right of each plot. **(B)** Nef mediated CD4 downregulation functions of LTS and controls. Red box and whiskers denote the median and interquartile range, with values indicated on the plot. P-value is calculated using the Mann-Whitney U-test. **(C)** Comparison of Nef mediated HLA downregulation function among LTS and controls. **(D)** Relationship between Nef-mediated CD4 and HLA downregulation functions in individual and combined cohorts, assessed using Spearman's correlation.

duplicated in HXB2 and NL4.3 (at codons 65-68 and 69-72, respectively), whereas this did not occur in our native subtype A sequences (or those of other subtypes, based on LANL). To ensure that our sequence-function analysis of Vpu reflected natural sequence variation in subtype A, we kept residues 60-62 in our alignment and removed the duplicate VEMG motif at residues 65-68. The full Nef and Vpu alignments used in these analyses are provided in **Supplementary Data File**; **Tables S1**

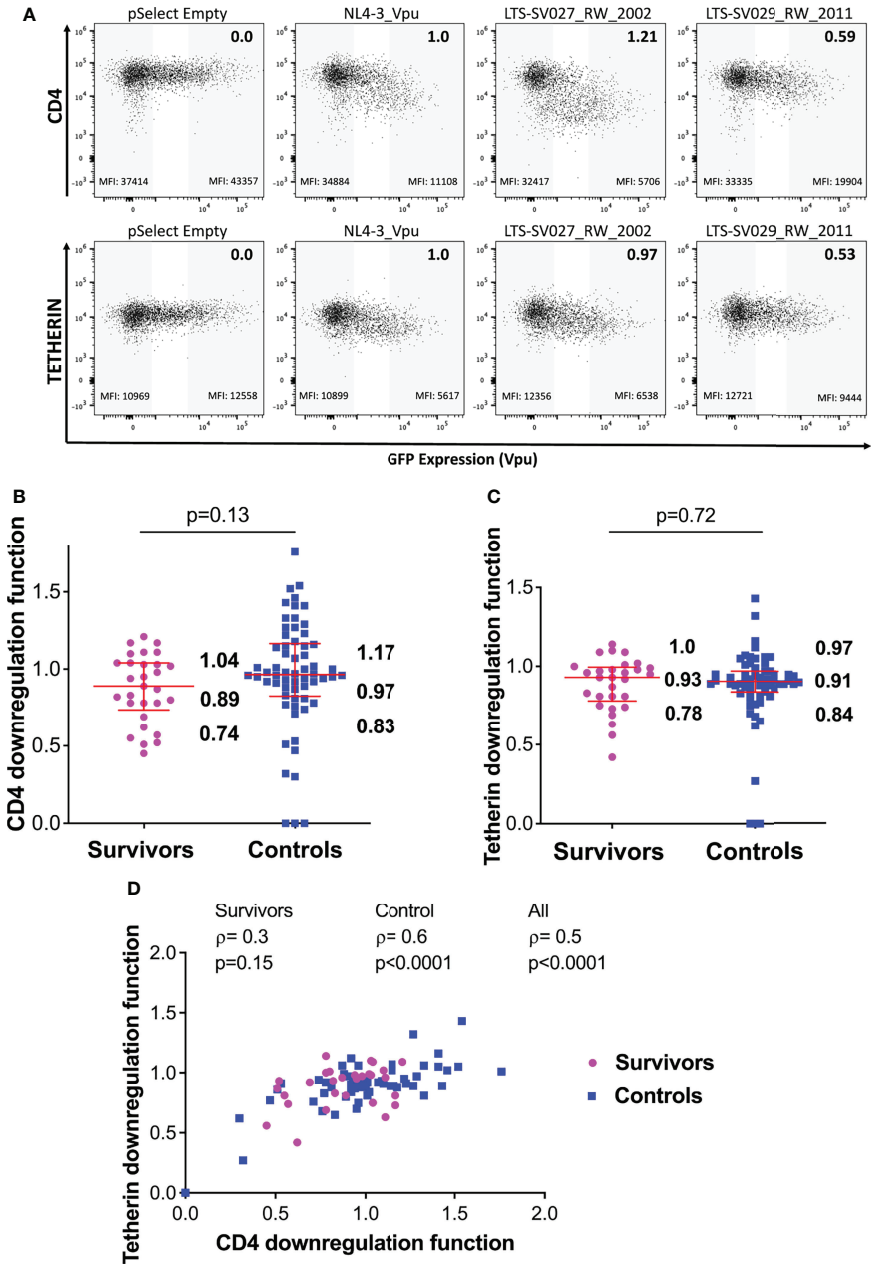

FIGURE 4 | Vpu-mediated CD4 and Tetherin downregulation function in survivors and controls. **(A)** Representative flow cytometry plots showing downregulation of CD4 (top) or tetherin (bottom) following transfection of negative control (pSelect empty vector), positive control (NL4.3 Vpu), a representative functional clone and a representative poorly-functional clone. Gray shading at the left of each plot denotes the GFP-negative (untransfected) gate used for quantification, whereas grey shading at the right denotes the corresponding GFP-high (Vpu-expressing) gate. Median fluorescence intensity (MFI) of receptor expression is indicated at the bottom of each gate, and the NL4.3-normalized downregulation function (calculated as described in the Methods) is indicated in the top right of each plot. **(B)** Vpu mediated CD4 downregulation functions of LTS and controls. Red box and whiskers denote the median and interquartile range, with values indicated on the plot. P-value is calculated using the Mann-Whitney U-test. **(C)** Comparison of Vpu mediated Tetherin downregulation function among LTS and controls. **(D)** Relationship between Vpu-mediated CD4 and Tetherin downregulation functions in individual and combined cohorts, assessed using Spearman's correlation.

and **S2**. The full results of our sequence-function analysis are shown in **Supplementary Data File**; **Tables S3–S6**; here, multiple comparisons were addressed using a false-discovery rate (q-value) approach (36).

Using a predefined significance threshold of $p<0.05$ and $q<0.4$, and a median functional difference of ≥ 5% between sequences having or lacking the amino acid of interest, we identified polymorphisms at 15 Nef codons that were associated with its

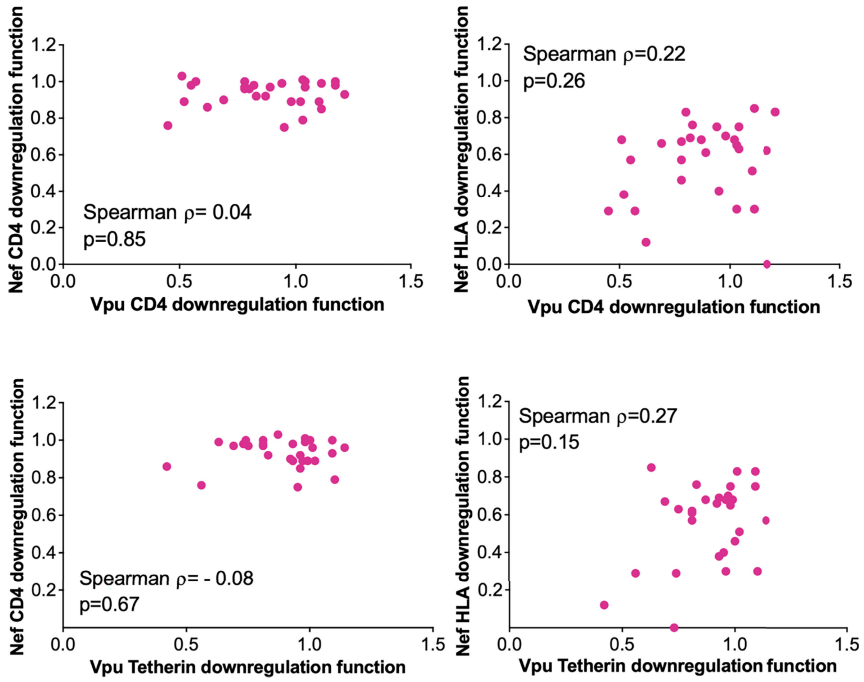

FIGURE 5 | Relationship between within-host *Nef* and *Vpu* functions in the survivor cohort. Relationships are assessed using Spearman's correlation.

HLA downregulation function (namely at residues 3, 9, 11, 14, 40, 56, 89, 105, 155, 157, 161, 184, 191, 196 and 206) (**Supplementary Data File**; **Table S4**). We also identified polymorphisms at seven of Vpu's codons that were associated with its CD4 downregulation function: 2, 3, 5, 7, 45, 60 and 68 (**Supplementary Data File**; **Table S5**); as well as polymorphisms at nine of Vpu's codons that were associated with its Tetherin downregulation function: 2, 26, 30, 58, 62, 68, 69, 70, 77 (**Supplementary Data File**; **Table S6**). We did not identify any residues associated with Nef-mediated CD4 downregulation function that met these criteria (**Supplementary Data File**; **Table S3**).

Three of these polymorphisms occurred at codons where the population consensus differed between cohorts (Nef residues 56 and 184; Vpu residue 2; see **Figures 2C, D**). However, the distribution of residues Nef 56V/A and Vpu 2T/L did not differ significantly between cohorts (Fisher's exact test, p=0.2 for Nef and p=0.16 for Vpu), so we did not pursue these further. Of the identified associations, we selected polymorphisms at Nef 184E, as well as Vpu 60D and Vpu 62E for *in vitro* validation. Nef 184E, a minority variant at this residue, was present in five (of 29; 17.2%) LTS clones compared to two (of 104; 1.9%) control clones (Fisher's exact test, p=0.006), and was associated with impaired HLA downregulation function. Vpu 60D/E and 62D/E were of interest since they were located within the motif absent in HXB2 and NL4.3, and because the D60E substitution, an uncommon variant at this position, was associated with the single largest negative effect on Vpu-mediated CD4 downregulation function (-44%) in our study (**Supplementary Data File**; **Table S5**). To test the impact of Nef 184E, we synthesized codon-optimized clones based on isolate KC906874 from the control cohort, that encoded the parental 184R or the mutant R184E. We then compared the abilities of these clones to downregulate CD4 and HLA using our reporter cell assay in at least three replicate experiments. In agreement with our expectations, the R184E substitution significantly reduced Nef's ability to downregulate HLA (p=0.006) (**Figure 7A**). We also observed that this mutation impaired CD4 downregulation compared to the parental clone (p=0.04) (**Figure 7B**).

Next, to test the impact of polymorphisms at Vpu codons 60 and 62, we synthesized codon-optimized clones based on isolate MT116708 from the control cohort that encoded the parental sequence, which featured D60 and E62. We also synthesized mutants encoding D60E or E62D, as well as a mutant that lacked residues 60-62 (consistent with NL4.3/HXB2). The relative abilities of each clone to downregulate CD4 and Tetherin were then assessed using our reporter cell assay in at least three replicate experiments. We observed that deletion of residues 60-62, located in the second alpha-helix of Vpu, abrogated CD4 downregulation function (p<0.0001) but reduced Tetherin downregulation function only modestly (p=0.07) (**Figures 7C, D**). In addition, consistent with our expectations, we found that D60E reduced CD4 downregulation function (p=0.0008), while E62D had no effect (p=0.73) (**Figure 7C**). Neither D60E nor E62D significantly altered Tetherin downregulation function compared to the parental clone (p=0.70 and p=0.86, respectively) (**Figure 7D**), though the modest enhancement by E62D was in line with our sequence/function analyses. Together, these observations indicate that Nef polymorphism 184E may attenuate function in an HIV-1 subtype A context. In addition, these findings suggest a potential role for Vpu residue 60 in modulating CD4 downregulation function in this subtype.

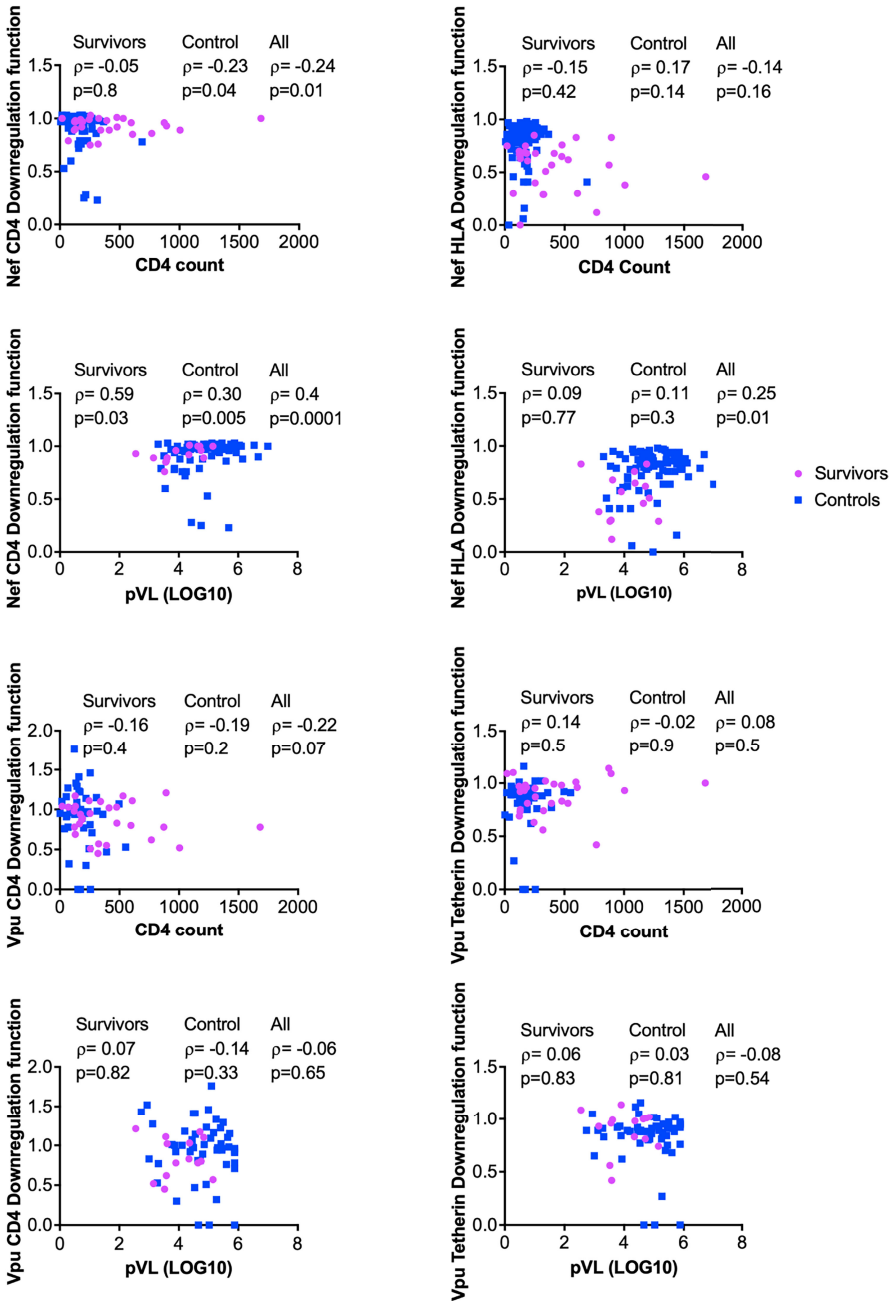

FIGURE 6 | Relationship between *Nef* and *Vpu* functions and HIV clinical parameters (CD4 and pVL). Relationships were assessed within survivors, within controls, and in combined cohorts, using Spearman's correlation.

CONCLUSION AND DISCUSSION

We investigated the sequence and function of HIV-1 accessory proteins Nef and Vpu in a unique cohort of 29 LTS individuals from Rwanda, who had survived with HIV-1 subtype A infection for a median of 19.3 years without antiretroviral treatment. LTS-derived clones did not display obvious genetic defects or deletions in Nef or Vpu that would be expected to affect their function. Furthermore, the sequences of LTS clones intermingled on a phylogenetic tree with those of 104 Nef and 62 Vpu clones from cART-naïve individuals living with HIV-1 subtype A from the same geographic region, suggesting that the LTS phenotype was not attributable to infection with a shared attenuated HIV-1 strain.

Overall, we observed that LTS Nef clones displayed significantly lower abilities to downregulate CD4 and HLA

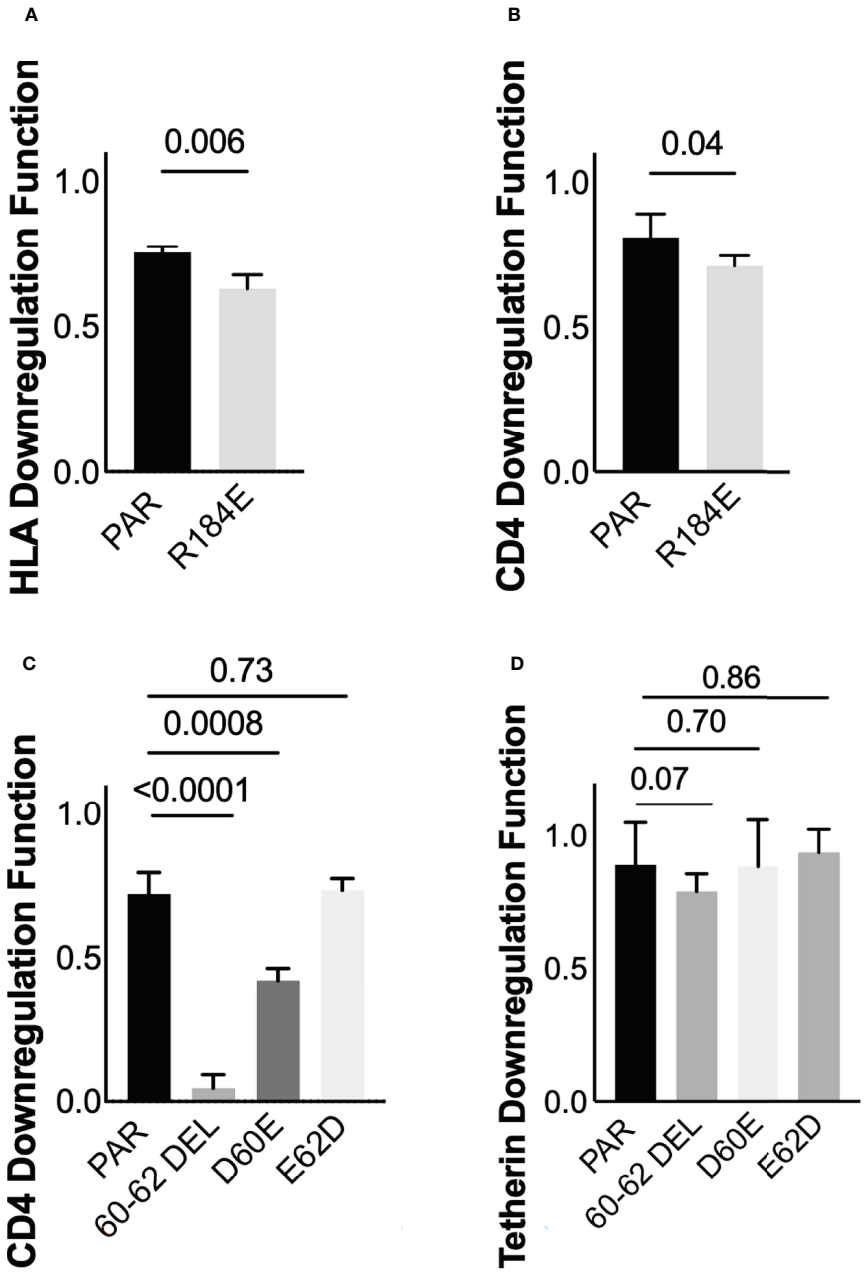

FIGURE 7 | Verification of residues associated with *Nef* and *Vpu* functions **(A)** Nef-mediated HLA downregulation function of the parental (PAR) clone expressing R184, and the mutant harboring R184E. Results are expressed as mean of 3 replicate measurements with error bars denoting the median and interquartile range. **(B)** Same as A, but for Nef-mediated CD4 downregulation function **(C)** Vpu-mediated CD4 downregulation function of the parental (PAR) clone expressing D60 and E62, along with mutants harboring the 60-62 deletion, D60E or E62D substitutions **(D)** Same as C, but for Vpu-mediated Tetherin downregulation function.

class I compared to control Nef clones. In contrast, both LTS and control Vpu clones downregulated CD4 and Tetherin to a similar degree. We also observed consistent positive correlations between Nef-mediated CD4 downregulation function *in vitro* and CD4 cell count as well as plasma viral load *in vivo*, while no similar correlation with HIV-1 clinical markers was found for Vpu. Together, these results suggest that impaired function of Nef, but not Vpu, contributes to slower progression in the LTS group; an observation that is consistent with prior studies from our group and others that found reduced Nef function in HIV-1 elite controllers and long-term non-progressors (24, 26, 42, 43).

In a linked sequence-function analysis of Nef, we identified polymorphisms at 15 Nef codons that were associated with differences in HLA downregulation, while no residues were

associated with CD4 downregulation using pre-defined thresholds for significance. Of these, Nef 184E was found in a higher proportion of LTS clones (17.2%) versus control clones (1.9%), and introducing it into a participant Nef clone significantly reduced HLA and CD4 downregulation function, supporting the importance of this naturally arising polymorphism in modulating Nef function in HIV-1 subtype A. In a similar analysis of Vpu, we identified polymorphisms at seven and nine of Vpu's codons that were associated with differences in CD4 and Tetherin downregulation, respectively. Of these, Vpu D60 and E62 were selected for further testing. Introducing D60E into a participant Vpu clone significantly reduced its ability to downregulate CD4 but not Tetherin, while introducing E62D did not affect downregulation of either protein. Notably, deletion of Vpu residues 60-62, which are present in most circulating HIV-1 sequences but absent in HXB2 and NL4.3, resulted in a near complete loss of CD4 downregulation activity, while Tetherin downregulation was largely unaffected. It is intriguing that NL4.3 Vpu remains highly functional despite lacking residues 60-62. We attribute this outcome to an unusual insertion that occurs at residues 65-68 only in the HXB2/NL4.3 lineage, which may compensate deletion of 60-62 by stabilizing alpha-helix 2, but additional studies will be needed to test this hypothesis. Even though Vpu function was not clearly associated with the LTS phenotype in our study, these findings nevertheless highlight polymorphic residues in Vpu that may contribute to modulation of CD4 downregulation function in HIV-1 subtype A, as well as other subtypes.

This retrospective study was restricted to individuals with a rare phenotype for whom viable specimens were available, which limited our statistical power to identify associations between sequence, function, and clinical markers of viral pathogenesis. The analyses of viral polymorphisms associated with protein function should be interpreted with caution, since observations based on individual clones may not be generalizable. In particular, the dataset did not allow us to perform an in-depth analysis of secondary mutations that might modulate the impact of Nef or Vpu polymorphisms; thus, additional studies of residues that covary with Nef 184E or Vpu 60D/62E could enhance efforts to identify functionally important motifs in these proteins. Furthermore, the lack of an association between Vpu and clinical markers should consider the relatively small size of the LTS group. Nevertheless, our final analysis of paired Nef and Vpu clones from 29 LTS is among the largest studies to examine HIV-1 accessory protein function in non-progressors. In addition, our assessment of LTS living with HIV-1 subtype A infection extends prior studies that looked only at subtype B. Given our focus on these two accessory proteins, we cannot rule out possible contributions of other viral genes to the LTS phenotype. Furthermore, we have not examined potential host genetic or immunological factors that may also result in relative control of HIV-1. Future studies will be needed to address these important issues, as well as investigate potential links between Nef function and reservoir size in long-term survivors living with non-B subtypes (44). Despite these limitations, our findings clearly indicate that impaired Nef function is associated with long-term survival in the context of HIV-1 subtype A.

IMPLICATIONS

Understanding the host and viral factors that contribute to control of HIV-1 infection can improve our knowledge of the biology of viral pathogenesis and may also provide new insights to inform the design of vaccines or therapies to prevent, treat or possibly cure HIV. The results of this study indicate that impaired Nef function contributes to slower disease progression in African long-term survivors living with untreated HIV-1 subtype A infection. This observation is consistent with prior studies in the context of subtype B infection, and further supports ongoing efforts to target Nef using novel antiviral therapies. Moreover, our analyses identified natural polymorphisms that impair Nef and Vpu function, which may highlight critical motifs on these proteins that can serve as new targets for therapeutic development.

DATA AVAILABILITY STATEMENT

The datasets presented in this study can be found in **Supplementary Material**. Sequences are submitted to GenBank: accession numbers ON044919-ON044988 (for LTS clones); KC906733-KC907077 and MT116441-MT116772 (for control clones).

ETHICS STATEMENT

The studies involving human participants were reviewed and approved by Rwanda National Ethics committee, Emory University Institutional Review Board, and Simon Fraser University Research Ethics Board. All participants provided written informed consent.

AUTHOR CONTRIBUTIONS

GU, MB and ZB conceived and designed the experiments. GU, JKM, and SJ performed the experiments and analyzed the data. FM, H-SH, and HS contributed to data analysis. GL, HB, CM, PH, JNM, JH, EK, SA and EH provided study specimens or data. GU prepared the manuscript. All authors reviewed the article and approved the final submitted version.

FUNDING

This project was funded by the Canadian Institutes of Health Research (CIHR; PJT-148621). The UARTO cohort was supported by grants from the National Institutes of Health, USA (R01 MH054907 and P30 AI027763). GU was supported

by the Queen Elizabeth Scholars program, a partnership between the Rideau Hall Foundation, Community Foundations of Canada, Universities Canada and Canadian universities; and the Sub-Saharan African Network for TB/HIV Research Excellence (SANTHE), a DELTAS Africa Initiative [grant # DEL-15-006]. The DELTAS Africa Initiative is an independent funding scheme of the African Academy of Sciences (AAS) Alliance for Accelerating Excellence in Science in Africa (AESA) and supported by the New Partnership for Africa Development Planning and Coordinating Agency (NEPAD Agency) with funding from the Wellcome Trust [grant # 107752/Z/15/Z] and the UK government. HS is supported by a CIHR Canada Graduate Scholarship Masters award. ZB is the recipient of a Scholar Award from the Michael Smith Foundation for Health Research. The views expressed in this publication are those of the author(s) and not necessarily those of AAS, NEPAD Agency, Wellcome Trust, the UK government or other funders.

ACKNOWLEDGMENTS

We thank the study participants for making this work possible. We also acknowledge the staff of Projet San Francisco, the Centre for Family Health Research and the UARTO project for their support. We also thank Chanson J. Brumme, Sarah Speckmaier and Anna Appah for their assistance during data collection and analysis.

SUPPLEMENTARY MATERIAL

The Supplementary Material for this article can be found online at: https://www.frontiersin.org/articles/10.3389/fviro.2022.917902/full#supplementary-material

REFERENCES

1. Pantaleo G, Fauci AS. Immunopathogenesis of HIV Infection. *Annu Rev Microbiol* (1996) 50:825–54. doi: 10.1146/annurev.micro.50.1.825
2. Vergis EN, Mellors JW. Natural History of HIV-1 Infection. *Infect Dis Clin North Am* (2000) 14:809–25. doi: 10.1016/S0891-5520(05)70135-5
3. Poorolajal J, Hooshmand E, Mahjub H, Esmailnasab N, Jenabi E. Survival Rate of AIDS Disease and Mortality in HIV-Infected Patients: A Meta-Analysis. *Public Health* (2016) 139:3–12. doi: 10.1016/j.puhe.2016.05.004
4. Walker BD, Yu XG. Unravelling the Mechanisms of Durable Control of HIV-1. *Nat Rev Immunol* (2013) 13:487–98. doi: 10.1038/nri3478
5. Gurdasani D, Iles L, Dillon DG, Young EH, Olson AD, Naranbhai V, et al. A Systematic Review of Definitions of Extreme Phenotypes of HIV Control and Progression. *AIDS* (2014) 28:149–62. doi: 10.1097/QAD.0000000000000049
6. Moyano A, Ndung'u T, Mann JK. Determinants of Natural HIV-1 Control. *AIDS Rev* (Online ahead of print). doi: 10.24875/AIDSRev.21000048
7. Dean M, Carrington M, Winkler C, Huttley GA, Smith MW, Allikmets R, et al. Genetic Restriction of HIV-1 Infection and Progression to AIDS by a Deletion Allele of the CKR5 Structural Gene. Hemophilia Growth and Development Study, Multicenter AIDS Cohort Study, Multicenter Hemophilia Cohort Study, San Francisco City Cohort, ALIVE Study. *Science* (1996) 273:1856–62. doi: 10.1126/science.273.5283.1856
8. Fellay J, Shianna KV, Ge D, Colombo S, Ledergerber B, Weale M, et al. A Whole-Genome Association Study of Major Determinants for Host Control of HIV-1. *Science* (2007) 317:944–7. doi: 10.1126/science.1143767
9. Hartana CA, Yu XG. Immunological Effector Mechanisms in HIV-1 Elite Controllers. *Curr Opin HIV AIDS* (2021) 16:243–8. doi: 10.1097/COH.0000000000000693
10. Blanquart F, Wymant C, Cornelissen M, Gall A, Bakker M, Bezemer D, et al. Viral Genetic Variation Accounts for a Third of Variability in HIV-1 Set-Point Viral Load in Europe. *PloS Biol* (2017) 15:e2001855. doi: 10.1371/journal.pbio.2001855
11. Wang B. Viral Factors in non-Progression. *Front Immunol* (2013) 4:355. doi: 10.3389/fimmu.2013.00355
12. Mlcochova P, Apolonia L, Kluge SF, Sridharan A, Kirchhoff F, Malim MH, et al. Immune Evasion Activities of Accessory Proteins Vpu, Nef and Vif are Conserved in Acute and Chronic HIV-1 Infection. *Virology* (2015) 482:72–8. doi: 10.1016/j.virol.2015.03.015
13. Song YE, Cyburt D, Lucas TM, Gregory DA, Lyddon TD, Johnson MC. ßTrCP is Required for HIV-1 Vpu Modulation of CD4, GaLV Env, and BST-2/Tetherin. *Viruses* (2018) 10:573. doi: 10.3390/v10100573
14. Khan N, Geiger JD. Role of Viral Protein U (Vpu) in HIV-1 Infection and Pathogenesis. *Viruses* (2021) 13:1466. doi: 10.3390/v13081466
15. Pham TN, Lukhele S, Hajjar F, Routy JP, Cohen EA. HIV Nef and Vpu Protect HIV-Infected CD4+ T Cells From Antibody-Mediated Cell Lysis Through Down-Modulation of CD4 and BST2. *Retrovirology* (2014) 11:15. doi: 10.1186/1742-4690-11-15
16. Veillette M, Desormeaux A, Medjahed H, Gharsallah NE, Coutu M, Baalwa J, et al. Interaction With Cellular CD4 Exposes HIV-1 Envelope Epitopes Targeted by Antibody-Dependent Cell-Mediated Cytotoxicity. *J Virol* (2014) 88:2633–44. doi: 10.1128/JVI.03230-13
17. Veillette M, Coutu M, Richard J, Batraville LA, Dagher O, Bernard N, et al. The HIV-1 Gp120 CD4-Bound Conformation is Preferentially Targeted by Antibody-Dependent Cellular Cytotoxicity-Mediating Antibodies in Sera From HIV-1-Infected Individuals. *J Virol* (2015) 89:545–51. doi: 10.1128/JVI.02868-14
18. Malim MH, Emerman M. HIV-1 Accessory Proteins–Ensuring Viral Survival in a Hostile Environment. *Cell Host Microbe* (2008) 3:388–98. doi: 10.1016/j.chom.2008.04.008
19. Sugden SM, Bego MG, Pham TN, Cohen EA. Remodeling of the Host Cell Plasma Membrane by HIV-1 Nef and Vpu: A Strategy to Ensure Viral Fitness and Persistence. *Viruses* (2016) 8:67. doi: 10.3390/v8030067
20. Kestler H, Ringler DJ, Mori K, Panicali DL, Sehgal PK, Daniel MD, et al. Importance of the Nef Gene for Maintenance of High Virus Loads and for Development of AIDS. *Cell* (1991) 65:651–62. doi: 10.1016/0092-8674(91)90097-I
21. Alexander L, Weiskopf E, Greenough TC, Gaddis NC, Auerbach MR, Malim MH, et al. Unusual Polymorphisms in Human Immunodeficiency Virus Type 1 Associated With Nonprogressive Infection. *J Virol* (2000) 74:4361–76. doi: 10.1128/JVI.74.9.4361-4376.2000
22. Foster JL, Garcia JV. Role of Nef in HIV-1 Replication and Pathogenesis. *Adv Pharmacol* (2007) 55:389–409. doi: 10.1016/S1054-3589(07)55011-8
23. Rhodes DI, Ashton L, Solomon A, Carr A, Cooper D, Kaldor J, et al. Characterization of Three Nef-Defective Human Immunodeficiency Virus Type 1 Strains Associated With Long-Term Nonprogression. Australian Long-Term Nonprogressor Study Group. *J Virol* (2000) 74:10581–8. doi: 10.1128/JVI.74.22.10581-10588.2000
24. Mwimanzi P, Markle TJ, Martin E, Ogata Y, Kuang XT, Tokunaga M, et al. Attenuation of Multiple Nef Functions in HIV-1 Elite Controllers. *Retrovirology* (2013) 10:1. doi: 10.1186/1742-4690-10-1
25. Mann JK, Chopera D, Omarjee S, Kuang XT, Le AQ, Anmole G, et al. Nef-Mediated Down-Regulation of CD4 and HLA Class I in HIV-1 Subtype C Infection: Association With Disease Progression and Influence of Immune Pressure. *Virology* (2014) 468-470:214–25. doi: 10.1016/j.virol.2014.08.009
26. Chen J, Tibroni N, Sauter D, Galaski J, Miura T, Alter G, et al. Modest Attenuation of HIV-1 Vpu Alleles Derived From Elite Controller Plasma. *PloS One* (2015) 10:e0120434. doi: 10.1371/journal.pone.0120434

27. Umviligihozo G, Cobarrubias KD, Chandrarathna S, Jin SW, Reddy N, Byakwaga H, et al. Differential Vpu-Mediated CD4 and Tetherin Downregulation Functions Among Major HIV-1 Group M Subtypes. *J Virol* (2020) 94:e00293–20. doi: 10.1128/JVI.00293-20
28. Mann JK, Byakwaga H, Kuang XT, Le AQ, Brumme CJ, Mwimanzi P, et al. Ability of HIV-1 Nef to Downregulate CD4 and HLA Class I Differs Among Viral Subtypes. *Retrovirology* (2013) 10:100. doi: 10.1186/1742-4690-10-100
29. Jin SW, Mwimanzi FM, Mann JK, Bwana MB, Lee GQ, Brumme CJ, et al. Variation in HIV-1 Nef Function Within and Among Viral Subtypes Reveals Genetically Separable Antagonism of SERINC3 and SERINC5. *PloS Pathog* (2020) 16:e1008813. doi: 10.1371/journal.ppat.1008813
30. Rahimi A, Anmole G, Soto-Nava M, Escamilla-Gomez T, Markle T, Jin SW, et al. *In Vitro* Functional Assessment of Natural HIV-1 Group M Vpu Sequences Using a Universal Priming Approach. *J Virol Methods* (2017) 240:32–41. doi: 10.1016/j.jviromet.2016.11.004
31. Gaschen B, Kuiken C, Korber B, Foley B. Retrieval and on-the-Fly Alignment of Sequence Fragments From the HIV Database. *Bioinformatics* (2001) 17:415–8. doi: 10.1093/bioinformatics/17.5.415
32. Larsson A. AliView: A Fast and Lightweight Alignment Viewer and Editor for Large Datasets. *Bioinformatics* (2014) 30:3276–8. doi: 10.1093/bioinformatics/btu531
33. Guindon S, Dufayard JF, Lefort V, Anisimova M, Hordijk W, Gascuel O. New Algorithms and Methods to Estimate Maximum-Likelihood Phylogenies: Assessing the Performance of PhyML 3.0. *Syst Biol* (2010) 59:307–21. doi: 10.1093/sysbio/syq010
34. Rambaut A. (2016). FigTree.
35. Siepel AC, Halpern AL, Macken C, Korber BT. A Computer Program Designed to Screen Rapidly for HIV Type 1 Intersubtype Recombinant Sequences. *AIDS Res Hum Retroviruses* (1995) 11:1413–6. doi: 10.1089/aid.1995.11.1413
36. Storey JD, Tibshirani R. Statistical Significance for Genomewide Studies. *Proc Natl Acad Sci U.S.A.* (2003) 100:9440–5. doi: 10.1073/pnas.1530509100
37. Allen S, Tice J, Van De Perre P, Serufilira A, Hudes E, Nsengumuremyi F, et al. Effect of Serotesting With Counselling on Condom Use and Seroconversion Among HIV Discordant Couples in Africa. *BMJ* (1992) 304:1605–9. doi: 10.1136/bmj.304.6842.1605
38. Strebel K. HIV Accessory Proteins Versus Host Restriction Factors. *Curr Opin Virol* (2013) 3:692–9. doi: 10.1016/j.coviro.2013.08.004
39. Haller C, Muller B, Fritz JV, Lamas-Murua M, Stolp B, Pujol FM, et al. HIV-1 Nef and Vpu are Functionally Redundant Broad-Spectrum Modulators of Cell Surface Receptors, Including Tetraspanins. *J Virol* (2014) 88:14241–57. doi: 10.1128/JVI.02333-14
40. Pickering S, Hue S, Kim EY, Reddy S, Wolinsky SM, Neil SJ. Preservation of Tetherin and CD4 Counter-Activities in Circulating Vpu Alleles Despite Extensive Sequence Variation Within HIV-1 Infected Individuals. *PloS Pathog* (2014) 10:e1003895. doi: 10.1371/journal.ppat.1003895
41. Kwon Y, Kaake RM, Echeverria I, Suarez M, Karimian Shamsabadi M, Stoneham C, et al. Structural Basis of CD4 Downregulation by HIV-1 Nef. *Nat Struct Mol Biol* (2020) 27:822–8. doi: 10.1038/s41594-020-0463-z
42. Tobiume M, Takahoko M, Yamada T, Tatsumi M, Iwamoto A, Matsuda M. Inefficient Enhancement of Viral Infectivity and CD4 Downregulation by Human Immunodeficiency Virus Type 1 Nef From Japanese Long-Term Nonprogressors. *J Virol* (2002) 76:5959–65. doi: 10.1128/JVI.76.12.5959-5965.2002
43. Toyoda M, Ogata Y, Mahiti M, Maeda Y, Kuang XT, Miura T, et al. Differential Ability of Primary HIV-1 Nef Isolates To Downregulate HIV-1 Entry Receptors. *J Virol* (2015) 89:9639–52. doi: 10.1128/JVI.01548-15
44. Omondi FH, Chandrarathna S, Mujib S, Brumme CJ, Jin SW, Sudderuddin H, et al. HIV Subtype and Nef-Mediated Immune Evasion Function Correlate With Viral Reservoir Size in Early-Treated Individuals. *J Virol* (2019) 93:e01832–18. doi: 10.1128/JVI.01832-18

Conflict of Interest: The authors declare that the research was conducted in the absence of any commercial or financial relationships that could be construed as a potential conflict of interest.

Publisher's Note: All claims expressed in this article are solely those of the authors and do not necessarily represent those of their affiliated organizations, or those of the publisher, the editors and the reviewers. Any product that may be evaluated in this article, or claim that may be made by its manufacturer, is not guaranteed or endorsed by the publisher.

frontiers | Frontiers in Virology

REVIEW
published: 29 June 2022
doi: 10.3389/fviro.2022.917941

Toward a Functional Cure for HIV-1 Infection: The Block and Lock Therapeutic Approach

*Benni Vargas and Nicolas Sluis-Cremer**

Division of Infectious Diseases, Department of Medicine, University of Pittsburgh School of Medicine, Pittsburgh, PA, United States

The persistence of latent, replication-competent HIV-1 proviruses in resting CD4+ T cells, and other cellular reservoirs, represents a major barrier to a cure. This reservoir is impervious to the immune system and to antiretroviral therapy, but has the potential to produce infectious rebound virus if antiretroviral therapy is interrupted. There are multiple ongoing efforts to identify and/or develop novel therapeutic strategies to eliminate or silence this latent reservoir of HIV-1 infection. One of these strategies is termed "block and lock". The "block" refers to a therapeutic agent's capacity to inhibit (or "block") transcription of HIV-1 proviruses, while the "lock" refers to its capacity to induce permanent silencing of the proviruses, typically *via* repressive epigenetic modifications. The "block and lock" approach elicits a functional, rather than sterilizing, cure for HIV-1 infection. This review article focuses on therapeutic approaches (i.e., small molecules, nucleic acids and recombinant proteins) that have been identified to block and, in some cases, lock HIV-1 in the latent state. We also touch on critical research that needs to be accomplished to advance this approach into humans.

Keywords: HIV-1, latency, functional cure, block and lock, epigenetic

OPEN ACCESS

Edited by:
Akio Adachi,
Kansai Medical University, Japan

Reviewed by:
Akifumi Takaori-Kondo,
Kyoto University, Japan
Hirofumi Akari,
Kyoto University, Japan
Zeger Debyser,
KU Leuven, Belgium

***Correspondence:**
Nicolas Sluis-Cremer
nps2@pitt.edu

Specialty section:
This article was submitted to Fundamental Virology, a section of the journal Frontiers in Virology

Received: *11 April 2022*
Accepted: *30 May 2022*
Published: *29 June 2022*

Citation:
Vargas B and Sluis-Cremer N (2022) Toward a Functional Cure for HIV-1 Infection: The Block and Lock Therapeutic Approach. Front. Virol. 2:917941. doi: 10.3389/fviro.2022.917941

INTRODUCTION

HIV-1 is a single-stranded positive-sense enveloped RNA retrovirus that causes acquired immunodeficiency syndrome (AIDS), a condition affecting ~ 36 million people worldwide. Antiretroviral therapy (ART) effectively restricts virus replication, and people living with HIV-1 infection on ART lead relatively healthy lives, as virus replication is suppressed to under the limit of detection of clinically used assays (currently, 20 HIV-1 RNA copies/ml of plasma). ART, however, is not curative and low-levels of persistent viremia can be detected by ultra-sensitive assays in the majority of infected individuals (1). Though the source of this viremia is likely to be variable and multi-faceted across each individual, in virologically suppressed individuals it is unclear if there is ongoing viral replication (2) and most replication-competent HIV-1 proviral DNA is found in resting $CD4^+$ T cells (3). Other cell types such as hematopoietic stem cells, macrophages, and

monocytes have been shown to possess proviral DNA, though they are not considered a major constituent of the reservoir (4–6). The reservoir of latent HIV-1 that resides in resting CD4+ T cells is thought to constitute the major hurdle to a HIV-1 cure (3) since it is unrecognized by the immune system, unaffected by ART, may produce infectious virus particles, and can contribute to either ongoing viremia during ART or HIV-1 viral rebound if treatment is paused.

Therapeutic approaches to eradicate the reservoir of latent HIV-1 infection in resting CD4+ T cells include (1): transplantation of hematopoietic stem cells engineered to lack the viral co-receptor CCR5 (2); gene editing to cleave the HIV-1 genome; and (3) a "shock and kill" approach that reverses latency thus rendering the infected cells vulnerable to immune clearance mechanisms, including therapeutic or immunomodulatory enhancement strategies (7–10). There are, however, limitations associated with each of these approaches, including scalability (particularly for hematopoietic stem cell treatment), the ability to deliver gene editing vehicles to all cells constituting the reservoir *in vivo*, and difficulties associated with the viral latency reversal in all, and not just a subset, of infected cells. As an alternative, the "block and lock" strategy involves long-term silencing of HIV-1 proviruses to prevent viral rebound following therapy cessation (11–13). The "block" refers to therapeutic agents, or latency promoting agents (LPAs), that inhibit (or "block") the transcription of latent HIV-1 proviruses. LPAs can specifically target viral proteins (i.e., Tat or integrase) and, in addition to their "blocking" phenotype, they may also elicit antiviral activity (i.e., inhibit ongoing HIV-1 replication). Alternatively, LPAs could target host proteins and elicit only a "blocking" phenotype. The "lock" refers to the agent's ability to induce permanent silencing of HIV-1 proviruses, typically *via* repressive epigenetic modifications. This approach elicits a functional, rather than sterilizing, cure. In this review, we discuss recent reports that encompass the block and lock strategy.

VIRAL AND CELLULAR FACTORS THAT REGULATE HIV-1 TRANSCRIPTION

The gene expression of HIV-1 is regulated by viral proteins and host factors. The HIV-1-encoded regulatory protein, trans-activator of transcription (Tat), vastly enhances viral transcription efficiency (14). Tat binds to the trans-activation response (TAR) RNA region that is situated at the 5′ end of HIV-1 transcripts and recruits the RNA polymerase II (Pol) II positive transcription elongation factor p-TEFb (15–17). p-TEFb is a cyclin dependent kinase that consists of cyclin-dependent kinase 9 (CDK9) and cyclin T1. In metabolically active cells, CDK9 and cyclin T1 are secluded in the 7SK ribonucleoprotein (RNP) RNA-protein complex. CDK9 and cyclin T1 are liberated from the 7SK RNP and bind to TAR RNA in complex with Tat and organize the assembly of a super elongation complex (SEC) along with several additional proteins. p-TEFb phosphorylates the 5,6-dichloro-1-β-D-ribofuranosylbenzimidazole sensitivity inducing factor (DSIF) and negative elongation factor (NELF), and importantly the carboxyl terminal domain of the large subunit of RNA Pol II which promotes the transition into the productive synthesis of mRNAs through transcriptional elongation. Of note, CDK9 and cyclin T1 function is decreased in resting $CD4^+$ T cells that harbor HIV-1 proviral DNA. As such therapeutic strategies that further negatively regulate Tat and/or p-TEFb activity would act as potent block and lock agents. HIV-1 transcription is mediated by the 5'-long terminal repeat (LTR) and is often restricted *in vivo*. Specifically, the binding sites in the LTR for several transcription factors includes nuclear factor kappa B (NF-κB), nuclear factor of activated T cell (NFAT), signal transducer and activator of transcription 5 (STAT5), activator protein 1 (AP-1) and Sp1. In resting CD4+ T cells, many of these viral transcription factors are sequestered, thereby fostering HIV-1 latency (18). Three precisely positioned nucleosomes within the 5′-LTR, namely Nuc-0, Nuc-1, and Nuc-2, also regulate HIV-1 transcription. In particular,the repressive Nuc-1 is positioned immediately downstream of the transcription start site (TSS) and represses viral transcription.

HIV-1 latency is established and regulated through a multitude of host and viral epigenetic and genetic mechanisms. Active viral transcription is mediated by Tat and the multiple activating co-factor complexes, whereas viral latency is promoted by epigenetic regulators that promote nucleosome occupancy at the 5' HIV-1 LTR promoter region. The class I histone deacetylases (HDACs), HDAC-1, -2 and -3, play a major role in the repressive heterochromatin environment that enforces HIV-1 latency (19–22). Following T cell activation, histone acetylation surrounding Nuc-1 increases significantly, concomitant with removal of the HDACs. Many other histone-modifying enzymes are recruited to the 5'-LTR by host cell transcription factors as well as Tat, of which may also be subject to post-translational modification by various factors. The mammalian SWI/SNF (SWItch/Sucrose Non-Fermentable) chromatin remodeling complex, the ATP-dependent BRG1/BRM associated factor (BAF), also contributes to HIV-1 transcriptional repression (23). In latent cells containing proviral DNA, BAF complexes promote nucleosome density immediately downstream of the HIV-1 TSS. The polybromo-associated BAF (PBAF) complex, which is closely related to BAF and possess several of the same subunits, substitutes BAF and induces removal of the repressive Nuc-1, leading to HIV-1 transcription activation and reversing latency. All of the viral proteins and host factors involved in the foundation and maintenance of HIV-1 latency represent viable targets for the development of block and lock cure strategies.

The preservation of cell identity as well as cellular lineage commitment relies on the combination of many factors including signaling pathways, transcription factors, and the genetic/epigenetic machinery. These regulatory factors have

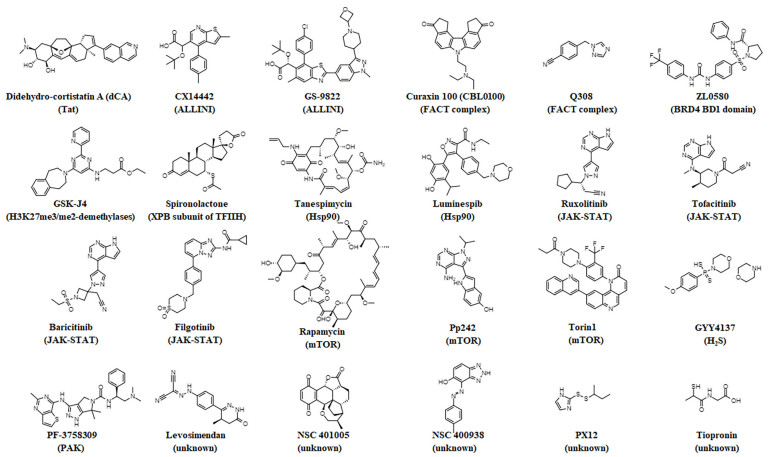

FIGURE 1 | Chemical structures of small molecules that elicit a block and lock phenotype. The molecule's target is noted in parentheses.

many intersections and they modulate the pattern of gene expression. Thus, it is not surprising that these cellular signaling pathways also play a critical role in the conservation of proviral latency and, as described below, several studies have reported that inhibition or activation of key proteins in these pathways can elicit a block and lock effect.

Below, we highlight several small molecules that have been reported to inhibit the reversal of HIV-1 latency and induce a block and lock phenotype. The structures of these small molecules are illustrated in **Figure 1**. **Figure 2** provides a graphical illustration of the molecular mechanisms involved in suppressing viral latency.

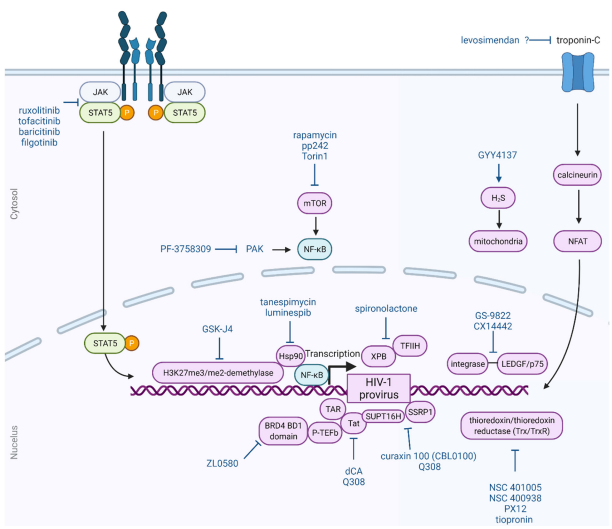

FIGURE 2 | Block and lock approach as a functional cure for HIV-1 infection. The block and lock approach involves long-term durable silencing of viral gene expression. Small molecule can elicit this phenotype by affecting multiple different host and viral proteins and pathways, as illustrated here. This Figure was created using BioRender.com.

SMALL MOLECULES THAT TARGET HIV-1 PROTEINS

Didehydro-Cortistatin A (dCA)

dCA is a synthetic analog derived from cortistatin A, which is naturally produced steroidal alkaloid from *Corticium simplex*. dCA has been shown to bind to the basic domain of Tat and is a potent inhibitor of viral transcription (24). dCA blocks HIV-1 reactivation from latency in primary CD4+ T cells from HIV-1 patients and in several other cellular models of latency (25). Importantly, dCA mediated inhibition of Tat promotes a repressive heterochromatin environment at the HIV-1 promoter, marked by decreased histone H3 lysine 27 (H3K27) acetylation levels at Nuc-1 and limited PBAF recruitment (26). In an *in vivo* murine model of HIV-1 infection, dCA reduced the viral mRNA burden in mouse tissues, and both reduced and delayed HIV-1 rebound following the cessation of ART (27). HIV-1 resistance to dCA is associated with mutations in the LTR that augment the basal levels of HIV-1 transcription by 10- to 30-fold, and with mutations in the viral accessory proteins Nef and Vpr that increase NF-κB nuclear translocation, which promotes transcription from the HIV-1 promoter (28). Collectively, these studies demonstrate a proof-of-concept that latency promoting agents can be used to suppress ongoing transcriptional events under ART, and can significantly delay and/or reduce viral rebound levels in upon treatment interruption.

Allosteric Integrase Inhibitors (ALLINIs)

HIV-1 preferentially integrates into actively transcribed gene-dense regions. This selectivity is driven by direct interaction between HIV-1 integrase and the lens epithelium–derived growth factor (LEDGF/p75), a host protein that acts as a transcriptional coactivator, binding various proteins to active transcription units through recognition of the trimethylated histone H3 at lysine 36 (H3K36me3) (29). ALLINIs, also referred to as LEDGINs, non-catalytic-site integrase inhibitors (NCINI) or multimeric integrase inhibitors (MINI), bind to

HIV-1 integrase at the integrase- LEDGF/p75 interaction site, perturb the viral-host protein interaction, and inhibit HIV-1 integration (30, 31). As expected by an HIV-1 integrase inhibitor, the ALLINI CX14442 was found to reduce the number of integrated proviruses. However, CX14442 also retargeted the site of residual HIV-1 integration away from active chromatin (32). Specifically, proviruses were integrating into less-gene-dense regions with a more repressive epigenetic environment, and were shifted away from H3K36me3, which lowered HIV-1 transcription. Similar results were noted with GS-9822, also an ALLINI, in that residual provirus was both more latent and refractory to reactivation, and were integrated away from genes and gene-dense chromatin, resulting in a more repressive heterochromatin environment (33). Collectively, these studies suggest that if HIV-1-infected individuals are treated early with ART regimens that include an ALLINI, the replication-competent viral reservoir in resting CD4+ T cells will be transcriptionally impaired, thus mimicking a "locked" phenotype.

SMALL MOLECULES THAT TARGET EPIGENETIC PROTEINS

Inhibitors of the Facilitates Chromatin Transcription (FACT) Complex

The FACT proteins suppressor of Ty 16 homolog (SUPT16H) and structure specific recognition protein 1 (SSRP1) represses HIV-1 transcription and induce viral latency (34). Depletion of SUPT16H or SSRP1 protein in cell line models of HIV-1 latency, increases transcriptional initiation and transcriptional elongation and is able to reverse latent HIV-1. Similar observations were reported with a primary CD4+ T cell model of HIV-1 latency. Curaxin 100 (CBL0100) is a small molecule that targets the FACT complex and was found to inhibit both HIV-1 reactivation and replication in *in vitro* and *ex vivo* models of virus latency (35). From a mechanistic perspective, CBL0100 targeted HIV-1 transcriptional elongation and decreased the occupancy of FACT and Pol II at the HIV-1 LTR promoter region. Recently, another small molecule, Q308, was also found to inhibit HIV-1 gene transcription mediated by Tat and selectively decreases FACT expression levels (36).

Inhibitors of Bromodomain Containing 4 (BRD4)

A family of proteins called the bromodomain and extraterminal (BET) proteins are host epigenetic factors marked by 2 N-terminal bromodomains that recognize acetylated histones in chromatin. BRD4, a member of this family, plays a crucial role in HIV-1 transcriptional regulation (37). Specifically, BRD4 competes with Tat for host p-TEFb/CDK9 which results in HIV-1 transcription elongation. The pan-BET inhibitor JQ1, which non-selectively targets both N-terminal bromodomains of all BET proteins, disables the interaction between BRD4 and Tat and reactivates latent HIV-1 infection (38–40). Niu et al. identified ZL0580, a small molecule, that selectively binds to BD1 domain of BRD4. ZL0580 enforced HIV-1 latency in both *in vitro* and *ex vivo* cell models of latency by preventing the transactivation of Tat as well as transcription elongation and also induced repressive heterochromatin structure at the HIV-1 LTR promoter (41). Combinatorial treatment of CD4+ T cells derived from aviremic HIV-infected individuals with both ZL0580 and ART demonstrated that ZL0580 promoted suppression of HIV-1and led to a delay in viral rebound after interruption of ART.

Inhibitors of the Lysine Demethylases 6A and 6B

H3K27 tri-methylation (H3K27me3) and DNA methylation are correlated with suppression of viral reactivation at the HIV-1 LTR, whereas H3K4 tri-methylation (H3K4me3) is associated with HIV-1 expression (42). Ethyl 3-((6-(4,5-dihydro-1H-benzo [d]azepin-3(2H)-yl)-2-(pyridin-2-yl)pyrimidin-4-yl)amino) propanoate (GSK-J4) is a strong inhibitor of UTX/KDM6A and JMJD3/KDM6B—both of which are the H3K27me3/me2-demethylases. In HIV-1 latently infected cells from patients, GSK-J4 was able to inhibit latent HIV-1 reactivation and promoted methylation of DNAat certain the 5'-LTR region of latent HIV-1 by facilitating engagement of DNA methyltransferase 3 alpha to HIV-1 LTR (43). However, silencing of HIV-1 through epigenetic mechanisms required continuous addition of GSK-J4 and the effect was lost quickly after drug removal. DNA methylation additionally was shortly lost after drug removal, which suggests active and fast demethylation of the DNA in the HIV-1 promoter region. As such, inhibitors of lysine methylases could be used in therapeutic approaches to induce the "block" but not "lock" phenotype.

Proteasomal Degradation of the Xeroderma Pigmentosum Type B (XPB) Subunit of the Transcription Factor IIH (TFIIH)

The transcription factor TFIIH enhances transcription initiation by inducing the DNA strands to open up near the transcription start site and phosphorylating and activating the carboxyl terminal domain of RNA Pol II. The aldosterone, spironolactone, mediates the proteasomal degradation of the XPB subunit of TFIIH as well as represses acute HIV-1 infection *in vitro* (44). While spironolactone readily inhibits HIV-1 transcription by decreasing Pol II recruitment to the HIV-1 genome, perpetual pretreatment with the drug was not able to maintain sustained epigenetic suppression of HIV-1 upon interruption of the drug, since the virus is reactivated when XPB reemerges. However, spironolactone by itself without ART was found to maintain transcriptional silencing of HIV-1.

Inhibitors of Heat Shock Protein 90 (Hsp90)

Heat shock induces overexpression of Hsp90 and leads to the activation of inducible cellular transcription factors. Specifically, heat shock facilitates HIV-1 transcription through activation of Hsp90 activity, which induces HIV-1-specific essential host cell

transcription factors (NF-κB, NFAT, and STAT5), while inhibition of Hsp90 significantly reduces their gene expression (45). Of note, the Hsp90 inhibitors tanespimycin (17-(allylamino)-17-demethoxygeldanamycin) and luminespib (5-[2,4-dihydroxy-5-(propan-2-yl)phenyl]-*N*-ethyl-4-{4-[(morpholin-4-yl)methyl]phenyl}-1,2-oxazole-3-carboxamide) were found to prevent HIV-1 expression for up to 11 weeks in HIV-1-infected humanized NOD scid IL-2Rγ$^{-/-}$ bone marrow-liver-thymus mice after treatment interruption (46). These data suggest that supplementing ART with Hsp90 inhibitors could possibly prevent rebound viremia from persistent HIV reservoirs.

SMALL MOLECULES THAT TARGET CELL SIGNALING PATHWAYS

Janus Kinase 2 (Jak)-STAT Inhibitors

The replication-competent latent HIV-1 reservoir resides within memory CD4+ T cells — central, transitional, and effector — all of which must be exposed to the γ-C receptor cytokines (IL-2, IL-7 and IL-15) for their long-term persistence (47). STAT-5 phosphorylation (pSTAT5) is induced following the exposure of the respective γ-C receptor cytokines cytokines with their respective receptors which facilitates anti-apoptotic signaling and increased T cell division. Given that there are several binding sites for pSTAT5 within the HIV-1 LTR, IL-2, IL-7 and IL-15 have been shown to enhance viral expression from infected cells. Ruxolitinib and tofacitinib are two FDA-approved Jak inhibitors that were both shown to block reactivation of latent proviruses in a primary CD4+ T cell model of HIV-1 latency (48). pSTAT5 has also been shown to strongly correlate with high levels of integrated viral DNA, and Jak inhibitors can decrease the amount of CD4+ T cells harboring integrated viral DNA (49). Other Jak inhibitors, including baricitinib and filgotinib, also inhibit virus production from latently infected cells, STAT5 phosphorylation and homeostatic proliferation (50, 51). Recently, an AIDS Clinical Trial Group multi-site Phase 2a study (A5336) has evaluated ruxolitinib, which has shown remarkable efficacy and safety in virally suppressed patients living with HIV-1, including a notable reduction in key markers associated with viral persistence (52). Collectively, these studies suggest that Jak inhibitors are a therapeutic strategy to block key events of T cell activation that modulate HIV-1 persistence.

Mammalian Target of Rapamycin (mTOR) Inhibitors

A genome-wide short hairpin (sh) RNA screen identified that the mTOR complex regulates HIV-1 latency (53). Knockdown of the mTOR complex or small molecule inhibition of mTOR activity suppressed latency reversal in several HIV-1 latency models and in patient cells from HIV-infected individuals. This inhibition was due in part to diminished phosphorylation of CDK9. While this study suggests that inhibition of mTOR may have therapeutic potential, other studies have reported that inhibition of mTOR had minimal effects on HIV-1 latency reversal (54, 55).

Activation of Kelch-Like ECH-Associated Protein 1 (Keap1) - Nuclear Factor Erythroid-2-Related Factor 2 (Nrf2) Pathway by Hydrogen Sulfide (H_2S)

Reactivation of latent HIV-1 is associated with decreased expression of the H_2S producing enzyme cystathionine-γ-lyase and downregulation of endogenous H_2S (56). Chemical complementation of cystathionine-γ-lyase activity with a slow-releasing H_2S donor, morpholin-4-ium 4-methoxyphenyl (morpholino) phosphinodithioate (GYY4137), was found to suppress HIV-1 gene expression by promoting the Keap1-Nrf2 pathway, blocking NF-κB, and engaging the epigenetic silencer, Yin Yang 1 (YY1), to the HIV-1 promoter (56). Combinatorial treatment of GYY4137 and ART prevented viral rebound in latently infected CD4+ T cells from ART-suppressed patients and demonstrated no adverse effect on proviral content or CD4+ T cell subsets, showing that the reduction in viral rebound is due to inhibition of transcription and not due to a reduction of a select group of infected cells.

Inhibitors of P21 (RAC1) Activated Kinases (PAKs)

Our laboratory utilized the 24ST1NLESG cell line model of HIV-1 latency to high-throughput screen a structurally diverse library cell permeable, medically active kinase inhibitors, which targets a comprehensive array of signaling pathways, to identify small molecule inhibitors of HIV-1 latency reversal (55). The screen was carried with or without co-treatment of three latency-reversing agents—prostratin, JQ-1, and panobinostat— each of which having distinct mechanisms of action. We found 12 kinase inhibitors that inhibited HIV-1 latency reversal regardless of the latency reversal agent used in the screen. Of these, PF-3758309, a pan-PAK inhibitor, was identified to be the most potent. The 50% inhibitory concentrations (IC_{50}) in the 24ST1NLESG cells ranged from 0.1 to 1 nM (selectivity indices, >3,300), and for PF-3758309 was also shown to inhibit HIV-1 reversal from latency in CD4+ T cells isolated from HIV-1-infected donors. More recently, we have shown that PAK1 and PAK2 are abundantly expressed in resting CD4+ T cells, and that knockdown of PAK1 and PAK2 in 24ST1NLESG cells inhibits HIV-1 reactivation, mostly likely by decreasing NF-κB expression (unpublished data).

SMALL MOLECULES WITHOUT DEFINED MECHANISMS OF ACTION FOUND IN HIGH THROUGHPUT SCREENS

Levosimendan, an FDA-approved drug to currently treat heart failure, was found as an inhibitor of HIV-1 latency reversal *via* screening of a compound library containing FDA-approved molecules (57). Levosimendan was found to exhibit potent inhibition of HIV-1 latency reversal in several cell lines of latency by affecting the HIV-1 LTR-Tat transcriptional axis,

and in primary CD4+ T cells also inhibited both HIV-1 latency reversal and acute replication.

Lu et al. used time-lapse fluorescence microscopy to measure HIV-1 gene-expression dynamics and identify latency promoting agents that would be otherwise disregarded when screening solely for mean gene expression (58). Following a screen of 1,806 compounds they identified NSC 401005, NSC 400938, PX12, and tiopronin, all of which are functionally and structurally similar to inhibitors of thioredoxin reductase, an enzyme whose function is to maintain redox balance in host cells. These molecules reduced reversal of HIV-1 latency in both Jurkat and primary cell models.

BLOCK AND LOCK APPROACHES USING NUCLEIC ACIDS

Short Hairpin (sh)/Small Interfering (si) RNA

The siRNA molecule siPromA targets the multiple NF-κB sites in the HIV-1 LTR promoter to elicit silencing of viral transcription through repressive epigenetic marks (59). si143, which also targets the HIV-1 5'-LTR, similarly induces transcriptional gene silencing (59). Further studies showed that cells expressing PromA, 143, or both, demonstrated significant resistance to viral reactivation that was correlated with significant changes in the levels of H3K27me3, Argonaute RISC Component 1 (AGO1) and HDAC1 in the LTR, which are associated with reduced HIV-1 reactivation (60). LTR362 is an RNA sequence that also targets the multiple NF-κB binding sites in the HIV-1 LTR and has overlap with the siPromA sequence (61). In a humanized mouse model of HIV-1 infection, LTR362 in combination with a HIV-1 glycoprotein 120 (gp120) aptamer and two RNAs targeting the viral mRNAs of Tat and rev inhibited viral reactivation and raised CD4+ T cell counts relative to controls. However, LTR362 did not appear to facilitate epigenetic silencing of the 5′-LTR, with inhibition against HIV-1 infection being related to the post-transcriptional regulation of rev and Tat.

Long Non-Coding (lnc) RNA

Saayman et al., identified a lncRNA that induced HIV-1 gene silencing *in vitro* through the recruitment of a chromatin-remodeling complex, involving DNA methyltransferase 3 alpha (DNMT3a), enhancer of zeste homolog 2 (EZH2), and HDAC1 to the HIV-1 LTR promoter (62). Li et al., identified a lncRNA termed NRON that suppressed virus transcription by promoting Tat degradation (63).

Repurposed *Clustered Regularly Interspaced Short Palindromic Repeats* (CRISPR)/CRISPR Associated Protein 9 (Cas9)

Olson et al., sought to silence HIV-1 proviruses by constructing a nuclease-deficient disabled Cas9 (dCas9) linked to the transcriptional repressor domain derived from Kruppel-associated box (KRAB) (64). They found that dCas9-KRAB along with unique guide RNAs (gRNAs) inhibit HIV-1 transcription and expression of latent HIV-1 proviruses, and that this suppression is associated with chromatin changes, including reduced H3 histone acetylation and increased histone H3 lysine 9 trimethylation, epigenetic marks that are correlated with suppression of transcription. Collectively, these studies suggest that genomic approaches could form part of a "toolkit" for block-and-lock strategies.

7SK Oligonucleotide Mimetics

Yamayoshi et al., developed oligonucleotides that mimic the function of 7SK and showed them to be potent inhibitors of HIV-1 LTR specific transcription (65). Interestingly, the inhibitory effects were shown to be increased by co-transfection with plasmids expressing Tat. Taken together, these data suggest that 7SK mimics may have a potential to be a therapeutic strategy for HIV-1 block and lock strategies.

BLOCK AND LOCK APPROACHES USING RECOMBINANT PROTEINS

NullBasic

NullBasic is a 101 amino acid transdominant Tat mutant with an modified basic domain in amino acid positions 49-57, that includes the TAR-binding region, which inhibits viral gene expression *via* competition with HIV-1 Tat, but also through blocking Rev-mediated transport of HIV-1 mRNA (66). Retroviral vectors that expressed NullBasic were transduced into CD4+ T cells and demonstrated inhibition of HIV-1 transcription and replication *via* reduced Pol II occupancy at the LTR region and diminished H3K9 acetylation (67). NullBasic retroviral transduction of primary human CD4+ T cells as well as transplantation in a NOD scid gamma mouse model showed viral RNA was undetectable in plasma samples for up to two weeks post-infection and markedly decreased HIV-1 RNA levels in CD4+ T cells derived from tissue (68).

Hexamethylene-bis-Acetamide-Inducible Transcript 1 (HEXIM1)-Tat Chimera

As described above (2. Viral and cellular factors that regulate HIV-1 transcription), Tat binds to the TAR RNA element and facilitates recruitment of the Pol II positive transcription elongation factor p-TEFb. In cells, p-TEFb is held by 7SK snRNP, and Tat can remove p-TEFb from the 7SK snRNP, where it is sequestered and rendered inactive by HEXIM1. Leoz et al., reported that a fusion protein that combined the Tat and HEXIM1 functional domains, strongly reduced HIV-1 gene expression, by competing with the interaction between Tat, TAR and P-TEFb (69). In lymphocyte T cell line models of HIV latency, the fusion protein reduced the spread of infection as well as HIV-1, with minor impacts on cellular metabolism and transcription. This study is a proof-of-concept of innovative approaches to disrupt HIV transcription by competing for RNA-protein interactions by utilizing peptide.

OTHER APPROACHES TO INHIBIT HIV-1 LATENCY REVERSAL

Vanadium Pentoxide (V_2O_5) Nanosheets

V_2O_5 nanosheets are similar to natural glutathione peroxidase activity in that they reduce reactive oxygen species correlated with HIV-1 infection (70). V_2O_5 nanosheets catalyze reactive oxygen species neutralization in HIV-1-infected cells and inhibit HIV-1 reactivation and replication, through modulation of the expression of pathways regulating redox balance, HIV-1 transactivation (*e.g.*, NF-κB), inflammation, and apoptosis. V_2O_5 nanosheets also block HIV-1 reactivation upon treatment with prostratin of latently infected CD4+ T cells from HIV-infected individuals on ART. V_2O_5 could be used with other agents to enforce HIV-1 latency and elicit the "block and lock" phenotype.

CONCLUSIONS

As described above, numerous diverse approaches have been identified to elicit a "block and lock" phenotype to inhibit reactivation of latent HIV-1 infection in CD4+ T cells. These approaches include small molecules, nucleic acids, and recombinant proteins. Currently, it is unknown whether any single approach will deliver sufficiently long-term silencing of latent proviruses to facilitate a functional HIV-1 cure. As such combination studies using two or more approaches should be rigorously explored *in vitro* and in appropriate animal models. While some of the therapeutic agents discussed in this application have been tested in humanized mice models of HIV-1 infection, none have progressed to clinical trials, with the exception of the Jak inhibitor ruxolitinib. However, it is not known whether ruxolitinib treatment resulted in block and lock phenotype in the clinical trial, as this measurement was not included as an end point in the study. A key issue for many of the therapeutic agents described in this review relates to target specificity as well as their impact on normal cell function. For example, small molecules that target epigenetic proteins or cell signaling pathways will fundamentally alter the functioning of other cellular processes which, in the long-term, may promote toxicity or adverse events in humans. In this regard, molecules that specifically target viral proteins (e.g. dCA or ALLINIs) may have a therapeutic advantage. To this end, to effectively develop a "block and lock" functional cure strategy the field requires the following advancements; (i) the discovery and development of potent molecules with appropriate safety and pharmacokinetic/pharmacodynamic properties such that they can be used clinically; (ii) the development of delivery systems for these molecules that specifically target latent reservoir cells; and (iii) appropriate clinical trials to assess efficacy and safety in HIV-1-infected individuals.

AUTHOR CONTRIBUTIONS

BV and NS-C co-wrote the review article. All authors contributed to the article and approved the submitted version.

FUNDING

This work was supported by a grant (R21AI57392-01) from the National Institutes of Health in the USA to NS-C.

REFERENCES

1. Jacobs JL, Halvas EK, Tosiano MA, Mellors JW. Persistent HIV-1 Viremia on Antiretroviral Therapy: Measurement and Mechanisms. *Front Microbiol* (2019) 10:2383. doi: 10.3389/fmicb.2019.02383
2. Bale MJ, Kearney MF. Review: HIV-1 Phylogeny During Suppressive Antiretroviral Therapy. *Curr Opin HIV AIDS* (2019) 14(3):188–93. doi: 10.1097/COH.0000000000000535
3. Siliciano JD, Siliciano RF. *In Vivo* Dynamics of the Latent Reservoir for HIV-1: New Insights and Implications for Cure. *Annu Rev Pathol* (2022) 17:271–94. doi: 10.1146/annurev-pathol-050520-112001
4. Kruize Z, Kootstra NA. The Role of Macrophages in HIV-1 Persistence and Pathogenesis. *Front Microbiol* (2019) 10:2828. doi: 10.3389/fmicb.2019.02828
5. Mitchell BI, Laws EI, Ndhlovu LC. Impact of Myeloid Reservoirs in HIV Cure Trials. *Curr HIV/AIDS Rep* (2019) 16(2):129–40. doi: 10.1007/s11904-019-00438-5
6. Sebastian NT, Collins KL. Targeting HIV Latency: Resting Memory T Cells, Hematopoietic Progenitor Cells and Future Directions. *Expert Rev Anti Infect Ther* (2014) 12(10):1187–201. doi: 10.1586/14787210.2014.956094
7. Lee PH, Keller MD, Hanley PJ, Bollard CM. Virus-Specific T Cell Therapies for HIV: Lessons Learned From Hematopoietic Stem Cell Transplantation. *Front Cell Infect Microbiol* (2020) 10:298. doi: 10.3389/fcimb.2020.00298
8. Khanal S, Schank M, El Gazzar M, Moorman JP, Yao ZQ. HIV-1 Latency and Viral Reservoirs: Existing Reversal Approaches and Potential Technologies, Targets, and Pathways Involved in HIV Latency Studies. *Cells.* (2021) 10 (2):475. doi: 10.3390/cells10020475
9. Karuppusamy KV, Babu P, Thangavel S. The Strategies and Challenges of CCR5 Gene Editing in Hematopoietic Stem and Progenitor Cells for the Treatment of HIV. *Stem Cell Rev Rep* (2021) 17(5):1607–18. doi: 10.1007/s12015-021-10145-7
10. Xun J, Zhang X, Guo S, Lu H, Chen J. Editing Out HIV: Application of Gene Editing Technology to Achieve Functional Cure. *Retrovirol.* (2021) 18(1):39. doi: 10.1186/s12977-021-00581-1
11. Vansant G, Bruggemans A, Janssens J, Debyser Z. Block-And-Lock Strategies to Cure HIV Infection. *Viruses.* (2020) 12(1):84. doi: 10.3390/v12010084
12. Ahlenstiel CL, Symonds G, Kent SJ, Kelleher AD. Block and Lock HIV Cure Strategies to Control the Latent Reservoir. *Front Cell Infect Microbiol* (2020) 10:424. doi: 10.3389/fcimb.2020.00424
13. Moranguinho I, Valente ST. Block-And-Lock: New Horizons for a Cure for HIV-1. *Viruses.* (2020) 12(12):1443. doi: 10.3390/v12121443
14. Rice AP. The HIV-1 Tat Protein: Mechanism of Action and Target for HIV-1 Cure Strategies. *Curr Pharm Des* (2017) 23(28):4098–102. doi: 10.2174/1381612823666170704130635
15. Asamitsu K, Okamoto T. The Tat/P-TEFb Protein-Protein Interaction Determining Transcriptional Activation of HIV. *Curr Pharm Des* (2017) 23 (28):4091–7. doi: 10.2174/1381612823666170710164148
16. Karn J. Tackling Tat. *J Mol Biol* (1999) 293(2):235–54. doi: 10.1006/jmbi.1999.3060

17. Spector C, Mele AR, Wigdahl B, Nonnemacher MR. Genetic Variation and Function of the HIV-1 Tat Protein. *Med Microbiol Immunol* (2019) 208 (2):131–69. doi: 10.1007/s00430-019-00583-z
18. Mbonye U, Karn J. The Molecular Basis for Human Immunodeficiency Virus Latency. *Annu Rev Virol* (2017) 4(1):261–85. doi: 10.1146/annurev-virology-101416-041646
19. Zaikos TD, Painter MM, Sebastian Kettinger NT, Terry VH, Collins KL. Class 1-Selective Histone Deacetylase (HDAC) Inhibitors Enhance HIV Latency Reversal While Preserving the Activity of HDAC Isoforms Necessary for Maximal HIV Gene Expression. *J Virol* (2018) 92(6):e02110–17. doi: 10.1128/JVI.02110-17
20. Barton KM, Archin NM, Keedy KS, Espeseth AS, Zhang YL, Gale J, et al. Selective HDAC Inhibition for the Disruption of Latent HIV-1 Infection. *PloS One* (2014) 9(8):e102684. doi: 10.1371/journal.pone.0102684
21. Keedy KS, Archin NM, Gates AT, Espeseth A, Hazuda DJ, Margolis DM. A Limited Group of Class I Histone Deacetylases Acts to Repress Human Immunodeficiency Virus Type 1 Expression. *J Virol* (2009) 3(10):4749–56. doi: 10.1128/JVI.02585-08
22. Huber K, Doyon G, Plaks J, Fyne E, Mellors JW, Sluis-Cremer N. Inhibitors of Histone Deacetylases: Correlation Between Isoform Specificity and Reactivation of HIV Type 1 (HIV-1) From Latently Infected Cells. *J Biol Chem* (2011) 286(25):22211–8. doi: 10.1074/jbc.M110.180224
23. Mahmoudi T. The BAF Complex and HIV Latency. *Transcription.* (2012) 3 (4):171–6. doi: 10.4161/trns.20541
24. Mousseau G, Clementz MA, Bakeman WN, Nagarsheth N, Cameron M, Shi J, et al. An Analog of the Natural Steroidal Alkaloid Cortistatin A Potently Suppresses Tat-Dependent HIV Transcription. *Cell Host Microbe* (2012) 12 (1):97–108. doi: 10.1016/j.chom.2012.05.016
25. Mousseau G, Kessing CF, Fromentin R, Trautmann L, Chomont N, Valente ST. The Tat Inhibitor Didehydro-Cortistatin A Prevents HIV-1 Reactivation From Latency. *mBio.* (2015) 6(4):e00465. doi: 10.1128/mBio.00465-15
26. Li C, Mousseau G, Valente ST. Tat Inhibition by Didehydro-Cortistatin A Promotes Heterochromatin Formation at the HIV-1 Long Terminal Repeat. *Epigenet Chromatin* (2019) 12(1):23. doi: 10.1186/s13072-019-0267-8
27. Kessing CF, Nixon CC, Li C, Tsai P, Takata H, Mousseau G, et al. In Vivo Suppression of HIV Rebound by Didehydro-Cortistatin A, a "Block-And-Lock" Strategy for HIV-1 Treatment. *Cell Rep* (2017) 21(3):600–11. doi: 10.1016/j.celrep.2017.09.080
28. Mousseau G, Aneja R, Clementz MA, Mediouni S, Lima NS, Haregot A, et al. Resistance to the Tat Inhibitor Didehydro-Cortistatin A Is Mediated by Heightened Basal HIV-1 Transcription. *mBio.* (2019) 10(4):e01750–18. doi: 10.1128/mBio.01750-18
29. Lesbats P, Engelman AN, Cherepanov P. Retroviral DNA Integration. *Chem Rev* (2016) 116(20):12730–57. doi: 10.1021/acs.chemrev.6b00125
30. Christ F, Voet A, Marchand A, Nicolet S, Desimmie BA, Marchand D, et al. Rational Design of Small-Molecule Inhibitors of the LEDGF/p75-Integrase Interaction and HIV Replication. *Nat Chem Biol* (2010) 6(6):442–8. doi: 10.1038/nchembio.370
31. Engelman A, Kessl JJ, Kvaratskhelia M. Allosteric Inhibition of HIV-1 Integrase Activity. *Curr Opin Chem Biol* (2013) 17(3):339–45. doi: 10.1016/j.cbpa.2013.04.010
32. Vranckx LS, Demeulemeester J, Saleh S, Boll A, Vansant G, Schrijvers R, et al. LEDGIN-Mediated Inhibition of Integrase-LEDGF/p75 Interaction Reduces Reactivation of Residual Latent HIV. *EBioMed.* (2016) 8:248–64. doi: 10.1016/j.ebiom.2016.04.039
33. Bruggemans A, Vansant G, Balakrishnan M, Mitchell ML, Cai R, Christ F, et al. GS-9822, a Preclinical LEDGIN Candidate, Displays a Block-and-Lock Phenotype in Cell Culture. *Antimicrob Agents Chemother* (2021) 65(5): e02328–20. doi: 10.1128/AAC.02328-20
34. Huang H, Santoso N, Power D, Simpson S, Dieringer M, Miao H, et al. FACT Proteins, SUPT16H and SSRP1, Are Transcriptional Suppressors of HIV-1 and HTLV-1 That Facilitate Viral Latency. *J Biol Chem* (2015) 290(45):27297–310. doi: 10.1074/jbc.M115.652339
35. Jean MJ, Hayashi T, Huang H, Brennan J, Simpson S, Purmal A, et al. Curaxin CBL0100 Blocks HIV-1 Replication and Reactivation Through Inhibition of Viral Transcriptional Elongation. *Front Microbiol* (2017) 8:2007. doi: 10.3389/fmicb.2017.02007
36. Zhou CL, Huang YF, Li YB, Liang TZ, Zheng TY, Chen P, et al. A New Small-Molecule Compound, Q308, Silences Latent HIV-1 Provirus by Suppressing Tat- and FACT-Mediated Transcription. *Antimicrob Agents Chemother* (2021) 65(12):e0047021. doi: 10.1128/AAC.00470-21
37. Alamer E, Zhong C, Hajnik R, Soong L, Hu H. Modulation of BRD4 in HIV Epigenetic Regulation: Implications for Finding an HIV Cure. *Retrovirol.* (2021) 18(1):3. doi: 10.1186/s12977-020-00547-9
38. Li Z, Guo J, Wu Y, Zhou Q. The BET Bromodomain Inhibitor JQ1 Activates HIV Latency Through Antagonizing Brd4 Inhibition of Tat-Transactivation. *Nucleic Acids Res* (2013) 41(1):277–87. doi: 10.1093/nar/gks976
39. Zhu J, Gaiha GD, John SP, Pertel T, Chin CR, Gao G, et al. Reactivation of Latent HIV-1 by Inhibition of BRD4. *Cell Rep* (2012) 2(4):807–16. doi: 10.1016/j.celrep.2012.09.008
40. Banerjee C, Archin N, Michaels D, Belkina AC, Denis GV, Bradner J, et al. BET Bromodomain Inhibition as a Novel Strategy for Reactivation of HIV-1. *J Leukoc Biol* (2012) 92(6):1147–54. doi: 10.1189/jlb.0312165
41. Niu Q, Liu Z, Alamer E, Fan X, Chen H, Endsley J, et al. Structure-Guided Drug Design Identifies a BRD4-Selective Small Molecule That Suppresses HIV. *J Clin Invest* (2019) 129(8):3361–73. doi: 10.1172/JCI120633
42. Boehm D, Ott M. Host Methyltransferases and Demethylases: Potential New Epigenetic Targets for HIV Cure Strategies and Beyond. *AIDS Res Hum Retroviruses* (2017) 33(S1):S8–S22. doi: 10.1089/aid.2017.0180
43. Nguyen K, Dobrowolski C, Shukla M, Cho WK, Luttge B, Karn J. Inhibition of the H3K27 Demethylase UTX Enhances the Epigenetic Silencing of HIV Proviruses and Induces HIV-1 DNA Hypermethylation But Fails to Permanently Block HIV Reactivation. *PloS Pathog* (2021) 17(10):e1010014. doi: 10.1371/journal.ppat.1010014
44. Mori L, Jenike K, Yeh YJ, Lacombe B, Li C, Getzler A, et al. The XPB Subunit of the TFIIH Complex Plays a Critical Role in HIV-1 Transcription and XPB Inhibition by Spironolactone Prevents HIV-1 Reactivation From Latency. *J Virol* (2020) 95(4):e01247–20. doi: 10.1128/JVI.01247-20
45. Anderson I, Low JS, Weston S, Weinberger M, Zhyvoloup A, Labokha AA, et al. Heat Shock Protein 90 Controls HIV-1 Reactivation From Latency. *Proc Natl Acad Sci USA* (2014) 111(15):E1528–37. doi: 10.1073/pnas.1320178111
46. Joshi P, Maidji E, Stoddart CA. Inhibition of Heat Shock Protein 90 Prevents HIV Rebound. *J Biol Chem* (2016) 291(19):10332–46. doi: 10.1074/jbc.M116.717538
47. Chomont N, El-Far M, Ancuta P, Trautmann L, Procopio FA, Yassine-Diab B, et al. HIV Reservoir Size and Persistence are Driven by T Cell Survival and Homeostatic Proliferation. *Nat Med* (2009) 15(8):893–900. doi: 10.1038/nm.1972
48. Gavegnano C, Detorio M, Montero C, Bosque A, Planelles V, Schinazi RF. Ruxolitinib and Tofacitinib Are Potent and Selective Inhibitors of HIV-1 Replication and Virus Reactivation *In Vitro*. *Antimicrob Agents Chemother* (2014) 58(4):1977–86. doi: 10.1128/AAC.02496-13
49. Gavegnano C, Brehm JH, Dupuy FP, Talla A, Ribeiro SP, Kulpa DA, et al. Novel Mechanisms to Inhibit HIV Reservoir Seeding Using Jak Inhibitors. *PloS Pathog* (2017) 13(12):e1006740. doi: 10.1371/journal.ppat.1006740
50. de Armas LR, Gavegnano C, Pallikkuth S, Rinaldi S, Pan L, Battivelli E, et al. The Effect of JAK1/2 Inhibitors on HIV Reservoir Using Primary Lymphoid Cell Model of HIV Latency. *Front Immunol* (2021) 12:720697. doi: 10.3389/fimmu.2021.720697
51. Yeh YJ, Jenike KM, Calvi RM, Chiarella J, Hoh R, Deeks SG, et al. Filgotinib Suppresses HIV-1-Driven Gene Transcription by Inhibiting HIV-1 Splicing and T Cell Activation. *J Clin Invest* (2020) 130(9):4969–84. doi: 10.1172/JCI137371
52. Marconi VC, Moser C, Gavegnano C, Deeks SG, Lederman MM, Overton ET, et al. Randomized Trial of Ruxolitinib in Antiretroviral-Treated Adults With Human Immunodeficiency Virus. *Clin Infect Dis* (2022) 74(1):95–104. doi: 10.1093/cid/ciab212
53. Besnard E, Hakre S, Kampmann M, Lim HW, Hosmane NN, Martin A, et al. The mTOR Complex Controls HIV Latency. *Cell Host Microbe* (2016) 20 (6):785–97. doi: 10.1016/j.chom.2016.11.001
54. Martin AR, Pollack RA, Capoferri A, Ambinder RF, Durand CM, Siliciano RF. Rapamycin-Mediated mTOR Inhibition Uncouples HIV-1 Latency Reversal From Cytokine-Associated Toxicity. *J Clin Invest* (2017) 127(2):651–6. doi: 10.1172/JCI89552

55. Vargas B, Giacobbi NS, Sanyal A, Venkatachari NJ, Han F, Gupta P, et al. Inhibitors of Signaling Pathways That Block Reversal of HIV-1 Latency. *Antimicrob Agents Chemother* (2019) 63(2):e01744–18. doi: 10.1128/AAC.01744-18
56. Pal VK, Agrawal R, Rakshit S, Shekar P, Murthy DTN, Vyakarnam A, et al. Hydrogen Sulfide Blocks HIV Rebound by Maintaining Mitochondrial Bioenergetics and Redox Homeostasis. *Elife.* (2021) 10:e68487. doi: 10.7554/eLife.68487
57. Hayashi T, Jean M, Huang H, Simpson S, Santoso NG, Zhu J. Screening of an FDA-Approved Compound Library Identifies Levosimendan as a Novel Anti-HIV-1 Agent That Inhibits Viral Transcription. *Antiviral Res* (2017) 146:76–85. doi: 10.1016/j.antiviral.2017.08.013
58. Lu Y, Bohn-Wippert K, Pazerunas PJ, Moy JM, Singh H, Dar RD. Screening for Gene Expression Fluctuations Reveals Latency-Promoting Agents of HIV. *Proc Natl Acad Sci USA* (2021) 118(11):e2012191118. doi: 10.1073/pnas.2012191118
59. Ahlenstiel C, Mendez C, Lim ST, Marks K, Turville S, Cooper DA, et al. Novel RNA Duplex Locks HIV-1 in a Latent State *via* Chromatin-Mediated Transcriptional Silencing. *Mol Ther Nucleic Acids* (2015) 4(10):e261. doi: 10.1038/mtna.2015.31
60. Méndez C, Ledger S, Petoumenos K, Ahlenstiel C, Kelleher AD. RNA-Induced Epigenetic Silencing Inhibits HIV-1 Reactivation From Latency. *Retrovirol.* (2018) 15(1):67. doi: 10.1186/s12977-018-0451-0
61. Zhou J, Lazar D, Li H, Xia X, Satheesan S, Charlins P, et al. Receptor-Targeted aptamer-siRNA Conjugate-Directed Transcriptional Regulation of HIV-1. *Theranostics.* (2018) 8(6):1575–90. doi: 10.7150/thno.23085
62. Saayman S, Ackley A, Turner AW, Famiglietti M, Bosque A, Clemson M, et al. An HIV-Encoded Antisense Long Noncoding RNA Epigenetically Regulates Viral Transcription. *Mol Ther* (2014) 22(6):1164–75. doi: 10.1038/mt.2014.29
63. Li J, Chen C, Ma X, Geng G, Liu B, Zhang Y, et al. Long Noncoding RNA NRON Contributes to HIV-1 Latency by Specifically Inducing Tat Protein Degradation. *Nat Commun* (2016) 7:11730. doi: 10.1038/ncomms11730
64. Olson A, Basukala B, Lee S, Gagne M, Wong WW, Henderson AJ. Targeted Chromatinization and Repression of HIV-1 Provirus Transcription With Repurposed CRISPR/Cas9. *Viruses.* (2020) 12(10):1154. doi: 10.3390/v12101154
65. Yamayoshi A, Fukumoto H, Hayashi R, Kishimoto K, Kobori A, Koyanagi Y, et al. Development of 7SK snRNA Mimics That Inhibit HIV Transcription. *ChemMedChem.* (2021) 16(20):3181–4. doi: 10.1002/cmdc.202100422
66. Apolloni A, Lin MH, Sivakumaran H, Li D, Kershaw MH, Harrich D. A Mutant Tat Protein Provides Strong Protection From HIV-1 Infection in Human CD4+ T Cells. *Hum Gene Ther* (2013) 24(3):270–82. doi: 10.1089/hum.2012.176
67. Jin H, Li D, Sivakumaran H, Lor M, Rustanti L, Cloonan N, et al. Shutdown of HIV-1 Transcription in T Cells by Nullbasic, a Mutant Tat Protein. *mBio.* (2016) 7(4):e00518-16. doi: 10.1128/mBio.00518-16
68. Jin H, Sun Y, Li D, Lin MH, Lor M, Rustanti L, et al. Strong *In Vivo* Inhibition of HIV-1 Replication by Nullbasic, a Tat Mutant. *mBio.* (2019) 10(4):e01769–19. doi: 10.1128/mBio.01769-19
69. Leoz M, Kukanja P, Luo Z, Huang F, Cary DC, Peterlin BM, et al. HEXIM1-Tat Chimera Inhibits HIV-1 Replication. *PloS Pathog* (2018) 14(11):e1007402. doi: 10.1371/journal.ppat.1007402
70. Singh S, Ghosh S, Pal VK, Munshi M, Shekar P, Narasimha Murthy DT, et al. Antioxidant Nanozyme Counteracts HIV-1 by Modulating Intracellular Redox Potential. *EMBO Mol Med* (2021) 13(5):e13314. doi: 10.15252/emmm.202013314

Conflict of Interest: The authors declare that the research was conducted in the absence of any commercial or financial relationships that could be construed as a potential conflict of interest.

Publisher's Note: All claims expressed in this article are solely those of the authors and do not necessarily represent those of their affiliated organizations, or those of the publisher, the editors and the reviewers. Any product that may be evaluated in this article, or claim that may be made by its manufacturer, is not guaranteed or endorsed by the publisher.

frontiers | Frontiers in Virology

TYPE Review
PUBLISHED 25 July 2022
DOI 10.3389/fviro.2022.934892

OPEN ACCESS

EDITED BY
Akio Adachi,
Kansai Medical University, Japan

REVIEWED BY
Yasuko Tsunetsugu Yokota,
Tokyo University of Technology, Japan
Rajesh Thippeshappa,
Texas Biomedical Research Institute,
United States

*CORRESPONDENCE
Hiroaki Takeuchi,
htake.molv@tmd.ac.jp
Sayaka Sukegawa,
sayaka.sukegawa.molv@tmd.ac.jp

SPECIALTY SECTION
This article was submitted to Fundamental Virology, a section of the journal Frontiers in Virology

RECEIVED 03 May 2022
ACCEPTED 29 June 2022
PUBLISHED 25 July 2022

CITATION
Sukegawa S and Takeuchi H (2022) Toward the unveiling of HIV-1 dynamics: Involvement of monocytes/macrophages in HIV-1 infection. *Front. Virol.* 2:934892. doi: 10.3389/fviro.2022.934892

Toward the unveiling of HIV-1 dynamics: Involvement of monocytes/macrophages in HIV-1 infection

Sayaka Sukegawa* and Hiroaki Takeuchi*

Department of Molecular Virology, Tokyo Medical and Dental University, Tokyo, Japan

HIV-1 targets the monocyte/macrophage lineage and CD4+ T cells for its replication. The efficiency of infection, replication, and cell-to-cell spread differs between these cell types. These differences are caused by various factors such as viral tropism, viral proteins, host factors, and cell proliferation. However, the precise mechanisms of how macrophages influence HIV-1 infection have not been fully elucidated. Macrophages are long-lived cells susceptible to infection predominantly with R5-tropic strains of HIV-1. Although co-receptor use switches from CCR5 to CXCR4 in up to 50% of patients during AIDS progression, R5-tropic strains remain predominant in the remaining patients. Compared to HIV-1-infected T cells, infected macrophages are less susceptible to HIV-induced cytopathic effects and survive for more than a few weeks. Efforts to cure HIV-1 may be thwarted by the existence of reservoir cells that cannot be targeted by ART. Resting CD4+ T lymphocytes are thought to be the primary reservoir cells, but recent studies demonstrated that monocyte/macrophage lineage cells may also act as viral reservoirs. This review will focus on the impact of monocytes/macrophages during HIV-1 replication, the establishment of the reservoirs, and recent approaches toward HIV-1 eradication by specifically targeting monocyte/macrophage lineage cells.

KEYWORDS

monocyte, macrophage, HIV-1, immunity, CD4+ T cells, viral tropism, HIV-1 reservoir

The mode of HIV-1 entry into macrophages

Macrophages have a crucial role in capturing foreign entities by endocytosing or phagocytosing pathogens as the first line of defense. They contribute to the adaptive immune response by presenting antigens to T cells, and to innate immunity by regulating inflammation *via* cytokine secretion (1). Macrophages express several receptors on their plasma membranes, including pattern-recognition receptors (PRRs), which contribute

significantly to recognizing pathogens for phagocytosis. Phagocytosed proteins are processed and presented in histocompatibility complex class II (MHC class II) to activate CD4+ T lymphocytes, while exogenous proteins such as viral proteins are presented on histocompatibility complex class I (MHC class I) to activate CD8+ T lymphocytes. In addition, the phagocytosed proteins can be presented on MHC class I, which is called cross-presentation. Macrophages and dendritic cells (DCs) play a critical role as antigen-presenting cells (APCs). Once pathogens are phagocytosed, these cells degrade and ingest exogenous proteins, then cross-present antigens on MHC class I to activate CD8+ cytotoxic T lymphocytes (2). PRRs function as sensors that rapidly initiate innate immune responses after binding with pathogen-associated molecular patterns (PAMPs) (3). Interferons (IFNs), secreted after the recognition of PAMPs by PRRs, have the potential to inhibit HIV-1 infection. IFNs also induce the expressions of several interferon-stimulated genes (ISGs), including SAMHD1, APOBEC3, Mx2 → MX2, tetherin, SERINC, and Siglec-1, which are well-known host factors that restrict HIV-1 replication (4). The functions of these host factors in HIV-1 replication are described in detail in the following section.

Despite their role in the clearance of pathogens, monocytes/macrophages as well as CD4+ T cells are targeted by HIV-1 for its replication. HIV-1 entry into the host cell begins with the attachment of viral envelope (Env) to CD4+ T-cell surface receptors, resulting in the exposure of the V3 loop of Env-gp120 following conformational changes induced by attachment. Sequentially, chemokine receptors CXCR4 or CCR5 are bound by Env-gp120, allowing insertion of viral Env-gp41 into the cell membrane and entrance of the viral capsid core into the host cell (5, 6). Macrophages are long-lived cells expressing CD4 as the primary receptor and chemokine receptors CXCR4 and CCR5 as co-receptors imbuing susceptibility to infection with HIV-1. The R5- and dual-tropic HIV-1 strains preferentially infect macrophages and memory-type CD4+ T lymphocytes by utilizing the CCR5 co-receptor, whereas most other CD4+ T lymphocytes are infected with X4-tropic viruses utilizing CXCR4. Co-receptor usage is thus one of the factors determining virus susceptibility, with several other factors such as differences in host cell proliferation and the existence of viral protein or host factors being significantly associated with disease progression after HIV-1 infection (7, 8). Generally, R5-tropic viruses are predominant at the early stages of infection and are associated with cell-to-cell transmission in individuals, whereas X4-tropic viruses usually emerge later (9). At this time, co-receptor usage switches from CCR5 to CXCR4, according to disease progression from acute to chronic infection in up to 50% of AIDS patients (9). However, R5-tropic virus predominance is sustained in the remaining patients. It is still unclear which conditions or factors are associated with facilitating this switch in tropism, but the series of HIV-1 infections with X4- or R5/X4-dual tropic HIV-1 are strongly associated with progression to AIDS by accelerating the reduction of CD4+ T cells (9).

Host and viral proteins involved in HIV-1 replication in myeloid lineage cells

Several factors are involved in the regulation of HIV replication, and a sufficient supply of nucleotides (dNTPs) is essential for efficient reverse transcription and the subsequent production of proviral DNA. Because the concentration of cellular dNTPs is strictly regulated by host cell cycle status, the characteristics of reverse transcription in non-dividing myeloid cells and activated CD4+ T cells are different. Cell cycle status greatly affects the level of ribonucleotide reductase subunit R2, which determines the amount of dNTPs available for reverse transcription (RT) (10). In addition, sterile alpha motif domain and HD domain-containing protein 1 (SAMHD1) was reported to be a host factor restricting HIV-1 and Vpx-deficient HIV-2 replication at the RT stage by depleting intracellular dNTPs in non-dividing cells such as DCs, macrophages, and resting CD4+ T cells (11–13) (**Figure 1**). It was reported that dNTP levels are approximately 130- to 250-fold lower in macrophages than in activated CD4+ T cells (14). HIV-2 Vpx counteracts the function of SAMHD1 by its degradation in a proteasome-dependent manner. In HIV-1, cyclin L2 promotes the proteasomal degradation of SAMHD1 (15). Thus far, the important roles of several other host factors including APOBEC3F, APOBEC3G, tetherin, and MX2 have also been implicated in HIV-1 replication in monocytes/macrophages (**Figure 1**). The apolipoprotein B editing complex (APOBEC) is a family of cellular cytidine deaminases. The APOBEC3 family is incorporated into nascent virions, which induce G-to-A hypermutation in the target cell. The viral cDNA produced by this mutation leads to HIV-1 genome changes, resulting in the inhibition of HIV-1 infection (16–18). HIV-1 Vif counteracts the function of this through proteasomal degradation. Macrophages express APOBEC3G, APOBEC3F, and APOBEC3DE, which are all upregulated by IFN-α stimulation. Similar to other APOBEC family members, APOBEC3A (A3A) is also upregulated by stimulation with IFN-α secreted during innate immune responses (18, 19). Interestingly, A3A is highly expressed in monocytes, whereas its expression is weak in fully differentiated macrophages (19). As the result of the silencing of A3A, HIV-1 infected monocytes increase virus replication. This differential expression level of A3A is tightly connected to the susceptibility to HIV-1 infection (16, 19). Myxovirus-resistance protein 2 (MX2, also known as MXB) is another well-known host viral restriction factor expressed in monocytes/macrophages and CD4 + T cells. MX2 protein limits HIV-1 replication by restricting nuclear import and repressing proviral DNA integration into

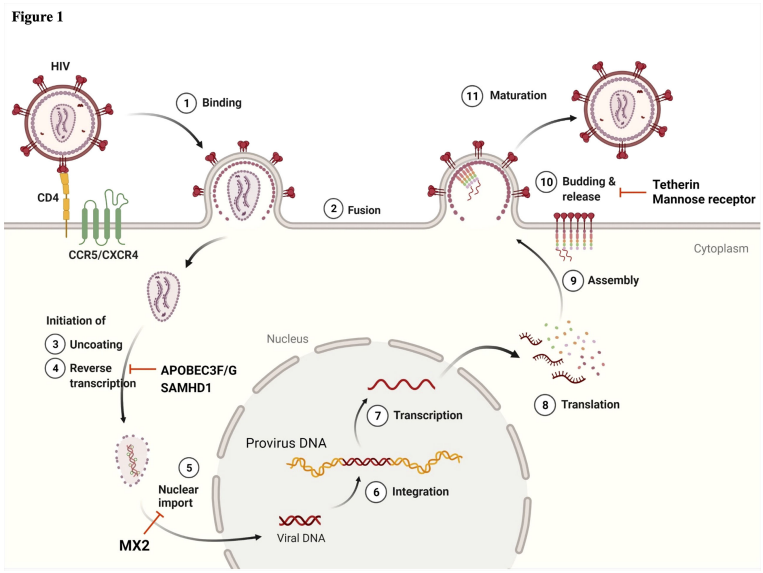

FIGURE 1
Schematic of the HIV-1 life cycle and host factors regulating HIV-1 replication in myeloid lineage cells. ① Viral infection begins by interactions between the viral envelope (Env) and the host cell receptor, CD4, and subsequently with the co-receptors CXCR4 or CCR5. ② This binding enables the fusion of virus to the host cell membrane and the release of viral cores into the cytoplasm. Once the viral core is released, ③ the uncoating and ④ reverse transcription (RT) of viral RNA are initiated in the cytoplasm. Virion-incorporated APOBEC3F/G and target cell SAMHD1 play a role in the inhibition of RT. ⑤ Viral content is transported to the nuclear pore, and uncoating and RT may then be completed. MX2 inhibits nuclear import. Following the completion of RT, ⑥ the viral genome is integrated into the host chromatin DNA. ⑦ Proviral DNA is transcribed and ⑧ translated into the Gag polyprotein. ⑨ Gag polyproteins are assembled at the plasma membrane and ⑩ initiate the viral budding and release of immature virions. Tetherin and mannose receptor (hMRC1) contribute to the inhibition of viral release. ⑪ For viral release from the cell membrane, viral protease cleaves Gag polyproteins, and mature virions are entirely released from the cell membrane. Image created with BioRender.com.

host chromatin (20–23) (**Figure 1**). This protein is a member of the RNA polymerase II-associated factor 1 (PAF1) family, identified in HeLa-CD4 cells by siRNA screening to identify restriction host factors in HIV-1 replication. A previous study reported that PAF1 was expressed in monocytes/macrophages in addition to T lymphocytes, and that the PAF1 complex (PAF1c) had a role in the inhibition of HIV replication by repressing RT and proviral DNA integration (24). There are two possible mechanisms of PAF1c restriction: first, according to their observations, a large quantity of PAF1 complex is localized in the nucleus. The interaction of PAF1 and RNA polymerase II is thought to be involved in mRNA transcription, elongation, and stability (25); second, the interaction with SKI8 (WDR61), which is part of the SKI complex, is associated with mRNA decay (25). Furthermore, the interactions of PAF1/SKI8 with DNA and RNA in the cytoplasm allow it to function as a PRR. Tetherin (BST-2, also known as CD317) is highly expressed on the surface of macrophages, in contrast to its absence or low-level expression by CD4+ T cells. Tetherin plays a crucial role in retaining progeny virions in infected cells and preventing their release (**Figures 1** and **2A**). However, Vpu, an accessory protein of HIV-1, antagonizes this function by downregulating tetherin by interfering with the trafficking of newly synthesized and recycling of tetherin proteins from the plasma membrane (26–29). In 2015, the serine incorporator (SERINC) family, especially SERINC3 and SERINC5 members, was newly identified as a host factor antagonized by Nef protein, which inhibited infection by progeny viruses (**Figure 2C**). The mechanism involves the incorporation of these proteins into newly synthesized virus particles, resulting in interference with their fusion to secondary target cells (30, 31). Furthermore, Zutz et al. revealed that endogenous SERINC5 is highly expressed in differentiated monocyte-derived macrophages at levels sufficient to exert antiviral effects in these primary cells but not in monocytes themselves (32). To date, it is clear that Env glycoprotein has a crucial role in the function of SERINC3/5, but its precise mechanisms of action remain incompletely understood (33–36). Neuropilin-1 (NRP-1), a transmembrane protein, was newly identified in 2021 by Wang et al., and shown to inhibit progeny virus infection (**Figure 2C**) (37). This protein is highly expressed on the cell surface of macrophages and DCs but not on stimulated or resting CD4+ T cells. Virion-incorporated NRP-1 inhibits their attachment to secondary target cells and consequently contributes to the suppression of infectivity, affecting HIV-1 transmission in a myeloid lineage cell-specific manner.

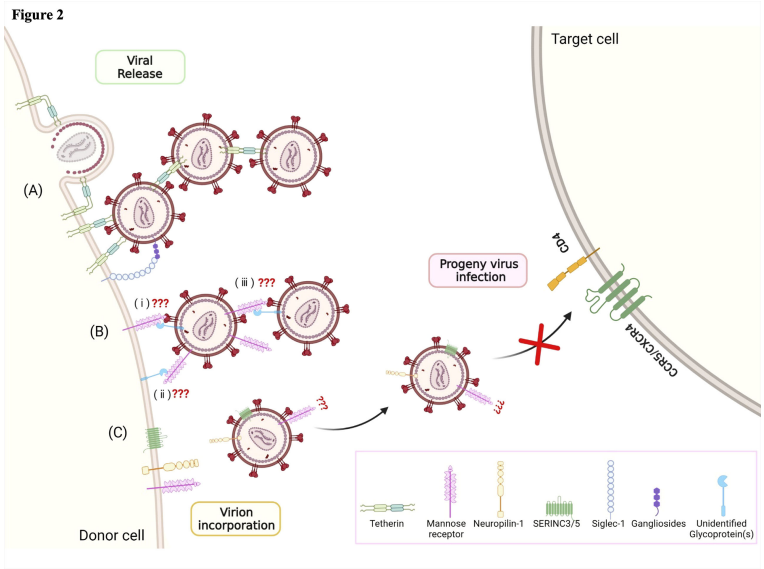

FIGURE 2
Host factors regulating the late phase of the HIV-1 life cycle, from viral release to progeny virus infection. Various cellular host factors including tetherin, mannose receptor (hMRC1), neuropilin-1 (NRP-1), SERINC3/5, and Siglec-1 are highly expressed on the surface of the plasma membrane. **(A)** Tetherin and Siglec-1 play a role in capturing viral particles at the budding step. **(B)** hMRC1 also inhibits viral particle release. It is hypothesized that (i) hMRC1 expressed on the cell surface may interact with Env glycoprotein and/or unidentified host glycoprotein(s) associated with viral particles. (ii) Unidentified host glycoprotein(s) expressed on the cell surface may interact with hMRC1 associated with viral particles. (iii) Viral particle-associated hMRC1 may interact with Env glycoprotein and/or unidentified host glycoprotein(s). However, the precise mechanisms are still unclear. **(C)** Virion-incorporated SERINC3/5 and NRP-1 contribute to the inhibition of progeny virus infection through interference with the binding step. Image created with BioRender.com.

In addition to the host factors described above, several viral accessory proteins, including Vif, Vpr, Vpu, Vpx, and Nef, also contribute to the regulation of HIV-1 replication in macrophages. Although the functions of most of these viral accessary proteins are well characterized, the precise role of Vpr is still poorly understood. Vpr has multiple biological functions, including the nuclear import of viral preintegration complex (PIC), repression of HIV-1 transcription, G2 cell cycle arrest, enhancement of the expression and processing of Env glycoprotein in macrophages, and induction of host protein degradation by recruitment of the E3 ubiquitin ligase complex (1, 38). Vpr is packaged into nascent virions (39) through interactions with the P6 domain of the viral Gag precursor (40). Vpr primarily localizes to the nucleus/nuclear envelope in PBMCs and macrophages (41, 42), and an observation by Desai et al. indicated that a substantial amount of Vpr incorporated into virus particles was released from the PIC and accumulated in the nucleus, suggesting a role for Vpr in the early stages of HIV-1 infection (43). However, the effect of virion-incorporated Vpr in the first round of infection of macrophages has not been revealed (44, 45). Vpr has a critical role in HIV-1 replication in monocytic cell lines including THP-1 or primary macrophages, but not in CD4+ T cells (i.e., Vpr-defective HIV-1 is severely restricted in macrophages) (46). Indeed, Mashiba et al. recently reported that Vpr promoted HIV-1 infection in non-dividing cells such as macrophages (44, 45). This evidence suggests the existence of host factors suppressing HIV-1 replication, which is counteracted by Vpr. Numerous host factors neutralized by Vpr have been identified including HTLF, CCDC137, MCM10, TET2, and LAPTM5 (44, 47–50). Despite the functional analyses of these Vpr-associated host factors, the exact role of Vpr in HIV-1 replication, especially in macrophages, is unclear and further study is required.

Cell-to-cell transmission

As described by Law et al., in addition to cell-free transmission, HIV-1 spreads *via* cell-to-cell contact through virological synapses (VS) *in vivo* (41). These are formed when the viral envelopes on the plasma membrane of HIV-1-infected cells bind to uninfected CD4+ T cells (51). Modes of cell-to-cell transmission are classified according to the cellular structures involved, i.e., filopodial bridges, membrane nanotubes (also known as TNT), and virological synapses (**Figure 3A**). The key feature of this mode of spread is that, in general, the effectiveness of HIV-1 infection is >10-fold greater than for cell-free infection of CD4+ T cells (52–56). Similar to the cell-to-cell transmission

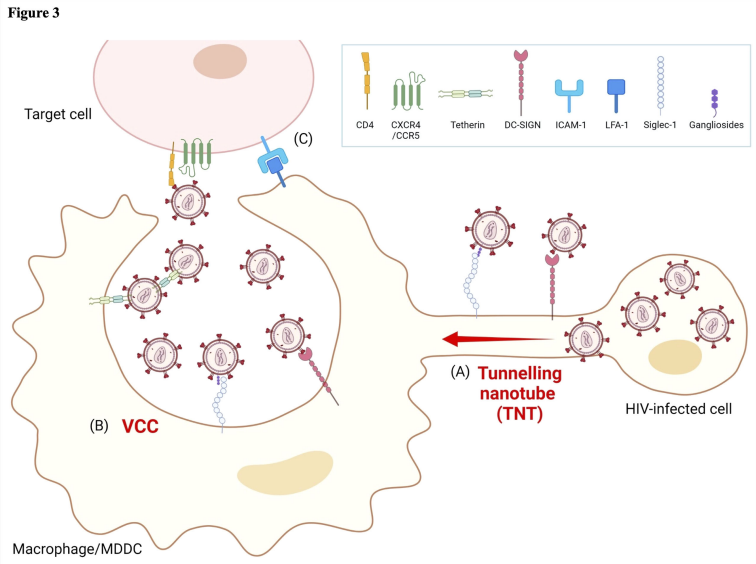

FIGURE 3
Models of HIV-1 cell-to-cell transmission in myeloid lineage cells. **(A)** HIV-1-infected cells form tunneling nanotubes (TNT) to transport infectious viral particles to other target cells by utilizing attachment receptors such as Siglec-1 or DC-SIGN. **(B)** Infected macrophages form unique virus-containing particles (VCC) and retain infectious viral particles through the association of tetherin, Siglec-1, or DC-SIGN with Env glycoprotein. When encountering other target cells, VCC containing either free virions or host factor(s)-associated virions may release infectious virus. **(C)** The binding of adhesion molecules LFA-1 and ICAM-1 has a well-characterized role in stabilizing virological synapse (VS) formation and contributes to cell-to-cell HIV-1 transmission. Image created with BioRender.com.

between CD4+ T cells, infected macrophages/monocyte-derived dendritic cells (MDDCs) recruit CD4, CCR5, LFA-1, ICAM-1, Gag proteins, and envelope glycoproteins, at the site of cell–cell contact, described as VS formation. More recently, it was reported that cell-to-cell contact between infected macrophages/MDDCs and CD4+ T cells was stabilized by interactions between gp120-CD4 and LFA-1-ICAM-1 and might be very effective for HIV-1 transmission (**Figure 3C**) (57). Previous studies suggested that DC-SIGN, a C-type lectin expressed on immature DCs, has a role in capturing HIV-1 particles through interactions with envelope glycoproteins and the subsequent transfer of infectious particles to other cells (**Figure 3B**) (58). Another member of the C-type lectin family, sialic acid-binding Ig-like lectin 1 (Siglec-1, also known as CD169), expressed on the surface of DCs and macrophages, also captures infectious particles *via* sialyl lactose-containing gangliosides exposed on the envelope, and thus also contributes to cell-to-cell transmission (**Figure 2A**) (59). Furthermore, Dupont et al. recently reported that TNT was highly positive for Siglec-1 and was required for TNT-mediated HIV-1 transmission in macrophages, as shown by silencing Siglec-1 (**Figure 3A**) (60). As described above, infected macrophages also significantly contribute to the cell-to-cell transmission through the formation of VS between infected macrophages and uninfected CD4+ T cells, which leads to the transfer of a high multiplicity of HIV-1 to the latter (61). Several groups also reported that this mode of infection is less sensitive to certain classes of antiretroviral therapies (ARTs) and reverse transcriptase (RT) inhibitors (62–64), and is more resistant to neutralizing antibodies against specific Env epitopes (65, 66).

In contrast to the mechanisms of viral assembly in infected CD4+ T cells, viral particles accumulate on the plasma membrane and in intracellular tetraspanin-enriched virus-containing compartments (VCCs) in productively infected macrophages (**Figure 3B**) (67–70). VCCs rapidly change transmission mode to VS in a cytoskeleton-dependent manner. The structural features of VCC are similar to those of late endosomes or multivesicular bodies (MVB), but are distinguished from them in terms of acidity. Thus, VCCs are non-acidic and non-degrading compartments (71–73). As described in *Section 2*, tetherin is a critical host factor regulating HIV-1 release that is highly expressed on the surface of macrophages (**Figures 1** and **2A**), but not or only at a low level on CD4+ T cells (26, 27). Thus, tetherin effectively restricts HIV-1 release from the cell surface of macrophages rather than from CD4+ T cells, and this function is antagonized by the viral protein Vpu (27). In addition to the inhibition of cell-free viruses, tetherin has a role in forming VCC and potentially contributes to restricting cell-to-cell transmission (**Figure 3B**). Tetherin retains HIV-1 virions at the plasma membrane, which are subsequently internalized into VCC (74–76). Recently, Hammonds et al. reported that lectins such as Siglec-1, expressed on DCs and macrophage cell surfaces, play

a crucial role in forming VCC (**Figure 3B**) (72). That study demonstrated that VCC formation is not necessary for macrophage infection but is necessary for cell-to-cell viral transmission from infected macrophages to CD4+ T cells (72). HIV-1 virions captured and internalized in VCCs through Siglec-1 are potentially protected from innate immune responses. Thus, captured HIV-1 infectious virions can transfer to target CD4+ T cells through VS, a mechanism independent of normal virus replication (77, 78). Human mannose receptor C-type 1 (hMRC1) also significantly contributes to the spread of infection through cell-to-cell transmission. Its function in HIV-1 infection is described in detail in the next section.

Contribution of mannose receptor during HIV-1 replication

The human mannose receptor C-type1 (hMRC1), designated CD260, is a 175-kDa type I transmembrane glycoprotein belonging to the C-type lectin family. It is expressed on most tissue macrophage surfaces, DCs, selected lymphatic cells, liver endothelial cells, and vaginal epithelial cells (79). This protein contains three types of extracellular domains, namely, CR (cysteine-rich domain), FNII (fibronectin type II repeat), and eight tandem CRD (C-type carbohydrate recognition domains) (79). The CRD domains have a crucial role in capturing foreign bodies, including HIV-1. Recently, it was shown to be involved in capturing pathogens including bacteria and fungi, as well as viruses like HIV-1 (79). In HIV-1 infection, hMRC1 binds to viral Env through interactions mediated by glycosylated mannose residues on Env (80–82). Intriguingly, unlike typical virus entry, this uptake of HIV-1 mediated by hMRC1 does not lead to productive infection (82, 83), but the phagocytosed pathogen contributes to antigen presentation (84, 85). However, Nguyen and Hildreth provided evidence that hMRC1 on the macrophage surface facilitates virus transmission to CD4+ T cells (81). Several factors regulate this function of hMRC1, including viral proteins such as Vpr, Tat, and Nef, as well as unidentified host factors, but the precise mechanisms remain unclear. Sukegawa et al. demonstrated that hMRC1 inhibits virus release from HIV-1-infected macrophages in a BST-2-independent manner (86) (**Figure 2B**). Interestingly, the amount of endogenously expressed hMRC1 was significantly downregulated after virus infection. It is assumed that the virus counteracts the function of hMRC1-mediated inhibition of virion release by removing hMRC1 from the cell surface. This reduction of hMRC1 has been reported in several other papers, both *in vivo* and *in vitro*. Koziel et al. reported a modest reduction of hMRC mRNA in HIV-1-positive patients (87). Other investigators have reported the relevance of viral proteins such as Nef, Tat, and Vpr. Vigerust et al. reported that Nef induced the surface repression of hMRC1 without affecting steady-state levels but interfered with the recycling of mannose receptors to the cell surface (88). In addition, HIV-1 Tat was reported to inhibit transcription from the rat mannose receptor promoter (89). However, recently, Lubow et al. reported that the contribution of Tat to the downregulation of mannose receptors was insignificant (53). Furthermore, they implicated the involvement of Nef and Vpr in the downregulation of hMRC1 and indicated that cooperation between Vpr and Nef induced a synergistic reduction of hMRC1 (53). Thus, Vpr downregulates the transcription of hMRC1, and Nef removes hMRC1 from the cell surface through lysosomal degradation, causing a further reduction of hMRC1. It was also demonstrated that the downregulation of Env expression by hMRC1 was counteracted by Vpr through rescue from lysosomal degradation, which increased the formation of VS and facilitated cell-to-cell transmission between macrophages and CD4+ T cells (53, 56). This evidence demonstrates the significant impact of hMRC1 during HIV-1 replication in macrophages and on the normal function of host immune defense by capturing pathogens.

HIV-1 reservoirs in macrophages

As noted above, CD4+T lymphocytes are considered the primary HIV-1 reservoir cells. The contribution of monocytes/macrophages remains controversial (7). However, there is evidence showing the contribution of tissue-resident macrophages in establishing HIV-1 reservoirs. The earliest study was reported by Gartner et al. in 1986 (90). Due to the difficulty of obtaining primary tissue-resident macrophages, non-human primate models have been widely used to investigate the association of infectious virus dynamics with disease progression *in vivo* (90–92). In 2001, Igarashi et al. confirmed the contribution of macrophages in HIV-1 reservoirs utilizing SHIV in a macaque model (93). That report observed the persistence of SHIV infection in tissue macrophages under the depletion of CD4+ T cells according to disease progression in the macaque. Furthermore, the administration of potent RT inhibitors effectively blocked HIV-1 circulating in CD4+ T cells but not in macrophages, demonstrating that tissue macrophages can sustain viral replication independently.

Reservoirs in macrophages start to become established a few days after the initial HIV-1 infection and are sustained during the asymptomatic stage of disease in these long-lived cells (7). In contrast to the loss of CD4+ T cells during the progression to AIDS, infected macrophages are less susceptible to HIV-induced

cytopathic effects (7) and are more resistant to CD8+ cytotoxic T lymphocyte (CTL)-mediated killing (94). Hence, they may survive for more than a few weeks (1) and can therefore persistently infect cells as they are also poorly targeted by ART (i.e., they are less susceptible to some antiretroviral drugs). In fact, recent *in vivo* studies revealed the contribution of monocytes/macrophages as reservoirs. Honeycutt et al. developed humanized myeloid-only mouse models (MoM) unable to support human lymphocyte development (95). Using these models, they reported the detection of rebound viremia in three of nine mice 7 weeks after the discontinuation of ART (96). This report thus provided novel evidence that monocytes/macrophages can be a source of rebound viremia following ART cessation. Furthermore, Ganor et al. demonstrated that integrated HIV-1 DNA, HIV-1 RNA, and p24 were predominantly detected in urethral macrophages rather than CD4+ T lymphocytes in HIV-1-infected patients on ART (97).

The central nervous system (CNS, microglia) is also considered another tissue-resident macrophage reservoir (98, 99). Within a few days after primary infection, HIV-1 entered the CNS through the blood–brain barrier (BBB) *via* infected monocytes rather than CD4+ T cells (100, 101). In the CNS, HIV-1 persists predominantly in tissue-resident macrophages, such as microglia and perivascular macrophages differentiated from monocytes. More recently, Joseph et al. reported the isolation of R5-tropic virus from the cerebrospinal fluid (CSF) of ART-treated patients, suggesting that HIV-1 is continuously replicating in CNS reservoirs (102, 103). As with other reservoir cells, HIV-1-infected microglia are also long-lived, and unlike other hematopoietic reservoirs, the turnover of microglia is very slow, with only 28% of these cells renewed annually (104). Thus, HIV-1-infected microglia potentially sustain lifetime reservoirs in infected individuals. As described above, monocytes/macrophages, as well as CD4+ T cells, contribute to the persistence of infection and represent reservoirs *in vivo*. Importantly, some antiretroviral drugs such as protease inhibitors, saquinavir, and ritonavir exhibited a 2- to 10-fold lower activity in infected macrophages relative to chronically infected lymphocytes (105, 106). Moreover, Gavegnano et al. showed that the intracellular concentrations of nucleoside analog active metabolites in macrophages were 5- to 140-fold lower than in lymphocytes, contributing to significantly weaker antiviral activity (107). These features may also contribute to the persistence of HIV-1-infected macrophages and result in the establishment of HIV-1 reservoirs and the evolution of drug-resistant viruses.

The current approach towards HIV-1 eradication

Viral replication in HIV-infected individuals is controlled by combination antiretroviral therapy (cART), which mainly targets viral enzymes. However, latently infected reservoirs and drug-resistant viruses are still a significant barrier to curing HIV-1. To this end, several strategies such as gene therapy using CRISPR, vaccines to boost anti-HIV immune responses, and immunotherapy with broadly neutralizing antibodies have been investigated. In addition to these strategies, the "Shock and Kill" approach to reducing the size of reservoirs is a current challenge, whereby latency-reversing agents (LRAs) reactivate latently infected provirus (the shock) and induce cell death mediated by cytopathic effects, apoptosis, or CTL response (the kill), combined with ART treatment to prevent the occurrence of a new infection. This strategy is still under development (108), and some small-molecule chemical compounds, including histone deacetylase inhibitors (HDACi) (e.g., SAHA/vorinostat) (109), bromodomain and extraterminal domain inhibitors (BETi) (e.g., JQ1) (110), and protein kinase C (PKC) agonists [e.g., Prostratin, PEP-005 (ingenole-3-angelate) and bryostatin-1] (111), are being intensively investigated as candidate LRAs. Several groups have reported that using an LRA, active via a single mechanism, might not lead to effective viral reactivation in reservoir cells, and combinations of drug candidates with different mechanisms of action will be needed to enhance proviral activation. Currently, combining the BRD4 inhibitor (JQ1) and PKC agonist(s) (e.g., Prostratin, PEP-005) might be the most effective means of reactivating the HIV-1 provirus (7, 108). Despite the potent effects of LRA or a combination of LRAs on *ex vivo* or *in vitro* analyses, multiple clinical trials have failed to reduce latent reservoir size sufficiently, and none have shown superior therapeutic effects compared with current cART (112). A reason for this may be that different responses to LRAs by several types of latent reservoirs (7, 113) are influenced by the size and chromosomal location of the integrated provirus (114) in HIV-1 reservoirs. Therefore, the development of new LRAs or combination therapies of several LRAs to induce efficient provirus reactivation remains an unmet need.

Author contributions

HT and SS contributed to the conception and wrote all sections of the manuscript. All authors contributed to manuscript revision, read, and approved the submitted version.

Funding

This work was supported by: grant 21fk0410023s0303, 22fk0410052s0101 for Research Program on HIV/AIDS from Japan Agency for Medical Research and Development to HT,

Takeda Science Foundation to SS. The founder had no role in decision to publish or preparation of the manuscript

Conflict of interest

The authors declare that the research was conducted in the absence of any commercial or financial relationships that could be construed as a potential conflict of interest.

Publisher's note

References

1. Lubow J, Collins KL. Vpr is a VIP: HIV vpr and infected macrophages promote viral pathogenesis. *Viruses* (2020) 12(8):809. doi: 10.3390/v12080809

2. Muntjewerff EM, Meesters LD, van den Bogaart G. Antigen cross-presentation by macrophages. *Front Immunol* (2020) 11:1276. doi: 10.3389/fimmu.2020.01276

3. Yin X, Langer S, Zhang Z, Herbert KM, Yoh S, König R, et al. Sensor sensibility-HIV-1 and the innate immune response. *Cells* (2020) 9(1):254. doi: 10.3390/cells9010254

4. Rojas M, Luz-Crawford P, Soto-Rifo R, Reyes-Cerpa S, Toro-Ascuy D. The landscape of IFN/ISG signaling in HIV-1-Infected macrophages and its possible role in the HIV-1 latency. *Cells* (2021) 10(9):2378. doi: 10.3390/cells10092378

5. Chen B. Molecular mechanism of HIV-1 entry. *Trends Microbiol* (2019) 27:878–91. doi: 10.1016/j.tim.2019.06.002

6. Moeser M, Nielsen JR, Joseph SB. Macrophage tropism in pathogenic HIV-1 and SIV infections. *Viruses* (2020) 12(10):1077. doi: 10.3390/v12101077

7. Hendricks CM, Cordeiro T, Gomes AP, Stevenson M. The interplay of HIV-1 and macrophages in viral persistence. *Front Microbiol* (2021) 12:646447. doi: 10.3389/fmicb.2021.646447

8. Borrajo A, Ranazzi A, Pollicita M, Bellocchi MC, Salpini R, Mauro MV, et al. Different patterns of HIV-1 replication in MACROPHAGES is led by Co-receptor usage. *Medicina (Kaunas)* (2019) 55(6):297. doi: 10.3390/medicina55060297

9. He S, Wu Y. Relationships between HIV-mediated chemokine coreceptor signaling, cofilin hyperactivation, viral tropism switch and HIV-mediated CD4 depletion. *Curr HIV Res* (2019) 17:388–96. doi: 10.2174/1570162X17666191106112018

10. Kennedy EM, Amie SM, Bambara RA, Kim B. Frequent incorporation of ribonucleotides during HIV-1 reverse transcription and their attenuated repair in macrophages. *J Biol Chem* (2012) 287:14280–8. doi: 10.1074/jbc.M112.348482

11. Laguette N, Sobhian B, Casartelli N, Ringeard M, Chable-Bessia C, Ségéral E, et al. SAMHD1 is the dendritic- and myeloid-cell-specific HIV-1 restriction factor counteracted by vpx. *Nature* (2011) 474:654–7. doi: 10.1038/nature10117

12. Lahouassa H, Daddacha W, Hofmann H, Ayinde D, Logue EC, Dragin L, et al. SAMHD1 restricts the replication of human immunodeficiency virus type 1 by depleting the intracellular pool of deoxynucleoside triphosphates. *Nat Immunol* (2012) 13:223–8. doi: 10.1038/ni.2236

13. Hrecka K, Hao C, Gierszewska M, Swanson SK, Kesik-Brodacka M, Srivastava S, et al. Vpx relieves inhibition of HIV-1 infection of macrophages mediated by the SAMHD1 protein. *Nature* (2011) 474:658–61. doi: 10.1038/nature10195

14. Diamond TL, Roshal M, Jamburuthugoda VK, Reynolds HM, Merriam AR, Lee KY, et al. Macrophage tropism of HIV-1 depends on efficient cellular dNTP utilization by reverse transcriptase. *J Biol Chem* (2004) 279:51545–53. doi: 10.1074/jbc.M408573200

15. Kyei GB, Cheng X, Ramani R, Ratner L. Cyclin L2 is a critical HIV dependency factor in macrophages that controls SAMHD1 abundance. *Cell Host Microbe* (2015) 17:98–106. doi: 10.1016/j.chom.2014.11.009

16. Berger G, Durand S, Fargier G, Nguyen XN, Cordeil S, Bouaziz S, et al. APOBEC3A is a specific inhibitor of the early phases of HIV-1 infection in myeloid cells. *PloS Pathog* (2011) 7:e1002221. doi: 10.1371/journal.ppat.1002221

17. Ikeda T, Molan AM, Jarvis MC, Carpenter MA, Salamango DJ, Brown WL, et al. HIV-1 restriction by endogenous APOBEC3G in the myeloid cell line THP-1. *J Gen Virol* (2019) 100:1140–52. doi: 10.1099/jgv.0.001276

18. Peng G, Greenwell-Wild T, Nares S, Jin W, Lei KJ, Rangel ZG, et al. Myeloid differentiation and susceptibility to HIV-1 are linked to APOBEC3 expression. *Blood* (2007) 110:393–400. doi: 10.1182/blood-2006-10-051763

19. Stavrou S, Ross SR. APOBEC3 proteins in viral immunity. *J Immunol* (2015) 195:4565–70. doi: 10.4049/jimmunol.1501504

20. Buffone C, Kutzner J, Opp S, Martinez-Lopez A, Selyutina A, Coggings SA, et al. The ability of SAMHD1 to block HIV-1 but not SIV requires expression of MxB. *Virology* (2019) 531:260–8. doi: 10.1016/j.virol.2019.03.018

21. Goujon C, Moncorgé O, Bauby H, Doyle T, Ward CC, Schaller T, et al. Human MX2 is an interferon-induced post-entry inhibitor of HIV-1 infection. *Nature* (2013) 502:559–62. doi: 10.1038/nature12542

22. Wang X, Wang H, Liu MQ, Li JL, Zhou RH, Zhou Y, et al. IFN-λ inhibits drug-resistant HIV infection of macrophages. *Front Immunol* (2017) 8:210. doi: 10.3389/fimmu.2017.00210

23. Kane M, Yadav SS, Bitzegeio J, Kutluay SB, Zang T, Wilson SJ, et al. MX2 is an interferon-induced inhibitor of HIV-1 infection. *Nature* (2013) 502:563–6. doi: 10.1038/nature12653

24. Liu L, Oliveira NM, Cheney KM, Pade C, Dreja H, Bergin AM, et al. A whole genome screen for HIV restriction factors. *Retrovirology* (2011) 8:94. doi: 10.1186/1742-4690-8-94

25. Zhu B, Mandal SS, Pham AD, Zheng Y, Erdjument-Bromage H, Batra SK, et al. The human PAF complex coordinates transcription with events downstream of RNA synthesis. *Genes Dev* (2005) 19:1668–73. doi: 10.1101/gad.1292105

26. Schindler M, Rajan D, Banning C, Wimmer P, Koppensteiner H, Iwanski A, et al. Vpu serine 52 dependent counteraction of tetherin is required for HIV-1 replication in macrophages, but not in ex vivo human lymphoid tissue. *Retrovirology* (2010) 7:1. doi: 10.1186/1742-4690-7-1

27. Miyagi E, Andrew AJ, Kao S, Strebel K. Vpu enhances HIV-1 virus release in the absence of bst-2 cell surface down-modulation and intracellular depletion. *Proc Natl Acad Sci U.S.A.* (2009) 106:2868–73. doi: 10.1073/pnas.0813223106

28. Schmidt S, Fritz JV, Bitzegeio J, Fackler OT, Keppler OT. HIV-1 vpu blocks recycling and biosynthetic transport of the intrinsic immunity factor CD317/tetherin to overcome the virion release restriction. *mBio* (2011) 2:e00036–00011. doi: 10.1128/mBio.00036-11

29. Dubé M, Paquay C, Roy BB, Bego MG, Mercier J, Cohen EA. HIV-1 vpu antagonizes BST-2 by interfering mainly with the trafficking of newly synthesized BST-2 to the cell surface. *Traffic* (2011) 12:1714–29. doi: 10.1111/j.1600-0854.2011.01277.x

30. Rosa A, Chande A, Ziglio S, De Sanctis V, Bertorelli R, Goh SL, et al. HIV-1 nef promotes infection by excluding SERINC5 from virion incorporation. *Nature* (2015) 526:212–7. doi: 10.1038/nature15399

31. Usami Y, Wu Y, Göttlinger HG. SERINC3 and SERINC5 restrict HIV-1 infectivity and are counteracted by nef. *Nature* (2015) 526:218–23. doi: 10.1038/nature15400

32. Zutz A, Schölz C, Schneider S, Pierini V, Münchhoff M, Sutter K, et al. SERINC5 is an unconventional HIV restriction factor that is upregulated during myeloid cell differentiation. *J Innate Immun* (2020) 12:399–409. doi: 10.1159/000504888

33. Sood C, Marin M, Chande A, Pizzato M, Melikyan GB. SERINC5 protein inhibits HIV-1 fusion pore formation by promoting functional inactivation of envelope glycoproteins. *J Biol Chem* (2017) 292:6014–26. doi: 10.1074/jbc.M117.777714

34. Beitari S, Ding S, Pan Q, Finzi A, Liang C. Effect of HIV-1 env on SERINC5 antagonism. *J Virol* (2017) 91(4):e02214–16. doi: 10.1128/JVI.02214-16

35. Chen YC, Sood C, Marin M, Aaron J, Gratton E, Salaita K, et al. Super-resolution fluorescence imaging reveals that serine incorporator protein 5 inhibits

human immunodeficiency virus fusion by disrupting envelope glycoprotein clusters. *ACS Nano* (2020) 14:10929–43. doi: 10.1021/acsnano.0c02699

36. Zhang X, Shi J, Qiu X, Chai Q, Frabutt DA, Schwartz RC, et al. CD4 expression and env conformation are critical for HIV-1 restriction by SERINC5. *J Virol* (2019) 93. doi: 10.1128/JVI.00544-19

37. Wang S, Zhao L, Zhang X, Zhang J, Shang H, Liang G. Neuropilin-1, a myeloid cell-specific protein, is an inhibitor of HIV-1 infectivity. *Proc Natl Acad Sci U.S.A.* (2022) 119(2):e2114884119. doi: 10.1073/pnas.2114884119

38. Fabryova H, Strebel K. Vpr and its cellular interaction partners: R we there yet? *Cells* (2019) 8(11):1310. doi: 10.3390/cells8111310

39. Cohen EA, Dehni G, Sodroski JG, Haseltine WA. Human immunodeficiency virus vpr product is a virion-associated regulatory protein. *J Virol* (1990) 64:3097–9. doi: 10.1128/jvi.64.6.3097-3099.1990

40. Bachand F, Yao XJ, Hrimech M, Rougeau N, Cohen EA. Incorporation of vpr into human immunodeficiency virus type 1 requires a direct interaction with the p6 domain of the p55 gag precursor. *J Biol Chem* (1999) 274:9083–91. doi: 10.1074/jbc.274.13.9083

41. Lu YL, Spearman P, Ratner L. Human immunodeficiency virus type 1 viral protein r localization in infected cells and virions. *J Virol* (1993) 67:6542–50. doi: 10.1128/jvi.67.11.6542-6550.1993

42. Jacquot G, Le Rouzic E, David A, Mazzolini J, Bouchet J, Bouaziz S, et al. Localization of HIV-1 vpr to the nuclear envelope: impact on vpr functions and virus replication in macrophages. *Retrovirology* (2007) 4:84. doi: 10.1186/1742-4690-4-84

43. Desai TM, Marin M, Sood C, Shi J, Nawaz F, Aiken C, et al. Fluorescent protein-tagged vpr dissociates from HIV-1 core after viral fusion and rapidly enters the cell nucleus. *Retrovirology* (2015) 12:88. doi: 10.1186/s12977-015-0215-z

44. Wang Q, Su L. Vpr enhances HIV-1 env processing and virion infectivity in macrophages by modulating TET2-dependent IFITM3 expression. *mBio* (2019) 10 (4):e01344–19. doi: 10.1128/mBio.01344-19

45. Mashiba M, Collins DR, Terry VH, Collins KL. Vpr overcomes macrophage-specific restriction of HIV-1 env expression and virion production. *Cell Host Microbe* (2014) 16:722–35. doi: 10.1016/j.chom.2014.10.014

46. Balliet JW, Kolson DL, Eiger G, Kim FM, McGann KA, Srinivasan A, et al. Distinct effects in primary macrophages and lymphocytes of the human immunodeficiency virus type 1 accessory genes vpr, vpu, and nef: Mutational analysis of a primary HIV-1 isolate. *Virology* (1994) 200:623–31. doi: 10.1006/viro.1994.1225

47. Lahouassa H, Blondot ML, Chauveau L, Chougui G, Morel M, Leduc M, et al. HIV-1 vpr degrades the HLTF DNA translocase in T cells and macrophages. *Proc Natl Acad Sci U.S.A.* (2016) 113:5311–6. doi: 10.1073/pnas.1600485113

48. Zhang F, Bieniasz PD. HIV-1 vpr induces cell cycle arrest and enhances viral gene expression by depleting CCDC137. *Elife* (2020) 9:e55806. doi: 10.7554/eLife.55806

49. Romani B, Shaykh Baygloo N, Aghasadeghi MR, Allahbakhshi E. HIV-1 vpr protein enhances proteasomal degradation of MCM10 DNA replication factor through the Cul4-DDB1[VprBP] E3 ubiquitin ligase to induce G2/M cell cycle arrest. *J Biol Chem* (2015) 290:17380–9. doi: 10.1074/jbc.M115.641522

50. Zhao L, Wang S, Xu M, He Y, Zhang X, Xiong Y, et al. Vpr counteracts the restriction of LAPTM5 to promote HIV-1 infection in macrophages. *Nat Commun* (2021) 12:3691. doi: 10.1038/s41467-021-24087-8

51. Piguet V, Sattentau Q. Dangerous liaisons at the virological synapse. *J Clin Invest* (2004) 114:605–10. doi: 10.1172/JCI22812

52. Sattentau Q. Avoiding the void: cell-to-cell spread of human viruses. *Nat Rev Microbiol* (2008) 6:815–26. doi: 10.1038/nrmicro1972

53. Lubow J, Virgilio MC, Merlino M, Collins DR, Mashiba M, Peterson BG, et al. Mannose receptor is an HIV restriction factor counteracted by vpr in macrophages. *Elife* (2020) 9:e51035. doi: 10.7554/eLife.51035

54. Del Portillo A, Tripodi J, Najfeld V, Wodarz D, Levy DN, Chen BK. Multiploid inheritance of HIV-1 during cell-to-cell infection. *J Virol* (2011) 85:7169–76. doi: 10.1128/JVI.00231-11

55. Martin N, Welsch S, Jolly C, Briggs JA, Vaux D, Sattentau QJ. Virological synapse-mediated spread of human immunodeficiency virus type 1 between T cells is sensitive to entry inhibition. *J Virol* (2010) 84:3516–27. doi: 10.1128/JVI.02651-09

56. Collins DR, Lubow J, Lukic Z, Mashiba M, Collins KL. Vpr promotes macrophage-dependent HIV-1 infection of CD4+ T lymphocytes. *PloS Pathog* (2015) 11:e1005054. doi: 10.1371/journal.ppat.1005054

57. Lopez P, Koh WH, Hnatiuk R, Murooka TT. HIV Infection stabilizes macrophage-T cell interactions to promote cell-cell HIV spread. *J Virol* (2019) 93 (18):e00805–19. doi: 10.1128/JVI.00805-19

58. Geijtenbeek TB, Kwon DS, Torensma R, van Vliet SJ, van Duijnhoven GC, Middel J, et al. DC-SIGN, a dendritic cell-specific HIV-1-binding protein that enhances trans-infection of T cells. *Cell* (2000) 100:587–97. doi: 10.1016/S0092-8674(00)80694-7

59. Izquierdo-Useros N, Lorizate M, Puertas MC, Rodriguez-Plata MT, Zangger N, Erikson E, et al. Siglec-1 is a novel dendritic cell receptor that mediates HIV-1 trans-infection through recognition of viral membrane gangliosides. *PloS Biol* (2012) 10:e1001448. doi: 10.1371/journal.pbio.1001448

60. Dupont M, Souriant S, Balboa L, Vu Manh TP, Pingris K, Rousset S, et al. Tuberculosis-associated IFN-I induces siglec-1 on tunneling nanotubes and favors HIV-1 spread in macrophages. *Elife* (2020) 9:e52535. doi: 10.7554/eLife.52535

61. Groot F, Welsch S, Sattentau QJ. Efficient HIV-1 transmission from macrophages to T cells across transient virological synapses. *Blood* (2008) 111:4660–3. doi: 10.1182/blood-2007-12-130070

62. Sigal A, Kim JT, Balazs AB, Dekel E, Mayo A, Milo R, et al. Cell-to-cell spread of HIV permits ongoing replication despite antiretroviral therapy. *Nature* (2011) 477:95–8. doi: 10.1038/nature10347

63. Duncan CJ, Russell RA, Sattentau QJ. High multiplicity HIV-1 cell-to-cell transmission from macrophages to CD4+ T cells limits antiretroviral efficacy. *Aids* (2013) 27:2201–6. doi: 10.1097/QAD.0b013e3283632ec4

64. Agosto LM, Zhong P, Munro J, Mothes W. Highly active antiretroviral therapies are effective against HIV-1 cell-to-cell transmission. *PloS Pathog* (2014) 10:e1003982. doi: 10.1371/journal.ppat.1003982

65. Schiffner T, Sattentau QJ, Duncan CJ. Cell-to-cell spread of HIV-1 and evasion of neutralizing antibodies. *Vaccine* (2013) 31:5789–97. doi: 10.1016/j.vaccine.2013.10.020

66. Dufloo J, Bruel T, Schwartz O. HIV-1 cell-to-cell transmission and broadly neutralizing antibodies. *Retrovirology* (2018) 15:51. doi: 10.1186/s12977-018-0434-1

67. Carter CA, Ehrlich LS. Cell biology of HIV-1 infection of macrophages. *Annu Rev Microbiol* (2008) 62:425–43. doi: 10.1146/annurev.micro.62.081307.162758

68. Deneka M, Pelchen-Matthews A, Byland R, Ruiz-Mateos E, Marsh M. In macrophages, HIV-1 assembles into an intracellular plasma membrane domain containing the tetraspanins CD81, CD9, and CD53. *J Cell Biol* (2007) 177:329–41. doi: 10.1083/jcb.200609050

69. Nkwe DO, Pelchen-Matthews A, Burden JJ, Collinson LM, Marsh M. The intracellular plasma membrane-connected compartment in the assembly of HIV-1 in human macrophages. *BMC Biol* (2016) 14:50. doi: 10.1186/s12915-016-0272-3

70. Mlcochova P, Pelchen-Matthews A, Marsh M. Organization and regulation of intracellular plasma membrane-connected HIV-1 assembly compartments in macrophages. *BMC Biol* (2013) 11:89. doi: 10.1186/1741-7007-11-89

71. Jouve M, Sol-Foulon N, Watson S, Schwartz O, Benaroch P. HIV-1 buds and accumulates in "nonacidic" endosomes of macrophages. *Cell Host Microbe* (2007) 2:85–95. doi: 10.1016/j.chom.2007.06.011

72. Hammonds JE, Beeman N, Ding L, Takushi S, Francis AC, Wang JJ, et al. Siglec-1 initiates formation of the virus-containing compartment and enhances macrophage-to-T cell transmission of HIV-1. *PloS Pathog* (2017) 13:e1006181. doi: 10.1371/journal.ppat.1006181

73. Tan J, Sattentau QJ. The HIV-1-containing macrophage compartment: a perfect cellular niche? *Trends Microbiol* (2013) 21:405–12. doi: 10.1016/j.tim.2013.05.001

74. Giese S, Marsh M. Tetherin can restrict cell-free and cell-cell transmission of HIV from primary macrophages to T cells. *PloS Pathog* (2014) 10:e1004189. doi: 10.1371/journal.ppat.1004189

75. Chu H, Wang JJ, Qi M, Yoon JJ, Chen X, Wen X, et al. Tetherin/BST-2 is essential for the formation of the intracellular virus-containing compartment in HIV-infected macrophages. *Cell Host Microbe* (2012) 12:360–72. doi: 10.1016/j.chom.2012.07.011

76. Blanchet FP, Stalder R, Czubala M, Lehmann M, Rio L, Mangeat B, et al. TLR-4 engagement of dendritic cells confers a BST-2/tetherin-mediated restriction of HIV-1 infection to CD4+ T cells across the virological synapse. *Retrovirology* (2013) 10:6. doi: 10.1186/1742-4690-10-6

77. Dupont M, Sattentau QJ. Macrophage cell-cell interactions promoting HIV-1 infection. *Viruses* (2020) 12(5):492. doi: 10.3390/v12050492

78. Martinez-Picado J, McLaren PJ, Telenti A, Izquierdo-Useros N. Retroviruses as myeloid cell riders: What natural human siglec-1 "Knockouts" tell us about pathogenesis. *Front Immunol* (2017) 8:1593. doi: 10.3389/fimmu.2017.01593

79. Azad AK, Rajaram MV, Schlesinger LS. Exploitation of the macrophage mannose receptor (CD206) in infectious disease diagnostics and therapeutics. *J Cytol Mol Biol* (2014) 1(1):1000003. doi: 10.13188/2325-4653.1000003

80. Fanibunda SE, Modi DN, Gokral JS, Bandivdekar AH. HIV gp120 binds to mannose receptor on vaginal epithelial cells and induces production of matrix metalloproteinases. *PloS One* (2011) 6:e28014. doi: 10.1371/journal.pone.0028014

81. Nguyen DG, Hildreth JE. Involvement of macrophage mannose receptor in the binding and transmission of HIV by macrophages. *Eur J Immunol* (2003) 33:483–93. doi: 10.1002/immu.200310024

82. Trujillo JR, Rogers R, Molina RM, Dangond F, McLane MF, Essex M, et al. Noninfectious entry of HIV-1 into peripheral and brain macrophages mediated by the mannose receptor. *Proc Natl Acad Sci U.S.A.* (2007) 104:5097–102. doi: 10.1073/pnas.0611263104

83. Pontow SE, Kery V, Stahl PD. Mannose receptor. *Int Rev Cytol* (1992) 137b:221–44. doi: 10.1073/pnas.0611263104

84. Geijtenbeek TB, Gringhuis SI. C-type lectin receptors in the control of T helper cell differentiation. *Nat Rev Immunol* (2016) 16:433–48. doi: 10.1038/nri.2016.55

85. Taylor PR, Gordon S, Martinez-Pomares L. The mannose receptor: linking homeostasis and immunity through sugar recognition. *Trends Immunol* (2005) 26:104–10. doi: 10.1016/j.it.2004.12.001

86. Sukegawa S, Miyagi E, Bouamr F, Farkašová H, Strebel K. Mannose receptor 1 restricts HIV particle release from infected macrophages. *Cell Rep* (2018) 22:786–95. doi: 10.1016/j.celrep.2017.12.085

87. Koziel H, Eichbaum Q, Kruskal BA, Pinkston P, Rogers RA, Armstrong MY, et al. Reduced binding and phagocytosis of pneumocystis carinii by alveolar macrophages from persons infected with HIV-1 correlates with mannose receptor downregulation. *J Clin Invest* (1998) 102:1332–44. doi: 10.1172/JCI560

88. Vigerust DJ, Egan BS, Shepherd VL. HIV-1 nef mediates post-translational down-regulation and redistribution of the mannose receptor. *J Leukoc Biol* (2005) 77:522–34. doi: 10.1189/jlb.0804454

89. Caldwell RL, Egan BS, Shepherd VL. HIV-1 tat represses transcription from the mannose receptor promoter. *J Immunol* (2000) 165:7035–41. doi: 10.4049/jimmunol.165.12.7035

90. Gartner S, Markovits P, Markovitz DM, Betts RF, Popovic M. Virus isolation from and identification of HTLV-III/LAV-producing cells in brain tissue from a patient with AIDS. *Jama* (1986) 256:2365–71. doi: 10.1001/jama.1986.03380170081023

91. Micci L, Alvarez X, Iriele RI, Ortiz AM, Ryan ES, McGary CS, et al. CD4 depletion in SIV-infected macaques results in macrophage and microglia infection with rapid turnover of infected cells. *PloS Pathog* (2014) 10:e1004467. doi: 10.1371/journal.ppat.1004467

92. Cai Y, Sugimoto C, Liu DX, Midkiff CC, Alvarez X, Lackner AA, et al. Increased monocyte turnover is associated with interstitial macrophage accumulation and pulmonary tissue damage in SIV-infected rhesus macaques. *J Leukoc Biol* (2015) 97:1147–53. doi: 10.1189/jlb.4A0914-441R

93. Igarashi T, Brown CR, Endo Y, Buckler-White A, Plishka R, Bischofberger N, et al. Macrophage are the principal reservoir and sustain high virus loads in rhesus macaques after the depletion of CD4+ T cells by a highly pathogenic simian immunodeficiency virus/HIV type 1 chimera (SHIV): Implications for HIV-1 infections of humans. *Proc Natl Acad Sci U.S.A.* (2001) 98:658–63. doi: 10.1073/pnas.98.2.658

94. Clayton KL, Collins DR, Lengieza J, Ghebremichael M, Dotiwala F, Lieberman J, et al. Resistance of HIV-infected macrophages to CD8(+) T lymphocyte-mediated killing drives activation of the immune system. *Nat Immunol* (2018) 19:475–86. doi: 10.1038/s41590-018-0085-3

95. Honeycutt JB, Wahl A, Baker C, Spagnuolo RA, Foster J, Zakharova O, et al. Macrophages sustain HIV replication *in vivo* independently of T cells. *J Clin Invest* (2016) 126:1353–66. doi: 10.1172/JCI84456

96. Honeycutt JB, Thayer WO, Baker CE, Ribeiro RM, Lada SM, Cao Y, et al. HIV Persistence in tissue macrophages of humanized myeloid-only mice during antiretroviral therapy. *Nat Med* (2017) 23:638–43. doi: 10.1038/nm.4319

97. Ganor Y, Real F, Sennepin A, Dutertre CA, Prevedel L, Xu L, et al. HIV-1 reservoirs in urethral macrophages of patients under suppressive antiretroviral therapy. *Nat Microbiol* (2019) 4:633–44. doi: 10.1038/s41564-018-0335-z

98. Williams DW, Anastos K, Morgello S, Berman JW. JAM-a and ALCAM are therapeutic targets to inhibit diapedesis across the BBB of CD14+CD16+ monocytes in HIV-infected individuals. *J Leukoc Biol* (2015) 97:401–12. doi: 10.1189/jlb.5A0714-347R

99. Kruize Z, Kootstra NA. The role of macrophages in HIV-1 persistence and pathogenesis. *Front Microbiol* (2019) 10:2828. doi: 10.3389/fmicb.2019.02828

100. León-Rivera R, Veenstra M, Donoso M, Tell E, Eugenin EA, Morgello S, et al. Central nervous system (CNS) viral seeding by mature monocytes and potential therapies to reduce CNS viral reservoirs in the cART era. *mBio* (2021) 12 (2):e03633–20. doi: 10.1128/mBio.03633-20

101. Davis LE, Hjelle BL, Miller VE, Palmer DL, Llewellyn AL, Merlin TL, et al. Early viral brain invasion in iatrogenic human immunodeficiency virus infection. *Neurology* (1992) 42:1736–9. doi: 10.1212/WNL.42.9.1736

102. Akiyama H, Gummuluru S. HIV-1 persistence and chronic induction of innate immune responses in macrophages. *Viruses* (2020) 12(7):711. doi: 10.3390/v12070711

103. Joseph SB, Kincer LP, Bowman NM, Evans C, Vinikoor MJ, Lippincott CK, et al. Human immunodeficiency virus type 1 RNA detected in the central nervous system (CNS) after years of suppressive antiretroviral therapy can originate from a replicating CNS reservoir or clonally expanded cells. *Clin Infect Dis* (2019) 69:1345–52. doi: 10.1093/cid/ciy1066

104. Réu P, Khosravi A, Bernard S, Mold JE, Salehpour M, Alkass K, et al. The lifespan and turnover of microglia in the human brain. *Cell Rep* (2017) 20:779–84. doi: 10.1016/j.celrep.2017.07.004

105. Wong ME, Jaworowski A, Hearps AC. The HIV reservoir in monocytes and macrophages. *Front Immunol* (2019) 10:1435. doi: 10.3389/fimmu.2019.01435

106. Perno CF, Newcomb FM, Davis DA, Aquaro S, Humphrey RW, Caliò R, et al. Relative potency of protease inhibitors in monocytes/macrophages acutely and chronically infected with human immunodeficiency virus. *J Infect Dis* (1998) 178:413–22. doi: 10.1086/515642

107. Gavegnano C, Detorio MA, Bassit L, Hurwitz SJ, North TW, Schinazi RF. Cellular pharmacology and potency of HIV-1 nucleoside analogs in primary human macrophages. *Antimicrob Agents Chemother* (2013) 57:1262–9. doi: 10.1128/AAC.02012-12

108. Maina EK, Adan AA, Mureithi H, Muriuki J, Lwembe RM. A review of current strategies towards the elimination of latent HIV-1 and subsequent HIV-1 cure. *Curr HIV Res* (2021) 19:14–26. doi: 10.2174/1570162X18999200819172009

109. Matalon S, Rasmussen TA, Dinarello CA. Histone deacetylase inhibitors for purging HIV-1 from the latent reservoir. *Mol Med* (2011) 17:466–72. doi: 10.2119/molmed.2011.00076

110. Boehm D, Calvanese V, Dar RD, Xing S, Schroeder S, Martins L, et al. BET bromodomain-targeting compounds reactivate HIV from latency *via* a tat-independent mechanism. *Cell Cycle* (2013) 12:452–62. doi: 10.4161/cc.23309

111. Sánchez-Duffhues G, Vo MQ, Pérez M, Calzado MA, Moreno S, Appendino G, et al. Activation of latent HIV-1 expression by protein kinase c agonists. a novel therapeutic approach to eradicate HIV-1 reservoirs. *Curr Drug Targets* (2011) 12:348–56. doi: 10.2174/138945011794815266

112. Rodari A, Darcis G, Van Lint CM. The current status of latency reversing agents for HIV-1 remission. *Annu Rev Virol* (2021) 8:491–514. doi: 10.1146/annurev-virology-091919-103029

113. Grau-Expósito J, Luque-Ballesteros L, Navarro J, Curran A, Burgos J, Ribera E, et al. Latency reversal agents affect differently the latent reservoir present in distinct CD4+ T subpopulations. *PloS Pathog* (2019) 15:e1007991. doi: 10.1371/journal.ppat.1007991

114. Einkauf KB, Osborn MR, Gao C, Sun W, Sun X, Lian X, et al. Parallel analysis of transcription, integration, and sequence of single HIV-1 proviruses. *Cell* (2022) 185:266–282.e215. doi: 10.1016/j.cell.2021.12.011

frontiers | Frontiers in Virology

TYPE Original Research
PUBLISHED 30 August 2022
DOI 10.3389/fviro.2022.932187

OPEN ACCESS

EDITED BY
Akio Adachi,
Kansai Medical University, Japan

REVIEWED BY
George N. Pavlakis,
National Cancer Institute (NIH), United States
Maxim Totrov,
Molsoft (United States), United States

*CORRESPONDENCE
Shuzo Matsushita
shuzo@kumamoto-u.ac.jp

†These authors have contributed equally to this work and share first authorship

SPECIALTY SECTION
This article was submitted to Fundamental Virology, a section of the journal Frontiers in Virology

RECEIVED 29 April 2022
ACCEPTED 08 August 2022
PUBLISHED 30 August 2022

CITATION
Kaku Y, Matsumoto K, Kuwata T, Zahid MdH, Biswas S, Gorny MK and Matsushita S (2022) Development and characterization of a panel of anti-idiotype antibodies to 1C10 that cross-neutralize HIV-1 subtype B viruses. *Front. Virol.* 2:932187. doi: 10.3389/fviro.2022.932187

Development and characterization of a panel of anti-idiotype antibodies to 1C10 that cross-neutralize HIV-1 subtype B viruses

Yu Kaku[1†], Kaho Matsumoto[1†], Takeo Kuwata[1], Hasan Md Zahid[1], Shashwata Biswas[1], Miroslaw K. Gorny[2] and Shuzo Matsushita[1*]

[1]Clinical Retrovirology, Joint Research Center for Human Retrovirus Infection, Kumamoto University, Kumamoto, Japan, [2]Department of Pathology, New York University (NYU) School of Medicine, New York, NY, United States

The V3 loop of the human immunodeficiency virus type 1 (HIV-1) envelope protein (Env) is one of the conserved immunogenic regions targeted by neutralizing antibodies (nAb). Two different binding modes of anti-V3 abs have been reported in studies using two V3 mimotopes: the ladle-type and cradle-type. We previously isolated a ladle-type nAb, 1C10, that potently and broadly neutralized clade B viruses. Despite its potent neutralization activity, 1C10 possesses no unique features in its amino acid sequence. We hypothesized that the neutralization potency of 1C10 is derived from its antigen-binding characteristics, which are not a consequence of the two previously reported binding modes of anti-V3 nAbs. To analyze epitope-paratope interactions between 1C10 and the V3 loop, we produced five anti-idiotypic antibodies (anti-Id abs) from mice immunized with 1C10 nAb. The idiotopes of the anti-Id Abs on the 1C10 heavy chain were estimated by alanine scanning, germline reversion mutagenesis, and a 1C10 sibling clone. Next-generation sequencing combined with homology modeling revealed contact between R315 at the tip of the V3 loop and 1C10 by D53 of CDRH2 and Phe/Asp of CDRH3. These amino acids were enriched in the anti-Id-ab-reactive B cell receptors encoded by the IGHV3-30 gene. We also found that 20% of HIV-infected individuals had abs specific to the anti-Id abs, as well as both of the V3 mimotopes, that did not respond to the linear V3 peptide. Our findings showed that the anti-Id abs induced by 1C10 recognized a key amino acid formation essential for steric interactions between the ladle-type nAb and the V3 loop. We also revealed the coexistence of anti-V3 ab reactivity to V3 loop mimotopes and to the anti-Id abs in HIV-positive individuals.

KEYWORDS

HIV-1, neutralizing antibody, vaccine, anti-idiotypic antibody, anti-V3 antibody

Introduction

Eliciting potent neutralization antibodies (nAbs) is the ultimate goal of the development of vaccines against human immunodeficiency virus type 1 (HIV-1). To date, various vaccines have been developed to induce nAbs targeting the conserved regions of the virus (1–7). The V3 loop of the HIV-1 envelope protein is a target for nAbs, of which glycan epitopes are specifically targeted by broadly neutralizing antibodies (bnAbs) and glycan-independent epitopes are recognized by most anti-V3 antibodies (abs) (8–14). Two types of the latter epitopes have been identified thus far, ladle-like and cradle-like epitopes, which are recognized by V3 mimotopes (15–17). In the binding of anti-V3 Abs to the two epitopes, ladle-type abs recognize the hydrophobic face of the circlet region, in which Gly-Phe-Gly-Arg/Gln (GPGR/Q) at the tip of the V3 loop is found along heavy chain complementarity-determining region 3 (CDRH3) (18–20). Conversely, cradle-type abs attach to the epitope by binding to the band and circlet regions on both sides of the V3 loop. In other words, the former type of binding mode requires a long CDRH3, which forms the handle of the "ladle", and the latter type requires a binding cavity consisting of both a heavy chain and a light chain, which form the "cradle." In fact, cradle-type abs are predominantly derived from the IGHV5-51 gene paired with light chain variable region (VL) lambda gene, and are detected in vaccinees' plasma as non- or weak-nAbs (15, 16, 21, 22). However, it remains unclear if ladle-type abs possess any unique structural features other than the longer-length CDRH3, especially those that are derived from the same immunoglobulin gene segment and can be elicited by vaccination.

From an elite controller, we previously isolated 1C10, which is a potent ladle-type anti-V3 Ab capable of neutralizing 80% of clade B viruses, including 30% of primary isolates of a major subtype in Japan (23). Despite its potent and broad-spectrum neutralization ability, 1C10, which is encoded by the major immunoglobulin gene IGHV3-30, has features common to many antibody types, including an 18-amino-acid-long CDRH3 region. In contrast, bnAbs possess a higher somatic hypermutation (SHM) rate, longer length CDRH3, and novel nucleotide insertions or deletions compared with most antibodies (12, 24–32). Although the details of 1C10's neutralization potency have not yet been revealed, the induction of 1C10 requires no specific conditions and can be elicited by a vaccine (23, 33, 34). In this study, we generated anti-idiotypic abs that bound to the paratope (or binding cavity) of 1C10 to analyze the key characteristics that make 1C10 a potent anti-V3 nAb. We also aimed to discover the steric structures shared by subgroups of ladle-type abs.

Materials and methods

Immunization of mice by 1C10 and generation of anti-Id abs

We injected 200 μg of 1C10 into the tail vein of each 6-week-old BALB/c mouse in a prime immunization and the same amount into the peritoneal cavity in further immunizations. After five immunizations at 2-week intervals, the mice were sacrificed and the spleens were extracted. We isolated B220+IgM-IgG+ B cells positive for 1C10 as single cells from the spleens by FACS AriaII (BD, NJ, USA). Following the method reported previously (35), we amplified variable regions of IgG heavy and light chains by RT-PCR and inserted each of the regions into respective expression vectors by means of murine IgG-specific primer pairs.

Competitive inhibition ELISA

After incubating a Maxisorp plate (Invitrogen, MA, USA) coated with 0.2 μg NNT-20 JR-FL overnight, which is V3 peptide of HIV-1 clade B strains JR-FL consisting of 20 amino acids (AAs) started from NNT (NNTRKSIHIGPGRAFYTTGE), the plate was blocked by adding 0.1% BSA/PBS for 30 minutes. Anti-Id abs were dispensed into each well at various concentrations from 1 μg to 39 ng and incubated for 30 minutes followed by the addition of 0.1 ng biotinylated 1C10 and 1 hour of incubation. Binding of 1C10 to NNT-20 JR-FL was detected by measuring the OD value (405 nm) following the addition of streptavidin-HRP and 2,2'-azino-bis(3-ethylbenzothiazoline)-6-sulfonic acid (ABTS).

Binding ELISA using 1C10 mutants and anti-Id abs

Germline reversion of 1C10 was achieved by AA-replacement of the 1C10 heavy chain variable region (VH) with IGHV3-30 AAs by overlap-extension PCR as we previously described (36). Purified germline 1C10 was dispensed onto a Maxisorp plate (Invitrogen, MA, USA) at 2 μg/well and incubated overnight. After blocking by the addition of 0.1% BSA/PBS, biotinylated anti-Id abs were added to each well as serially diluted concentrations from 1 μg to 39 ng and 1 hour of incubation. Binding of anti-Id abs to germline-reverted 1C10 was detected by measuring the OD value at a wavelength of 405 nm following the addition of streptavidin-HRP (ThermoFisher, MA, USA) and ABTS (Roche, Switzerland). The binding ELISA was also performed to assess the effect of

alanine-scanning mutagenesis of the 1C10 CDRH3 contact residues on binding to the anti-Id abs.

Single-cell sorting for 1C10 lineage analysis

Single-cell sorting was performed to isolate abs reactive to the anti-Id ab clones, as previously reported (35), from an HIV-infected patient who was an elite controller and had a plasma viral load constantly below the detection level. Briefly, after CD3-CD8-CD14-cells were negatively sorted from peripheral blood mononuclear cells (PBMCs) using a MojoSort magnet (BioLegend, CA, USA), CD19+CD27+7AAD-IgM-IgG+ B cells that bound to the anti-Id abs were sorted as single cells. The IgG variable regions from the sorted cells were amplified as described above and used for both sequence analysis and cloning into expression vectors for functional analysis. The sequence of the variable region was analyzed by International ImMunoGeneTics (IMGT) and Basic Local Alignment Search Tool (BLAST) searching. Functional analysis was performed using binding ELISA.

NGS analysis of anti-Id-ab-reactive B cell receptors

CD19+CD27+IgM-IgG+ B cells reactive to anti-Id abs #87 and #102 were isolated by single-cell sorting as a biased group and CD19+CD27+IgM-IgG+B cells were negatively sorted by MojoSort Magnet (BioLegend) as an unbiased group from PBMCs of the elite controller. Single-cell RNA-seq was performed using 10X Chromium (10X Genomics, CA, USA) following the manufacturer's protocol.

AlphaScreen for antigen-antibody binding

AlphaScreen (PerkinElmer, Switzerland) was performed to examine the binding between either 1C10 or 3-32 and the looped V3 mimotopes. Mixtures of 2 μg/ml and 20 μg/ml, respectively, were incubated for 40 minutes room temperature. Binding was detected by anti-hIgG acceptor beads and streptavidin donor beads 40 minutes after the addition of the analyte mixture.

Anti-Id-ab Fabs and plasma IgGs obtained from HIV-positive patients' plasma at 2 μg/ml and a 1:1000 dilution, respectively, were incubated for 40 minutes room temperature. Binding was measured by anti-6x His acceptor beads and protein A donor beads 40 minutes room temperature after the addition of the analyte mixture.

Statistics

Correlation coefficients (CC) were calculated by Pearson's correlation. The network map of CC among the contact residues was drawn using NetworkX.

Homology modeling and data visualization

A 1C10 homology model was constructed as described in our previous report (36). In detail, we selected four ladle abs, three unclassified abs, and two cradle abs for which the crystal structures were available as templates for homology modeling of 1C10. Homology models of 1C10 were generated with the SWISS-model (37). First, screening was completed using rigid-body docking simulations with a native V3 loop in zdock (38). Second, flexible-docking simulation by Rossie (39) was performed on the first and second ranked ladle abs and unclassified abs by zdock score. Among the four homology models, we chose the 1C10 homology model using 1334 as the template based on the highest Rossie score of 1369.64. A 1C10-V3 loop complex model was created using 1334 (PDB: 6DB7) and the JRFL V3 loop sequence. Structure models were depicted with Pymol (40), and interactions between the heavy chain and R315 at the tip of the V3 loop in the model were detected using AppA (41). The interface residues of the heavy chain and the V3 loop were identified with the Pymol script, InterfaceResidues.

Results

Specific inhibition of binding of 1C10 to V3 peptide by five anti-Id abs

Using mice immunized with 1C10, we created anti-Id abs against 1C10 as mouse-human chimeric antibodies consisting of murine variable regions and human constant regions. Of these, anti-Id abs specific to the paratope of 1C10 were selected by competitive inhibition against biotinylated anti-V3 abs showing binding to NNT-20 JR-FL (NNTRKSIHIGPGRAFYTTGE) in ELISA. Five different anti-Id ab clones showed interference, not between the V3 peptide and other ladle-type anti-V3 abs, such as KD-247, 5G2, 1D9, 19F8, and 717G2, but between the V3 peptide and 1C10 (Figure 1 and Supplementary Table 1).

Three predicted idiotopes of anti-Id abs determined by germline-reverted 1C10

We first assessed the region of the 1C10 paratope targeted by the anti-Id abs using 1C10 mutants. For this purpose, we

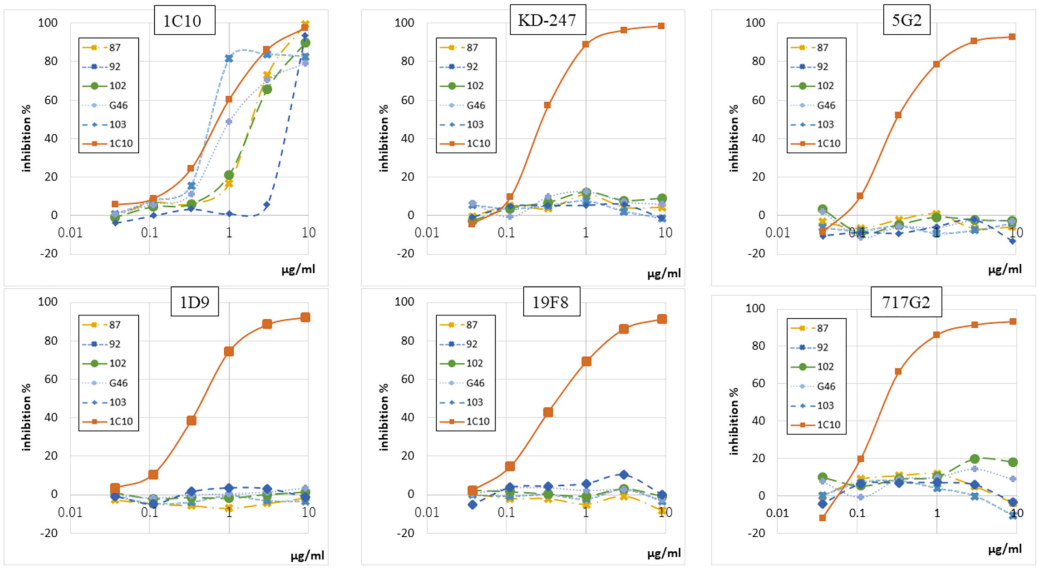

FIGURE 1
Five anti-Id abs inhibited only 1C10 among six anti-V3 abs. Binding-inhibition ability of five anti-Id abs (87, 92, 102, G46, and 103), which interfere with interactions between anti-V3 abs and NNT-20, was determined by binding-inhibition ELISA using five anti-V3 abs (1C10, KD-247, 5G2, 1D9, 19F8, 717G2) conjugated to biotin. Unconjugated 1C10 was used as a control binding inhibitor for all anti-V3 abs.

constructed germline-reverted forms of the 1C10 heavy chain VH (Supplementary Figure 1, Figure 2A). We found that all five anti-Id abs bound to the germline-reverted 1C10 mutants in various patterns but did not react to the inferred germline. The result indicated that #87, #102, and #103 had decreased binding potency to the CDR2 mutation, #92 had decreased binding potency to the FR3 mutation, and #G46 had decreased binding potency to the CDR1 mutation (Figure 2B).

We next assessed the effects of alanine substitutions at the contact residues of 1C10 CDRH3 that we previously predicted (36) on the anti-Id abs by binding ELISA. Among the contact residues (D95, D97, P100a, and D100b), interactions were observed between D95 and #103, D97 and #102, either or both P100a and D100b, and #87 and #92. While most of the alanine substitutions resulted in a reduced or unchanged interaction strength with anti-Id abs, all substitutions, other than D95, enhanced the affinity of #102 to 1C10 (Figure 2C).

Lineage specificity of the anti-Id abs for 1C10 lineage

To identify the conformation shared by abs in the 1C10 lineage, antibody-expressing B cells (CD19+CD27+IgM-IgG+) were sorted as single cells using all five anti-Id ab clones from PBMCs of the HIV-1-positive patient, who produced 1C10. From 326 antibody-expressing B cells, we extracted 35 antibody clones, including one 1C10 sibling clone, 3-32. The same AA sequence was shared between 3-32 and 1C10 CDR3, other than 23 AAs of the heavy chain and one AA of the light chain. This also corresponds to the fact that both ab clones are encoded by the same V gene and have the same CDR3 length (Figure 3A). The binding of 3-32 to both looped V3 peptides and the linear V3 peptide (NNT-20) significantly decreased in strength compared with that of 1C10 (Figure 3B).

According to our previous prediction (36), there is one contact residue in CDRH1 (N31), two contact residues in CDRH2 (D53 and D56), and one contact residue in FR3 (D61), in addition to the four contact residues in CDRH3. Of these positions, 3-32 possessed N31 and D56, which are mutated from germline AAs, as in 1C10, and V100b, which is different from the D100b of 1C10 (Figure 3A). Furthermore, 3-32 enhanced the binding of #102, despite the decreased interactions with the other four anti-Id ab clones (Figure 3C).

Deviation caused by the anti-Id abs explored by NGS

We analyzed the idiotopes that were shared by abs produced by an individual who produced 1C10 that were targeted by the anti-Id abs. On the basis of idiotopic analysis of 1C10 VH, we selected two CDRH2-specific anti-Id abs for NGS analysis, #87 and #102, with opposing affinities to mutations of the contact residues. We isolated CD2-CD14-CD16-CD36-CD43-Cd235a-B cells (unbiased B cells) as total B cells with magnet beads for

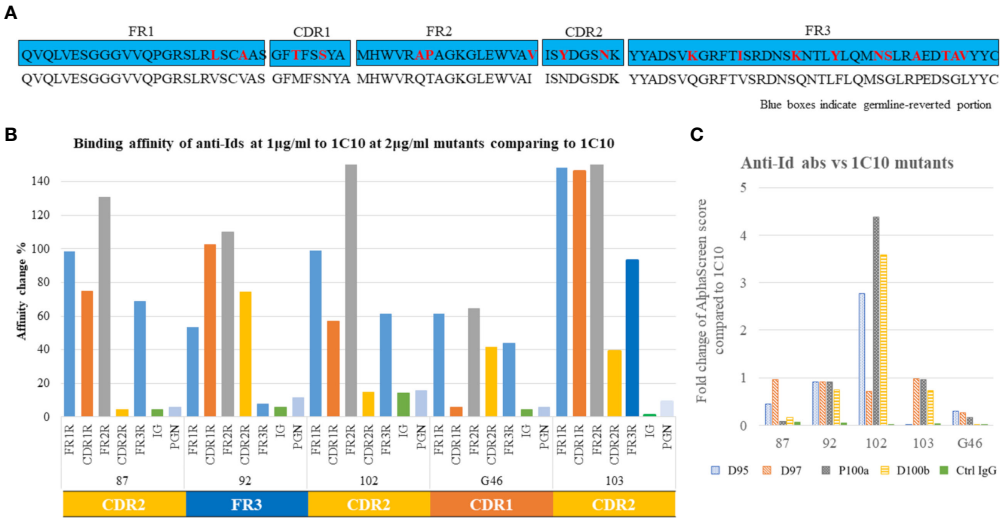

FIGURE 2
Idiotope classification. Germline reversion of 1C10 was created by overlap PCR to replace five portions of the heavy chain variable region (VH), including framework regions (FR)1-3 and complementarity determining regions (CDR)1-2, with their germline amino acid (AA) sequences. Germline sequences are shown in blue boxes, with replaced AAs as red letters, and the 1C10 sequence is shown below the blue box. **(A)** Binding of anti-Id abs to germline-reverted 1C10, including inferred germline (IG) and human polyclonal IgG (Ctrl IgG), was tested by binding ELISA and expressed as percentage affinity change, calculated as a relative value based on binding to 1C10. The binding patterns of the anti-Id abs resulted in three types: CDR1-, CDR2-, and FR3-specific types. **(B)** Alanine scanning mutagenesis was applied to four contact residues of 1C10 CDRH3 (D95, D97, P100a, and D100b). Binding ELISA was used to examine the binding of the anti-Id abs to the 1C10 mutants containing alanine **(C)**.

analysis of the whole BCR repertoire of the individual. We also sorted B cells (CD19+CD27+IgM-IgG+) expressing idiotypic abs capable of binding to #87 and #102 to analyze the BCRs expressed on the responder B cells (biased B cells). Single-cell RNA-seq of BCRs was performed on 21,179 BCRs of unbiased B cells and 2,164 BCRs of biased B cells by 10X chromium, and we found 1,008 CDRH3s and 1,253 CDRH3s from each BCR group. In the IGHV3 BCR, we focused on five Asp residues and one Asn residue at the same positions as the predicted contact residues of 1C10 shown in Figure 3A. Of interest, Phe/Asp (PD) at any place in CDRH3 were analyzed as residues corresponding to the P100a and D100b of the 1C10 CDRH3. We obtained BCRs containing 35 and 64 N31, 165 and 212 D53, 4 and 5 D56, 138 and 209 D95, and 9 and 19 PD from the unbiased and biased groups, respectively (Figure 4A). In addition to CDRH3 length and the mutation ratio of the IGHV gene, IGHV3 usage was also increased in the biased group compared to the unbiased group (55.7% vs 32.8%) (Figure 4B).

Although there were no correlations among the contact residues, once both BCR groups were classified by the possession of a single contact residue, several correlations appeared among the other contact residues. In the unbiased group, D56 and D97, and D53 and D95 correlated with the possession of N31 and D95, respectively. In the biased group, D53 and D97 were associated with PD when one of the two residues existed. Furthermore, in biased BCRs containing either D56 or PD in their CDRH3 region, N31 and D95 were correlated (Figure 5, Supplementary Figure 2). The results indicate the coexistence of these AAs in individual BCRs of each group; the AA pairs in the biased group, especially, implied the presence of epitopes for the anti-Id abs.

1C10 homology model

We selected a ladle-type ab, 1334, as a template for homology modeling based on its zdock score and Rossie score. The V and D segments of 1C10 and 1334 are encoded by IGHV3-30 and IGHV1-3, and IGHD2-21 and IGHD3-9, respectively, while the J segments of both antibodies are encoded by IGHJ4. The root mean square deviation of the 1C10 homology model and 1334 was 0.315, which was the lowest value among ladle-type abs, though it was higher than the unclassified and cradle-type abs. This difference was attributed to the longer CDRH3 of the ladle-type abs compared with other ab types (Supplementary Table 2, Figure 6A).

The 1C10-homology model constructed using SWISS-model exhibited a negatively charged binding cavity consisting of both heavy and light chains. More than half (57.0%) of this binding pocket is formed by the heavy chain, especially by CDRH3 (23.9%), and the remaining area (42.9%) is formed mainly by CDRL1 (23.2%) (data not shown).

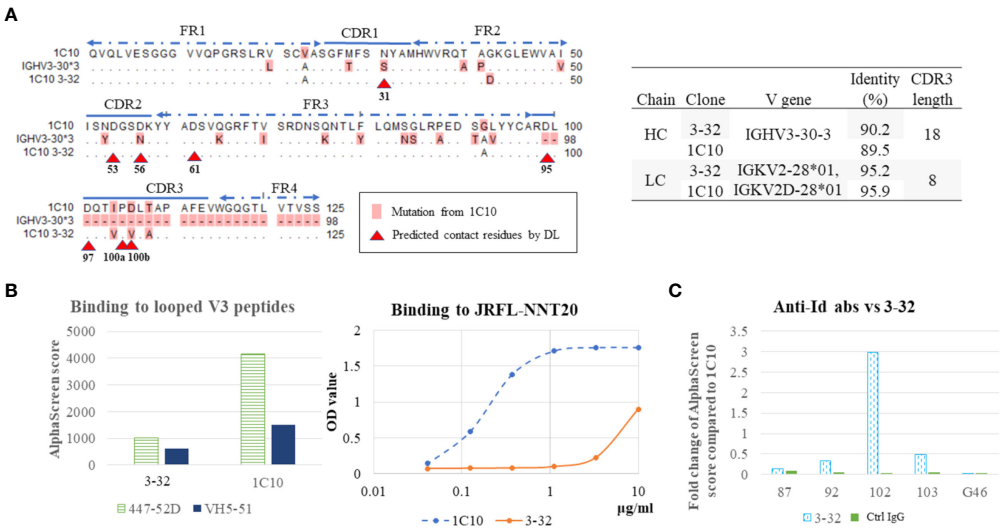

FIGURE 3
Antibody of 1C10 lineage bound weakly to V3 loops. Amino acid **(AA)** sequence alignment of heavy chain variable regions of 1C10, germline (IGHV3-30), and a sibling antibody of 1C10 lineage (3-32). The different AAs are highlighted as pink, and predicted contact residues detected by deep learning (DL) are indicated by red arrow heads. Gene usage of the two antibody clones was analyzed with the Basic Local Alignment Search Tool (BLAST) and results are in the table on the right **(A)**. Binding of 1C10 and 3-32 to two looped V3 mimotopes (447-52D and VH5-51) was tested by AlphaScreen, and binding to the linear V3 loop peptide (JRFL-NNT20) was assayed with ELISA **(B)**. Interaction between anti-Id antibodies and 3-32 were examined using AlphaScreen **(C)**.

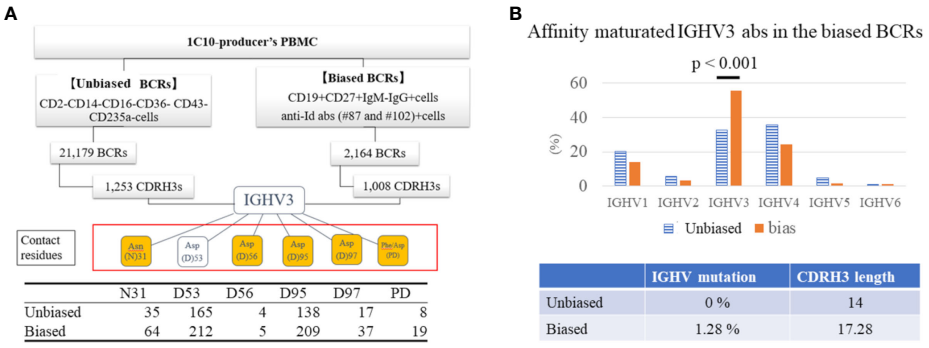

FIGURE 4
IGHV3 BCR responded to anti-Id abs. BCRs were analyzed in CD2-CD14-CD16-CD36-CD43-Cd235a B cells (unbiased BCRs) as total BCRs and in CD19+CD27+IgM-IgG+ B cells with response to anti-Id ab #87 and #102 (biased BCRs) respectively sorted from an elite controller. We obtained 1,253 CDRH3s from unbiased BCRs and 1,008 CDRH3s from biased BCRs. Finally, we analyzed five aspartic acid (Asp) residues and one asparagine (Asn) residue at the same positions as contact residues of 1C10 in IGHV3 abs. Amino acids (AAs) in orange boxes are mutated AAs from germline, of which N31 is located in CDR2, and sequential phenylalanine (Phe) and Asp residues (PD) are considered mutated AAs corresponding to P100a and D100b. The table at the bottom shows the number of IGHV3 CDRH3 regions containing each residue **(A)**. Unbiased and biased BCRs were compared for genes encoding immunoglobulin heavy chain variable (IGHV) regions, mutation ratio of AAs of IGHV, and length of CDRH3 **(B)**.

In this model, correlated contact residues detected by NGS analysis formed a part of the 1C10 binding pocket. In the complex model with the V3 loop, the R315 at the tip of the V3 loop was placed close to D53 or D100b of PD, which were correlated AAs in the biased group (Figure 6B). Interactive contact analysis of these close AAs by AppA also suggested the formation of strong interactions comprising hydrogen bonds, VdW interactions, and ionic interactions. This is comparable to the binding of 1334 to the V3 loop, which uses CDRH2, including N52, D53, and D54, and CDRH3, including

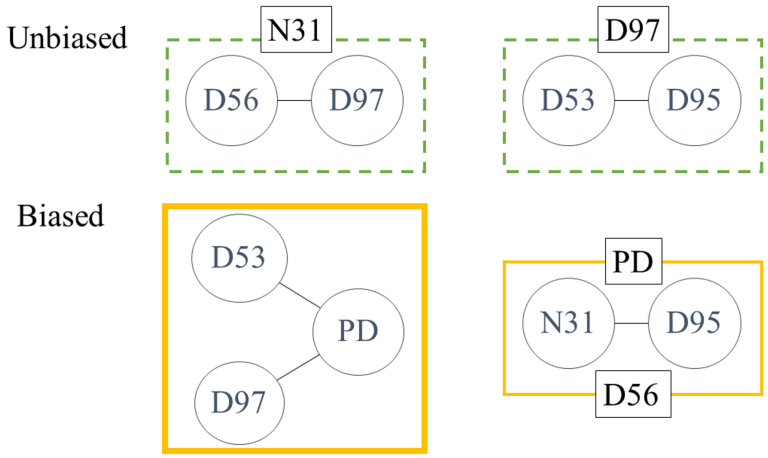

FIGURE 5
Correlated AAs in both samples. Within six subgroups of both unbiased and biased BCRs classified using one of the contact residues (N31, D53, D56, D95, D97, and PD), correlations among other contact residues were calculated by Pearson's correlation. Two correlations were detected in subgroups containing either N31 or D97 in unbiased BCRs. In biased BCRs, D53 and D97 were correlated to PD when the subgroup was chosen by the other residue. The correlation between N31 and D95 was seen in both PD and D56 subgroups. Amino acids are annotated by Kabat numbering.

D99. Intriguingly, the D99 of 1334 CDRH3 comprises a PD sequence with P98 (Figure 7, Table 1).

Correspondence between anti-Id abs and V3 peptides

We tested the polyclonal ab responses of HIV-positive patients' plasma samples and anti-Id ab binding to V3 peptides with AlphaScreen. We used the linear V3 peptide and cyclic V3 mimotopes (447-D and VH5-51 type peptides), which were reported to be involved in the differentiation into the two binding modes of anti-V3 abs (cradle-type and ladle-type) (15). Among the 44 plasma samples, there were 12 (27.2%) with reactivity to the anti-Id abs mixture, 10 (22.7%) with reactivity to the cyclic V3 peptides, and 5 (11.3%) with reactivity to the linear peptide. No correlation in reactivity was found between anti-Id abs and the linear peptide (NNT-20 JR-FL). Responders to the

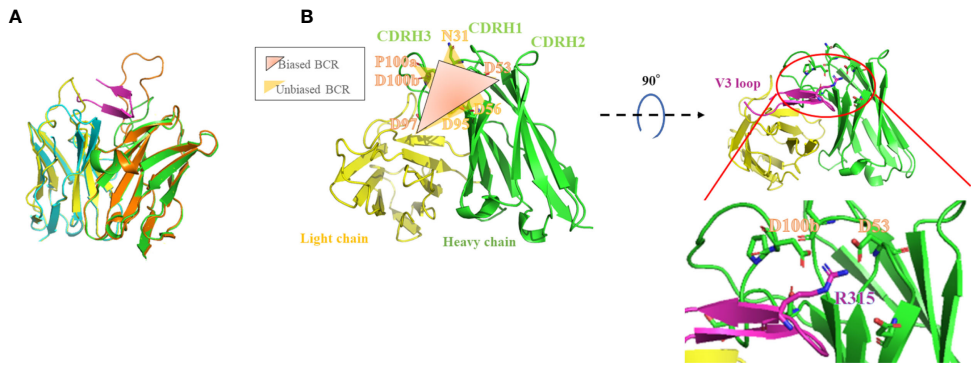

FIGURE 6
1C10 homology model illustrates contact residues on the adapted structure located close to the V3 tip region. The crystal structure of 1334 (PDB: 6db7) is superposed onto the 1C10 homology model. Heavy and light chains of 1334 are drawn as orange and light blue ribbons, respectively, and those of 1C10 are light green and light blue, respectively, and the V3 loop is magenta **(A)**. The structures composed by the correlated amino acids (AAs) in biased BCRs and unbiased BCRs are drawn in the 1C10 homology model as graduated dark orange triangles consisting of D53, D97, and PD, and yellow triangles consisting of N31, D56, and D97, and D53, D95, and D97, respectively (left). The positions of D53 of 1C10 CDRH2, D100b of 1C10 CDRH3, and R315 of the V3 loop are also depicted in the homology model (right) **(B)**. AAs are annotated by Kabat numbering.

10.3389/fviro.2022.932187

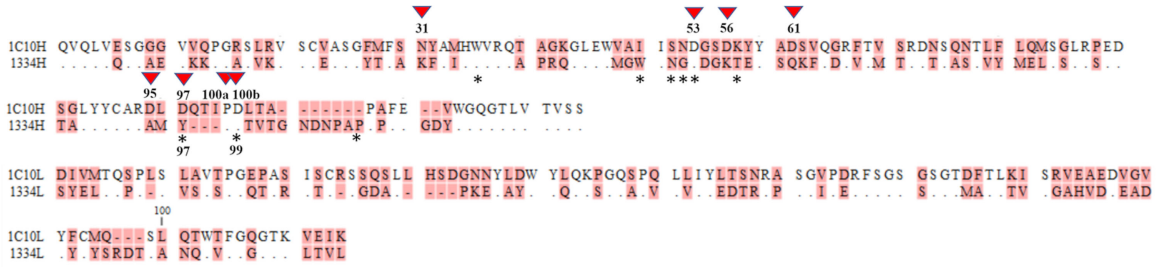

FIGURE 7
Contact residues between the V3 loop and 1C10 and 1334. Contact residues of the 1C10 heavy chain are numbered with down forward arrow heads and those of 1334 are indicated by asterisks. Different amino acids are highlighted in pink, and the same residues are shown by dots. Amino acids are annotated by Kabat numbering. The single asterisk and the double asterisk indicate the elite controller who produced 1C10 and a healthy donor, respectively.

anti-Id abs also bound to the cyclic peptides (Figure 8). Interestingly, the plasma IgG responses of the responders to each V3 mimotope were equally strong, other than the response of the elite controller who produced 1C10. This result suggests that the anti-Id abs form a structure similar to the steric structure shared by both cyclic V3 mimotopes but not by the linear V3 peptide.

Discussion

The purpose of this study was using anti-Id abs to investigate the structural features of 1C10 as a potent ladle-type anti-V3 nAb without a long CDRH3 and as an ab originated from the IGHV3 gene. Our data demonstrated that components of the 1C10 paratope shared among IGHV3 abs corresponded to the response to the V3 loop. For this purpose, we generated five anti-Id antibodies specific for the 1C10 paratope without cross-reactivity against other anti-V3 abs. The results of binding to germline-reverted 1C10s revealed that the five anti-Id ab clones should have unique steric structures that consist of at least two epitopes: an epitope bound by 1C10 contact-residue-like AAs on CDRH2 and CDRH3 and an epitope shared with the cyclic V3 loop of a mimotope. The anti-Id abs were specific to 1C10 and predominantly recognized the idiotopes on CDRH2. In addition, alanine replacement at contact residues also showed the existence of the idiotopes of 1C10 CDRH3 based on changes to the anti-Id ab binding potency. More evidence was provided by a 1C10 sibling clone showing many different AAs of CDR3 in 3-32, especially N31S, D56N, and D100bD, at contact residues, leading to a loss of affinity to the V3 loop and alterations to anti-Id ab recognition (Figures 4A, B). Our NGS data suggested that the anti-Id abs recognized the same AAs at the same positions or order as the contact residues of 1C10 CDRH3. In particular, D53 of CDRH2 correlated to D97 and PD of CDRH3 in the biased IGHV3 BCRs. Other combinations were found in D56 of CDRH2 or PD, N31 of CDRH1, and D95 of CDRH3. The homology model postulated strong interactions between D53 or D100b and R315, which is known to be a conserved immunogenic AA on the tip of the clade B virus V3 loop (11). The crystal structure determined for 1334 yielded evidence for the involvement of D53 and PD in contact between the V3 loop and ladle-type abs. This also gave rise to our interest in the interaction between 1334 and the anti-Id ab clones, which should be explored in more detail.

TABLE 1 Contact residues of interface between R315 and 1C10 or 1334.

	Contact AA	Hydrogen Bond	Hydrophobic	VdW	Ionic
1C10	D53	2	0	7	4
	D100b	1	0	5	4
1334	N52	0	0	2	0
	D53	1	0	3	4
	D54	1	0	4	4
	D99	1	0	4	3

Interactions between either D53 or D100b and R315 and 1334 heavy chains and R315 were analyzed by AppA. Amino acids are annotated by Kabat numbering.

In the binding assay, 27.2% (12/44) of HIV-infected patients were shown to possess plasma IgGs reactive to the anti-Id abs, of which 75% (9/12) also bound to both types of V3 mimotopes equally. Interestingly, only the elite controller, who produced 1C10, had plasma IgG that bound to the NNT-20 JRFL peptide, namely the linear peptide, and preferentially bound to the 447-52D mimotope rather than the VH5-51 mimotope. The relatively low plasma response, namely 22% (2/9, to the linear peptide in the anti-Id abs and V3 mimotope responders was considered to be a specific immune response in the moderately inflammatory chronic phase of HIV-1 infection, as opposed to a non-specific immune response in the acute phase. This plasma response specific to the V3 mimotopes consisted of both a

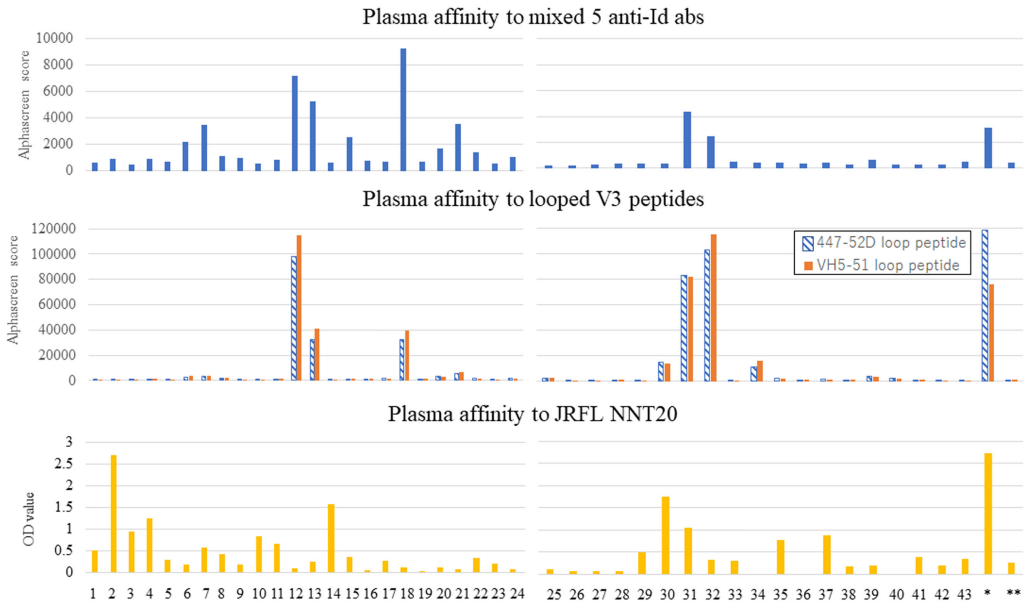

FIGURE 8
Affinity of 44 patients' plasma to anti-Id abs correlated to that to looped V3 peptides. Plasma samples from 44 HIV-positive patients were collected to investigate the binding of IgG in sera to a mixture of the five anti-Id abs, the looped V3 peptides (447-52D and VH5-51), and a linear V3 peptide (JRFL NNT20). The former two affinities were examined by AlphaScreen, and the latter affinity was shown by ELISA.

response to the 447-52D (ladle-type) mimotope and a response to the VH5-51 (cradle-type) mimotope. However, cradle-type abs specific to the VH5-51 mimotope have been reported to be vaccine-inducible abs with cross-neutralizing activities due to binding to conserved residues. Conversely, the ladle-type abs may be potent but are more specific to viruses with R315 at the tip of the V3 region (15, 21, 42–44).

Despite the current study's lack of crystal structural analyses, bioinformatic analysis using the anti-Id abs asserted that the anti-Id abs specifically recognize the D53 and D100b that form solid bonds between the 1C10 heavy chain and R315 of the V3 tip region. This contributed to results showing that the anti-Id abs targeted IGHV3-30 abs with higher SHM rates and a longer CDRH3 length, and the anti-Id abs derived a synchronized response to cyclic V3 mimotopes from HIV-infected individuals. These findings concur with the idea that, in addition to cradle-type abs, subgroups of ladle-type abs lacking the typical feature of a long CDRH3 are induced by vaccines.

Conclusion

In this report, we first described the remarkable features of mouse anti-Id abs raised against the potent cross-neutralizing human anti-V3 mAb 1C10. Our data indicate that the anti-Id abs target not only the distinctive AAs shared among 1C10-like abs but also the conformational epitope corresponding to epitopes of anti-V3 ab specific to cyclic V3 mimotopes. Of note, 20% of individuals chronically infected with HIV-1 produced anti-V3 abs cross-reactive to the anti-Id abs. These results help to confirm our hypothesis that subgroups of ladle-type abs are derived from a certain immunoglobulin gene and can be elicited by vaccination.

The findings may also lead to a strategy to induce 1C10-like anti-V3 nAbs in HIV-1-infected individuals using anti-Id abs, based on the idea that anti-Id abs mimic an antigen of their target antibody, which first appeared in the "idiotypic network theory" (45–47). By way of illustration, a recent study demonstrated bnAb precursor B cells can be activated by BCR cross-links with anti-Id abs (48). Further studies are needed to complete our comprehension of the effects of these anti-Id abs on responsive B cells; such studies may include structural analyses to investigate the interfaces within complexes of anti-Id abs and 1C10 as well as the V3 loop and 1C10, *in vivo* experiments to examine the abs induced by the anti-Id abs, and experiments to test the neutralization ability of 1C10-like abs.

Data availability statement

The datasets presented in this study can be found in online repositories. The names of the repository/repositories and accession number(s) can be found below: GenBank, accession numbers OP006668-OP006677.

Ethics statement

The studies involving human participants were reviewed and approved by the ethics committee for Clinical Research and Advanced Medical Technology at the Kumamoto University Medical School. The patients/participants provided their written informed consent to participate in this study. The animal study was reviewed and approved by Institutional Animal Care and Use Committee at Kumamoto University.

Author contributions

YK, KM, TK, and SM designed the experiments. YK generated anti-idiotypic antibodies, germline-reverted mutants and isolated B cells. YK, KM, HZ, and SB performed antibody cloning. YK performed binding and inhibition assay. MG produced V3 mimotopes. YK did homology modeling and next generation sequencing. YK, KM, TK, and SM interpreted data and prepared the figures and wrote the first draft and MG revised the draft. SM designed the study and SM and MG coordinated the study. All authors contributed to manuscript revision, read, and approved the submitted version.

Funding

This work was supported in part by Global Education and Research Center Aiming at the Control of AIDS, by JSPS KAKENHI Grant Number18H0285400 and by a grant for Research Program on HIV/AIDS from the Japan Agency for Medical Research and Development (JP19fk0410025h0001, JP20fk0410025h0002, JP21fk0410025h0003, JP22fk0410054h0001).

Acknowledgments

The looped V3 mimotopes were kindly gifted by MG. We thank Ms. Noriko Kuramoto, Yoko Kawanami, and Mikiko Shimizu for their assistance in the experiments, and Chie Hirai for her kind administrative assistance and Suzanne Leech, PhD, from Edanz (https://jp.edanz.com/ac) for editing a draft of this manuscript.

Conflict of interest

The authors declare that the research was conducted in the absence of any commercial or financial relationships that could be construed as a potential conflict of interest.

Publisher's note

All claims expressed in this article are solely those of the authors and do not necessarily represent those of their affiliated organizations, or those of the publisher, the editors and the reviewers. Any product that may be evaluated in this article, or claim that may be made by its manufacturer, is not guaranteed or endorsed by the publisher.

Supplementary material

The Supplementary Material for this article can be found online at: https://www.frontiersin.org/articles/10.3389/fviro.2022.932187/full#supplementary-material

References

1. Zagury D, Léonard R, Fouchard M, Réveil B, Bernard J, Ittelé D, et al. Immunization against AIDS in humans. *Nature* (1987) 326:249–50. doi: 10.1038/326249a0

2. Esparza J. A brief history of the global effort to develop a preventive HIV vaccine. *Vaccine* (2013) 31:3502–18. doi: 10.1016/j.vaccine.2013.05.018

3. Dolin R, Graham BS, Greenberg SB, Tacket CO, Belshe RB, Midthun K, et al. The safety and immunogenicity of a human immunodeficiency virus type 1 (HIV-1) recombinant gp160 candidate vaccine in humans. NIAID AIDS vaccine clinical trials network. *Ann Intern Med* (1991) 114:119–27. doi: 10.7326/0003-4819-114-2-119

4. Marovich MA. ALVAC-HIV vaccines: clinical trial experience focusing on progress in vaccine development. *Expert Rev Vaccines* (2004) 3(4 Suppl):S99–S104. doi: 10.1586/14760584.3.4.S99

5. Sanders RW, Derking R, Cupo A, Julien JP, Yasmeen A, de Val N, et al. A next-generation cleaved, soluble HIV-1 env trimer, BG505 SOSIP.664 gp140, expresses multiple epitopes for broadly neutralizing but not non-neutralizing antibodies. *PloS Pathog* (2013) 9:e1003618. doi: 10.1371/journal.ppat.1003618

6. Pauthner MG, Nkolola JP, Havenar-Daughton C, Murrell B, Reiss SM, Bastidas R, et al. Vaccine-induced protection from homologous tier 2 SHIV challenge in nonhuman primates depends on serum-neutralizing antibody titers. *Immunity* (2019) 50:241–52.e6. doi: 10.1016/j.immuni.2018.11.011

7. Rerks-Ngarm S, Pitisuttithum P, Nitayaphan S, Kaewkungwal J, Chiu J, Paris R, et al. Vaccination with ALVAC and AIDSVAX to prevent HIV-1 infection in Thailand. *N Engl J Med* (2009) 361:2209–20. doi: 10.1056/NEJMoa0908492

8. Burton DR, Ahmed R, Barouch DH, Butera ST, Crotty S, Godzik A, et al. A blueprint for HIV vaccine discovery. *Cell Host Microbe* (2012) 12:396–407. doi: 10.1016/j.chom.2012.09.008

9. Ringe RP, Ozorowski G, Rantalainen K, Struwe WB, Matthews K, Torres JL, et al. Reducing V3 antigenicity and immunogenicity on soluble, native-like HIV-1 env SOSIP trimers. *J Virol* (2017) 91:e00677–17. doi: 10.1128/JVI.00677-17

10. Escolano A, Gristick HB, Abernathy ME, Merkenschlager J, Gautam R, Oliveira TY, et al. Immunization expands b cells specific to HIV-1 V3 glycan in mice and macaques. *Nature* (2019) 570:468–73. doi: 10.1038/s41586-019-1250-z

11. Zolla-Pazner S. Improving on nature: focusing the immune response on the V3 loop. *Hum Antibodies* (2005) 14:69–72. doi: 10.3233/HAB-2005-143-403

12. Zolla-Pazner S, Edlefsen PT, Rolland M, Kong XP, deCamp A, Gottardo R, et al. Vaccine-induced human antibodies specific for the third variable region of HIV-1 gp120 impose immune pressure on infecting viruses. *EBioMedicine* (2014) 1:37–45. doi: 10.1016/j.ebiom.2014.10.022

13. Gottardo R, Bailer RT, Korber BT, Gnanakaran S, Phillips J, Shen X, et al. Plasma IgG to linear epitopes in the V2 and V3 regions of HIV-1 gp120 correlate with a reduced risk of infection in the RV144 vaccine efficacy trial. *PloS One* (2013) 8:e75665. doi: 10.1371/journal.pone.0075665

14. Gorny MK, Williams C, Volsky B, Revesz K, Cohen S, Polonis VR, et al. Human monoclonal antibodies specific for conformation-sensitive epitopes of V3 neutralize human immunodeficiency virus type 1 primary isolates from various clades. *J Virol* (2002) 76:9035–45. doi: 10.1128/JVI.76.18.9035-9045.2002

15. Gorny MK, Sampson J, Li H, Jiang X, Totrov M, Wang XH, et al. Human anti-V3 HIV-1 monoclonal antibodies encoded by the VH5-51/VL lambda genes define a conserved antigenic structure. *PloS One* (2011) 6:e27780. doi: 10.1371/journal.pone.0027780

16. Balasubramanian P, Kumar R, Williams C, Itri V, Wang S, Lu S, et al. Differential induction of anti-V3 crown antibodies with cradle- and ladle-binding modes in response to HIV-1 envelope vaccination. *Vaccine* (2017) 35:1464–73. doi: 10.1016/j.vaccine.2016.11.107

17. Kumar R, Pan R, Upadhyay C, Mayr L, Cohen S, Wang XH, et al. Functional and structural characterization of human V3-specific monoclonal antibody 2424 with neutralizing activity against HIV-1 JRFL. *J Virol* (2015) 89:9090–102. doi: 10.1128/JVI.01280-15

18. Jiang X, Burke V, Totrov M, Williams C, Cardozo T, Gorny MK, et al. Conserved structural elements in the V3 crown of HIV-1 gp120. *Nat Struct Mol Biol* (2010) 17:955–61. doi: 10.1038/nsmb.1861

19. Burton DR, Hangartner L. Broadly neutralizing antibodies to HIV and their role in vaccine design. *Annu Rev Immunol* (2016) 34:635–59. doi: 10.1146/annurev-immunol-041015-055515

20. Zolla-Pazner S, Cohen SS, Boyd D, Kong XP, Seaman M, Nussenzweig M, et al. Structure/Function studies involving the V3 region of the HIV-1 envelope delineate multiple factors that affect neutralization sensitivity. *J Virol* (2015) 90:636–49. doi: 10.1128/JVI.01645-15

21. Hessell AJ, McBurney S, Pandey S, Sutton W, Liu L, Li L, et al. Induction of neutralizing antibodies in rhesus macaques using V3 mimotope peptides. *Vaccine* (2016) 34:2713–21. doi: 10.1016/j.vaccine.2016.04.027

22. Balasubramanian P, Williams C, Shapiro MB, Sinangil F, Higgins K, Nádas A, et al. Functional antibody response against V1V2 and V3 of HIV gp120 in the VAX003 and VAX004 vaccine trials. *Sci Rep* (2018) 8:542. C. E. doi: 10.1038/s41598-017-18863-0

23. Ramirez Valdez KP, Kuwata T, Maruta Y, Tanaka K, Alam M, Yoshimura K, et al. Complementary and synergistic activities of anti-V3, CD4bs and CD4i antibodies derived from a single individual can cover a wide range of HIV-1 strains. *Virology* (2015) 475:187–203. doi: 10.1016/j.virol.2014.11.011

24. Roskin KM, Jackson K, Lee JY, Hoh RA, Joshi SA, Hwang KK, et al. Aberrant b cell repertoire selection associated with HIV neutralizing antibody breadth. *Nat Immunol* (2020) 21:199–209. doi: 10.1038/s41590-019-0581-0

25. Wu X, Yang ZY, Li Y, Hogerkorp CM, Schief WR, Seaman MS, et al. Rational design of envelope identifies broadly neutralizing human monoclonal antibodies to HIV-1. *Sci (New York NY)* (2010) 329:856–61. doi: 10.1126/science.1187659

26. Scheid JF, Mouquet H, Ueberheide B, Diskin R, Klein F, Oliveira TY, et al. Sequence and structural convergence of broad and potent HIV antibodies that mimic CD4 binding. *Sci (New York NY)* (2011) 333:1633–7. doi: 10.1126/science.1207227

27. Walker LM, Phogat SK, Chan-Hui PY, Wagner D, Phung P, Goss JL, et al. Broad and potent neutralizing antibodies from an African donor reveal a new HIV-1 vaccine target. *Sci (New York NY)* (2009) 326:285–9. doi: 10.1126/science.1178746

28. Walker LM, Huber M, Doores KJ, Falkowska E, Pejchal R, Julien JP, et al. Broad neutralization coverage of HIV by multiple highly potent antibodies. *Nature* (2011) 477:466–70. doi: 10.1038/nature10373

29. Bonsignori M, Hwang KK, Chen X, Tsao CY, Morris L, Gray E, et al. Analysis of a clonal lineage of HIV-1 envelope V2/V3 conformational epitope-specific broadly neutralizing antibodies and their inferred unmutated common ancestors. *J Virol* (2011) 85:9998–10009. doi: 10.1128/JVI.05045-11

30. Pejchal R, Doores KJ, Walker LM, Khayat R, Huang PS, Wang SK, et al. A potent and broad neutralizing antibody recognizes and penetrates the HIV glycan shield. *Sci (New York NY)* (2011) 334:1097–103. doi: 10.1126/science.1213256

31. Huang J, Ofek G, Laub L, Louder MK, Doria-Rose NA, Longo NS, et al. Broad and potent neutralization of HIV-1 by a gp41-specific human antibody. *Nature* (2012) 491:406–12. doi: 10.1038/nature11544

32. Doria-Rose NA, Schramm CA, Gorman J, Moore PL, Bhiman JN, DeKosky BJ, et al. Developmental pathway for potent V1V2-directed HIV-neutralizing antibodies. *Nature* (2014) 509:55–62. doi: 10.1038/nature13036

33. Maruta Y, Kuwata T, Tanaka K, Alam M, Valdez KP, Egami Y, et al. Cross-neutralization activity of single-chain variable fragment (scFv) derived from anti-V3 monoclonal antibodies mediated by post-attachment binding. *Jpn J Infect Dis* (2016) 69:395–404. doi: 10.7883/yoken.JJID.2015.667

34. Tanaka K, Kuwata T, Alam M, Kaplan G, Takahama S, Valdez K, et al. Unique binding modes for the broad neutralizing activity of single-chain variable fragments (scFv) targeting CD4-induced epitopes. *Retrovirology* (2017) 14:44. doi: 10.1186/s12977-017-0369-y

35. Kaku Y, Kuwata T, Zahid HM, Hashiguchi T, Noda T, Kuramoto N, et al. Resistance of SARS-CoV-2 variants to neutralization by antibodies induced in convalescent patients with COVID-19. *Cell Rep* (2021) 36:109385. doi: 10.1016/j.celrep.2021.109385

36. Kaku Y, Kuwata T, Gorny MK, Matsushita S. Prediction of contact residues in anti-HIV neutralizing antibody by deep learning. *Jpn J Infect Dis* (2020) 73:235–41. doi: 10.7883/yoken.JJID.2019.496

37. Waterhouse A, Bertoni M, Bienert S, Studer G, Tauriello G, Gumienny R, et al. SWISS-MODEL: homology modelling of protein structures and complexes. *Nucleic Acids Res* (2018) 46(W1):W296–303. doi: 10.1093/nar/gky427

38. Pierce BG, Hourai Y, Weng Z. Accelerating protein docking in ZDOCK using an advanced 3D convolution library. *PloS One* (2011) 6:e24657. doi: 10.1371/journal.pone.0024657

39. Lyskov S, Chou FC, Conchúir SÓ, Der BS, Drew K, Kuroda D, et al. Serverification of molecular modeling applications: The Rosetta online server that includes everyone (ROSIE). *PloS One* (2013) 8:e63906. doi: 10.1371/journal.pone.0063906

40. Schrödinger L, DeLano W. *PyMOL* (2020). Available at: http://www.pymol.org/pymol.

41. Nguyen MN, Verma CS, Zhong P. AppA: a web server for analysis, comparison, and visualization of contact residues and interfacial waters of antibody-antigen structures and models. *Nucleic Acids Res* (2019) 47(W1): W482–9. doi: 10.1093/nar/gkz358

42. Gorny MK, Wang XH, Williams C, Volsky B, Revesz K, Witover B, et al. Preferential use of the VH5-51 gene segment by the human immune response to code for antibodies against the V3 domain of HIV-1. *Mol Immunol* (2009) 46:917–26. doi: 10.1016/j.molimm.2008.09.005

43. Pan R, Qin Y, Banasik M, Lees W, Shepherd AJ, Cho MW, et al. Increased epitope complexity correlated with antibody affinity maturation and a novel binding mode revealed by structures of rabbit antibodies against the third variable loop (V3) of HIV-1 gp120. *J Virol* (2018) 92:e01894–17. doi: 10.1128/JVI.01894-17

44. Spencer DA, Malherbe DC, Vázquez Bernat N, Ádori M, Goldberg B, Dambrauskas N, et al. Polyfunctional tier 2-neutralizing antibodies cloned following HIV-1 env macaque immunization mirror native antibodies in a human donor. *J Immunol (Baltimore Md 1950)* (2021) 206:999–1012. doi: 10.4049/jimmunol.2001082

45. Lindenmann J. Speculations on idiotypes and homobodies. *Ann Immunol (Paris)* (1973) 124:171–84.

46. Jerne NK. Towards a network theory of the immune system. *Ann Immunol* (1974) 125C:373–89.

47. Kohler H, Pashov A, Kieber-Emmons T. The promise of anti-idiotype revisited. *Front Immunol* (2019) 10:808. doi: 10.3389/fimmu.2019.00808

48. Seydoux E, Wan YH, Feng J, Wall A, Aljedani S, Homad LJ, et al. Development of a VRC01-class germline targeting immunogen derived from anti-idiotypic antibodies. *Cell Rep* (2021) 36:109454. doi: 10.1016/j.celrep.2021.109454

frontiers | Frontiers in Virology

TYPE Original Research
PUBLISHED 01 November 2022
DOI 10.3389/fviro.2022.971293

OPEN ACCESS

EDITED BY
Akio Adachi,
Kansai Medical University, Japan

REVIEWED BY
Carine M. C. Van Lint,
Université libre de Bruxelles, Belgium
Mary Jane Potash,
Icahn School of Medicine at Mount Sinai, United States

*CORRESPONDENCE
Brian Wigdahl
bw45@drexel.edu

†PRESENT ADDRESS
John J. McAllister,
Anesthesia Company LLC, Luminis Health, Annapolis, MD, United States

‡These authors have contributed equally to this work

SPECIALTY SECTION
This article was submitted to Fundamental Virology, a section of the journal Frontiers in Virology

RECEIVED 16 June 2022
ACCEPTED 14 October 2022
PUBLISHED 01 November 2022

CITATION
McAllister JJ, Dahiya S, Berman R, Collins M, Nonnemacher MR, Burdo TH and Wigdahl B (2022) Altered recruitment of Sp isoforms to HIV-1 long terminal repeat between differentiated monoblastic cell lines and primary monocyte-derived macrophages. *Front. Virol.* 2:971293. doi: 10.3389/fviro.2022.971293

Altered recruitment of Sp isoforms to HIV-1 long terminal repeat between differentiated monoblastic cell lines and primary monocyte-derived macrophages

John J. McAllister[1†‡], Satinder Dahiya[2,3‡], Rachel Berman[2,3], Mackenzie Collins[2,3], Michael R. Nonnemacher[2,3,4], Tricia H. Burdo[5] and Brian Wigdahl[2,3,4*]

[1]Department of Microbiology and Immunology, Pennsylvania State University College of Medicine, Hershey, PA, United States, [2]Department of Microbiology and Immunology, Drexel University College of Medicine, Philadelphia, PA, United States, [3]Center for Neurovirology and Translational Neuroscience, Institute for Molecular Medicine and Infectious Disease, Drexel University College of Medicine, Philadelphia, PA, United States, [4]Sidney Kimmel Cancer Center, Thomas Jefferson University, Philadelphia, PA, United States, [5]Department of Microbiology, Immunology, and Inflammation, Center for Neurovirology and Gene Editing, School of Medicine, Temple University, Philadelphia, PA, United States

Human immunodeficiency virus type 1 (HIV-1) transcription in cells of the monocyte-macrophage lineage is regulated by interactions between the HIV-1 long terminal repeat (LTR) and a variety of host cell and viral proteins. Binding of the Sp family of transcription factors (TFs) to the G/C box array of the LTR governs both basal as well as activated LTR-directed transcriptional activity. The effect of monocytic differentiation on Sp factor binding and transactivation was examined with respect to the HIV-1 LTR. The binding of Sp1, full-length Sp3 and truncated Sp3 to a high affinity HIV-1 Sp element was specifically investigated and results showed that Sp1 binding increased relative to the binding of the sum of full-length and truncated Sp3 binding following chemically-induced monocytic differentiation in monoblastic (U-937, THP-1) and myelomonocytic (HL-60) cells. In addition, Sp binding ratios from PMA-induced cell lines were shown to more closely approximate those derived from primary monocyte-derived macrophages (MDMs) than did ratios derived from uninduced cell lines. The altered Sp binding phenotype associated with changes in the transcriptional activation mediated by the HIV-1 G/C box array. Additionally, analysis of post-translational modifications on Sp1 and Sp3 revealed a loss of phosphorylation on serine and threonine residues with chemically-induced differentiation indicating that the activity of Sp factors is additionally regulated at the level of post-translational modifications (PTMs).

KEYWORDS

HIV-1 LTR, Sp, G/C box array, transcription, monocytes

Introduction

HIV-1 infection within monocyte-macrophage lineage cells represent a crucial cellular reservoir that needs to be targeted and eliminated to achieve complete remission and superior patient outcomes in people living with HIV (PLWH; (1–5). Macrophages are more resistant to cytopathic effects of HIV-1 compared to T cells; as a result, these cells can harbor the virus for a longer period of time and can also traffic across the blood-brain barrier seeding virus into the brain (6–9). Productive infection of the monocyte-macrophage lineage is limited, in comparison to CD4+ T cells, due to the low surface expression of CD4 and HIV-1 co-receptors CCR5 and CXCR4; however, all are displayed on these cell types with the timing and quantity of receptor expression varying depending on the states of stimulation and differentiation of the given cell population (10–13). Circulating monocytes can be infected with HIV-1 and then differentiate into macrophages wherein post-integration latency is established. Once resident in tissues like the brain, these non-proliferative cells are capable of supporting viral gene expression and infectious virus production, albeit to a much lesser extent than activated T cells, with dissemination of virus to surrounding susceptible cells (7, 12, 14, 15). In addition, the production and release of viral proteins such as gp41, gp120, Tat, Vpr, and Nef impact neighboring cellular populations and have been shown to have neurotoxic properties (7, 12, 14, 15).

Monocytic cells are generated in the bone marrow from pluripotent stem cells, which retain the ability to differentiate into either granulocytes or cells of the monocyte-macrophage lineage. The process of differentiation is governed by activity of transcription factors (TFs) that bind *cis*-acting promoter elements to govern expression of myeloid-specific genes in response to extracellular cues (16). The Sp family of TFs is involved in the regulation of monocyte- and/or myeloid-specific gene expression (17, 18). Sp1 and AP-1 have been shown to act cooperatively in the myeloid-specific regulation of the CD11c leukocyte integrin promoter (19). Similarly, Sp1 and AP-2 have been implicated in regulating lysosomal acid lipase and acid sphingomyelinase during monocytic differentiation (20, 21). Sp1 is also known to interact with C/EBP factors in regulating expression of several genes in myeloid cells (22–24). Other myeloid cell-specific differentiation events have also been attributed to specific activity of Sp factors (25–27). Sp factors have also been implicated in the regulation of chondrocyte, adipocyte, and epithelial cell differentiation (28–30) as well as in neuronal differentiation (31–34).

The Sp family of TFs includes Sp1, Sp2, Sp3, and Sp4 (35, 36). The C-terminus of Sp1 contains three zinc fingers that facilitate DNA binding, while the N-terminus contains the transactivation domains. (17). Sp1, Sp3 and Sp4 share near-equivalent affinity for binding G/C rich sequences, while Sp2 prefers binding to an alternative G/T rich sequence (35–38). Sp1 and Sp3 are ubiquitously expressed, while Sp4 has been shown to be brain-restricted in its pattern of expression (34, 35, 39, 40). Post-translation modifications (PTMs) including phosphorylation, glycosylation, acetylation and sumoylation of the Sp family of TFs have been shown to regulate their DNA binding and transcriptional activity (41). For instance, phosphorylation of Sp1 on Serine 131 by HIV-1 Tat-mediated activation of DNA-dependent protein kinase increases transcription with no effect on DNA binding (42–44) whereas other reports have shown that dephosphorylation of Sp1 mediated increased transcription activity from IL-21R promoter upon T cell receptor stimulation (45). Similarly, dephosphorylation of Sp1 at Serine 59 and Threonine 681 by PP2A resulted in increased association of dephosphorylated Sp1 with chromatin; however, the impact on transcriptional regulation was not studied (46). Additionally, groups have shown that sumoylation of the Sp1 N-terminus and other Sp3 isoforms occurs at basal conditions and can decrease transcriptional activity *via* chromatin changes promoting local gene silencing (43).

With respect to HIV-1, Sp1 and Sp4 have been shown to function as activators of gene expression through their interactions with the G/C box array of the HIV-1 LTR, while both the full-length Sp3 and truncated Sp3 isoforms have been shown to act as repressors (7, 47, 48). In another report a host factor, interferon γ-inducible protein 16 (IFI16) has also been shown to bind at high levels to Sp1, sequestering it from interacting with the LTR of HIV-1, leading to inefficient transcription. (49, 50). To examine the role of Sp factors in regulating HIV-1 gene expression during the course of monocytic differentiation, a number of immature myeloid cell line models capable of chemically-induced differentiation along with primary monocyte-derived macrophages (MDM) were utilized to model monocytic differentiation (Figure 1). The HL-60 cell line represents a partially committed myeloid cell (51, 52), which retains the ability to differentiate toward either granulocytic or monocytic cell types following treatment with either dimethylsulfoxide (DMSO) or phorbol myristate acetate (PMA), respectively (53, 54). The U-937 and THP-1 cell lines represent committed monoblastic cells (55–58), which may be further differentiated along the monocytic pathway when treated with PMA (59).

Utilizing these *in vitro* model systems, the binding of the Sp1 activator protein to a high affinity HIV-1 Sp site was shown to increase relative to the binding of the Sp3 repressor isoforms following PMA-induced monocytic differentiation of HL-60, U-937 and THP-1 cell lines. Sp binding ratios from PMA-induced cells lines were also shown to more closely approximate those derived from primary MDMs than did ratios derived from uninduced cell lines. In addition, the altered Sp factor binding phenotype is associated with alterations in the transcriptional activation generated by a series of HIV-1 *cis*-acting Sp elements. Moreover, the PTM analysis on Sp1 and Sp3 proteins from

10.3389/fviro.2022.971293

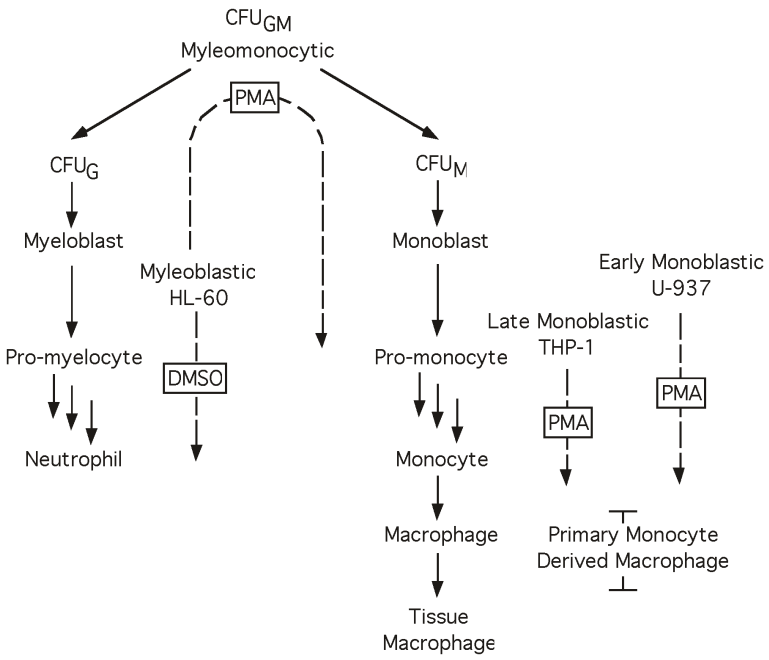

FIGURE 1
Myeloid differentiation. Diagrammatic representation of the process of myeloid differentiation. Cell lines and primary cell preparations are shown at their approximate stage in the differentiation process, dotted arrows indicate a cell line's ability to differentiate towards a given cell type in the presence of the boxed chemical inducer. When treated with PMA cell lines HL-60 (48 hrs), THP-1 and U-937 (24 hrs) differentiate toward the monocyte lineage. When treated with DMSO cell line HL-60 (48 hrs) differentiates toward the granulocyte lineage.

untreated and PMA-activated U-937 cells demonstrated a loss of phosphorylation on certain residues on Sp1 and Sp3 proteins showing potential functional contribution of these specific PTMs in regulating LTR-directed transcription.

Materials and methods

Cell culture

The human monocytic cell lines U-937 and THP-1 were grown in RPMI 1640 media (55, 56). The human myelomonocytic cell line HL-60 was grown in Dulbecco's media (51, 52). All media were supplemented with 10% heat-inactivated fetal bovine serum, antibiotics (penicillin, streptomycin, and kanamycin at 0.04 mg/ml each), L-glutamine (0.3 mg/ml), and sodium bicarbonate (0.05%). All cell lines were maintained at 37˚C in the presence of 5% CO_2 and 90% relative humidity. To induce monocytic differentiation, HL-60 cells were cultured in the presence of PMA (10 µM, Sigma) for 48 hr, while U-937 and THP-1 cells were cultured for 24 hr in the presence of 0.5 µM and 1.5 µM PMA, respectively (20, 60); for review see (59). Granulocytic differentiation of HL-60 cells was induced for 48 hr in the presence of DMSO (1.25%, Sigma) (53, 54).

Isolation and characterization of primary MDMs

Buffy coat preparations obtained from normal healthy individuals were centrifuged over a Ficoll gradient (300 x g) for 45 min (61) and the mononuclear fraction was collected and washed in Hank's balanced salt solution containing EDTA (0.5 mM final concentration). The cells were resuspended in Dulbecco's phosphate-buffered saline containing 10% human AB serum (US Biological) and HEPES buffer (2.5 mM). This preparation was subsequently centrifuged (550 x g) for 45 min over a 46% Percol solution (Pharmacia), and mononuclear cells were harvested at the resulting interface (62). Cells were washed with PBS and plated into 100-mm tissue culture plates (Falcon) at a density of 1 x 10^6 cell per ml. Following a 1 hr incubation at 37˚C in the presence of 5% CO_2 and 90% relative humidity, nonadherent T cells were removed by washing with RPMI 1640. Adherent T cells were subsequently maintained in RPMI 1640 supplemented with 10% heat-inactivated human AB serum (US biological), M-CSF (100 U/ml; R&D Systems), GM-CSF (40 U/ml; R&D Systems), antibiotics (penicillin, streptomycin, and kanamycin at 0.04 mg/ml each), L-glutamine (0.3 mg/ml), and sodium bicarbonate (0.05%). Cells were cultured at 37˚C in the presence of 5% CO_2 and 90% relative humidity for 5 to 10 days before use. The purity of monocytic preparations was assessed

three days after isolation. Purity was determined to be >95% by flow cytometry. Cells reactive with antibodies directed against either CD45, CD4 (dim) and CD14; or CD45, CD4 (dim) and CD15 (dim) were considered monocytic by previous definition (63). Assessment of the major contaminating cell populations within the monocytic cell preparations was assessed by flow cytometry utilizing antibodies directed against CD45, CD20, and CD15 (bright) for identification of B cells and granulocytes; and antibodies directed against CD45, CD4, CD3 for the identification of T cells. All antibodies were purchased from Becton Dickenson.

Nuclear extract preparation and electrophoretic mobility shift analyses

Small-scale nuclear extracts were prepared from low-passage, exponentially-growing cells as previously described (3). Briefly, cells (1×10^7) were collected by centrifugation, washed once with ice-cold 1× Dulbecco phosphate-buffered saline (Mediatech), and lysed in ice-cold lysis buffer [HEPES (10 mM) pH 7.9, KCl (10 mM), EDTA (0.1 mM), EGTA (0.1 mM), octylphenoxypolyethoxyethanol (IGEPAL; Rhodia) (0.4%), dithiothreitol (DTT; 1 mM), phenylmethylsulfonyl fluoride (PMSF; 0.5 mM), and HALT protease inhibitor cocktail (1:100; Thermo Scientific, Rockford, IL)]. After centrifugation ($1000 \times g$), the supernatant (cytoplasmic extract) was discarded. The pelleted nuclei were gently resuspended in nuclear extract buffer [HEPES (20 mM), NaCl (0.4 M), EDTA (1 mM), EGTA (1 mM), DTT (1 mM), PMSF (1 mM), and HALT protease inhibitor cocktail (1:100)], shaken vigorously on a rocker for 30 min at 4°C, and subjected to centrifugation for 10 min ($14{,}000 \times g$). The supernatant (nuclear extract) was then dialyzed two times for 45 minutes using mini dialysis units (Thermo Scientific, 2000 molecular weight cutoff) in dialysis buffer [HEPES (20 mM), KCl (100 mM), EDTA (0.2 mM), glycerol (20%), DTT (1 mM), and PMSF (1 mM)]. The nuclear extract was recovered from the dialysis units and transferred to an Eppendorf tube and stored at -80°C in small aliquots. The protein concentration was determined by Bradford assay as described by the manufacturer (Bio-Rad, Hercules, CA).

Double-stranded, gel-purified oligonucleotides for EMS analysis were prepared as previously described (64). The sequence of the probe used in these studies was derived from the HIV-1 subtype B consensus Sp site III, 5'-CCAGGGAGGCGTGGCCTGGG-3'. Oligonucleotides were synthesized by Integrated DNA Technologies (Coralville, IA) as previously described (64). For antibody supershift/abrogation analysis, the indicated antibody (2 µg per reaction) (Santa Cruz Biotechnologies, Santa Cruz, CA) was added to the reaction and incubated for 30 min at room temperature prior to addition of the labeled probe. Complexes were separated on a 4% native TGE gel.

Plasmid construction

Complementary single-stranded oligonucleotides representing the subtype B consensus HIV-1 core LTR sequence (-83 to +2, relative to the transcriptional start site) were synthesized and annealed. In addition, an HIV-1 natural variant Sp element that fails to recruit Sp family factors (GAAGCGTGGC; (65) was substituted for 1, 2 or all 3 Sp elements in three additional synthetic oligonucleotides. Substitution of variant Sp elements in place of subtype B consensus binding elements began at the NF-κB-proximal Sp site and sequentially moved toward the TATA element. The four resulting oligonucleotides were cloned into pGL3-Basic (Promega) to generate Sp(3x)TATA-Luc, Sp(2x)TATA-Luc, Sp (1x)TATA-Luc, and Sp(0x)TATA-Luc (Figure 8A). Sp(3x) TATA-Luc contains three subtype B consensus Sp binding elements. Sp(2x)TATA-Luc contains a low affinity Sp element at position III, and subtype B consensus elements at positions II and I. Sp(1x)TATA-Luc contains two low affinity Sp elements at positions III and II, and a subtype B consensus element at position I. Sp(0x)TATA-Luc contains three low affinity Sp elements (Figure 8). Each construct contains a functional HIV-1 LTR TATA box as well as additional sequence out to the start site of transcription. The sequence of each construct was confirmed prior to experimentation.

Transient transfections and luciferase assays

Reporter plasmids were transfected in the U-937 and THP-1 monoblastic cell lines using Fugene 6 transfection system (Promega, Madison, WI) while electroporation was utilized in the HL-60 myelomonocytic cell line. U-937 or THP-1 cells were seeded from exponentially growing, low passage cultures at 5 x 10^5 cells per ml growth medium and transfected with Fugene 6 in 35-mm plates (Falcon). Premixed Fugene (94 µl serum free RPMI with 6 µl Fugene) was added dropwise to 2.5 µg of the experimental luciferase vector (THP-1 and U-937) and either 200 ng pRL-CMV, or 100 ng pRL-TK Renilla internal control vector (THP-1 and U-937, respectively). After a 15-min incubation, the Fugene/DNA mixture was added directly to the cells. Cultures were incubated at 37°C for 24 hr. Cell extracts were harvested and assayed for luminescence using the Dual Luciferase Assay (Promega). HL-60 cells were seeded from exponentially growing, low passage cultures. The experimental luciferase vector (15 µg) and the pRL-CMV Renilla internal control vector (50 ng) were added to 5 x 10^6 cells in 250 µl of culture medium. Cells were subsequently electroporated (250 V and 960 µF) and transferred to 35-mm plates (Falcon) in 2 ml growth media. Cultures were incubated for 24 hr at 37°C. Cell extracts were prepared, and luminescence

was measured using the Dual Luciferase Assay (Promega). Chemical differentiating agents, DMSO (1.25%) or PMA (0.5 μM U-937, 1.0 μM HL-60 or 1.5 μM THP-1); were diluted in culture media and added to transfected cells 30 min after the addition of the DNA/Fugene mixture. In each case, firefly luminescence was normalized to Renilla luminescence to control for variability in transfection efficiency. Activity of the constructs is presented as the fold-increase in normalized firefly activity over the activity of the Sp(0x)TATA-Luc construct. Each transfection was performed in duplicate and repeated at least three separate times. Error bars indicate the standard deviation among data obtained from independent experiments.

Mass spectroscopy and post-translational modification (PTM) analyses on Sp1 and Sp3

Total protein was isolated from U-937 and U-937 PMA-treated cell pellets. The isolated proteins were then digested with trypsin in solution and enriched for phosphopeptides with Titanium dioxide (TiO2) column. The digested peptides were then extracted with 50% acetonitrile containing 5% formic acid, dried in a speedvac and resuspended in the appropriate mobile phase for LC-MS/MS analysis. A linear acetonitrile gradient was used to separate the tryptic peptides based on their hydrophobicity prior to MS analysis on a Thermo Scientific LTQ XL mass spectrometer and with a total run time of 90 min per sample. The samples were then analyzed separately by nano-LC-MS/MS and the PTM analyses for phosphorylation were performed. A data-dependent Top 5 method was used where a full MS scan from m/z 400-1500 was followed by MS/MS scans of the five most abundant ions. Each ion was subjected to CID (Collision Induced Dissociation) for fragmentation and peptide identification. Raw data files from each sample were then searched using Proteome Discoverer 1.4 (Thermo Scientific) and SEQUEST algorithm against FASTA databases for Sp1 (P08047.3) and Sp3 (Q02447) from UniProt. PhosphoRS 3.0 algorithm (integrated into the Proteome Discoverer) was used for phosphorylation site localization, whereas fixed value PSM Validator was used for PSM validation in database searches for Sp1 and Sp3. pRS site probabilities above 75% were used as a cutoff to obtain good evidence that a responsive site was truly phosphorylated.

Statistical analysis

The quantitative two-tailed student t-test was utilized and $p < 0.05$ was considered significant.

Results

Sp1 and Sp3 isoforms are present in myelomonocytic and monoblastic cell lines as well as primary MDMs

To investigate the relative amounts of the different Sp family TFs present during the course of monocytic differentiation it was necessary to identify the Sp family members present in each of the cell types examined. EMS analyses were performed utilizing a 20-bp oligonucleotide probe centered on the subtype B consensus HIV-1 Sp site III in conjunction with HL-60, U-937, THP-1 and primary MDM nuclear extracts. The U-937 and THP-1 nuclear extracts each generated four distinct DNA-protein complexes (Figure 2, lanes 1 and 6). Addition of antibody directed against Sp1 resulted in both the partial abrogation of complex A and the generation of a lower mobility complex (Figure 2, compare lanes 1 and 6 to lanes 2 and 7). Complexes B and C were shown to be reactive with antibody directed against Sp3 by a combination of abrogation (complexes B and C) and supershift (either complex B or complex C) (Figure 2, compare lanes 1 and 6 to lanes 3 and 8). Consistent with the analysis of individual antibodies, the combined use of both Sp1 and Sp3 antibodies resulted in both the abrogation of complexes A, B and C and the generation of multiple low mobility complexes (Figure 2, lanes 4 and 9). Sp4 antibody did not react significantly with any of the complexes in reactions containing U-937 or THP-1 nuclear extract. Complex D was unaffected by the presence of any of the Sp antibodies examined and has been shown to be nonspecific by competition with homologous and non-homologous competitors (data not shown). EMS reactions containing HL-60 nuclear extract generated DNA-protein complexes consistent with complexes A through D in the U-937 and THP-1 extracts (Figure 2, compare lane 11 to lanes 1 and 6). Complex A and B was found to contain Sp1 while complexes B and C were found to contain Sp3 (Figure 2, lanes 11-14). In addition to these four complexes, a fifth high mobility complex was observed (Figure 2, lane 11, complex E). This complex was shown to be partially abrogated in the presence of either Sp1 or Sp3 antibody. Use of both Sp1 and Sp3 antibody resulted in nearly complete abrogation of complex E, suggesting that this high mobility complex may represent proteolytic Sp factor fragments, which retain their DNA-binding activity (27). Analysis of the primary MDM extract also yielded complexes similar to those observed in the U-937, THP-1 and HL-60 analysis. Complex A was shown to contain Sp1 (Figure 2, compare lane 16 and 17). Although complexes B and C appeared in low abundance, supershift analysis with Sp3 antibody yielded a faint low mobility complex consistent with the presence of Sp3 containing DNA-protein complexes (Figure 2, lane 18). As before, complex D was

10.3389/fviro.2022.971293

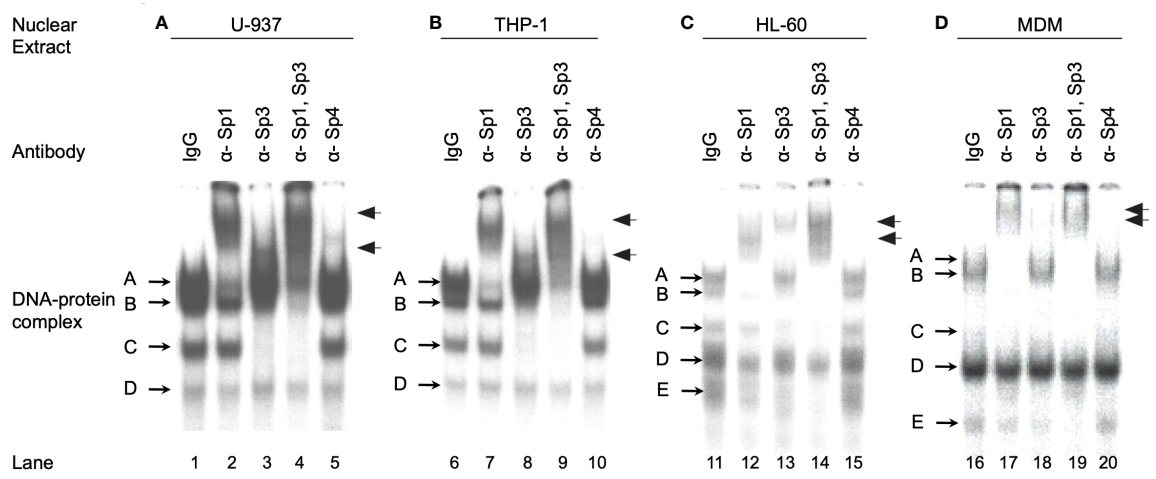

FIGURE 2
Monocytic Sp TFs bind a high affinity HIV-1 Sp binding site. EMS analyses using the HIV-1 subtype B consensus Sp site III were performed as described in the Materials and Methods. Binding reactions included 6 µg of U-937 **(A)**, THP-1 **(B)**, or HL-60 **(C)** nuclear extract with 60,000 cpm radiolabled probe (approximately 1 ng). MDM nuclear extract (20 µg) **(D)** was also reacted with 60,000 cpm of radiolabled probe. Antisera (1 µl) was added as indicated. DNA-protein complexes are labeled A through E, while supershifted DNA-protein complexes are indicated with arrows. This was performed as three independent experiments with a representative image presented.

shown to be nonspecific by competition analysis (data not shown). A fifth complex (complex E), similar to that observed in EMS reactions utilizing HL-60 nuclear extract (Figure 2C), again demonstrated partial abrogation in the presence of either Sp1 or Sp3 antisera (Figure 2, lanes 17 and 18). Use of both Sp1 and Sp3 antibodies resulted in nearly complete abrogation of the complex (Figure 2, lane 19).

Alterations in the relative binding of Sp1 and Sp3 during differentiation of a myelomonocytic cell line

It was observed in initial studies that the ratio of Sp1 to Sp3 might vary among nuclear extracts prepared from primary MDM, monoblastic (U-937 and THP-1) and myelomonoblastic (HL-60) cell populations. To determine whether alterations in the relative binding of Sp family activators (Sp1) and Sp family repressors (full-length and truncated Sp3) occurred during the course of monocytic differentiation, the binding of Sp factors was examined in a probe titration EMS analysis under conditions where each of the three major Sp complexes could be quantitated. Increasing amounts of a 20-bp probe centered on the HIV-1 subtype B consensus Sp site III was reacted with a constant amount of nuclear extract. When the probe is saturated with respect to the available binding protein, the relative abundance of each complex will primarily reflect the relative amounts of protein in the extract capable of binding probe. Under these conditions, a comparison of unstimulated, DMSO-stimulated, and PMA-stimulated HL-60 nuclear extracts (Figure 3A) provides an indication of the relative levels of Sp factors present in myelomonocytic cells (unstimulated), granulocytic cells (DMSO-treated), and monocytic cells (PMA-treated).

Quantitation of the resulting DNA-protein complexes and subsequent comparison of the complex intensities at saturation (Figure 3B) allows identification of the relative levels of each DNA-protein complex. The relative levels of Sp1 and Sp3 demonstrated little or no difference when nuclear extracts of untreated and DMSO-treated HL-60 cells were examined. In each case, the level of Sp1 relative to full-length Sp3 was approximately 2:1 (Figure 3C). Similarly, the level of Sp1 relative to truncated Sp3 was also approximately 2:1, while the level of full-length Sp3 relative to truncated Sp3 was nearly 1:1 in both extracts (Figure 3C). In contrast to the similarity among the Sp1- and Sp3-containing complexes, the intensity of the nonspecific complex D and the Sp1-Sp3 reactive low mobility complex E (Figure 3A) were notably reduced following DMSO treatment. Overall, it appears that DMSO treatment, which approximates myeloid differentiation (53), has little impact on the relative binding levels of Sp1, full-length Sp3, or truncated Sp3 to the HIV-1 subtype B consensus Sp site III.

In contrast to the Sp ratios observed between untreated and DMSO-treated HL-60 nuclear extracts, a comparison of untreated and PMA-treated HL-60 nuclear extracts yielded a different result. The level of Sp1 relative to full-length Sp3 was approximately 2:1 in each case (Figure 3C). However, the level of Sp1 relative to truncated Sp3 increased from 2:1 in untreated HL-60 nuclear extracts to nearly 3.6:1.0 in PMA-treated extracts (Figure 3C, middle panel). Similarly, the ratio of full-length Sp3 relative to truncated Sp3 increased from just under 1:1 in

10.3389/fviro.2022.971293

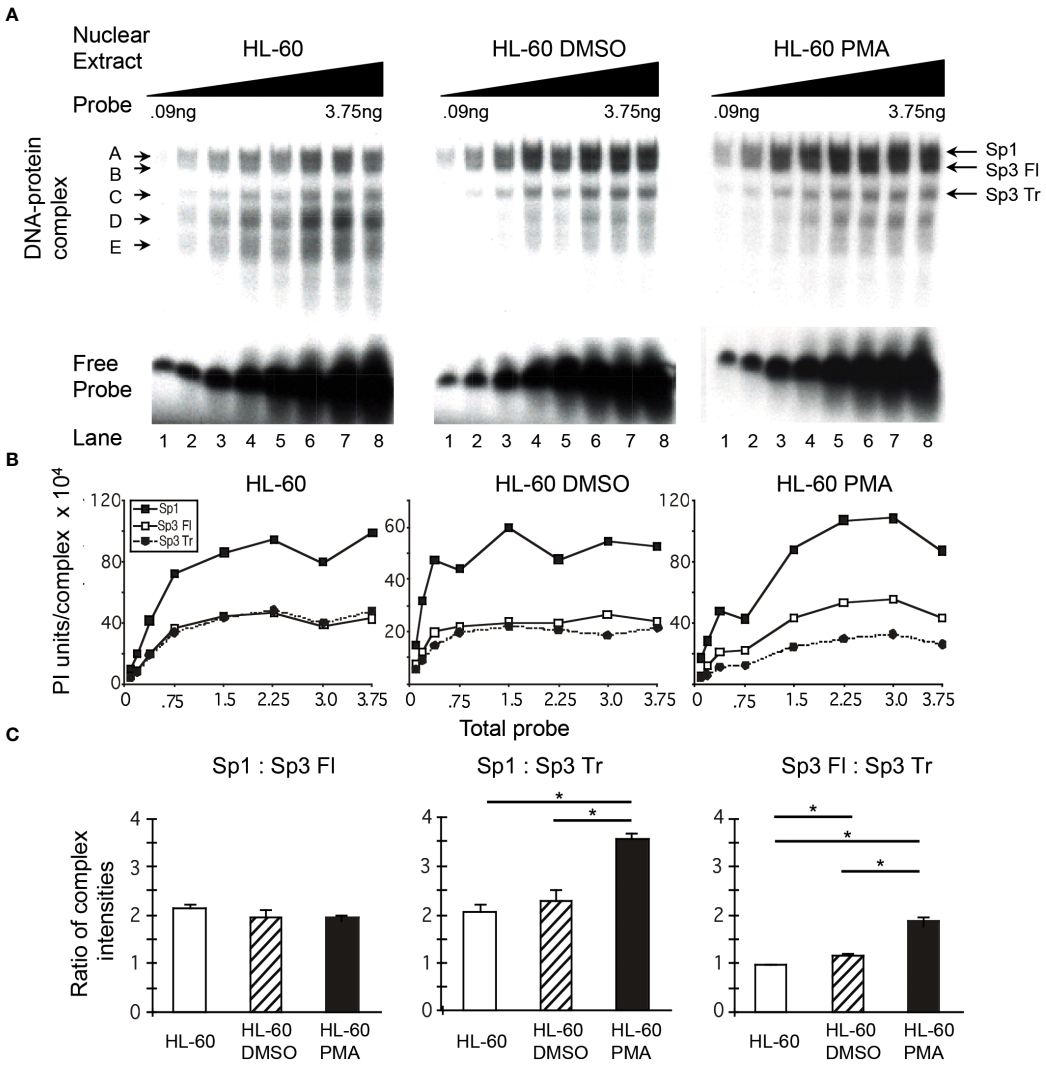

FIGURE 3
Relative levels of Sp factor binding in the myleomonocytic HL-60 cell line are altered with the addition of the chemical differentiating agent, PMA. Relative Sp factor binding was examined by EMS probe titration analyses. **(A)** Untreated, DMSO-treated, and PMA-treated HL-60 nuclear extracts (6 µg) were reacted with increasing amounts of labeled HIV-1 Sp site III probe (12,500 to 500,000 cpm; 0.09 to 3.75 ng). Complexes were separated utilizing a 2-hr electrophoresis interval through a 4% acrylamide gel to retain unbound probe and facilitate subsequent analysis. DNA-protein complexes are labeled A through E; arrows indicate the position of low mobility Sp-related complexes. Representative image shown. **(B)** Untreated, DMSO-treated, and PMA-treated HL-60 nuclear extracts (6 µg) were reacted with increasing amounts of labeled HIV-1 Sp site III probe (12,500 to 500,000 cpm; 0.09 to 3.75 ng). Complexes were subjected to a 3-hr electrophoresis interval utilizing 4% acrylamide to allow for greater separation and a more accurate subsequent quantitation of the resulting DNA-protein complexes. Unbound probe was not retained. DNA-protein complexes were quantitated and graphed as phosphorimager units per complex. Representative graph shown. **(C)** DNA-protein complexes intensities **(B)** were averaged at saturation and their relative levels compared within a given gel. This process was repeated three times and the average of the three relative intensities was graphed for each pair of DNA-protein complexes examined: Sp1 relative to full-length Sp3 (Sp3 Fl), Sp1 relative to truncated Sp3 (Sp3 Tr), and Sp3 Fl relative to Sp3 Tr. Comparisons between all were evaluated by the quantitative two-tailed student t-test and $p < 0.05$ was considered significant (*).

untreated extracts to nearly 2:1 in PMA-treated nuclear extracts. As with the DMSO-treated extracts, complexes D and E (Figure 3A) were noticeably reduced following differentiation. Overall, it appears that PMA treatment, which approximates monocytic differentiation (54), causes an increase in both Sp1 and full-length Sp3 relative to truncated Sp3.

Alterations in the relative binding of Sp1 and Sp3 during differentiation of two monoblastic cell lines

To determine if the changes in relative Sp factor binding observed during the chemical differentiation of HL-60 cells was

cell type-specific or related to a more general physiologic process, similar experiments were performed using the U-937 and THP-1 monoblastic cell lines. Nuclear extracts from untreated and PMA-treated cells were utilized in probe titration analyses under conditions in which each of the three Sp complexes could be separately quantitated (U-937, Figure 4A; THP-1, Figure 5A). Subsequent quantitation and comparison of complex intensities at saturation allowed for comparisons of relative factor binding profiles (U-937, Figure 4B; THP-1, Figure 5B).

Significant alterations in relative factor binding were observed with chemical differentiation of U-937 cells with PMA. The level of Sp1 relative to full-length Sp3 in untreated U-937 cells was similar to that seen in untreated HL-60 cells, nearly 2:1 in each case (compare Figures 3C, 4C). This ratio increased to 3:1 in PMA-treated U-937 nuclear extracts (Figure 4C). The level of Sp1 relative to truncated Sp3 in untreated U-937 cells was again similar to that observed in nuclear extract prepared from untreated HL-60 cells (compare Figure 3C, 4C). However, this ratio increased from 1.8:1.0 in untreated U-937 nuclear extract to approximately 5.6:1.0 in nuclear extract prepared from PMA-treated U-937 cells (Figure 4C). The level of full-length Sp3 relative to truncated Sp3 was again near equivalent in nuclear extracts derived from untreated U-937 and HL-60 cells, approximately 1:1 in each case (compare Figures 3C, 4C). Examination of nuclear extracts from PMA-treated U-937 cells yielded a 2:1 ratio between full-length Sp3 and truncated Sp3 (Figure 4C). In summary, the Sp factor ratios observed in nuclear extracts prepared from the U-937 cell line were consistent with those observed in extracts prepared from the HL-60 cell line, in that a relative increase in Sp1 over both full-length and truncated Sp3 was observed following PMA-induced monocytic differentiation.

Relative Sp factor ratios were also examined in THP-1 monoblastic nuclear extracts. The level of Sp1 relative to full-length Sp3 in untreated THP-1 nuclear extracts (Figure 5C) was similar to those observed in untreated U-937 (Figure 4C) and HL-60 extracts (Figure 3C). Nuclear extracts prepared from PMA-treated THP-1 cells exhibited Sp1 to full-length Sp3 ratios of 2.7:1.0, a value above that of untreated U-937 and THP-1 extracts, but below that of PMA-treated U-937 extracts (Figure 5C). The level of Sp1 relative to truncated Sp3 in untreated THP-1 extracts (2.7:1.0) was above that observed with U-937 (2:1) and HL-60 (2:1) nuclear extracts (THP-1, Figure 5C; U-937, Figure 4C; HL-60, Figure 3C). Similar to previous results, nuclear extracts prepared from PMA-treated THP-1 cells exhibited an increase in the Sp1 to truncated Sp3 ratio as compared to the ratio observed with extracts prepared from untreated THP-1 cells (compare 4.3:1.0 to 2.7:1.0, respectively; Figure 5C). The full-length Sp3 to truncated Sp3 ratio obtained with nuclear extracts prepared from untreated THP-1 cells (Figure 5C) was slightly above those ratios generated from U-937 (Figure 4C) and HL-60 (Figure 3C) nuclear extract. However, nuclear extracts prepared from PMA-treated THP-1 cells exhibited little or no increase in the full-length Sp3 to truncated Sp3 ratio compared to extracts prepared from untreated THP-1 cells (Figure 5C). In summary, the use of the THP-1 monoblastic cell line as a model of PMA-induced monocytic differentiation yielded results similar to those observed in the U-937 monoblastic and HL-60 myeloblastic cell lines. In each case, the activating Sp1 was found to increase relative to the repressor Sp3 isoforms.

Relative binding of Sp1 and Sp3 isoforms in primary MDMs

To determine whether the increase in relative Sp1 binding observed during chemical differentiation of monoblastic and myelomonocytic cell lines was a direct result of a monocytic differentiation process or a process specific to monocytic cell lines and thus unrelated to the differentiation process that occurs in primary monocytic cell populations *in vivo*, the relative binding of Sp factors in primary MDMs was examined. MDMs are known to differentiate during the process of isolation from peripheral blood. Hence, it was hypothesized that Sp factor binding ratios derived from MDM nuclear extracts would be similar to those observed in chemically differentiated nuclear extracts, if the alterations in Sp factor ratios were dependent on the process of monocytic differentiation.

MDM nuclear extracts were utilized in probe titration analyses (Figure 6A) under conditions in which each of the major Sp complexes could be quantitated (Figure 6B). The ratio of Sp1 relative to full-length Sp3 was 3:1 (MDM, Figure 6C), a value similar to ratios derived from PMA-treated U-937 (Figure 4C) and THP-1 (Figure 5C) nuclear extracts (3.0:1.0 and 2.8:1.0, respectively) and greater than the value obtained with PMA-treated HL-60 nuclear extracts (Figure 3C, 2.1:1.0). The level of Sp1 relative to truncated Sp3 was 3.7:1.0 (MDM, Figure 6C), a level similar to PMA-treated HL-60 (Figure 3C) and THP-1 (Figure 5C) cells (3.6:1.0 and 4.3:1.0, respectively), but somewhat below the level derived from PMA-treated U-937 cells (Figure 4C, 5.6:1.0). The level of full-length Sp3 relative to truncated Sp3 was 1.3:1.0 in primary MDM nuclear extracts (Figure 6C). When compared to chemically-differentiated cell lines exhibiting ratios between 1.6:1.0 and 1.9:1.0, it was apparent that MDM nuclear extracts exhibit less binding of full-length Sp3 relative to truncated Sp3 (MDM, Figure 6C; U-937, Figure 4C; THP-1, Figure 5C; HL-60, Figure 3C).

Because Sp1 activates transcription from the HIV-1 LTR while both Sp3 isoforms act as transcriptional repressors (47), a comparison of activator to repressor ratios [Sp1/(Full length Sp3 + Truncated Sp3)], may allow for a more succinct view of the functional impact of different levels of Sp factor binding (Figure 7). Nuclear extracts from untreated cell lines, modeling undifferentiated monoblastic cells, each exhibited lower activator/repressor ratios than their PMA differentiated counterparts, indicating a potential increase in transcriptional activation from

10.3389/fviro.2022.971293

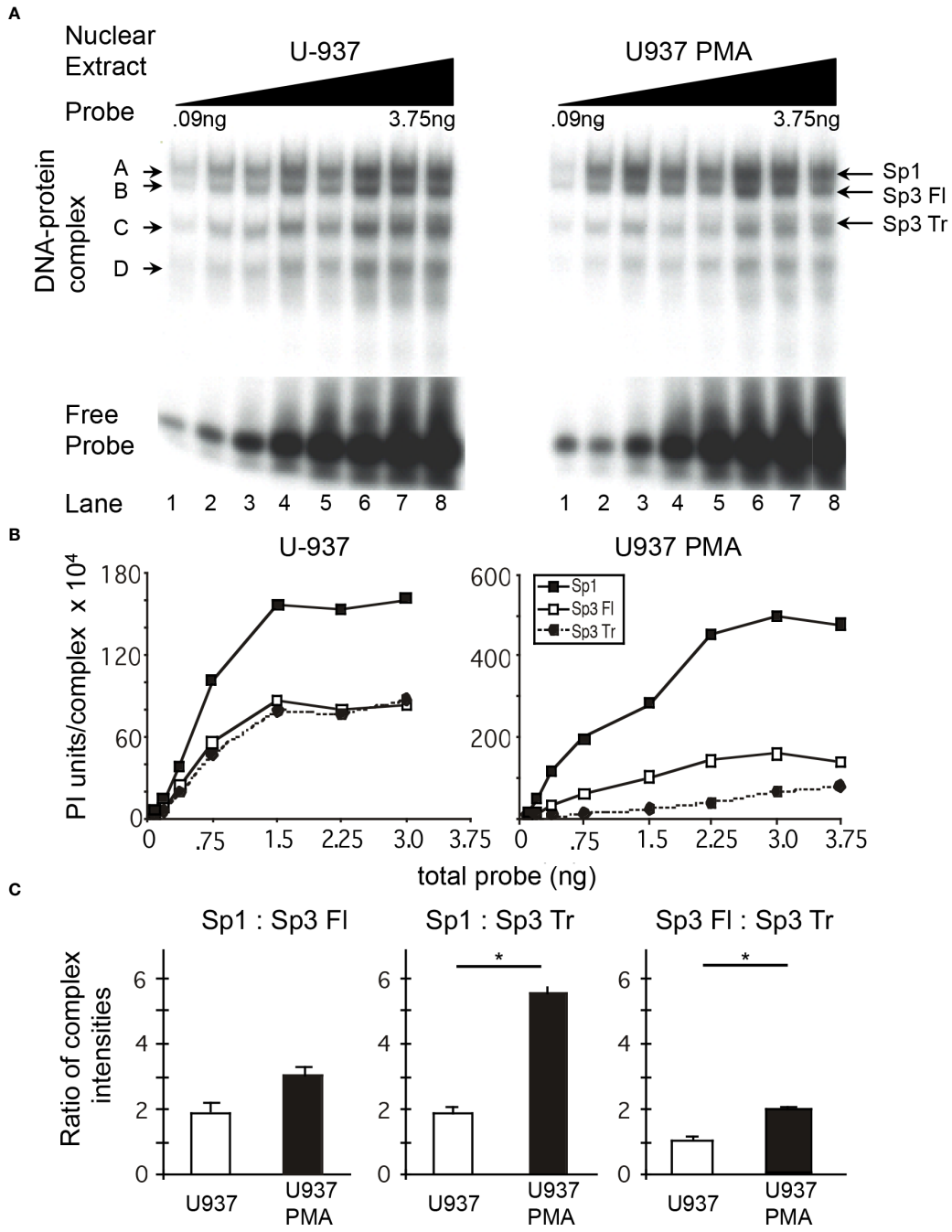

FIGURE 4
Relative levels of Sp factor binding in the monoblastic U-937 cell line varies with the addition of the chemical differentiating agent, PMA. Relative Sp factor binding was examined by EMS probe titration analyses. **(A)** Untreated and PMA-treated U-937 nuclear extracts (6 µg) were reacted with increasing amounts of labeled HIV-1 Sp site III probe (12,500 to 500,000 cpm; 0.09 to 3.75 ng). Complexes were separated by a 2-hr electrophoresis interval through a 4% acrylamide gel to retain unbound probe to facilitate subsequent analysis. DNA-protein complexes are labeled A through D; arrows indicate the position of low mobility Sp-related complexes. Representative image shown. **(B)** Untreated and PMA-treated U-937 nuclear extracts (6 µg) were reacted with increasing amounts of labeled HIV-1 Sp site III probe (12,500 to 500,000 cpm; 0.09 to 3.75 ng). Complexes were subjected to a 3-hr electrophoresis interval utilizing 4% acrylamide to allow for greater separation and a more accurate subsequent quantitation of the resulting DNA-protein complexes. Unbound probe was not retained. DNA-protein complexes were quantitated and graphed as phosphorimager units per complex. Representative graph shown. **(C)** DNA-protein complex intensities **(B)** were averaged at saturation and their relative levels compared within a given gel. This process was repeated three times and the average of the three relative intensities was graphed for each pair of DNA-protein complexes examined: Sp1 relative to Sp3 Fl, Sp1 relative to Sp3 Tr, and Sp3 Fl relative to Sp3 Tr. Comparisons between all were evaluated by the quantitative two-tailed student t-test and $p < 0.05$ was considered significant (*).

10.3389/fviro.2022.971293

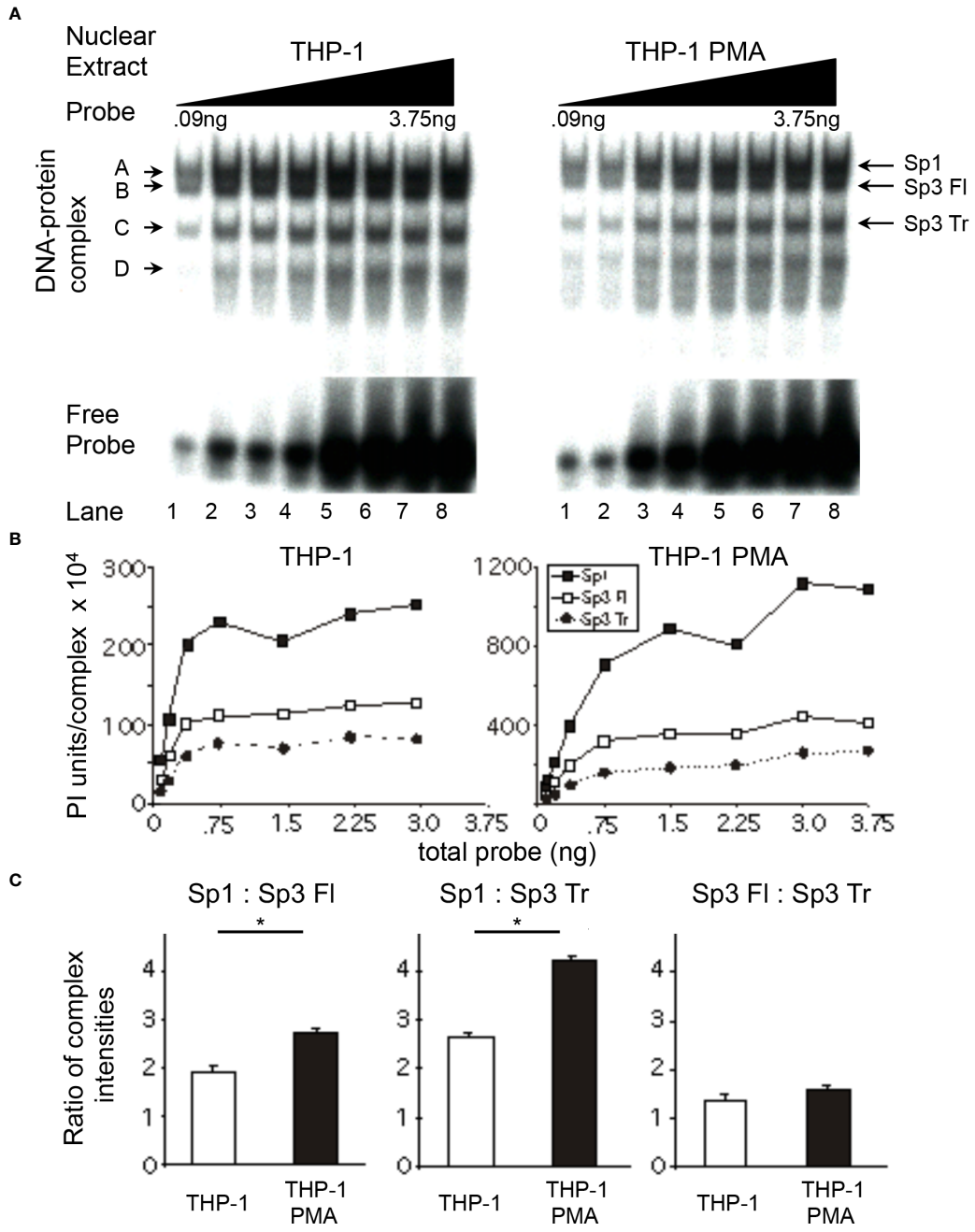

FIGURE 5
Relative levels of Sp factor binding in the monoblastic THP-1 cell line varies with the addition of the chemical differentiating agent, PMA. Relative Sp factor binding was examined by EMS probe titration analyses. **(A)** Untreated and PMA-treated THP-1 nuclear extracts (6 µg) were reacted with increasing amounts of labeled HIV-1 Sp site III probe (12,500 to 500,000 cpm; 0.09 to 3.75 ng). Complexes were separated by a 2-hr electrophoresis interval utilizing 4% acrylamide gel to retain unbound probe to facilitate subsequent analysis. DNA-protein complexes are labeled A through D; arrows indicate the position of low mobility Sp-related complexes. Representative image shown. **(B)** Untreated and PMA-treated THP-1 nuclear extracts (6 µg) were reacted with increasing amounts of labeled HIV-1 Sp site III probe (12,500 to 500,000 cpm; 0.09 to 3.75 ng). Complexes were subjected to a 3-hr electrophoresis interval utilizing 4% acrylamide to allow for greater separation and a more accurate subsequent quantitation of the DNA-protein complexes. Unbound probe was not retained. DNA-protein complexes were quantitated and graphed as phosphorimager units per complex. Representative graph shown. **(C)** DNA-protein complexes intensities **(B)** were averaged at plateau and their relative levels compared within a given gel. This process was repeated three times and the average of the three relative intensities was graphed for each pair of DNA-protein complexes examined: Sp1 relative to full-length Sp3, Sp1 relative to Sp3 Tr, and Sp3 Fl relative to Sp3 Tr. Comparisons between all were evaluated by the quantitative two-tailed student t-test and $p < 0.05$ was considered significant (*).

10.3389/fviro.2022.971293

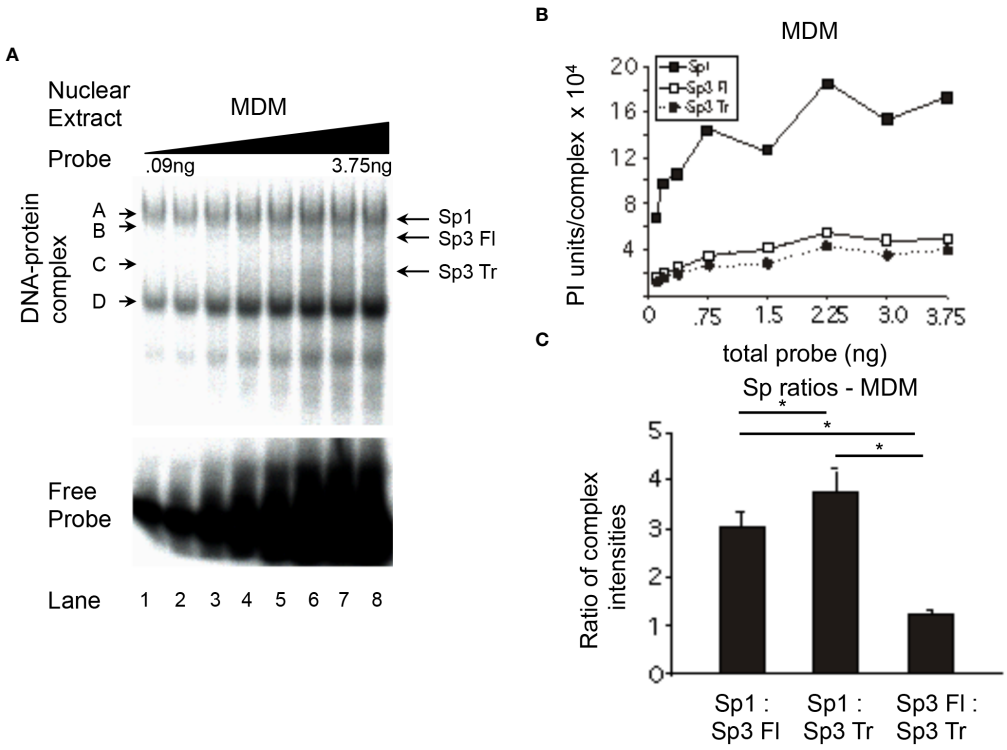

FIGURE 6
Relative levels of Sp factor binding in primary MDMs. Relative Sp factor binding was examined by EMS probe titration analyses. **(A)** Primary MDM nuclear extracts (20 µg) were reacted with increasing amounts of labeled HIV-1 Sp site III probe (12,500 to 500,000 cpm; 0.09 to 3.75 ng). Complexes were separated by a 2-hr electrophoresis interval utilizing 4% acrylamide gel to retain unbound probe for subsequent analysis. DNA-protein complexes are labeled A through D; arrows indicate the position of low mobility Sp-related complexes. Representative image shown. **(B)** Primary MDM nuclear extracts (6 µg) were reacted with increasing amounts of labeled HIV-1 Sp site III probe (12,500 to 500,000 cpm.; 0.09 to 3.75 ng). Complexes were subjected to a 3-hr electrophoresis interval utilizing 4% acrylamide to allow for greater separation and a more accurate subsequent quantitation of the DNA-protein complexes. Unbound probe was not retained. DNA-protein complexes were quantitated and graphed as phosphorimager units per complex. **(C)** DNA-protein complexes intensities Representative graph shown. **(B)** were averaged at saturation and their relative levels compared within a given gel. This process was repeated three times and the average of the three relative intensities was graphed for each pair of DNA-protein complexes examined: Sp1 relative to Sp3 Fl, Sp1 relative to Sp3 Tr, and Sp3 Fl relative to Sp3 Tr. Comparisons between all were evaluated by the quantitative two-tailed student t-test and $p < 0.05$ was considered significant (*).

HIV-1 promoters containing active *cis*-acting Sp elements following monocytic differentiation. In the case of the HL-60 and U-937 nuclear extracts, each exhibited a nearly 1:1 ratio of activating Sp factors to repressing Sp factors. Following chemical differentiation with PMA, these ratios increased to 1.9:1.0 and 2.0:1.0, respectively (Figure 7). However, DMSO-induced granulocytic differentiation of the HL-60 myelomonocytic cell line generated a much smaller change in the activator/repressor ratio (compare 1.0:1.0 untreated to 1.2:1.0 treated) implying that the change in Sp factor recruitment observed with PMA-treatment were more a function of monocytic differentiation, than granulocytic differentiation. Nuclear extracts prepared from untreated cells exhibited similar levels of activating and repressing Sp factors (compare THP-1, 1.1:1.0; U-937, 0.9:1.0; and HL-60, 1.0:1.0; Figure 7). Interestingly, nuclear extracts from PMA-differentiated THP-1 cells, exhibited a smaller increase in the activator/repressor ratio (compare 1.1:1.0 untreated to 1.7:1.0 PMA-treated, Figure 7) than did nuclear extracts from either PMA-differentiated HL-60 or U-937 cells (compare 1.0:1.0 untreated to 1.9:1.0 PMA-treated, HL-60; and 0.9:1.0 untreated to 2.0:1.0 PMA-treated U-937; Figure 7). When the activator/repressor ratio of primary MDM (1.7:1.0) was compared to that of the cell lines examined, it was clear that primary MDMs have Sp factor binding profiles which more closely resemble profiles from chemically-differentiated monoblastic and myelomonoblastic cell lines as compared to their untreated counterparts (Figure 7).

Impact of altered Sp factor binding on transcriptional activity of subtype B consensus HIV-1 *cis*-acting Sp elements

To examine the effect of the altered Sp factor ratios on HIV-1 LTR-directed gene expression in the absence of any confounding

10.3389/fviro.2022.971293

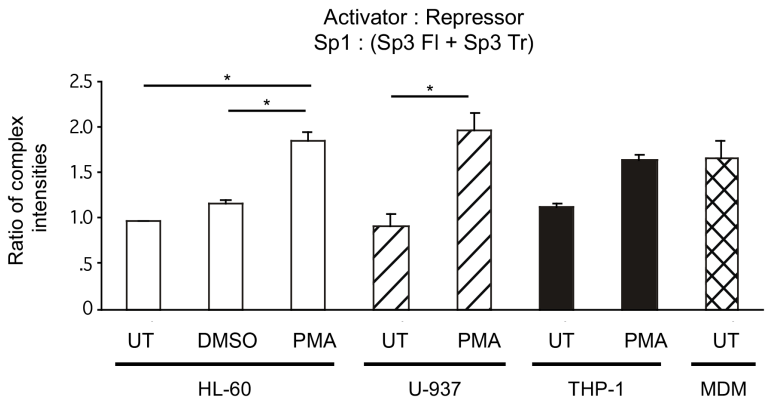

FIGURE 7
Comparisons of relative Sp family activator to repressor levels in untreated and chemically differentiated cell lines as well as primary MDM. To facilitate an examination of the effect of changing Sp factor binding on Sp-mediated activation of the HIV-1 LTR, results from Figures 3–6 have been coalesced to illustrate Sp1 (total activator) to the sum of both Sp3 isoforms (total repressor). Results from untreated and chemically differentiated cell lines are presented along with results from primary MDM. Statistical analysis between the three basal cells lines show no statistical difference. PMA treated cells cell lines were all statistically significantly higher than their basal comparator. Most important is that there was not a statistical difference between the PMA-treated cell lines and primary MDMs in this ratio. Comparisons between all were evaluated by the quantitative two-tailed student t-test and $p < 0.05$ was considered significant (*).

effects from non-Sp related changes in the transcriptional factor milieu which might be induced following monocyte differentiation, analyses were performed with a series of constructs containing only the TATA box and Sp elements. Specifically, transient transfection-reporter gene analyses were performed on truncated HIV-1 subtype B LTR-luciferase constructs containing three, two, one or no active *cis*-acting Sp elements (Figure 8A). To test the impact of altered Sp factor binding ratios on the activity of these constructs, fold-activation of the Sp(0x)TATA construct following the addition of one, two or three active Sp elements was examined in the HL-60, U-937 and THP-1 cell lines both in their undifferentiated and chemical-differentiated states. When these studies were performed in the HL-60 cell line, the addition of each active Sp element caused a sequential increase in promoter activity [Sp(0x)TATA ≤ Sp(1x)TATA < Sp(2x)TATA < Sp(3x)TATA] in both untreated and PMA-treated HL-60 cells (Figure 8B). The activity of each individual construct relative to that of the Sp(0x)TATA construct was then compared in untreated and chemically differentiated cells. Similar increases in activity were observed when both the Sp(1x)TATA and the Sp(2x)TATA constructs were examined (Figure 8B). However, the Sp(3x)TATA construct generated a small increase in promoter activity in PMA-treated cells than in untreated cells (compare 17-fold in untreated to 27-fold in PMA-treated; Figure 8B). This increase in fold-activation of the Sp(0x)TATA construct in the presence of PMA was qualitatively consistent with the 92% elevation in Sp activator binding observed in PMA-treated HL-60 nuclear extracts (compare untreated and PMA-treated HL-60 cells; Figure 7).

When these constructs were examined in U-937 cells, the addition of each active Sp element again caused a sequential increase in promoter activity [Sp(0x)TATA ≤ Sp(1x)TATA < Sp(2x)TATA < Sp(3x)TATA] in both untreated and PMA-treated U-937 cells (Figure 8C). When the activity of each individual construct relative to that of the Sp(0x)TATA construct was compared in untreated and chemically differentiated cells, significant differences were observed. When examined in untreated U-937 cells the Sp(1x)TATA construct resulted in no increase in activity over the Sp(0x) TATA construct, however a 1.8-fold increase in activity was observed when the constructs were tested in PMA-treated U-937 cells (Figure 8C). Similarly, the untreated Sp(2x)TATA construct generated a 3.3-fold increase in activity relative the Sp(0x)TATA construct in untreated cells, and a 14-fold increase in this activity in PMA-treated cells (Figure 8C). The Sp(3x)TATA construct, containing three active Sp elements, generated activity 5.7-fold over that of the Sp(0x) TATA construct in untreated cells, while the same comparison in PMA-treated cells yielded a 38-fold increase in promoter activity (Figure 8C). These results are consistent with results observed in HL-60 cells, in that a 116% increase in the relative levels of Sp family activators observed in PMA-treated extracts (compare untreated and PMA-treated U-937 cells; Figure 8) qualitatively correlates with the increased levels of LTR-luciferase activity observed in the presence of PMA.

10.3389/fviro.2022.971293

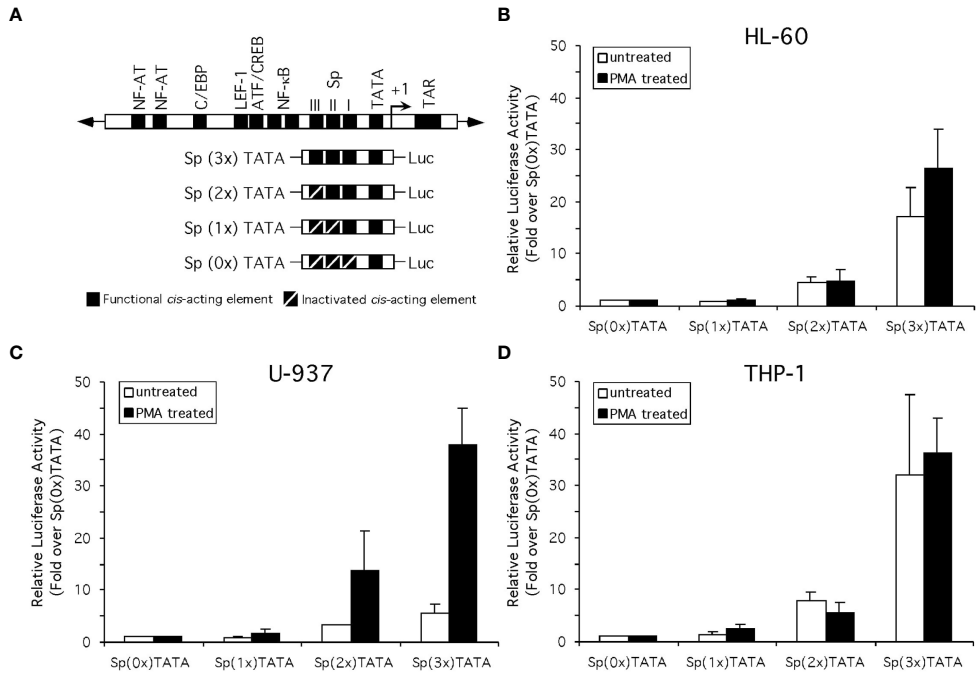

FIGURE 8
Altered Sp factor binding correlated with chemical differentiation alters the activity of the Sp elements of the HIV-1 LTR. **(A)** Diagrammatic depiction of the truncated LTR-Luciferase constructs examined. **(B)** Standard reporter gene analysis utilizing the dual luciferase reporter gene system (see Materials and Methods for details) was employed to determine the effect of chemically-induced monocytic differentiation on the activity of constructs containing three, two, one or no active Sp *cis*-acting elements. Results compare the activity of constructs in the HL-60 **(B)**, U-937 **(C)**, and THP-1 **(D)** cells in the absence or presence of PMA treatment. Activity is shown as fold-increase over the Sp(0x)TATA construct. Individual experiments were performed in duplicate and repeated at least three times. Error bars represent the standard deviation between the replicate experiments.

Similar to observations in HL-60 and U-937 cells, the addition of each active Sp element caused a sequential increase in promoter activity [Sp(0x)TATA ≤ Sp(1x)TATA < Sp(2x)TATA < Sp(3x)TATA] in both untreated and PMA-treated THP-1 cells (Figure 8D). As before, the activity of each individual construct relative to that of the Sp(0x)TATA construct was compared in untreated and chemically differentiated cells. Unlike the results obtained with HL-60 or U-937 cells, a comparison of construct activity in untreated and PMA-treated THP-1 cells generated little or no difference in activity relative to the Sp(0x)TATA construct (Figure 8D). The lack of a PMA-induced increase in the activation of the Sp-containing LTR-Luciferase constructs may be related to the smaller (47%) increase in the binding of Sp family activators relative to repressors observed with THP-1 nuclear extracts following PMA treatment (compare untreated and PMA-treated THP-1 cells; Figure 8). Cumulatively, results from the HL-60, U-937 and THP-1 cell lines indicate that enhancement of Sp1 factor binding relative to Sp3 isoform binding may influence, but not fully predict, the transcriptional activity generated from the *cis*-acting Sp elements of the HIV-1 LTR.

Identification of phosphorylation changes on Sp1 and Sp3 upon PMA-induced differentiation of promonocytic U-937 cells

It is well established that activity and stability of cellular TFs is regulated by PTMs including phosphorylation, glycosylation, acetylation, ubiquitination, methylation and sumoylation [reviewed in (66)]. For the Sp family of TFs, PTMs have been shown to influence several functional aspects including protein-protein interactions, sequence-specific DNA binding, and transcriptional activity (41). To evaluate the changes in PTMs on Sp1 and Sp3 in the process of monocytic differentiation, mass spectroscopy analysis was performed as described above. U-937 promocytic cells were utilized in this analysis as these cells demonstrated a good separation of transcriptional activity between untreated and PMA-treated conditions (see Figure 8C). Untreated and 0.5 μM PMA-treated U-937 cells were lysed and subjected to LC MS/MS analysis after trypsin digestion followed by PTM analyses as described above. Results identified loss of phosphorylation on S126, S137, S360, S365, T375, S376, S379, S765, S777, and S781 positions for Sp1

(Table 1). There was also a gain of phosphorylation at S127. Similarly, for Sp3, loss of phosphorylation was observed but only on the T574 residue (Table 2). The PTM analysis did not detect the well-studied amino acid residues in the transactivation domains of Sp1 and Sp3 including Ser131, T355 and others (43). It may be due to inefficient digestion with trypsin (data not shown) or uniqueness of the cell types and culture conditions utilized in this study. Nevertheless, the results identified additional novel sites where Sp1 and Sp3 were post-translationally modified upon activation in monocytic-lineage cells. Is the specific loss of phosphorylation on these residues a result of other competitive PTMs and what is their functional relevance to LTR-directed transcription? These questions are highly relevant and would require additional studies focused on mutating these residues and evaluating the impact on Sp1/Sp3 binding to cognate sites in the HIV-1 LTR and downstream transcriptional activation.

Discussion

Cells of the monocyte-macrophage lineage play critical roles in the function of immune system during infection by pathogens such as HIV-1. The process of monocytic differentiation induces a shift in the relative levels of Sp TFs with a favorable binding of the activating Sp1 over the two Sp3 isoforms. These alterations in Sp TFs appear to increase the transcriptional activity provided by the *cis*-acting Sp elements of the HIV-1 subtype B consensus LTR.

A comparison of Sp factor binding ratios derived from MDMs, chemically-differentiated cell lines, and their undifferentiated counterparts, illustrated that ratios derived from MDMs and chemically-differentiated cells more closely resemble each other than did ratios from undifferentiated cells (compare Figure 6C to Figures 3C, 4C, 5C). These results suggest that Sp factor binding ratios derived from chemically differentiated cells lines may act as an appropriate proxy for Sp factor binding in primary MDMs.

After demonstrating an alteration in the binding profiles of Sp factors following monocytic differentiation, it was of interest to examine the mechanism by which their binding profiles were altered. To this end, the level of both Sp1 and Sp3 were examined by western immunoblot analyses. Interestingly, no significant differences in the levels of Sp factors were detected between nuclear extracts derived from untreated and chemically differentiated U-937 or THP-1 cells (data not shown). Although a small increase in Sp factors was observed in HL-60 cells upon PMA-induced monocytic differentiation, a similar increase was also observed following DMSO-induced granulocytic differentiation (data not shown) indicating that the increased protein levels were not the likely cause of the altered factor binding. Hence, changes in Sp factor binding do not appear to be driven by changes in the nuclear concentrations of the Sp factors, though this observation could also be validated through chromatin immunoprecipitation and qPCR. Thus, it was hypothesized that Sp factor binding may be regulated by a post-translational mechanism. The PTM analysis on Sp1 and Sp3 upon differentiation with PMA revealed loss of phosphorylation on several residues on Sp1 and one such modification was seen on Sp3 (Tables 1, 2). The PTM data did not result in the detection of some of the reported phosphorylated residues in Sp1 and Sp3. This may be due a variety of factors including inefficient digestion with trypsin prior to MS/MS or it may be due to unique patterns of phosphorylation of Sp factors in the promonocytic U-937 cells. Additional studies will need to be performed that will involve the use of a combination of proteases (Chymotrypsin and trypsin) to generate superior digestion to yield smaller peptides and better coverage. In addition, in future studies in this regard, we would also want to perform these studies in other myeloid cells to see if there is differential phosphorylation in myeloid cell type populations. These studies are extensive and beyond the scope of this report. Additionally, the functional contribution of these newly-identified phosphorylation sites on Sp1 and Sp3 will be evaluated in context of LTR-directed transcription by sequentially mutating these residues coupled with additional functional studies to pinpoint the role of these residues with respect to the impact of Sp phosphorylation on regulating HIV-1 gene expression during differentiation and activation of this important lineage of cells.

After observing an increase in Sp1 binding relative to the two Sp3 isoforms, the mechanisms guiding altered Sp factor binding profiles and how they impact the activity of subtype B consensus HIV-1 LTR *cis*-acting Sp elements was examined. Because Sp1 has been shown to activate the HIV-1 LTR while both Sp3 isoforms have been shown to repress it (47), we hypothesized that an increase in Sp1 binding relative the Sp3 isoforms would correlate with increased LTR activity. To examine this hypothesis a series of truncated HIV-1 LTR constructs (-83 to +2 relative the transcriptional start site) containing a TATA box and either three, two, one or no active Sp binding elements were utilized in transient expression analyses in HL-60, U-937, and THP-1 cells in the absence or presence of PMA (Figure 8A). The activity of each construct was then compared to the activity of the construct containing no active Sp elements. This measure of relative activity facilitated a comparison of each construct activity in a given cell line in the absence or presence of PMA. Furthermore, one might anticipate a greater increase in the relative activity of a construct containing Sp elements in a cellular environment, which favors binding of the activating Sp1 over the repressing Sp3 isoforms. In general, assuming that the activation potential for the Sp factors themselves remains unchanged during differentiation, the increase in LTR activity observed with each additional Sp element would be greater after differentiation.

10.3389/fviro.2022.971293

TABLE 1 PTM (phosphorylation) analysis on Sp1 in promonocytic U-937 cells upon PMA stimulation.

Amino acid phosphorylated	Position in Sp1 sequence	U-937UT	U-937PMA
S	2	+	+
S	7	+	+
T	12	+	+
S	36	+	+
S	124	+	+
S	**126**	+	-
S	**127**	-	+
T	128	+	+
S	134	+	+
S	136	+	+
S	**137**	+	-
S	**360**	+	-
S	**365**	+	-
T	**375**	+	-
S	**376**	+	-
S	**379**	+	-
T	599	+	+
T	605	+	+
Y	608	+	+
S	612	+	+
S	617	+	+
Y	637	+	+
T	640	+	+
S	641	+	+
T	651	+	+
T	659	+	+
S	661	+	+
Y	662	+	+
T	668	+	+
S	670	+	+
T	679	+	+
T	681	+	+
S	698	+	+
S	702	+	+
T	707	+	+
S	**765**	+	-
S	**777**	+	-
S	**781**	+	-

(UT- untreated and PMA- PMA 0.5μM treated).
(+ indicates phosphorylation; - indicated no phosphorylation; phosphoR site probabilities of 75% or more were considered; green boxes highlight a dephosphorylation event and red box highlights phosphorylation).

TABLE 2 PTM (phosphorylation) analysis on Sp3 in promonocytic U-937 cells upon PMA stimulation.

Amino acid phosphorylated	Position in SP3 sequence	U-937UT	U-937PMA
T	2	+	+
S	113	+	+
T	115	+	+
T	117	+	+
T	118	+	+
S	563	+	+
S	566	+	+
T	567	+	+
T	570	+	+
T	574	+	-
T	601	+	+
T	613	+	+
Y	632	+	+
T	635	+	+
S	636	+	+
S	646	+	+
Y	657	+	+
T	663	+	+
S	665	+	+
T	674	+	+
T	676	+	+
S	687	+	+
S	693	+	+
T	702	+	+
S	711	+	+
S	712	+	+
S	713	+	+
T	714	+	+
S	718	+	+

(UT- untreated and PMA- PMA 0.5μM treated).
(+ indicates phosphorylation; - indicated no phosphorylation; phosphoR site probabilities of 75% or more were considered; green boxes highlight a dephosphorylation event).

Results from two of the three cell lines examined qualitatively support this hypothesis. The HL-60 and U-937 cell lines both exhibit increases in their activator to repressor ratio (Figure 7) and an increased relative activity of *cis*-acting Sp elements (Figures 8B, C) following chemically induced monocytic differentiation. However, the qualitative relationship between the activator to repressor ratio and the increase in relative activity of *cis*-acting Sp elements is significantly different. The HL-60 cell line exhibited a 92% increase in the activator to repressor ratio (Figure 7) and a 55% increase in the relative activity of the Sp(3x)TATA LTR-Luciferase construct (Figure 8B) with PMA treatment. While the U-937 cell line exhibited a 116% increase in the activator to repressor ratio (Figure 7) and a 5.6-fold increase in the relative activity of the Sp(3x)TATA LTR-Luciferase construct (Figure 8C) with PMA treatment. In addition, PMA treatment causes the Sp(1x)TATA and Sp(2x)TATA constructs to exhibit little increase in relative activity in HL-60 cells while a greater increase was observed in U-937 cells (compare Figure 8B to Figure 8C). Conversely, the THP-1 cell line did not appear to qualitatively or quantitatively adhere to our aforementioned

hypothesis. THP-1 cells exhibited a 47% increase in the activator to repressor ratio (Figure 7) and either a minor or no increase in the relative activity of the Sp(3x)TATA LTR-Luciferase construct (Figure 8D) upon PMA treatment. Taken together, these relationships imply that although Sp factor binding may influence the activity of *cis*-acting Sp elements it does not directly predict this activity, thus implying that factors or processes other than the ratio of Sp factor binding may also modulate the activation of *cis*-acting Sp elements. To further explore these findings, knockdowns of Sp1 and Sp3 may also be used to support our hypotheses however it has previously been shown that loss of Sp1 significantly dysregulates gene expression during differentiation (67).

One possible inference from these results is that the activation potential of the Sp factors themselves may be altered during the course of monocytic differentiation. An increase in the activation potential of the Sp factors following monocytic differentiation could explain how the small difference in increased activator to repressor ratios observed between HL-60 and U-937 cells following PMA treatment [compare a 92% increase (HL-60) to a 116% increase (U-937); Figure 7), could be coupled to such notable differences in increased relative activity of *cis*-acting Sp elements following PMA treatment [compare a 55% increase (HL-60) to a 5.6-fold increase (U-937); Figures 8B, C]. Similarly, in the THP-1 cell line a marginal change in the activating potential of Sp factors might explain the lack of a significant increase in the relative activity of the Sp(3x)TATA construct following (Figure 8D) the induction of a 42% increase in the activator to repressor ratio (Figure 7) following PMA treatment. Another potential explanation for these findings would hypothesize the existence of significant synergism between activating Sp family members. Such a synergism could be used to explain the large changes in transcriptional activity observed after smaller quantitative alterations in Sp factor recruitment in U-937s. Furthermore, the 42% increase in activating Sp factor binding coupled with only minor alterations in transcriptional activity observed following PMA treatment of THP-1 cells, could be explained if a certain threshold level of Sp activator binding was required before noticeable synergism is achieved. In addition to these, the PTMs on Sp factors showed some significant differences between the untreated and PMA-stimulated U-937 cells (Tables 1, 2). Additional studies in HIV-infected monocytic cell lines with induced differentiation, demonstrating altered PTMs of Sp isoforms would support the significance of this observation.

With respect to the HIV-1 gene regulation system, the alterations in Sp factor binding observed may have significance beyond that presently illustrated. HIV-1 LTR activity has been shown to be activated in the presence of either the viral transactivating protein, Tat, (68) or the viral accessory protein Vpr (69). Moreover, it has been shown that both Tat- and Vpr-mediated LTR activation is modulated through interactions with the G/C box array of the HIV-1 LTR and recruited Sp factors. Specifically, the loss of Sp elements in the HIV-1 LTR dramatically reduces Tat-mediated LTR activity in HeLa cells but only when all three are mutated but not basal activity (57). In Figure 8, we show that individual Sp binding site mutations in Sp binding site III contribute the most to basal and PMA-induced activity in various monocytic cells. However, previous studies from our group have shown that in HIV-1 replication experiments when Sp binding site III alone is mutated to prevent Sp1 and/or 3 binding, viral replication is reduced in Jurkat T cells and not U-937 monocytic cells (70). However, in this scenario Tat and Vpr would be present. This is interesting as the Tat inducibility of certain synthetic promoters has been shown to be Sp1-dependent (71) and Tat has been shown to induce the phosphorylation of Sp factors (42), a modification which might directly influence the DNA binding affinity of the Sp factors themselves. Evidence that Vpr-mediated LTR activation is influenced by an interaction between Vpr and the Sp1 HIV-1 LTR complex has also been reported (72, 73). In light of these studies, one might hypothesize that the altered recruitment of Sp factors during monocytic differentiation illustrated herein may likely impact Tat- and/or Vpr-mediated LTR activation or that Tat and/or Vpr may aid in stabilizing lower affinity Sp binding sites to help induce replication.

In summary, we have illustrated that the process of monocytic differentiation can induce a shift in the relative levels of Sp factor binding to an HIV-1 Sp element. This shift favors binding of the activated Sp1 over the two Sp3 isoforms. Such an alteration in Sp factor binding may have significance across a variety of Sp-dependent cellular and viral promoters present in cells of the monocyte-macrophage lineage during differentiation. Furthermore, the alteration in Sp factor binding was shown to alter the transcriptional activity provided by the *cis*-acting Sp elements of the HIV-1 subtype B consensus LTR. These observations may be attributed to the changes in PTMs on Sp isoforms upon receiving differentiation and activation stimuli as observed in U-937 cells. Finally, HIV-1 transcription and replication is driven through the LTR and cell phenotype and differentiation status impacts this. In fact, we have previously shown that all three Sp binding sites explored here have significantly different mean genetic differences between CXCR4-utilizing and CCR5-utilizing virus (proxy for T cell versus myeloid infection) and that these differential genetic signatures are predicted to impact the Sp binding phenotype at each Sp site (65, 70, 74). Taken together, this study adds to the importance of the Sp binding sites for viral replication and shows the isoforms of the proteins that can regulate the LTR in various differentiation states of myeloid lineages.

Data availability statement

All relevant data is contained within the article: The original contributions presented in the study are included in the article/supplementary material. Further inquiries can be directed to the corresponding author.

Author contributions

Conceptualization, JM., SD, BW; methodology, JM., SD, BW; formal analysis, SD, JM, MN, TB, BW; investigation, SD, JM, MN, TB, BW; resources, BW; data curation, SD, JM., MN, TB, BW; writing—original draft preparation, SD, JM, MN, TB, BW; writing—review and editing, SD, JM, RB, MC, MN, TB, BW; visualization, SD, JM, MN, TB, BW; supervision, MN, BW; project administration, MN, BW; funding acquisition, BW. All authors contributed to the article and approved the submitted version.

Funding

The authors were funded in part by the Public Health Service, National Institutes of Health, through grants from the National Institute of Mental Health (NIMH) R01 MH110360 (Contact PI, BW), the NIMH Comprehensive NeuroAIDS Center (CNAC) P30 MH092177 (KK, PI; BW, PI of the Drexel subcontract involving the Clinical and Translational Research Support Core), the Ruth L. Kirschstein National Research Service Award T32 MH079785 (PI, TB; BW, Principal Investigator of the Drexel University College of Medicine component). The contents of the paper are solely the responsibility of the authors and do not necessarily reflect the official views of the NIH.

Conflict of interest

The authors declare that the research was conducted in the absence of any commercial or financial relationships that could be construed as a potential conflict of interest.

Publisher's note

All claims expressed in this article are solely those of the authors and do not necessarily represent those of their affiliated organizations, or those of the publisher, the editors and the reviewers. Any product that may be evaluated in this article, or claim that may be made by its manufacturer, is not guaranteed or endorsed by the publisher.

References

1. Le Douce V, Herbein G, Rohr O, Schwartz C. Molecular mechanisms of HIV-1 persistence in the monocyte-macrophage lineage. *Retrovirology* (2010) 7:32. doi: 10.1186/1742-4690-7-32

2. Burdo TH, Lackner A, Williams KC. Monocyte/macrophages and their role in HIV neuropathogenesis. *Immunol Rev* (2013) 254(1):102–13. doi: 10.1111/imr.12068

3. Dahiya S, Liu Y, Nonnemacher MR, Dampier W, Wigdahl B. CCAAT enhancer binding protein and nuclear factor of activated T cells regulate HIV-1 LTR *via* a novel conserved downstream site in cells of the monocyte-macrophage lineage. *PloS One* (2014) 9(2):e88116. doi: 10.1371/journal.pone.0088116

4. Kumar A, Abbas W, Herbein G. HIV-1 latency in monocytes/macrophages. *Viruses* (2014) 6(4):1837–60. doi: 10.3390/v6041837

5. Avalos CR, Price SL, Forsyth ER, Pin JN, Shirk EN, Bullock BT, et al. Quantitation of productively infected monocytes and macrophages of SIV-infected macaques. *J Virol* (2016) 5643–56. doi: 10.1128/JVI.00290-16

6. Carter CA, Ehrlich LS. Cell biology of HIV-1 infection of macrophages. *Annu Rev Microbiol* (2008) 62:425–43. doi: 10.1146/annurev.micro.62.081307.162758

7. Kilareski EM, Shah S, Nonnemacher MR, Wigdahl B. Regulation of HIV-1 transcription in cells of the monocyte-macrophage lineage. *Retrovirology* (2009) 6:118. doi: 10.1186/1742-4690-6-118

8. Honeycutt JB, Wahl A, Baker C, Spagnuolo RA, Foster J, Zakharova O, et al. Macrophages sustain HIV replication *in vivo* independently of T cells. *J Clin Invest* (2016) 126(4):1353–66. doi: 10.1172/JCI84456

9. Sattentau QJ, Stevenson M. Macrophages and HIV-1: An unhealthy constellation. *Cell Host Microbe* (2016) 19(3):304–10. doi: 10.1016/j.chom.2016.02.013

10. Lee B, Sharron M, Montaner LJ, Weissman D, Doms RW. Quantification of CD4, CCR5, and CXCR4 levels on lymphocyte subsets, dendritic cells, and differentially conditioned monocyte-derived macrophages. *Proc Natl Acad Sci U.S.A.* (1999) 96(9):5215–20. doi: 10.1073/pnas.96.9.5215

11. Joly M, Pinto JM. CXCR4 and CCR5 regulation and expression patterns on T- and monocyte-macrophage cell lineages: implications for susceptibility to infection by HIV-1. *Math Biosci* (2005) 195(1):92–126. doi: 10.1016/j.mbs.2005.01.002

12. Kruize Z, Kootstra NA. The role of macrophages in HIV-1 persistence and pathogenesis. *Front Microbiol* (20192828) 10:2828. doi: 10.3389/fmicb.2019.02828

13. Wong ME, Jaworowski A, Hearps AC. The HIV reservoir in monocytes and macrophages. *Front Immunol* (2019) 10:1435. doi: 10.3389/fimmu.2019.01435

14. Hendricks CM, Cordeiro T, Gomes AP, Stevenson M. The interplay of HIV-1 and macrophages in viral persistence. *Front Microbiol* (2021) 12:646447. doi: 10.3389/fmicb.2021.646447

15. Veenhuis RT, Abreu CM, Shirk EN, Gama L, Clements JE. HIV Replication and latency in monocytes and macrophages. *Semin Immunol* (2021) 51:101472. doi: 10.1016/j.smim.2021.101472

16. Valledor AF, Borras FE, Cullell-Young M, Celada A. Transcription factors that regulate monocyte/macrophage differentiation. *J Leukoc Biol* (1998) 63 (4):405–17. doi: 10.1002/jlb.63.4.405

17. Li L, He S, Sun JM, Davie JR. Gene regulation by Sp1 and Sp3. *Biochem Cell Biol* (2004) 82(4):460–71. doi: 10.1139/o04-045

18. Resendes KK, Rosmarin AG. Sp1 control of gene expression in myeloid cells. *Crit Rev Eukaryot Gene Expr* (2004) 14(3):171–81. doi: 10.1615/CritRevEukaryotGeneExpr.v14.i3.20

19. Noti JD, Reinemann BC, Petrus MN. Sp1 binds two sites in the CD11c promoter *in vivo* specifically in myeloid cells and cooperates with AP1 to activate transcription. *Mol Cell Biol* (1996) 16(6):2940–50. doi: 10.1128/MCB.16.6.2940

20. Ries S, Buchler C, Langmann T, Fehringer P, Aslanidis C, Schmitz G. Transcriptional regulation of lysosomal acid lipase in differentiating monocytes is mediated by transcription factors Sp1 and AP-2. *J Lipid Res* (1998) 39(11):2125–34. doi: 10.1016/S0022-2275(20)32467-6

21. Langmann T, Buechler C, Ries S, Schaeffler A, Aslanidis C, Schuierer M, et al. Transcription factors Sp1 and AP-2 mediate induction of acid sphingomyelinase during monocytic differentiation. *J Lipid Res* (1999) 40 (5):870–80. doi: 10.1016/S0022-2275(20)32122-2

22. Friedman AD. Transcriptional regulation of granulocyte and monocyte development. *Oncogene* (2002) 21(21):3377–90. doi: 10.1038/sj.onc.1205324

23. Payton SG, Whetstine JR, Ge Y, Matherly LH. Transcriptional regulation of the human reduced folate carrier promoter c: synergistic transactivation by Sp1 and C/EBP beta and identification of a downstream repressor. *Biochim Biophys Acta* (2005) 1727(1):45–57. doi: 10.1016/j.bbaexp.2004.11.006

24. Richer E, Campion CG, Dabbas B, White JH, Cellier MF. Transcription factors Sp1 and C/EBP regulate NRAMP1 gene expression. *FEBS J* (2008) 275 (20):5074–89. doi: 10.1111/j.1742-4658.2008.06640.x

25. Kao WY, Briggs JA, Kinney MC, Jensen RA, Briggs RC. Structure and function analysis of the human myeloid cell nuclear differentiation antigen promoter: evidence for the role of Sp1 and not of c-myb or PU.1 in myelomonocytic lineage-specific expression. *J Cell Biochem* (1997) 65(2):231–44. doi: 10.1002/(sici)1097-4644(199705)65:2<231::aid-jcb8>3.0.co;2-v

26. Hauses M, Tonjes RR, Grez M. The transcription factor Sp1 regulates the myeloid-specific expression of the human hematopoietic cell kinase (HCK) gene through binding to two adjacent GC boxes within the HCK promoter-proximal region. *J Biol Chem* (1998) 273(48):31844–52. doi: 10.1074/jbc.273.48.31844

27. Rao J, Zhang F, Donnelly RJ, Spector NL, Studzinski GP. Truncation of Sp1 transcription factor by myeloblastin in undifferentiated HL60 cells. *J Cell Physiol* (1998) 175(2):121–8. doi: 10.1002/(SICI)1097-4652(199805)175:2<121::AID-JCP1>3.0.CO;2-Q

28. Apt D, Watts RM, Suske G, Bernard HU. High Sp1/Sp3 ratios in epithelial cells during epithelial differentiation and cellular transformation correlate with the activation of the HPV-16 promoter. *Virology* (1996) 224(1):281–91. doi: 10.1006/viro.1996.0530

29. Dharmavaram RM, Liu G, Mowers SD, Jimenez SA. Detection and characterization of Sp1 binding activity in human chondrocytes and its alterations during chondrocyte dedifferentiation. *J Biol Chem* (1997) 272 (43):26918–25. doi: 10.1074/jbc.272.43.26918

30. Tang QQ, Jiang MS, Lane MD. Repressive effect of Sp1 on the C/EBPalpha gene promoter: role in adipocyte differentiation. *Mol Cell Biol* (1999) 19(7):4855–65. doi: 10.1128/MCB.19.7.4855

31. Billon N, Carlisi D, Datto MB, van Grunsven LA, Watt A, Wang XF, et al. Cooperation of Sp1 and p300 in the induction of the CDK inhibitor p21WAF1/CIP1 during NGF-mediated neuronal differentiation. *Oncogene* (1999) 18 (18):2872–82. doi: 10.1038/sj.onc.1202712

32. Yoo J, Jeong MJ, Kwon BM, Hur MW, Park YM, Han MY. Activation of dynamin I gene expression by Sp1 and Sp3 is required for neuronal differentiation of N1E-115 cells. *J Biol Chem* (2002) 277(14):11904–9. doi: 10.1074/jbc.M111788200

33. Milagre I, Nunes MJ, Castro-Caldas M, Moutinho M, Gama MJ, Rodrigues E. Neuronal differentiation alters the ratio of sp transcription factors recruited to the CYP46A1 promoter. *J Neurochem* (2012) 120(2):220–9. doi: 10.1111/j.1471-4159.2011.07577.x

34. Guo H, Cao C, Chi X, Zhao J, Liu X, Zhou N, et al. Specificity protein 1 regulates topoisomerase IIbeta expression in SH-SY5Y cells during neuronal differentiation. *J Neurosci Res* (2014) 1374–83. doi: 10.1002/jnr.23403

35. Hagen G, Muller S, Beato M, Suske G. Cloning by recognition site screening of two novel GT box binding proteins: A family of Sp1 related genes. *Nucleic Acids Res* (1992) 20(21):5519–25. doi: 10.1093/nar/20.21.5519

36. Kingsley C, Winoto A. Cloning of GT box-binding proteins: A novel Sp1 multigene family regulating T-cell receptor gene expression. *Mol Cell Biol* (1992) 12 (10):4251–61. doi: 10.1128/mcb.12.10.4251-4261.1992

37. Hagen G, Muller S, Beato M, Suske G. Sp1-mediated transcriptional activation is repressed by Sp3. *EMBO J* (1994) 13(16):3843–51. doi: 10.1002/j.1460-2075.1994.tb06695.x

38. Terrados G, Finkernagel F, Stielow B, Sadic D, Neubert J, Herdt O, et al. Genome-wide localization and expression profiling establish Sp2 as a sequence-specific transcription factor regulating vitally important genes. *Nucleic Acids Res* (2012) 40(16):7844–57. doi: 10.1093/nar/gks544

39. Lalonde J, Saia G, Gill G. Store-operated calcium entry promotes the degradation of the transcription factor Sp4 in resting neurons. *Sci Signal* (2014) 7(328):ra51. doi: 10.1126/scisignal.2005242

40. Saia G, Lalonde J, Sun X, Ramos B, Gill G. Phosphorylation of the transcription factor Sp4 is reduced by NMDA receptor signaling. *J Neurochem* (2014) 129(4):743–52. doi: 10.1111/jnc.12657

41. Waby JS, Bingle CD, Corfe BM. Post-translational control of sp-family transcription factors. *Curr Genomics* (2008) 9(5):301–11. doi: 10.2174/138920208785133244

42. Chun RF, Semmes OJ, Neuveut C, Jeang KT. Modulation of Sp1 phosphorylation by human immunodeficiency virus type 1 tat. *J Virol* (1998) 72 (4):2615–29. doi: 10.1128/JVI.72.4.2615-2629.1998

43. Tan NY, Khachigian LM. Sp1 phosphorylation and its regulation of gene transcription. *Mol Cell Biol* (2009) 29(10):2483–8. doi: 10.1128/MCB.01828-08

44. Chu S. Transcriptional regulation by post-transcriptional modification–role of phosphorylation in Sp1 transcriptional activity. *Gene* (2012) 508(1):1–8. doi: 10.1016/j.gene.2012.07.022

45. Wu Z, Kim HP, Xue HH, Liu H, Zhao K, Leonard WJ. Interleukin-21 receptor gene induction in human T cells is mediated by T-cell receptor-induced Sp1 activity. *Mol Cell Biol* (2005) 25(22):9741–52. doi: 10.1128/MCB.25.22.9741-9752.2005

46. Vicart A, Lefebvre T, Imbert J, Fernandez A, Kahn-Perles B. Increased chromatin association of Sp1 in interphase cells by PP2A-mediated dephosphorylations. *J Mol Biol* (2006) 364(5):897–908. doi: 10.1016/j.jmb.2006.09.036

47. Majello B, De Luca P, Hagen G, Suske G, Lania L. Different members of the Sp1 multigene family exert opposite transcriptional regulation of the long terminal repeat of HIV-1. *Nucleic Acids Res* (1994) 22(23):4914–21. doi: 10.1093/nar/22.23.4914

48. Rohr O, Marban C, Aunis D, Schaeffer E. Regulation of HIV-1 gene transcription: From lymphocytes to microglial cells. *J Leukoc Biol* (2003) 74 (5):736–49. doi: 10.1189/jlb.0403180

49. Hotter D, Bosso M, Jonsson KL, Krapp C, Sturzel CM, Das A, et al. IFI16 targets the transcription factor Sp1 to suppress HIV-1 transcription and latency reactivation. *Cell Host Microbe* (2019) 25(6):858–872 e813. doi: 10.1016/j.chom.2019.05.002

50. Bosso M, Prelli Bozzo C, Hotter D, Volcic M, Sturzel CM, Rammelt A, et al. Nuclear PYHIN proteins target the host transcription factor Sp1 thereby restricting HIV-1 in human macrophages and CD4+ T cells. *PloS Pathog* (2020) 16(8): e1008752. doi: 10.1371/journal.ppat.1008752

51. Collins SJ, Gallo RC, Gallagher RE. Continuous growth and differentiation of human myeloid leukaemic cells in suspension culture. *Nature* (1977) 270 (5635):347–9. doi: 10.1038/270347a0

52. Gallagher R, Collins S, Trujillo J, McCredie K, Ahearn M, Tsai S, et al. Characterization of the continuous, differentiating myeloid cell line (HL-60) from a patient with acute promyelocytic leukemia. *Blood* (1979) 54(3):713–33. doi: 10.1182/blood.V54.3.713.713

53. Collins SJ, Ruscetti FW, Gallagher RE, Gallo RC. Terminal differentiation of human promyelocytic leukemia cells induced by dimethyl sulfoxide and other polar compounds. *Proc Natl Acad Sci U.S.A.* (1978) 75(5):2458–62. doi: 10.1073/pnas.75.5.2458

54. Lotem J, Sachs L. Regulation of normal differentiation in mouse and human myeloid leukemic cells by phorbol esters and the mechanism of tumor promotion. *Proc Natl Acad Sci U.S.A.* (1979) 76(10):5158–62. doi: 10.1073/pnas.76.10.5158

55. Sundstrom C, Nilsson K. Establishment and characterization of a human histiocytic lymphoma cell line (U-937). *Int J Cancer* (1976) 17(5):565–77. doi: 10.1002/ijc.2910170504

56. Tsuchiya S, Yamabe M, Yamaguchi Y, Kobayashi Y, Konno T, Tada K. Establishment and characterization of a human acute monocytic leukemia cell line (THP-1). *Int J Cancer* (1980) 26(2):171–6. doi: 10.1002/ijc.2910260208

57. Harrich D, Garcia J, Wu F, Mitsuyasu R, Gonazalez J, Gaynor R. Role of SP1-binding domains in *in vivo* transcriptional regulation of the human immunodeficiency virus type 1 long terminal repeat. *J Virol* (1989) 63(6):2585–91. doi: 10.1128/jvi.63.6.2585-2591.1989

58. Auwerx J. The human leukemia cell line, THP-1: A multifacetted model for the study of monocyte-macrophage differentiation. *Experientia* (1991) 47(1):22–31. doi: 10.1007/BF02041244

59. Koeffler HP. Induction of differentiation of human acute myelogenous leukemia cells: Therapeutic implications. *Blood* (1983) 62(4):709–21. doi: 10.1182/blood.V62.4.709.709

60. Lopez-Rodriguez C, Zubiaur M, Sancho J, Concha A, Corbi AL. An octamer element functions as a regulatory element in the differentiation-responsive CD11c integrin gene promoter: OCT-2 inducibility during myelomonocytic differentiation. *J Immunol* (1997) 158(12):5833–40.

61. Boyum A. Isolation of mononuclear cells and granulocytes from human blood. isolation of monuclear cells by one centrifugation, and of granulocytes by combining centrifugation and sedimentation at 1 g. *Scand J Clin Lab Invest Suppl* (1968) 97:77–89.

62. Gmelig-Meyling F, Waldmann TA. Separation of human blood monocytes and lymphocytes on a continuous percoll gradient. *J Immunol Methods* (1980) 33 (1):1–9. doi: 10.1016/0022-1759(80)90077-0

63. Graziani-Bowering GM, Graham JM, Filion LG. A quick, easy and inexpensive method for the isolation of human peripheral blood monocytes. *J Immunol Methods* (1997) 207(2):157–68. doi: 10.1016/S0022-1759(97)00114-2

64. Grant C, Nonnemacher M, Jain P, Pandya D, Irish B, Williams SC, et al. CCAAT/enhancer-binding proteins modulate human T cell leukemia virus type 1 long terminal repeat activation. *Virology* (2006) 348(2):354–69. doi: 10.1016/j.virol.2005.12.024

65. Millhouse S, Krebs FC, Yao J, McAllister JJ, Conner J, Ross H, et al. Sp1 and related factors fail to interact with the NF-kappaB-proximal G/C box in the LTR of a replication competent, brain-derived strain of HIV-1 (YU-2). *J Neurovirol* (1998) 4(3):312–23. doi: 10.3109/13550289809114532

66. Filtz TM, Vogel WK, Leid M. Regulation of transcription factor activity by interconnected post-translational modifications. *Trends Pharmacol Sci* (2014) 35 (2):76–85. doi: 10.1016/j.tips.2013.11.005

67. Gilmour J, O'Connor L, Middleton CP, Keane P, Gillemans N, Cazier JB, et al. Robust hematopoietic specification requires the ubiquitous Sp1 and Sp3 transcription factors. *Epigenet Chromatin* (2019) 12(1):33. doi: 10.1186/s13072-019-0282-9

68. Arya SK, Guo C, Josephs SF, Wong-Staal F. Trans-activator gene of human T-lymphotropic virus type III (HTLV-III). *Science* (1985) 229(4708):69–73. doi: 10.1126/science.2990040

69. Cohen EA, Terwilliger EF, Jalinoos Y, Proulx J, Sodroski JG, Haseltine WA. Identification of HIV-1 vpr product and function. *J Acquir Immune Defic Syndr* (1990) 3(1):11–8.

70. McAllister JJ, Phillips D, Millhouse S, Conner J, Hogan T, Ross HL, et al. Analysis of the HIV-1 LTR NF-kappaB-proximal sp site III: Evidence for cell type-specific gene regulation and viral replication. *Virology* (2000) 274(2):262–77. doi: 10.1006/viro.2000.0476

71. Kamine J, Subramanian T, Chinnadurai G. Sp1-dependent activation of a synthetic promoter by human immunodeficiency virus type 1 tat protein. *Proc Natl Acad Sci U.S.A.* (1991) 88(19):8510–4. doi: 10.1073/pnas.88.19.8510

72. Wang L, Mukherjee S, Jia F, Narayan O, Zhao LJ. Interaction of virion protein vpr of human immunodeficiency virus type 1 with cellular transcription factor Sp1 and trans-activation of viral long terminal repeat. *J Biol Chem* (1995) 270 (43):25564–9. doi: 10.1074/jbc.270.43.25564

73. Sawaya BE, Khalili K, Mercer WE, Denisova L, Amini S. Cooperative actions of HIV-1 vpr and p53 modulate viral gene transcription. *J Biol Chem* (1998) 273 (32):20052–7. doi: 10.1074/jbc.273.32.20052

74. Alexaki A, Quiterio SJ, Nonnemacher MR, Shah S, Liu Y, Banerjee A, et al. Modeling bone marrow progenitor cell differentiation and susceptibility to HIV-1 infection. *MOJ Immunol* (2014) 1(2):9. doi: 10.15406/moji.2014.01.00009

Frontiers in Virology

Explores viruses and their interactions with their hosts

A multidisciplinary journal which explores all biological and molecular aspects of viruses, with a focus on innovative investigative and analytical systems.

Discover the latest Research Topics

See more →

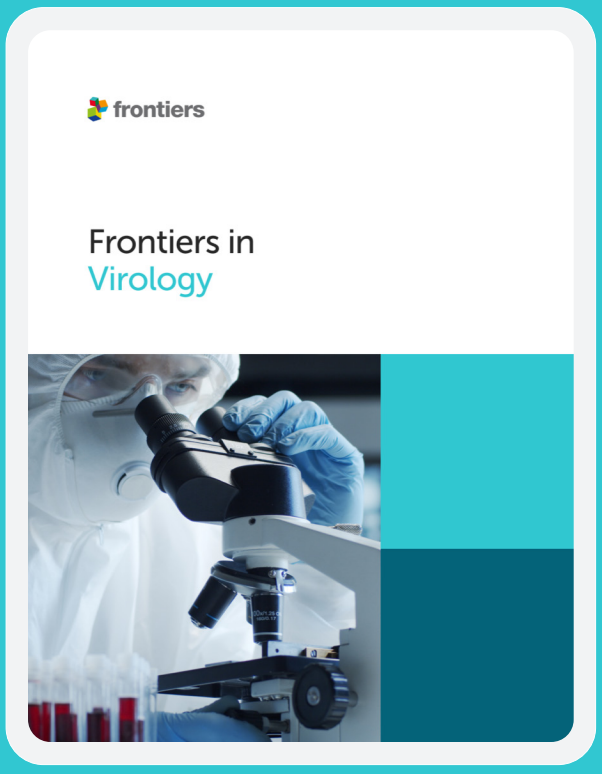

Frontiers

Avenue du Tribunal-Fédéral 34
1005 Lausanne, Switzerland
frontiersin.org

Contact us

+41 (0)21 510 17 00
frontiersin.org/about/contact